Final Report
Contract DOT-HS-031-1-159

Vehicle Handling Performance

Volume 1 of 2
Research Study

R. D. Ervin
P. Grote
P. S. Fancher
C. C. MacAdam
L. Segel

Highway Safety Research Institute
The University of Michigan
Huron Parkway and Baxter Road
Ann Arbor, Michigan

November 1972

Prepared for
National Highway Traffic Safety Administration
U. S. Department of Transportation
Washington, D.C. 20591

TECHNICAL REPORT STANDARD TITLE PAGE

1. Report No.	2. Government Accession No.	3. Recipient's Catalog No.

4. Title and Subtitle

VEHICLE HANDLING PERFORMANCE

5. Report Date
November, 1972

6. Performing Organization Code

7. Author(s)
R.D. Ervin, P. Grote, P.S. Fancher, C.C. MacAdam, L. Segel

8. Performing Organization Report No.
UM-HSRI-PF-72-2-2

9. Performing Organization Name and Address
Highway Safety Research Institute
The University of Michigan
Huron Parkway & Baxter Road
Ann Arbor, Michigan 48105

10. Work Unit No

11. Contract or Grant No.
DOT-HS-031-1-159

12. Sponsoring Agency Name and Address
National Highway Traffic Safety Administration
U.S. Department of Transportation
Washington, D.C. 20591

13. Type of Report and Period Covered
Final Report
6/71 - 11/72

14. Sponsoring Agency Code

15. Supplementary Notes

16. Abstract

The test methodology which was originally developed in the Vehicle Handling Test Procedures study was extensively refined in this program. Redesigned test apparatus was utilized in the conduct of refined test procedures on a sample of 12 contemporary passenger vehicles. The resulting data was reduced through a fully computerized data processing system. A permanent digital tape library was generated and will be preserved for public use.

Significant findings were made with respect to certain tire properties which impose a serious confounding influence on limit turning measurement.

The test vehicle sample was seen to exhibit a large range of emergency maneuvering capability. It was seen that certain vehicles exhibit properties which appear desirable over a great variety of maneuvers—while certain other vehicles exhibit consistently "poorer" performance, in terms of the safety-related hypotheses.

It is recommended that research be conducted to identify the causative mechanism behind the sensitivity of tire side force capability to shoulder wear. Research is recommended in the area of driver/vehicle system performance such that an evaluation can be made of the validity of certain expressed hypotheses related to interpretation of open-loop responses.

17. Key Words	18. Distribution Statement
Vehicle mechanics, vehicle performance, open-loop measures, limit performance, emergency maneuvers, test procedures, data base	Unlimited Availability

19. Security Classif. (of this report)	20. Security Classif. (of this page)	21. No. of Pages	22. Price
Unclassified	Unclassified		

Form DOT F 1700.7 (8-69)

TABLE OF CONTENTS

Volume 1

The contents of this report reflect the views of the Highway Safety Research Institute which is responsible for the facts and the accuracy of the data presented herein. The contents do not necessarily reflect the official views or policy of the National Highway Traffic Safety Administration.

FOREWORD

The research study reported herein was supported by the National Highway Traffic Safety Administration of the U.S. Department of Transportation. The contract technical manager was Svein I. Larsen.

This project was directed by the Highway Safety Research Institute of The University of Michigan at Ann Arbor. The testing activity was conducted with the support of the facilities and staff of the Texas Transportation Institute (TTI) at College Station, Texas.

In November, 1971, a pilot test program was begun at TTI, permitting the preliminary examination of several alternatives with respect to test procedure and logistics. A supplemental testing activity followed, beginning in March 1972, intending to resolve certain anomalies in the pilot test program data through an extensive set of tire properties experiments. In May, 1972, a full-scale test program was initiated, completing in September with the acquisition of a data base representing a sample of twelve contemporary passenger vehicles. The resulting base data has been stored permanently on digital magnetic tape for future public use.

The execution of tests on the 12th vehicle, an American Motors Ambassador, was supported by the American Motors Corporation. By mutual agreement with NHTSA, the resulting data is included within this report.

ACKNOWLEDGEMENTS

The test vehicles used in this study were prepared and initially outfitted under the direction of Mr. J. Boissonneault of HSRI.

The design of the electronics system in the new automatic controller was the responsibility of Mr. James Ackley.

Special acknowledgement is due to the subcontractor, Texas Transportation Institute (TTI). In particular, Mssrs. R. Young, R. Zimmer, L. Milberger and M. White of the TTI staff contributed extraordinary efforts to the success of the test activity.

We wish also to express sincere thanks to Mercedes Benz of North America, Inc., and to the Chrysler Corporation for the provision of test vehicles in this study.

1. INTRODUCTION

This report presents findings, conclusions and recommendations derived by the Highway Safety Research Institute (HSRI) in a research study for the National Highway Traffic Safety Administration (NHTSA) entitled "Vehicle Handling Performance." The objectives of the study involved:

1) review and refinement of test procedures derived in a parent NHTSA-sponsored study, "Vehicle Handling Test Procedures" (VHTP), which was completed by HSRI in 1970 [1]

2) application of these refined test procedures to the objective measurement of safety-related vehicle handling properties of a representative sample of vehicles

3) determination of the minimum physical requirements for the execution of these test procedures.

This report presents material which can be more fully understood if the reader is acquainted with the concepts and methods put forth in the above-cited report on the VHTP study. In that work, a rational pragmatic viewpoint was developed, from which a relationship between highway safety and vehicle performance was hypothesized.

Based on the hypothesis that such a relationship exists, this study refines and extends the performance measurement methodology developed earlier and applies this experimental method to the construction of a data library documenting six vehicle handling properties in objective terms. The objective measures selected express vehicle performance properties in the context of the hypothesized safety relationship.

Whereas the current state of highway safety research does not provide scientific proof for the hypothesized performance/safety relationship, it is postulated that this study provides safety-related performance data of value to the highway safety community, and whose value can be enhanced by further research.

The data library generated in this study contains measurements of vehicle handling performance exhibited at the limits of tire-road adhesion. It follows that these measures do not constitute an evaluation of the handling properties manifested in normal driving, but rather characterize the emergency maneuvering capability of the tire-vehicle system. Further, the term "open-loop" is applied to these measures since the driver has been removed as an active element in the system.

The report documents the further development of vehicle handling test procedures and the application of the developed methodology to a test sample. In Section 2, material related to the refinement of each basic element of the measurement methodology is presented. In this section, considerable reference is made to Appendices I - Automatic Vehicle Controller, II - Test Procedures, III - Tire Side Force Investigation, and V - Data Acquisition and Processing. Each of these topics is discussed in summary fashion in Section 2, in order to achieve continuity in the presentation.

Section 3 presents the results of the full-scale test program with a considerable number of references being made to Appendices IV - Test Sample Selection and VII - Full Scale Test Program Data Plots. However, summary treatments of these latter topics are provided in the text. With regard to the presentation of test data, "summary" is the key word. Section 3 presents sixteen data plots that serve as a

condensation of over one quarter of a million time histories that were recorded during the test program. A complete tape file of these test data will be preserved for public use, a documentation step believed to constitute a significant fruit of this study.

In Section 4, conclusions and recommendations are presented. Judgments and observations are expressed based upon vehicle-test data, tire-test data, overall test experience, and the authors' convictions relative to the directions that future research should take.

2. VEHICLE HANDLING TEST PROCEDURES: FURTHER DEVELOPMENTS

A review of the open-loop, limit-response test methodology developed by HSRI under an earlier contract entitled "Vehicle Handling Test Procedures" (VHTP) constituted the first major task of this study. The adequacy of the methodology developed in the prior study was evaluated in terms of the original objective, namely, the development of performance measures and test procedures that would provide an indicator of precrash safety quality. Five basic elements of this methodology were examined:

1. test facility
2. test apparatus
3. test procedure
4. data processing
5. data presentation

This review and examination led to the conclusion that refinements should be made in each of the above categories. These refinements are summarized below, together with the reasoning and evidence that led to the decisions that were made.

2.1 TEST FACILITY REFINEMENTS

The primary test facility needed to conduct open-loop limit maneuver measurements is a skid pad with adequate approaches for accelerating up to speed.

Whereas the original VHTP study involved testing that served primarily as a demonstration of feasibility, this program required the establishment of a high quality data

base, representative of the performance range in the vehicle population. Thus, the test surface irregularities that were tolerated in the early work were deemed excessive in view of the purposes of this program, and a new asphalt skid pad was constructed by the test subcontractor, Texas Transportation Institute, at their facility in College Station, Texas. This skid pad (Fig. 1) was constructed by applying two courses of bituminous asphalt over a concrete ramp formerly used for parking aircraft. The 1% inclination of this test surface provided ample drainage while assuring an essentially normal gravity vector for all possible vehicle trajectories. In addition to the improvement in test surface quality, the location of the skid pad also provided large runup and recovery areas which are necessary for open-loop tests.

The frictional properties of the test surface have an important influence on the results obtained in limit-response measurements. Using the ASTM method, dry skid numbers of 76-82 were obtained (averaged over the test surface) following the scrubbing of the new asphalt. Data will be presented later showing the peak lateral friction achieved on this surface by each tire represented in the test vehicle sample. Additionally, data will be presented relative to the stability of the peak lateral force achieved by tires on this surface as a function of ambient temperature and surface wetness.

The dimensions of the skid pad, nominally, 400 x 600 feet, were found to be more than adequate to conduct the limit response maneuvers developed in this program. A recommendation for minimum skid pad dimensions is given in Appendix VI.

2.2 TEST APPARATUS REFINEMENTS

In order to make open-loop maneuver measurements, the test process must prevent the driver from influencing the experiment. To this end, the original VHTP study defined

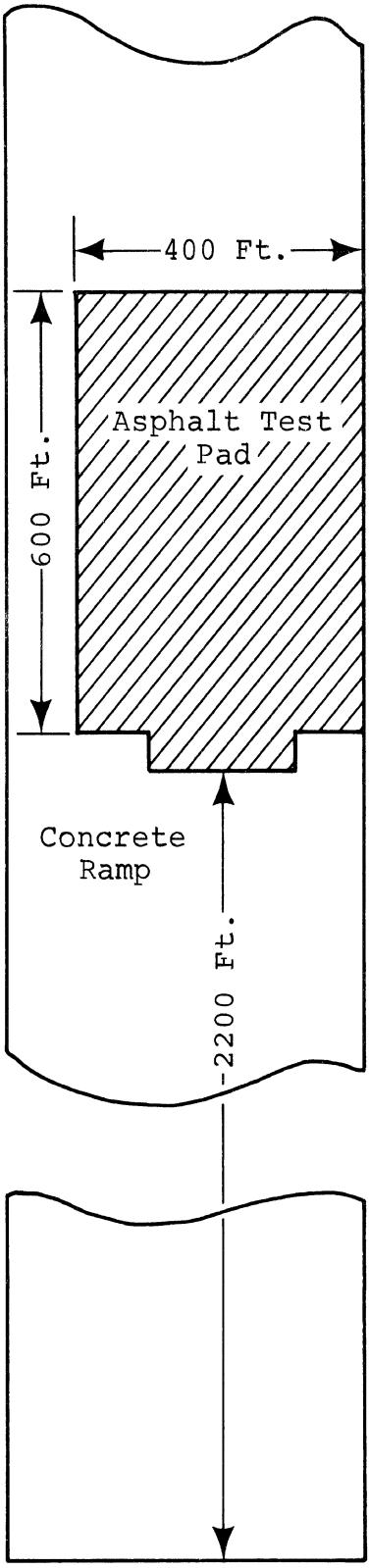

FIGURE 1

Test Area at Texas Transportation Institute

four maneuvers which could be conducted by a driver with his control inputs constrained by passive mechanisms. Two maneuvers were defined involving complex waveshapes of steering and braking and, in addition, critical phase relationships. Driver control was considered impractical. Accordingly, an automatic vehicle controller was designed, constructed, and utilized in these latter experiments. In the current program, this equipment was extensively redesigned to provide improved precision, repeatability, and utility of application as were deemed necessary to provide a high quality data base, covering a large sample of vehicles.

2.2.1 STEERING LIMITER. An adjustable device for limiting steering-wheel displacement was constructed (Fig. 2) to provide the following features:

1. The steer limiter was built as a complete assembly to replace the steering wheel of the test vehicle. This replacement was facilitated by mounting the limiter on a splined hub which was fabricated from a spare steering wheel procured for each test vehicle. Comprised of a rotor and a stator, the assembly was held fixed by a strap which fastened to the A pillar.

2. A graduated aximuth ring was included, providing a scale for steering level which could be "rezeroed," as necessary, to accommodate changes in the zero-steer setting deriving from front-end misalignment and tire wear.

3. A potentiometer for measuring steering displacement was permanently installed in the steering limiter, and was driven by a positive drive belt.

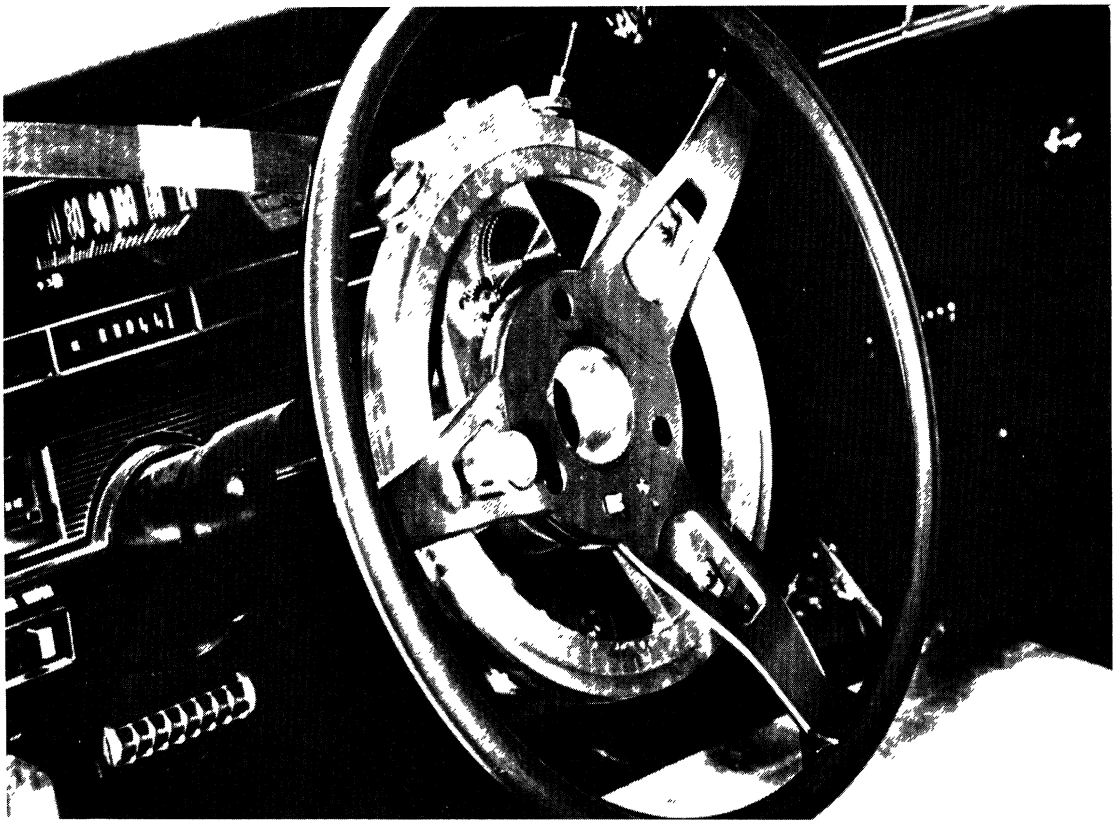

Figure 2.
Steering limiter assembly.

2.2.2 BRAKE LIMITER. The device constructed to limit driver-applied braking inputs utilized a concept that maintained a preset line pressure in contrast to the pedal displacement limiting device used in the VHTP study. By limiting line pressure, a precise control of brake input level was maintained. A hydraulic circuit (see Fig. 3) was constructed by which both pistons of the master cylinder dispense fluid into all four brakes as well as into the limiter section of the devised circuit. When the pressure of the brake system rises to equal the pressure in the bladder-type accumulator controlled by means of a high pressure source of nitrogen, further dispensing of fluid from the master cylinder results in virtually no additional pressure rise since the fluid flows into the accumulator. The small fluid displacements involved in actuating the brake system permit a procedure by which a driver can rapidly push the brake pedal to the floor, dispensing the complete fluid volume within the master cylinder, thereby appreciating a fixed level of line pressure equal to approximately 101% of the nitrogen-precharge level. A small storage bottle of nitrogen is carried in the test vehicle, permitting the operator to adjust the braking level rather quickly, incrementing up or down in pressure level as necessary. A pressure transducer (potentiometer) was incorporated into this pressure-limiting device to record brakeline pressure levels.

2.2.3 AUTOMATIC CONTROLLER. Three automatic controllers were constructed simultaneously (under separate support from three companion DOT contracts*) and incorporated the basic elements contained in the original controller, plus additional

*These contracts were the following: DOT-HS-031-1-(159), -(126), and -(143).

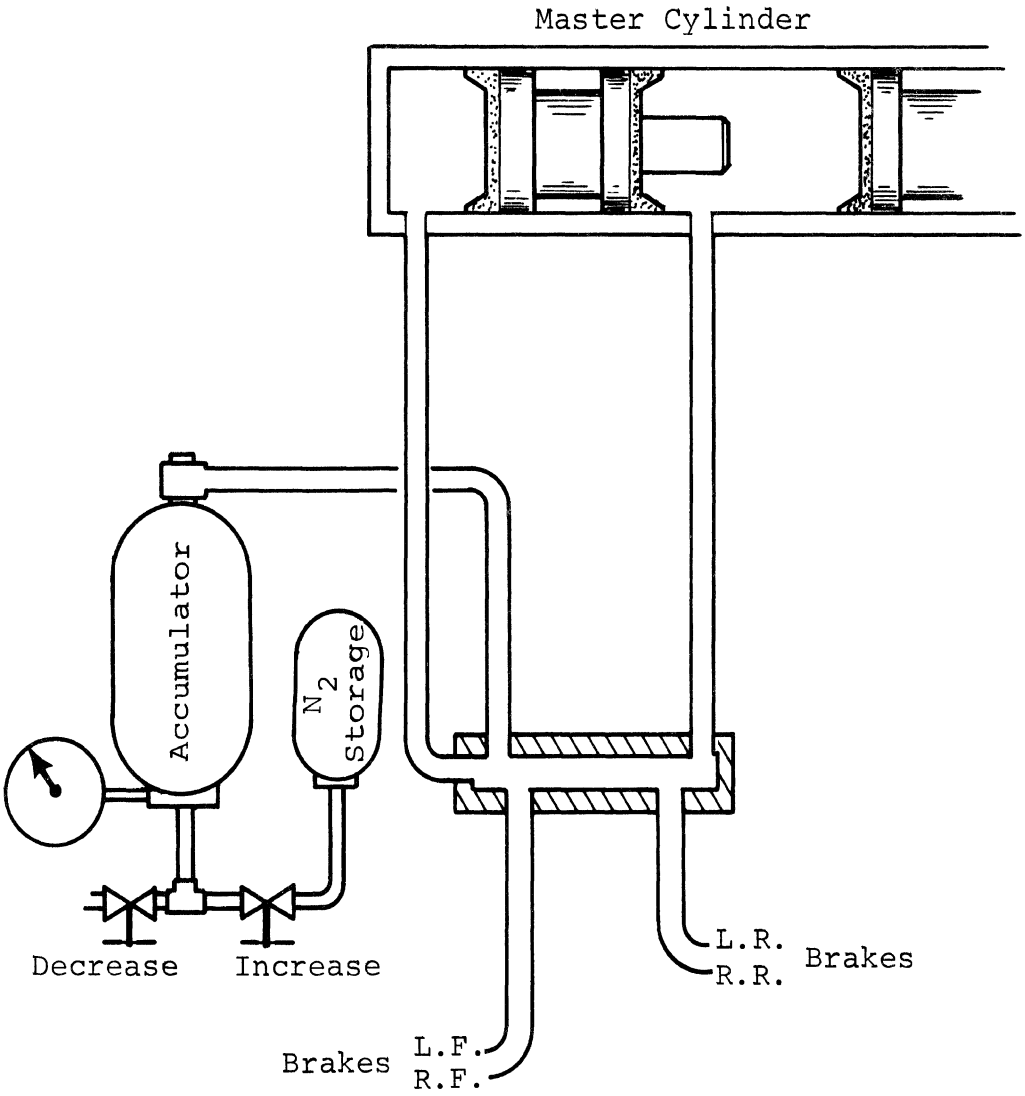

FIGURE 3

Schematic of Brakeline Pressure Limiting System

features deemed necessary to expedite the execution of this program.

The basic controller consists of three servomechanisms that respond to analog command signals deriving from a stored function programmer or by way of a radio link with a test operator. During test operations, the test vehicle is guided initially in a drone mode by an operator who is riding in a chase vehicle. With control stick command of steer, brake, and accelerator displacements, the operator manipulates the test vehicle to attain the appropriate velocity and spatial position to conduct the programmed maneuver. When the vehicle velocity matches a preset level, the programmed test begins, as does recording of the data in an on-board tape recorder. When the programmed maneuver is completed, the operator is again in control and guides the vehicle to a halt.

The following six major refinements were incorporated into the design of the new controller, thereby expanding upon the original concept to provide a test apparatus whose performance could be relied upon under a continuous testing routine:

1. A pressure-compensated, variable-displacement pump was mounted on the engine of the test vehicle to provide continuous hydraulic power, and thus a "continuous run" capability.

2. An abort-brake feature was made integral with the servo-brake actuator, thereby removing the earlier requirement for connections to brake-lines or master cylinder.

3. A fully solid-state, programmable function generator was designed, incorporating all system logic and program circuits on plug-in printed wiring boards. Quick adjust program selectors were provided to improve test efficiency.

4. Universal mounts were provided for the three servomechanisms to permit installation of the servo packages without requiring the fabrication of special brackets. (A typical installation is shown in Figure 4.)

5. A selectable high/low steering-gain adjustment was provided on the radio transmitter, permitting the test operator to control the vehicle adequately at high speeds (low gain) but still be capable of commanding large steer levels for "close quarters" maneuvering at low speeds (high gain).

6. Selection and control of the velocity to exist at the beginning of the test maneuver was provided by employing circuitry in which a preset value of velocity is compared with the velocity signal produced by a fifth wheel and the programmed function constrained to begin only when the compared difference passes through zero.

The detailed design of the automatic controller is presented in Appendix I.

In this program, the automatic controller was utilized to conduct three of the six vehicle handling test procedures in accordance with the findings developed in the exploratory experiments conducted during the pilot-test phase. In the full-scale test program, over 4500 programmed test maneuvers were conducted, using each of the three new controllers in rotation. On the basis of this test experience, a set of observations with respect to the facility and quality of vehicle testing with an automatic controller are set forth in Section 4 of this report.

Figure 4.

Servo actuators installed in a van-type vehicle

2.2.4 ADDITIONAL HARDWARE/INSTRUMENTATION REFINEMENTS. The following major hardware items were redesigned and constructed for use in this program:

1. A device (Fig. 5) that automatically provides a pneumatic lift of the fifth wheel whenever the vehicle spins to a large sideslip angle or lifts the wheel in response to driver command in the driver-controlled tests. In addition to the lift cylinder, a second pneumatic cylinder applies a brake to prevent the lifted wheel from articulating about its vertical hinge. This apparatus was found to be necessary to prevent the fifth wheel from being damaged during the spin outs that are frequently encountered in limit-response tests and during negotiation of the "rough road" course.

2. Universal-mount outriggers, for preventing vehicle rollover. This assembly was designed to provide weight and installation cost savings over the outrigger design used in the VHTP test program. Composed of struts fabricated from aluminum tubing and supporting spring-suspended caster wheels (Fig. 6), the assembly fits passenger cars of all sizes and is adjusted to touch the ground after 15° of body roll (Fig. 7). The outrigger weighs 88 lbs. and contributes 44.5 slug-ft^2 to the roll moment of inertia of the test vehicle.

3. Wheel rotation transducers utilizing photo-electric sensors providing a reliable inexpensive detector of wheel lockup occurrence. The transducers were configured such that the difference between the output signals from two photo transistors viewing the black/white mask on the wheel (Fig. 8) produced an oscillating square wave at a frequency synchronous with wheel speed.

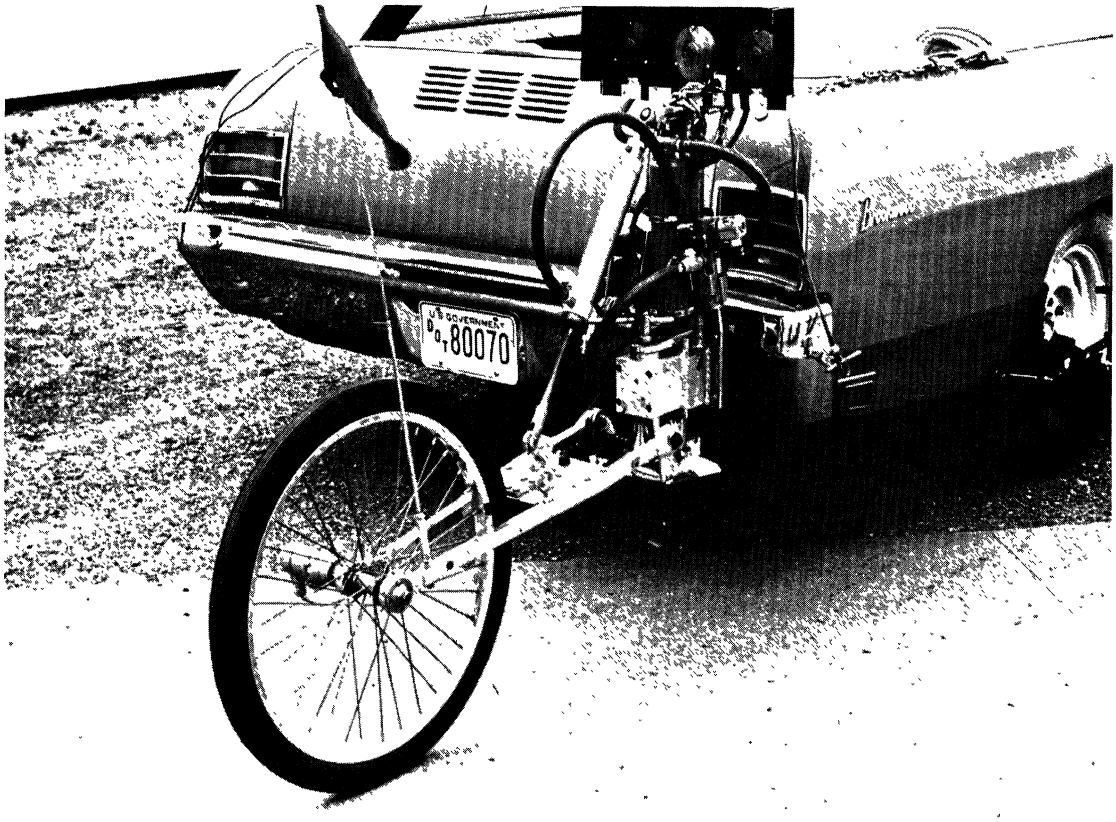

Figure 5.

Automatic lift 5th wheel assembly.

Figure 6.

Roll-restraining outrigger attachment

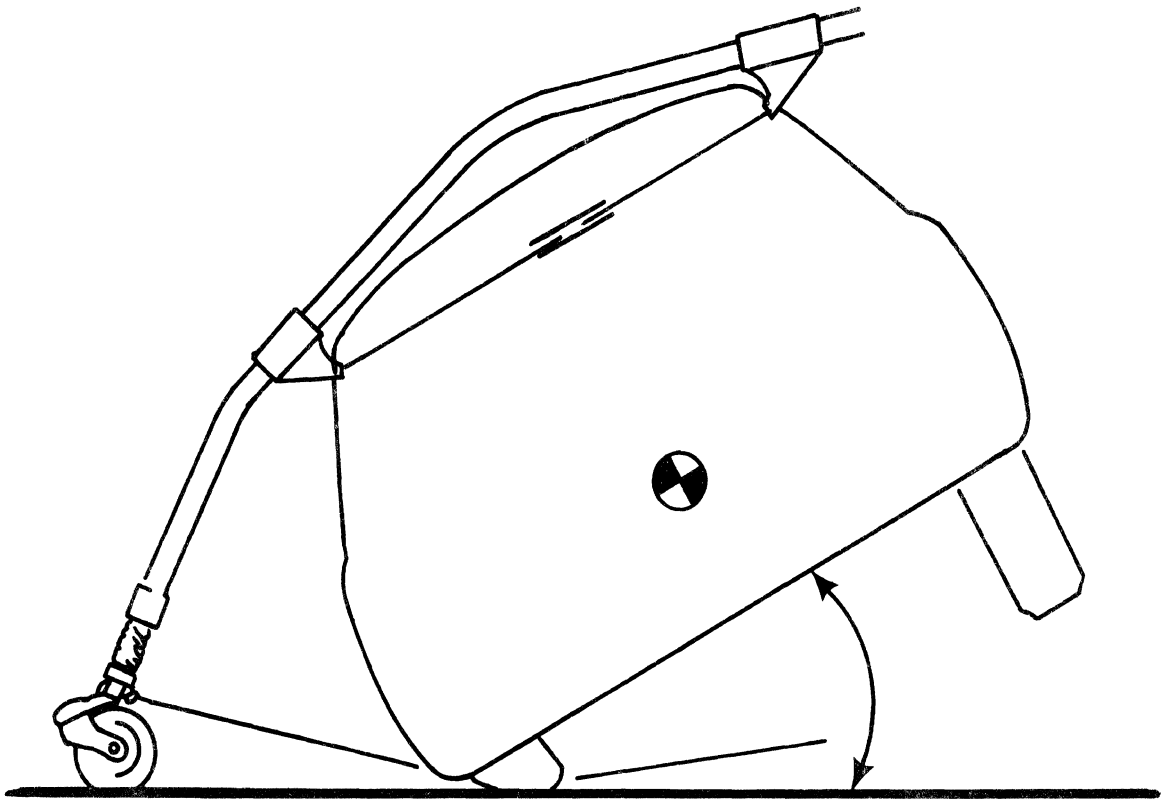

FIGURE 7

Outrigger Configuration for Rollover Restraint

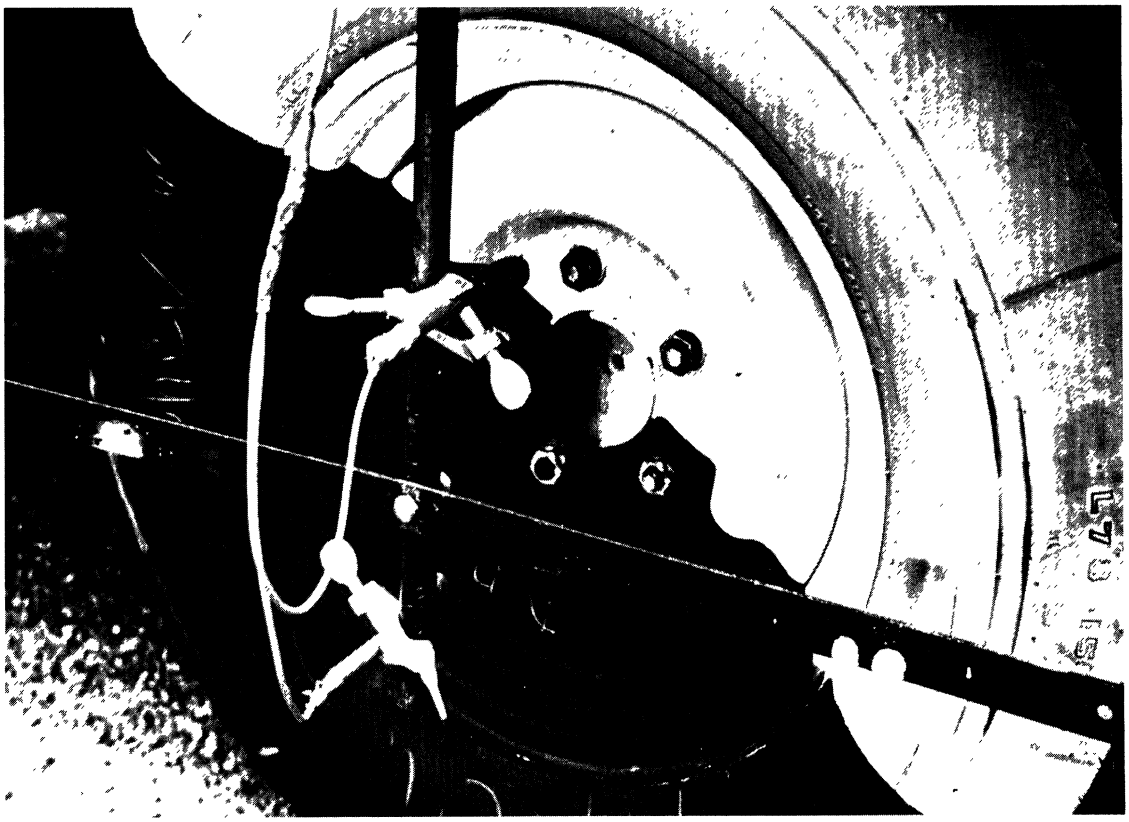

Figure 8.
Photoelectric wheel rotation transducer.

Refinements in data acquisition were made, constituting a significant improvement from the procedures used in the earlier VHTP program. In this program all of the response data were gathered on FM analog magnetic tape, thus providing the versatility and efficiency deriving from computerized data processing (see Section 2.4). Interface electronics were developed for scaling and calibrating the output of each transducer ahead of the tape recorder, and a control logic signal was provided to serve as a master reference for automatic processing of the data.

The test apparatus was assembled into two test "packages," one for the conduct of driver-controlled tests and the other for the automatically-controlled tests, thus permitting two parallel test activities to be maintained. Each package contained the following common elements:

- Automatic-lift fifth wheel
- Outrigger assembly
- Wheel rotation transducers (4)
- Gyro stabilized platform with accelerometers measuring A_x and A_y
- Yaw rate gyro
- Data interface module

The test package used in the driver-controlled tests also contained the following elements:

- Steer and brake limiter assemblies
- FM telemetry transmitter for remote data recording
- Power supplies
- Communications radio for coordination with the telemetry base operator. (In these tests, an FM telemetry receiver exists at a remote location with the test data recorded on FM magnetic tape.)

The automatic test package contained, in addition to the common elements:

- Automatic controller assembly
- Roll rate gyro
- FM tape recorder (on-board)

2.3 TEST PROCEDURE REFINEMENTS

Six basic test procedures were developed in the Vehicle Handling Test Procedures study [1], each directed towards assessing a specific performance property. Each of these test procedures involved control inputs or external disturbances selected to elicit a limit response, but which nevertheless were arbitrary and, in some cases, unsatisfactory. Accordingly, a Pilot Test Program was performed to examine potential improvements in procedural specifications. For each test, procedural modifications were examined by conducting experiments with a Ford Mustang outfitted for the driver-controlled maneuvers and a Dodge Coronet outfitted to perform the maneuvers conducted with the automatic controller.

In Appendix II, a complete specification for each test procedure is given, as refined through the pilot test program investigation, and later applied to the vehicle test sample in the full scale test program.

2.3.1 STRAIGHT-LINE BRAKING. This test involves the measurement of straight-line braking effectiveness. In the VHTP study it was performed at an initial velocity of 30 mph, with a program of brake inputs designed to permit a precise determination of deceleration achieved at the point of incipient wheel lock. In the pilot test program conducted in this study, tests were run to compare the relative merits of using 30 mph or 40 mph as the initial velocity. It was found that either initial speed could be consistently

achieved within 0.5 mph by having the driver apply the brake pedal, while coasting, when the velocity indicator crossed the desired value, thus eliminating a need for speed modulation.

The pilot tests indicated that the 40 mph test provided two significant advantages over the 30 mph test:

(1) a more severe test of the brake system performance is obtained because of the 78% increase in kinetic energy to be dissipated.

(2) An improved signal-to-noise ratio results with the higher initial velocity, from the viewpoint that a performance numeric is derived over longer stopping times.

Since the initial velocity of 40 mph could be achieved with precision comparable to that attained in 30 mph tests, the former was selected as the test procedure.

In addition to selecting the initial velocity, the pilot testing indicated that the lockup criterion (by which the sequencing of brake level is constrained) should be changed. The single-wheel lockup criterion, defined as the limit of controllable straight-line braking in the original VHTP tests, corresponds to a sublimit condition in those cases in which the prevailing level of brake imbalance may leave a substantial side force capability on the non-locked wheel of the same axle. Thus, the test procedure was changed to one in which brake levels would be incremented until both wheels on any axle were seen to lock prior to the vehicle attaining a velocity below 10 mph.

2.3.2 BRAKING IN A STEADY TURN. In the VHTP version, this test utilized the same procedure as the straight-line braking test, except the initial condition (instead of being a straight course equilibrium) was a 30 mph steady turn

producing a nominal lateral acceleration of 0.3g. Steering wheel displacement was held fixed throughout the maneuver.

Procedural refinements studied in the pilot test program included the examination of two initial velocities (30 and 40 mph) and two initial lateral accelerations (0.3 and 0.4g). It was found that each combination of these initial conditions could be performed easily, although the higher lateral acceleration imposed the burden of a substantially greater number of test runs. When this maneuver is executed with the initial value of A_y equal to 0.4g, in contrast to 0.3g, the lateral transfer of tire loading is increased by 33 percent, resulting in a wide band of pressure levels in which only the inside, unloaded wheels will lock. Further, in the 0.4g turn, the heavily loaded outside wheels require that a higher level of brake-line pressure be supplied to provide lockup of those wheels. A larger number of locked-wheel stops are required and presumably degrade the test procedure from the viewpoint of accelerated wearing of tires and increased testing time. Thus the 0.4g A_y test condition was considered undesirable, and the 0.3g initial condition was retained.

Braking from the higher initial velocity offered the same advantages observed in the straight-line braking tests and this observation led to the 40 mph initial velocity condition being selected for this procedure.

The pilot testing indicated a need for performing alternate left and right turns as a means of (1) balancing tire wear and (2) introducing the asymmetry factor* into the

*"Asymmetry" here refers to those differences in response which occur between left and right turning tests executed under the same nominal conditions.

basic measurement process, such that it may be either averaged out of the determined numeric or quantified as a stand-alone finding.

In view of the substantial load increase occurring on the outside tire in a turn, it is clearly inappropriate to constrain the incrementing of brake level by the obserance of single-wheel lockup. Although a substantial yaw disturbance can accompany the lockup of one unloaded wheel for certain vehicle configurations, this type of anomalous response is difficult to evaluate in the field. Thus, the procedure was structured to carry the sequence to an obvious limit condition—namely, two wheels locking on the front or rear even though a practical limit of controllability may have been reached at a lower level of braking.

2.3.3 TURNING ON A ROUGH SURFACE. In the VHTP study, the vehicle's ability to corner over a rough road was assessed by execution of a test involving steady turning over a disturbance grid whose fundamental frequencies of excitation covered the range of wheel-hop frequencies possessed by passenger cars. Whereas the previous procedure utilized three velocities over a disturbance array of fixed pitch to sweep frequency, a refinement was examined in which a constant velocity was used in traversing three different disturbance arrays. This refinement was motivated by the recognition that the concept of limit response, as applied to this test, involved an examination of resonance. The original procedure somewhat confounded the search for resonance, however, to the extent that both frequency and velocity were being varied at each condition, while the velocity change alone is known to have an effect on the side force output of the oscillating tire, as well as the magnitude of a yaw disturbance that might accrue over the fixed-length course.

In the VHTP study, the disturbance grid was constructed of 1 1/2 inch diameter steel pipe arranged parallel to one another at a nominal spacing of 4.4 ft. The grid elements adopted in this study were slabs of rubber tire tread stock, as first applied by the Cornell Aeronautical Laboratories [2] in similar test activities. These elements provide a "softer" profile to the tire (Fig. 9) and impose a relatively broad disturbance pulse on the vehicle compared to the 1 1/2 inch diameter elements used earlier. Three grid spacings were constructed, corresponding to excitations of 9, 11, and 14 Hz which frequencies span the range of typical wheel-hop frequencies with an approximately logarithmic distribution.

During the pilot tests, initial condition variables were examined, as was done for the two test procedures discussed above. Combinations of initial velocities of 30 and 40 mph (with grid spacings adjusted accordingly) and initial lateral accelerations of 0.3g and 0.4g were examined. It was found that the 40 mph test results in a dramatic attenuation in response severity in comparison to that resulting at 30 mph, apparently the result of tire dynamic factors as well as the reduction in test duration over a fixed-length disturbance grid. In running 30 mph tests at lateral accelerations of 0.3 and 0.4g, a substantial increase was observed in the relative disturbance occurring at the 0.4g level. Thus a 30 mph turn at a lateral acceleration of 0.4g over rubber strips, creating a road disturbance of 9, 11, and 14 Hz, was chosen as the revised procedure specification.

2.3.4 TRAPEZOIDAL STEER. This maneuver was originally called "Rapid Extreme Steering" or "Step Steer". It involved a rapid application of steering displacement up to a fixed level, following the removal of drive thrust. In the VHTP study, these maneuvers were conducted by a test

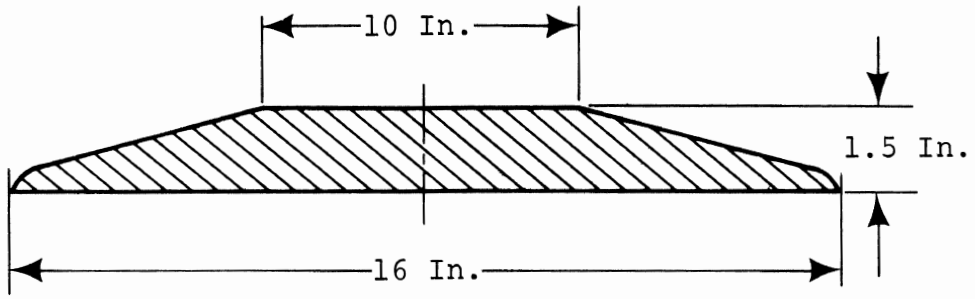

FIGURE 9

Cross-Section Through Rubber Tread Stock Elements

driver at an initial velocity of 30 mph. Alternate procedures were examined during the pilot test program of this study, in which the automatic controller was used exclusively.

A set of experiments was structured around a basic trapezoidal steer input definition (Fig. 10). The rate (or slope) of steer input was considered a control variable, as were steer level and initial velocity. Two sets of tests were run holding steer input ramp time and velocity fixed, while incrementing steer level. In the first set, with the initial velocity set at 30 mph and the ramp time set at 0.40 seconds, essentially overdamped time histories of yaw rate and lateral acceleration were observed with the test vehicle (Dodge Coronet) when the steering wheel was displaced over the following range of values:

$$\Delta_{SW} = N_g \times (4°), (6°), (8°), (12°), (16°), (20°)$$

Alternate left and right turns were made at each steer level, but no appreciable asymmetry of response was observed. A similar set of tests was made with the initial velocity equal to 40 mph. The same ramp time and steer levels were used. The results of this second test set showed comparable peak values of yaw rate and lateral acceleration, but the response of the vehicle was decidedly underdamped with significant overshoot of the quasi steady-state value. Also, the higher speed tests produced a substantial response asymmetry.

Tests were also performed to investigate the relative merits of using ramp time as an index variable for searching out the limit condition. Two sets of test runs were conducted with V_o = 40 mph and with steering level and ramp time adjusted as follows:

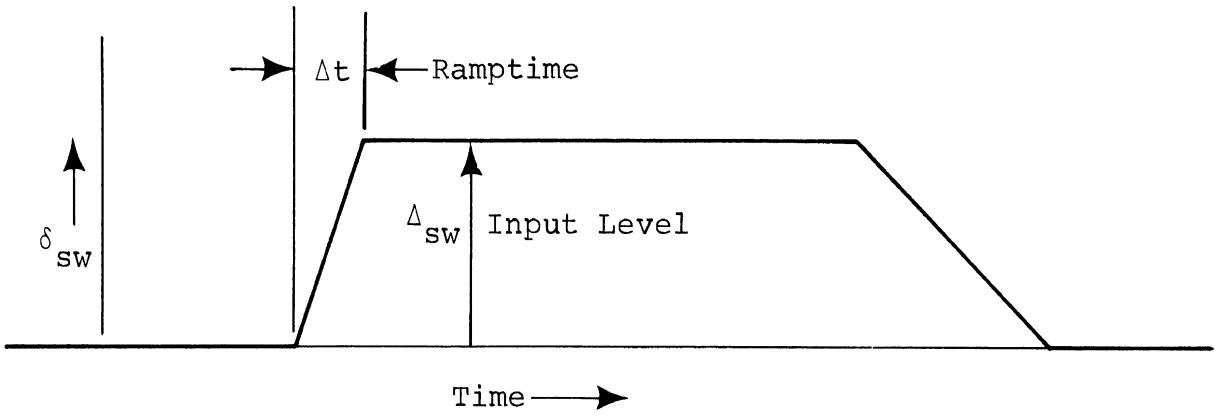

Figure 10.

Trapezoidal wave shape of steering input.

Set a: $\Delta_{SW} = N_g(8°)$

RAMP TIME, Δt = 0.2, 0.6, 1.0, 1.5, 2.0

Set b: $\Delta_{SW} = N_g(12°)$

RAMP TIME, Δt = 0.2, 0.6, 1.0, 1.5, 2.0

Both test series indicated that the peak values of yaw rate and lateral acceleration were generally insensitive to wide changes in ramp time. Although a longer delay was observed in attaining peak values of r and A_y with the longer Δt inputs, it was observed that the increase in both peaks, as obtained at Δt = 0.2 sec, was only about 7% greater than was obtained in the runs in which Δt = 2.0 sec. Clearly, the selection of ramp time as an index variable was unacceptable for the purpose of searching out limit performance.

Another set of runs was made with steer amplitude fixed at a large level, $\Delta_{SW} = N_g(16°)$, with the steering ramp time set to the relatively long interval of 1.5 sec. Velocity was indexed over a broad range (V_o = 30, 35, 40, 45, 48, 50, 52, 54, 56, 58, 60 mph) in an attempt to determine if any first-order change in the character of the vehicle's limit turn would derive from the level of initial velocity used in the test. The response data indicated a remarkable insensitivity to vehicle velocity at this high steer input level. Over the 30 to 60 mph range, peak (r) and (A_y) measurements remained within 10% of their values at 30 mph, although differences in the shape of the time history were observed as velocity increased.

On the basis of these pilot test findings, it was concluded that steer level was the appropriate index variable for this test and that the ramp time should be selected merely to represent an ergonomically reasonable value,

representative of the steering input rate that drivers might generate under emergency conditions.

After some deliberation, a constant delay time of 0.4 sec. was selected for use at all levels of steer input. It was rationalized that a constant delay time would provide for the lower steering rates that a driver would impose to reach low levels of steer displacement and the high panic rates which logically might accompany limit steering levels. The constant delay obviously forces a linear relationship between steer rate and steer level, but, for purposes of test simplicity, this selection appeared warranted.

An initial velocity of 40 mph was chosen for the trapezoidal steer procedure, constituting a compromise selection governed by the following major factors:

1. it was deemed desirable to employ a sufficiently high velocity such that 3 to 4 seconds would elapse before vehicle speed was excessively diminished, and,

2. the severe tire wear produced by this maneuver demanded that the velocity be minimized.

2.3.5 SINUSOIDAL STEER. This test was developed in the VHTP study to examine those vehicle response properties which might impose a significant challenge to a driver's ability to control the vehicle in an emergency lane change. It was hypothsized that the relative asymmetry of a vehicle's response to a symmetric sine wave of steering input would be representative of the degree of steer input asymmetry which a driver would be required to provide in order to assure a change of lanes with the final heading parallel to the initial heading. The original procedure involved the execution of a 2.0 sec period sine input of steering from a closed throttle condition at each of 4 initial velocities. Steering amplitude was indexed at each velocity level in a search for a limiting excursion in yaw response.

A considerable amount of pilot testing was performed to examine a group of widely differing test concepts with the objective of simulating an emergency lane change maneuver. The following sets of refinement tests were performed:

Set (a); Single sine waves were generated with 2.0 second periods, and amplitudes of $.5\Delta_{max}$, $.75\Delta_{max}$, and $1.0\Delta_{max}$ where Δ_{max} is the normalized steer amplitude defined as

$$\Delta_{sw_{max}} = 360 \left(\frac{N_g}{22.5}\right)\left(\frac{\ell}{10}\right)$$

Velocity was indexed through 30, 35, 40, 45, 48, 50, 52, 54, 56, 58, and 60 mph for each amplitude. This test series provided a dense matrix of runs with alternating left and right turns, in which increasing velocity generally results in greater asymmetry of vehicle response, producing a final heading other than the initial heading. In addition to asymmetry in the yaw velocity response, the test vehicle also exhibited gross differences in its response to a lane-change-to-the-left sine wave as opposed to a lane-change-to-the-right.

Sets (b) and (c): The design of these two test series derived from the recognition that the sine wave maneuver used in the VHTP study sacrificed realism in that the steer inputs were not constrained or normalized to provide a lateral displacement equivalent to a single lane width. The feasibility of developing such a normalizing scheme was examined in the pilot testing to be described below.

An analytical expression was developed relating the major variables of the sine-steer test to lateral displacement, assuming symmetry of vehicle response to steering and an absence of vehicle sideslip. The condensed form of this relationship is simply

$$\text{lateral displacement, } y = K \frac{T^2 V^2 \Delta_{sw}}{N_g \ell}$$

where

N_g = steering gear ratio

ℓ = wheelbase feet

T = period, sec.

V = velocity, ft/sec

Δ_{sw} = steering wheel angle

K = calibration factor

In order to utilize the above expression, an iterative set of runs were conducted at 15 mph, a speed at which a visual assessment of lateral displacement is feasible. The steering angle resulting in a 12-foot lateral displacement was experimentally determined for a sine-steer of 2.0 sec. period, yielding a value for the calibration factor, K. In test series (b), successive runs were made with steer amplitude fixed, varying velocity and period such that the expression remained satisfied for values of velocity equal to 30, 40, 45, 50, 54, 57, and 60 mph. A visual estimate of the lateral displacement was logged, and it was found that a gross attenuation of lateral displacement occurred with increasing velocity. Similarly, set (c), which exercised the same routine, with the exception that period was held fixed while solving the above relationship for steering amplitude at each velocity, showed a severe attenuation in lateral displacement response over the velocity range. The set (b) results ranged from 12 feet to about 2 feet while the set (c) results ranged from 12 feet to a few inches of lateral displacement being achieved at velocity levels ranging from 15 mph to 60 mph. These findings indicate a very strong role being played by dynamic factors and slip phenomena. The

conclusion was that the resolution of an effective normalization scheme for maintaining equivalent displacement criteria in the selection of inputs was beyond the scope of this program.

Set (d): Double sine waves, of the "over and back" variety, were examined. (See Figure 11.) When a single sine wave of steering was applied to the test vehicle, overcorrecting responses were generally obtained. That is, in a lane change to the left, the vehicle would overcompensate in the second half of the sine wave, bringing the vehicle to a terminal heading off to the right. Whenever "over and back" steer was applied, it was observed that the second steer cycle further exaggerated the asymmetry produced by the first wave, resulting in a rather ridiculous trajectory. It appears that the steer input consisting of a double sinusoid is not a viable procedure for open-loop testing. Without loop closure, the propagation of response asymmetries over long periods provides results which simply delay interpretation.

Set (e): A run was selected from the set (a) data and repeated in set (e) with increasing levels of corrective steering following the first sinusoid until the lane-change was observed to approximate a symmetrical trajectory (see Figure 12). The test procedure, as executed, requires careful observation and estimation on the part of the test operator, who must iterate to achieve the proper corrective input. Although the procedure was performed, it was judged to be unacceptably cumbersome and subjective.

As a result of the above-described experiments, it was decided that lane change performance was still best examined by means of single sine wave steering with velocity and amplitude variable. It was concluded that sine steer

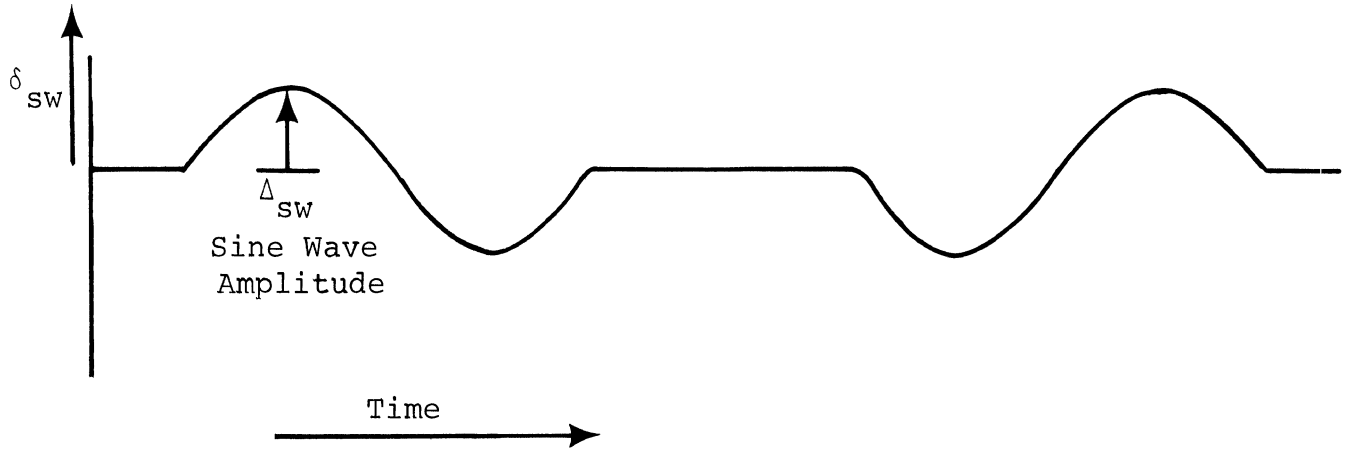

FIGURE 11

Double Sinusoid Waveform of Steering Input

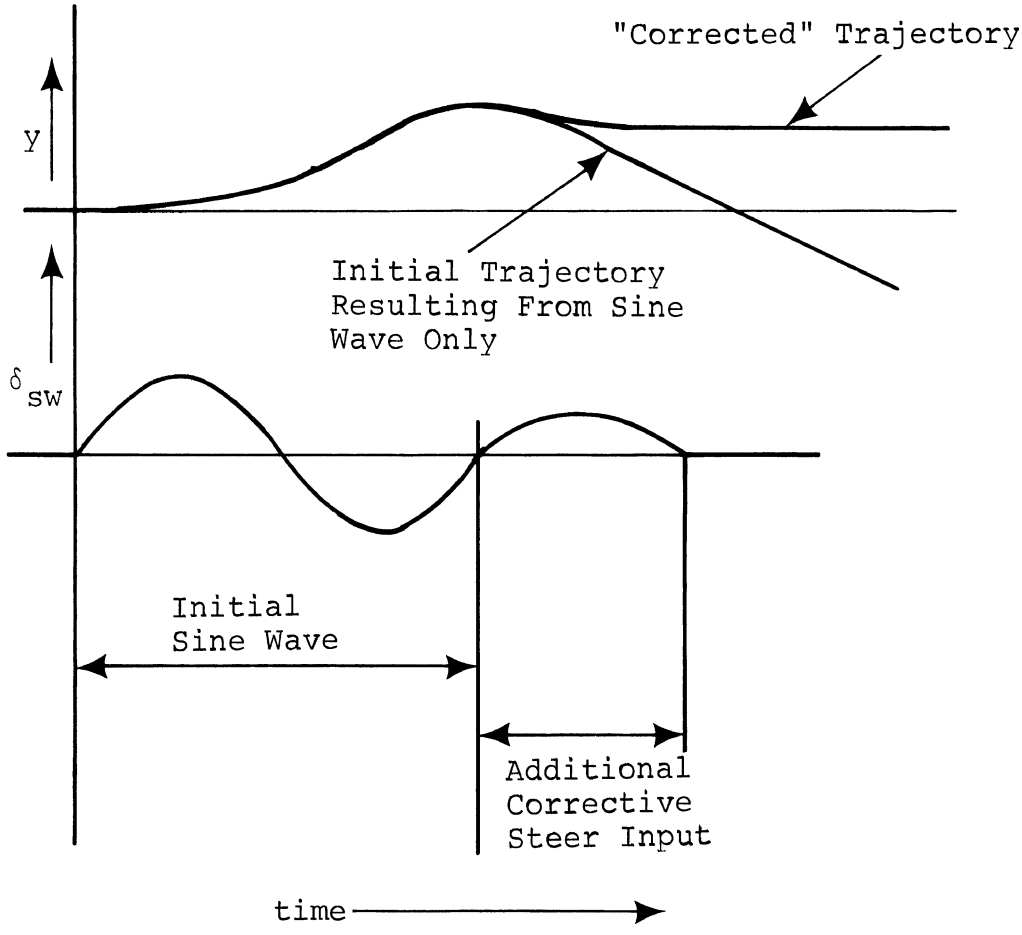

Figure 12.

Corrective steering inputs were added to the basic sine wave shape to force symmetric trajectories to result.

tests would be run at each of two initial velocities, 45 and 60 mph, with the amplitude of the sine wave determined by the following relationship:

$$\delta_{sw} = \frac{66}{V} \frac{\ell}{10} \sigma N_g$$

where σ = 2, 4, 6, 8, 12, 16. By means of this relationship, steer amplitude could be constrained to encompass the range of levels required to provide a lane change. (The relationship between the factors, V, ℓ, and N_g is determined on the basis of the kinematics of steady turning.)

In addition to the findings developed in the above summarized sets of tests, an observation was made relative to the control of test conditions for the sinusoidal steer maneuver. In the presence of a 20 mph wind, having a component of 12 to 15 mph normal to the vehicle's path, eighteen runs were made with the Dodge, using initial headings that alternated by 180 degrees and applying precisely the same sine wave steer input each time. (The velocity was the same in all runs.) Heading angle deviations with the wind from the left ranged from +26° to +92° with a mean of +51°. With identically the same inputs but with the wind from the right, measured deviation in heading angles ranged from -15° to +8°, with an average of -10°. Thus it appears that the lateral wind loading on the subject vehicle caused by the defined wind conditions can alter the asymmetry of its response to sinusoidal steering over a range at least equal to half of the range of the observed means, or 30 degrees. The large scatter attained is presumably the result of the nonuniformity of the wind conditions prevailing throughout the test series. This finding is admittedly crude, but it has serious implications with regard to the constraints that should be placed on the atmospheric conditions existing during open-loop testing.

2.3.6 DRASTIC STEER-BRAKE. This maneuver was developed to impose the maximum challenge to a vehicle's roll stability that could be derived solely from tire-road shear forces. The maneuver, as originally developed, involved a test sequence in which a half sine wave of steering is followed by a brief pulse of braking such as to cause the vehicle to attain a large sideslip angle and at the occasion of brake release, realize a virtual step input of side force.

The single anticipated refinement to the basic procedure developed in the VHTP study involved a tuning of the brake release time such that the resulting step input of side force (and thus roll moment) would coincide with the occasion of maximum roll angular momentum (Fig. 13), which timing would theoretically cause a maximum overshoot of the roll transient to occur. In the single series of tests that were executed to examine this concept, the soundness of this principle was indicated. In a later set of runs, however, it was observed that tuning brake release to coincide with the peak roll rate was not necessarily the singularly worst case under all conditions. Since roll motions are determined by the complex interaction of both nonlinear dampers and nonlinear springs (in the proximity of bump stop contact), there can apparently exist arrangements of characteristics which yield a larger roll rotation response when the brake release is timed to coincide with the peak angle achieved during the natural transient motion.

A set of drastic steer-brake runs was made in which brake-off times were varied over a range of 500 milliseconds. Starting with the timing in which brake release coincides with a sympathetic roll rate peak (referred to as t = 0 in Fig. 14), the peak value of roll angle attained following brake release was seen to increase to a maximum at t = 0.400 seconds and then fall off as the critical timing was

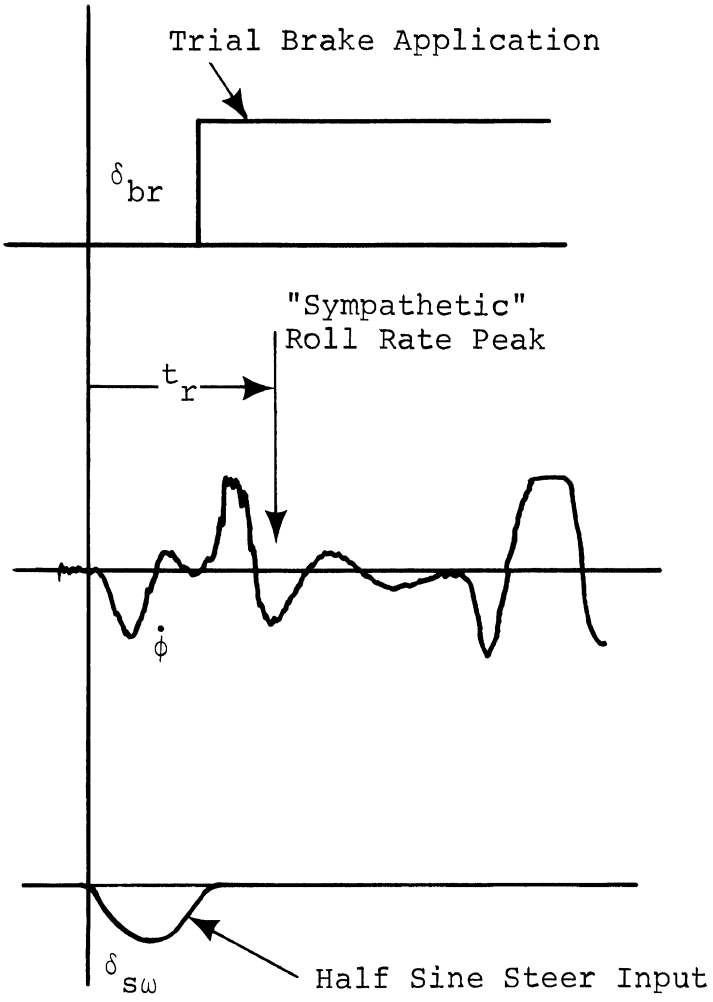

Figure 13.

At time t_r, the release of the brake input will cause the side force step to coincide with the occasion of maximum roll angular momentum.

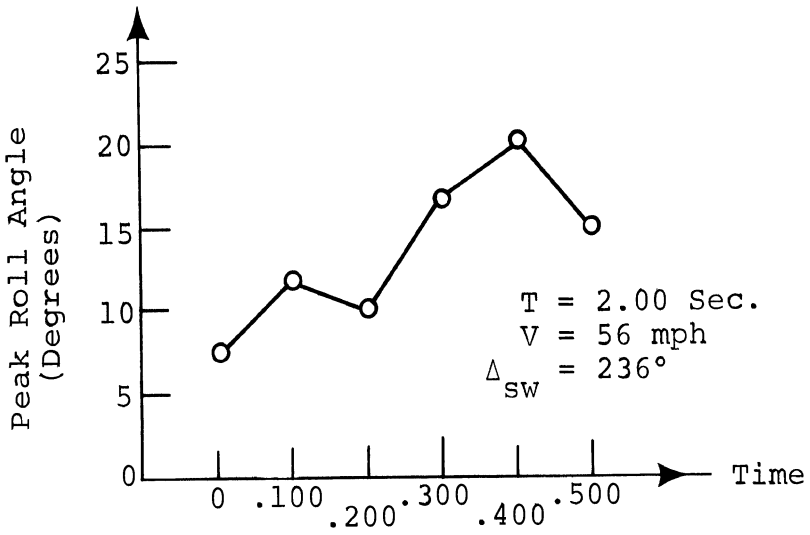

Figure 14.

Peak roll angle was seen to increase when brake release time was delayed as shown.

exceeded. These findings indicated that the refined procedure should include runs to be executed with brake release occurring both at the instant of peak roll rate and peak roll angle, such that the maximum possible roll response would be attained irrespective of the particular sensitivities of each test vehicle.

For reasons not altogether clear, the Dodge Coronet and certain other vehicles have shown an increase in the peak roll response produced in drastic steer-brake maneuvers as initial velocity is increased. Since it is generally true that tire shear force potential decreases with increasing velocity, the generality of this finding is

doubted. Nonetheless, it was concluded that the drastic steer-brake procedure should be executed at initial velocities of 50 and 60 mph.

2.3.7 REDUCED FRICTION COEFFICIENT TESTING. In addition to the experiments conducted to refine the test procedures developed earlier, a set of experiments was performed during the pilot test program to investigate the feasibility of providing an acceptably consistent low friction surface as a test condition.

Since the asphalt skid pad facility constructed at TTI for this program was intended from the beginning to provide as smooth and homogeneous a test surface as can be provided to accommodate large turning maneuvers, extreme care was taken in both the engineering and construction phases. Nevertheless, variations in surface elevation on the order of 3/8" are encountered regularly across the pad in the vicinity of the joints that are produced by each pass of the paving machine. Thus, when performing wet test experiments, it was not altogether surprising to record water depth measurements which ranged from less than 0.010 inches to greater than 0.100 inches. These measurements were made with a NASA-developed instrument utilizing a cluster of machined translucent prisms to probe depth levels to a least count of .010 inches. The depth measurement variations which cycled every 8 to 12 feet laterally, in the proximity of the paving matrix joints, also varied monotonically in relationship to the elapsed time between passes of the watering truck at any given location.

Since the large lateral excursions produced in open-loop handling experiments are not constrained to follow a prescribed trajectory, it becomes necessary to wet vast areas of test surface to account for both the undetermined and sequentially-indexed path curvature responses as well as the

longitudinal or "down range" uncertainty existing with respect to the precise location of maneuver initiation. As an example, the trapezoidal-steer maneuver requires a minimum rectangle having dimensions of 300 ft. down range and 200 ft. in the lateral direction. To wet this area once requires a minimum of 7 to 10 minutes with one watering truck. Since the natural percolation of the delivered water accomplishes the bulk of the level seeking within one minute of the passage of the spray bar, however, the surface becomes segregated into zones of significantly varying water depth long before the next test run begins.

Water depth variations of the order measured on the TTI skid pad facility are shown in the literature to have a profound influence on tire-road friction properties [3, 4]. Data presented in Reference 3 indicate that, at test velocities of 40 mph, normalized peak longitudinal force could be expected to vary from .55 to .7 and normalized peak lateral force from .35 to .65 with water depths ranging from .010 to .080 inches. At 60 mph, normalized peak longitudinal force shows a spread ranging from classic hydroplaning values (near 0.10) to a level of .60, while lateral force data illustrates an even greater sensitivity to water depth, with values ranging from near zero (full lift hydroplaning) to about .55, within the .010 to .080 inch band of water depths. Although the above-cited findings have not been obtained on actual road surfaces and thus should be considered as being valid primarily for demonstrating trends, the basic scaling has been corroborated by other investigators (e.g., see Reference 4) whose measurements have been made with tire force measurement trailers operated over paved road surfaces.

On the basis of the above observations, it appears that conducting open-loop turning maneuvers on large wetted surfaces does not constitute a viable method for establishing a data base of low coefficient limit-turning performance.

While this conclusion has profound implications on the comprehensiveness of the vehicle handling safety assessment that can be derived from open-loop vehicle testing, a broader view of the problem indicates a lessened impact from this finding. It can be argued that vehicle limit performance on low coefficient surfaces, below 0.4, is so overwhelmingly a matter of tire performance that little reason exists, conceptually, for confounding the examination of the tire/vehicle system performance in this regime by full scale testing of the vehicle. This matter will be treated again in Section 4 of this report.

2.3.8 TIRE SURFACE FRICTION STUDY. In the review of certain data generated during the pilot test program, large variations in peak lateral acceleration response were observed which could not be explained. It was hypothesized that such changes in peak acceleration performance could only be attributable to variation in friction properties at the tire-road interface. Recognizing that consistency of friction condition was critical to the viability of limit maneuver measurement, a substantial effort was undertaken to identify causes of the variation and to determine compensating test practices. The findings resulting from this investigation are presented in detail in Appendix III, and are summarized in this section.

The study concentrated on the investigation of certain tire properties which were felt to be potentially culpable factors in the variation phenomenon. Utilizing experiments with the HSRI Mobile Tire Tester, and full scale vehicle tests, the influence of four test condition variables on peak tire side force capability was examined.

1. Tire tread wear, as derives from the conduct of limit turning tests.

2. Drying time, as it affects the recovery of "dry pavement" friction properties following a rainfall.

3. Test surface temperature.

4. Test surface material.

A remarkable finding related to the influence of tire shoulder, or buttress, wear on peak side force capability was made during Mobile Tire Tester experiments and correlated with vehicle experiments. On certain tires it was found that side force improves dramatically as the buttress first begins to wear and eventually achieves steady-state at a normalized force level that can be as much as 40% higher than in the unworn state. In Figure 15 is shown the results of tire wearing tests performed with the Mobile Tire Tester on tires representing original equipment for the vehicles in the full scale test program sample. The indicated ranges of normalized side force measurements were made with each tire loaded to approximate the respective vehicle-imposed loads on the outside tires in a limit turn. All tires were operated at 20° slip angle and subjected to a series of test runs to obtain the performance bands indicated. Other data in Appendix III indicates the degree to which this wear sensitivity is correlated by vehicle test, in addition to providing measurements indicating the yaw-destabilizing influence of higher front tire wear rates during limit turning experiments.

The principal conclusion from these findings was that further refinement of test practice was necessary to minimize the otherwise inevitable degradation of cornering test results with non-steady tire side force output. A process was outlined by which sets of test tires would be worn in by preliminary limit cornering tests of sufficient number as to assure the achievement of steady-state performance. Although this procedure is clearly an artificial alteration of tire properties, it was deemed to be the only recourse for the

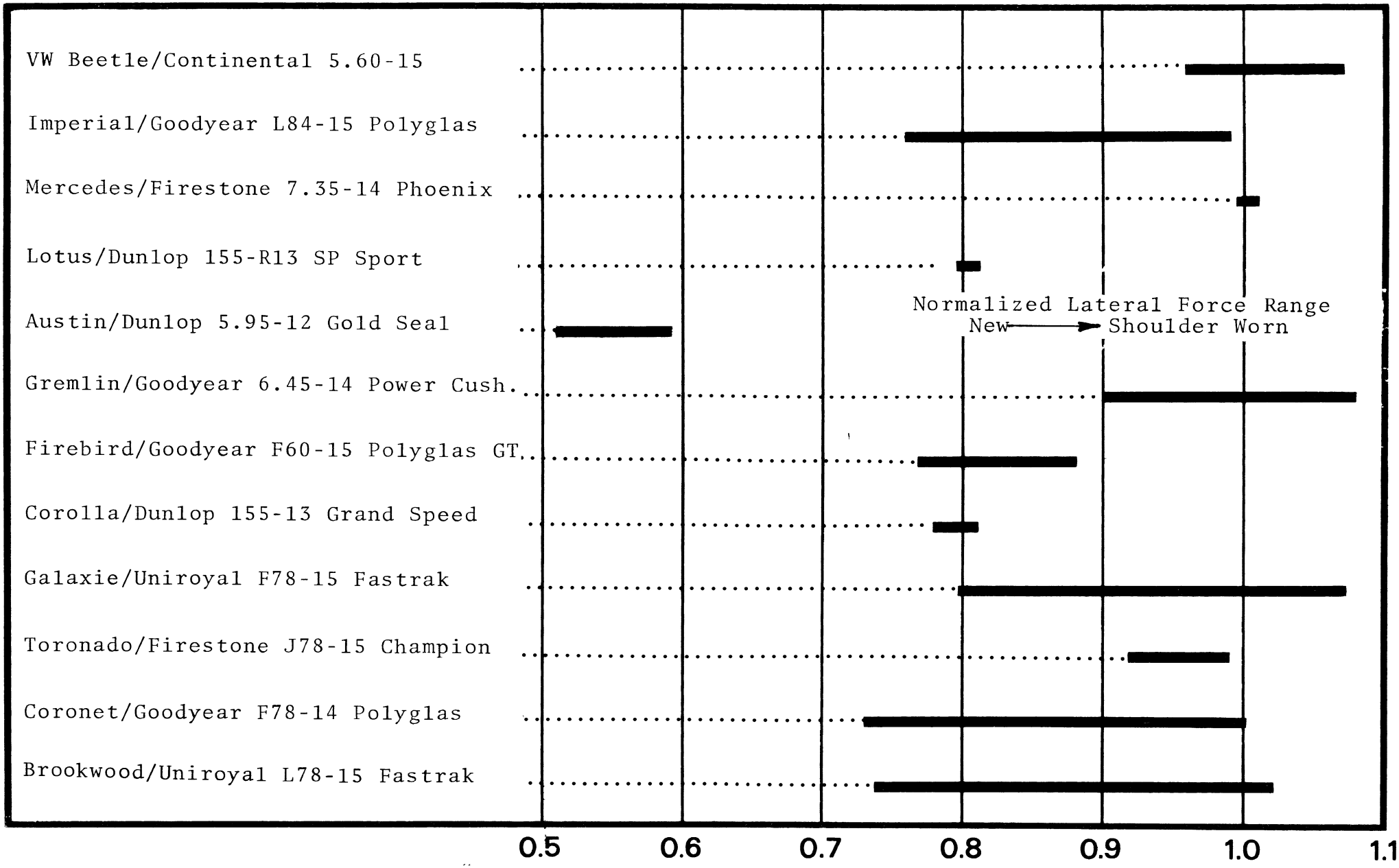

FIGURE 15
Normalized Lateral Force Range - Tires were run on a mobile tire test device gathering side force data as shoulder wear accumulated.

purposes of obtaining the vehicle performance data base in this study. An obvious philosophical conflict arises, however, in attempting to label the nominal condition of the data base experiments. They do not literally represent original equipment performance, nor do they necessarily represent a condition of usage which vehicles would be expected to exhibit in any normal driving mission. Further discussion of these matters is presented in the Conclusions and Recommendations section. It suffices here to summarize that a first-order source of vehicle turning response variability was identified, and that a compensating test practice was adopted, in an attempt to assure data consistency.

With regard to the three other potential sources of variability, data is presented in Appendix III indicating that

a) "dry pavement" friction properties were recovered following wetting of the asphalt test pad, as soon as the surface "appeared dry", that is, no perceptable darkening was noticeable in comparison to the dry "control" surface,

b) no monotonic effect on tire side force or vehicle limit turning capability is seen to derive from large changes in test surface temperature, over the range investigated,

c) no specific repeatability advantages were identified for a concrete surface compared to asphalt, in any of the experiments regarding tire wear or surface temperature.

Thus no refinements in test practice were found necessary in relation to the temperature, drying time, and surface material factors.

2.4 DATA PROCESSING REFINEMENTS

During the original VHTP study, raw data was recorded on light-beam oscillographs mounted in the test vehicle. Data processing and analysis was limited to visual interpretation of oscillograph traces: reading peak values of a given response variable, detecting values at critical points, etc. Such data processing and analysis is most laborious and thereby discourages efforts towards making a more sophisticated evaluation of time histories or towards performing continuous mathematical analyses.

In this program, major refinements in data processing were accomplished by resorting to analog magnetic tape recordings and computer analysis of these recordings. These changes led to the development of an efficient and flexible system for processing the raw data, eliminating the manual element as well as providing for the computation of other response variables. Detailed information on this data processing system will be found in Appendix V.

The tape-recorded data obtained in both the driver- and automatic-control test series were given identical formats to facilitate data analysis. The automatically-controlled vehicle tests employed on-board data recording whereas the data produced by the driver-controlled vehicle was transmitted via telemetry to a base station (see Fig. 16). Scales for each of the recorded variables were established during the pilot test program as guided by experience gained in the previous VHTP study.

The recorded raw data signals, as generated through an interface module (see Appendix V), were processed on HSRI's hybrid computer system (Fig. 17). Significant features of this data processing system are itemized below:

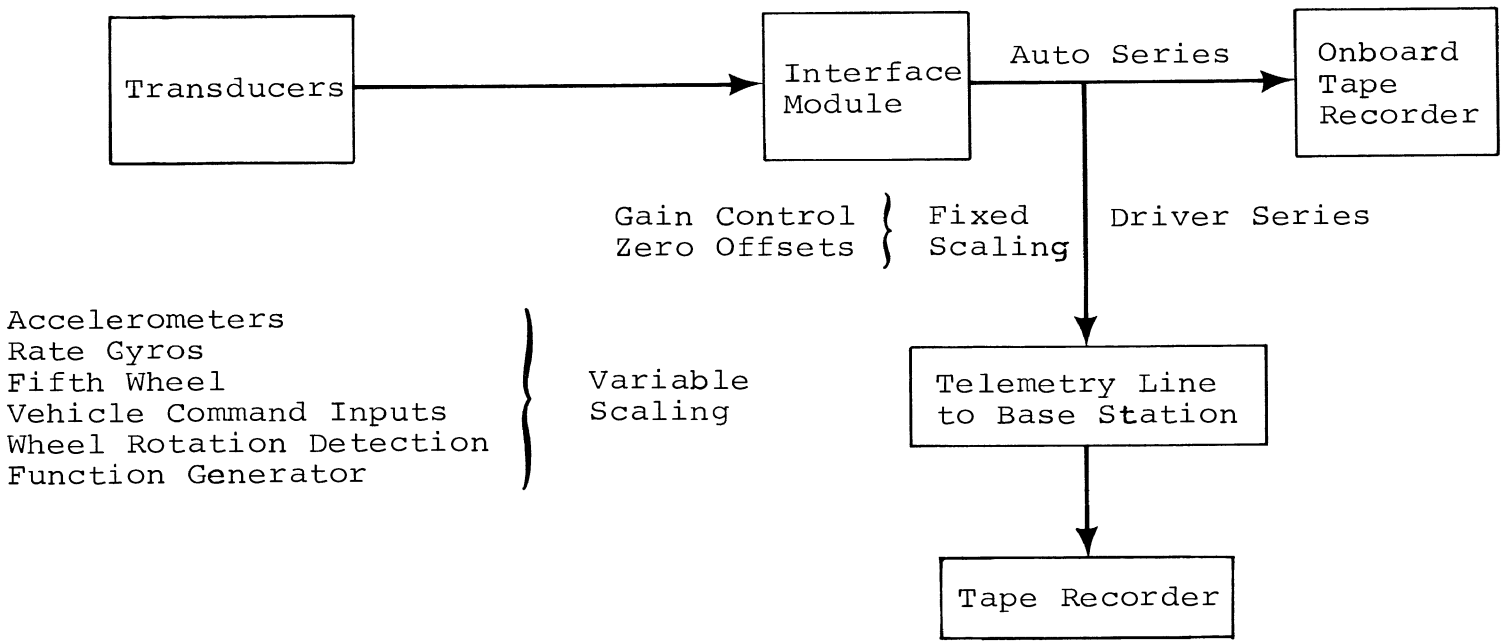

FIGURE 16

Data Acquisition System - Block Diagram

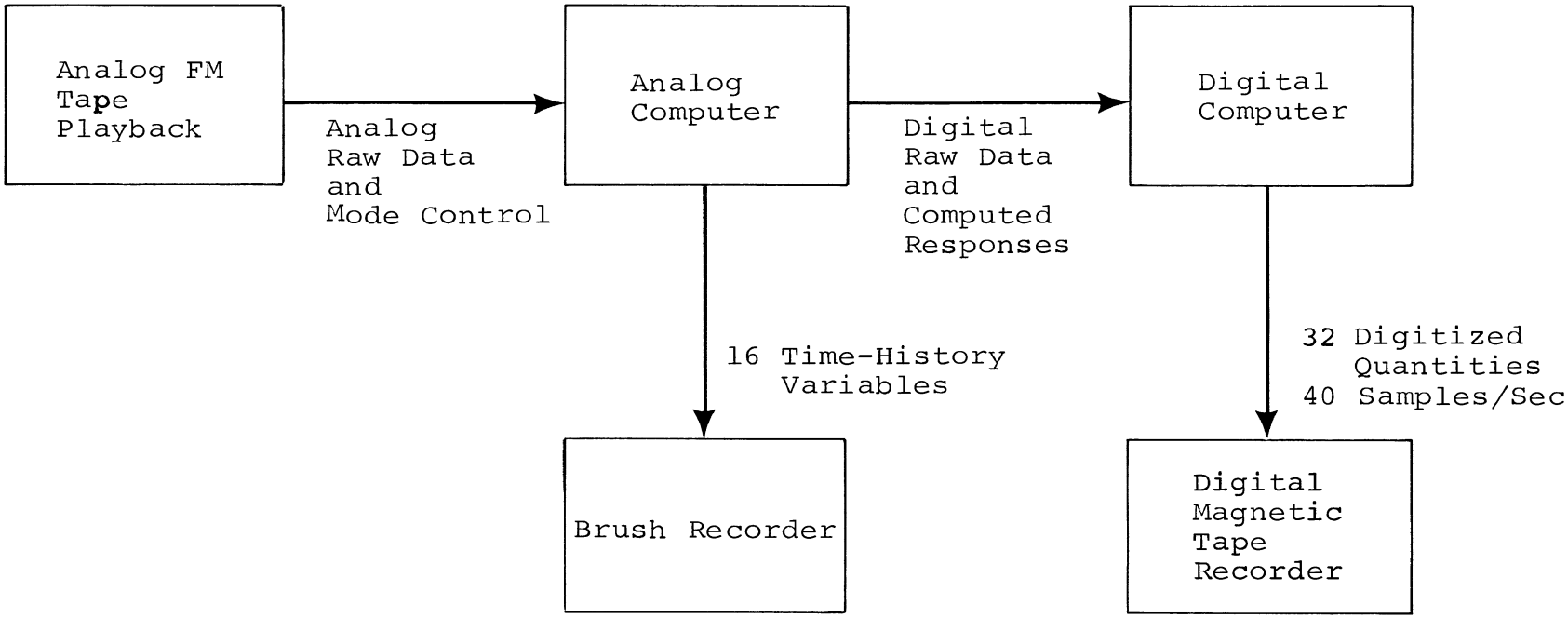

FIGURE 17
Data Processing System - Block Diagram

1. A mode-control signal was generated in the interface module to indicate the various calibration modes and test execution modes. The hybrid computer in operating on these signals automatically scaled for gain and nulled any zero shifts prior to making further computations.

2. The raw data signals were processed through analog circuits that represented the simple kinematic relationships required to determine the sideslip response and spatial trajectory of the test vehicle on a continuous basis.

3. The raw data signals and the computed variables were digitized for storage on digital magnetic tapes. These digital tapes form a library of the time histories produced in each test run performed on every vehicle tested in this program.

4. Using the digital tapes, further processing of all data was effected by computing response numerics for each test. With the aid of a variety of digital algorithms, the unwieldy time history format was reduced to a few numbers for each run, indicating the most significant properties of the vehicle's response.

5. A variety of output formats either exist or can be generated at will—the digital tapes mentioned above, pen-recorded analog traces of raw and computed variables, and digital listings.

2.5 VEHICLE PERFORMANCE DATA PRESENTATION AND INTERPRETATION—REVIEW AND REFINEMENTS

In many disciplines, the presentation of test data requires merely that the experiment be defined and the measured variables identified. In the context of acquiring measures of vehicle handling performance deemed to be safety relevant, data presentation itself lies at the heart of the problem. In addition to selecting limit maneuvers and the test procedures associated therewith, it is desirable that the data produced in these maneuvers be processed and presented so as to enhance both their meaning and relevance to safety issues. Without a relationship between performance measures (or performance numerics) and accident statistics established from research studies, the vehicle dynamicist and the test engineer must necessarily resort to pragmatism and intuition to derive data presentations which are interpretable in the safety context.

Each of the open-loop maneuvers, as finalized during the pilot testing conducted in this study, was re-examined with respect to refining limit maneuver performance numerics and their presentation format. This refinement is discussed herein, together with a discussion of the philosophical base upon which the relationship to safety is hypothesized. It must be emphasized that these hypotheses involve the identification of the relative safety quality of certain response categories and that absolute judgments with respect to safety are not offered.

It should be noted these refinements derive from the development of new concepts for evaluating vehicle response as well as from data processing developments which currently provide response variables previously unavailable.

2.5.1 STRAIGHT-LINE BRAKING. As in the VHTP study, maximum deceleration, wheels unlocked, has been identified as the principle performance measure of interest in this test. Data will be presented in the form shown in Figure 18, with distinctions provided for those runs which resulted in lockup of two wheels on the same axle. It is hypothesized that the occurrence of this condition represents a safety-relevant limit to the controllable range of straight-line braking, because of:

a) the absence of steering control which accompanies the locking of both front wheels, and

b) the classical directional instability which accompanies lockup of both rear wheels.

The ordinate variable, "average longitudinal acceleration," is a digital average of the longitudinal accelerations produced over the time span during which the vehicle slowed from 35 mph to 10 mph. This velocity "window" is chosen to avoid the complications resulting from variabilities in initial velocity and brake-pedal application rates at test initiation and to eliminate the influence on average deceleration that derive from the increase in braking effectiveness occurring at low rubbing speeds between lining and drum/disc. This latter effect is of concern because it tends to bias upward the average deceleration performance of a motor vehicle without contributing significantly to minimizing stopping distance.

2.5.2 BRAKING IN A STEADY TURN. Three data plots have been developed for presentation of vehicle response in this maneuver. The first plot, shown in Figure 19, is identical to that used to demonstrate straight-line braking effectiveness. The two other presentations, Figures 20 and 21,

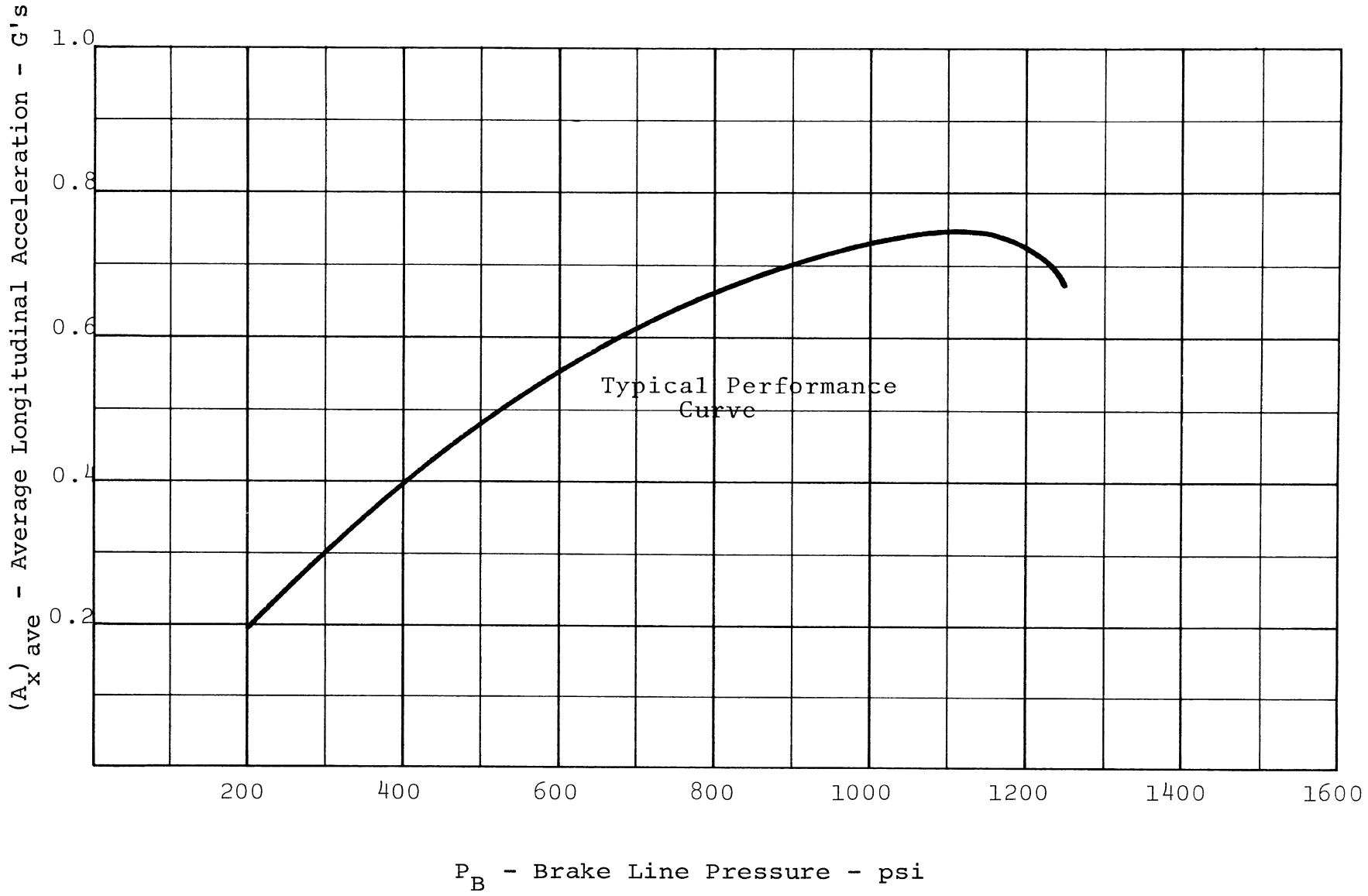

Figure 18. Straight line braking plot format

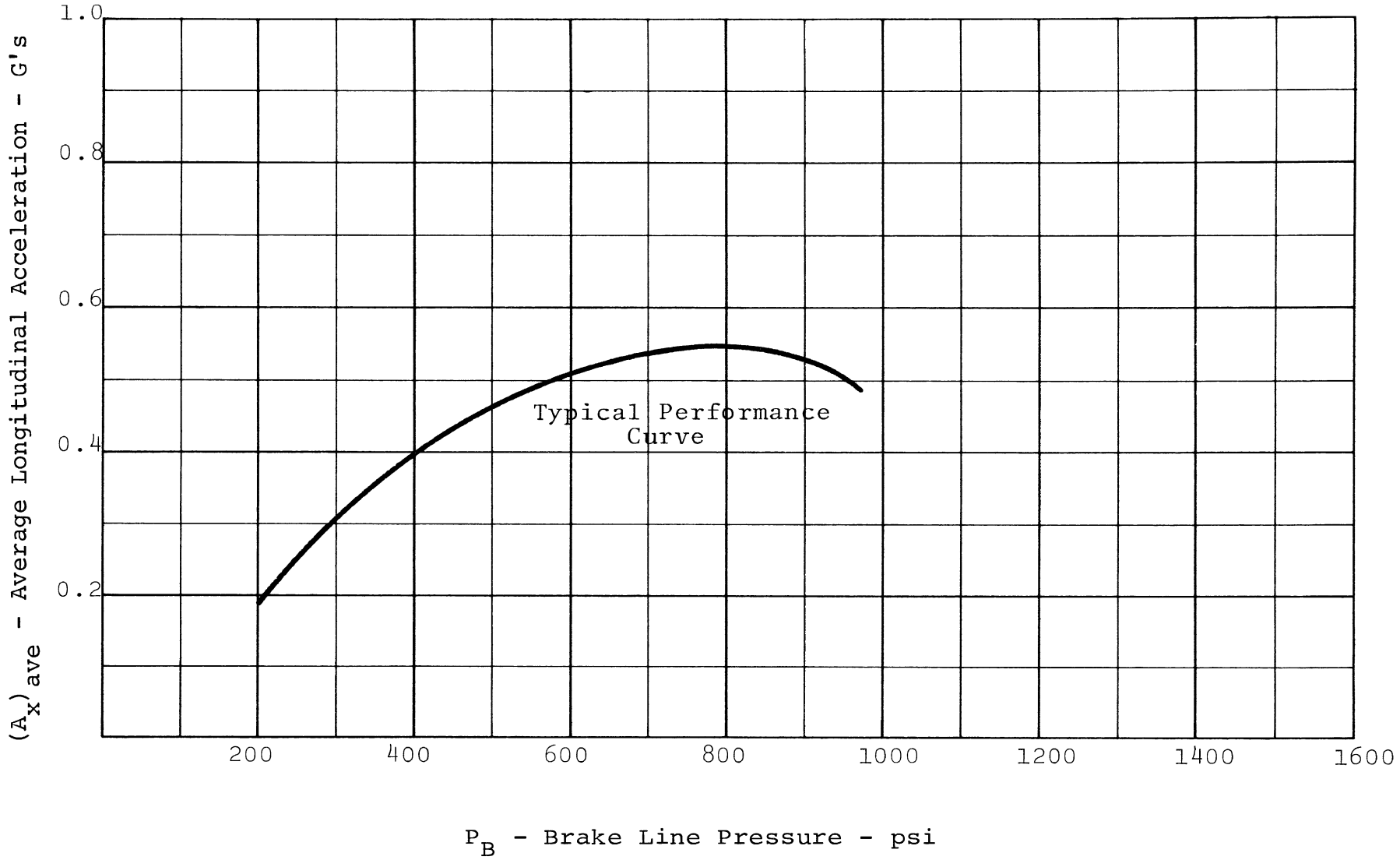

Figure 19. Braking in a turn plot format

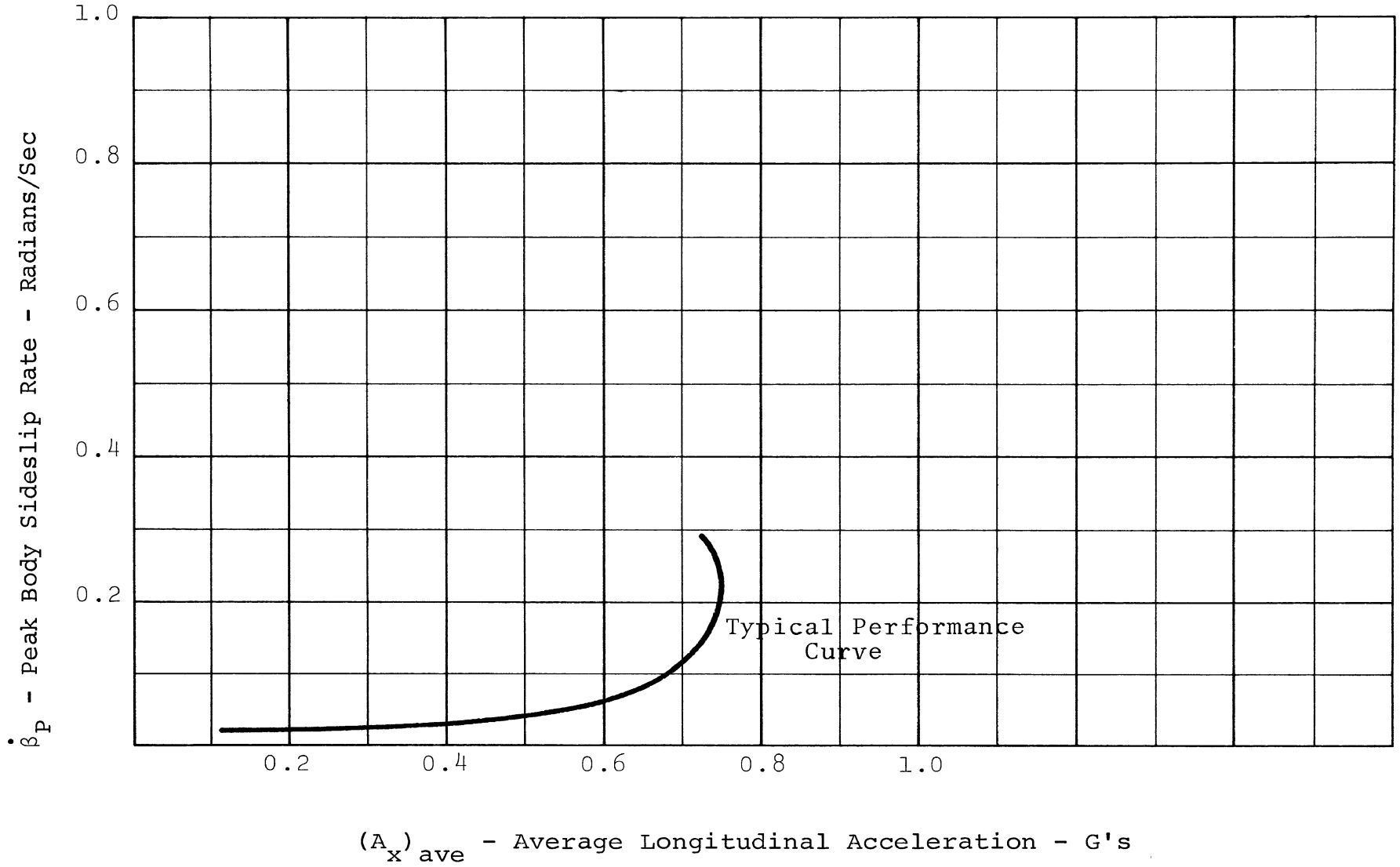

Figure 20. Braking in a turn plot format

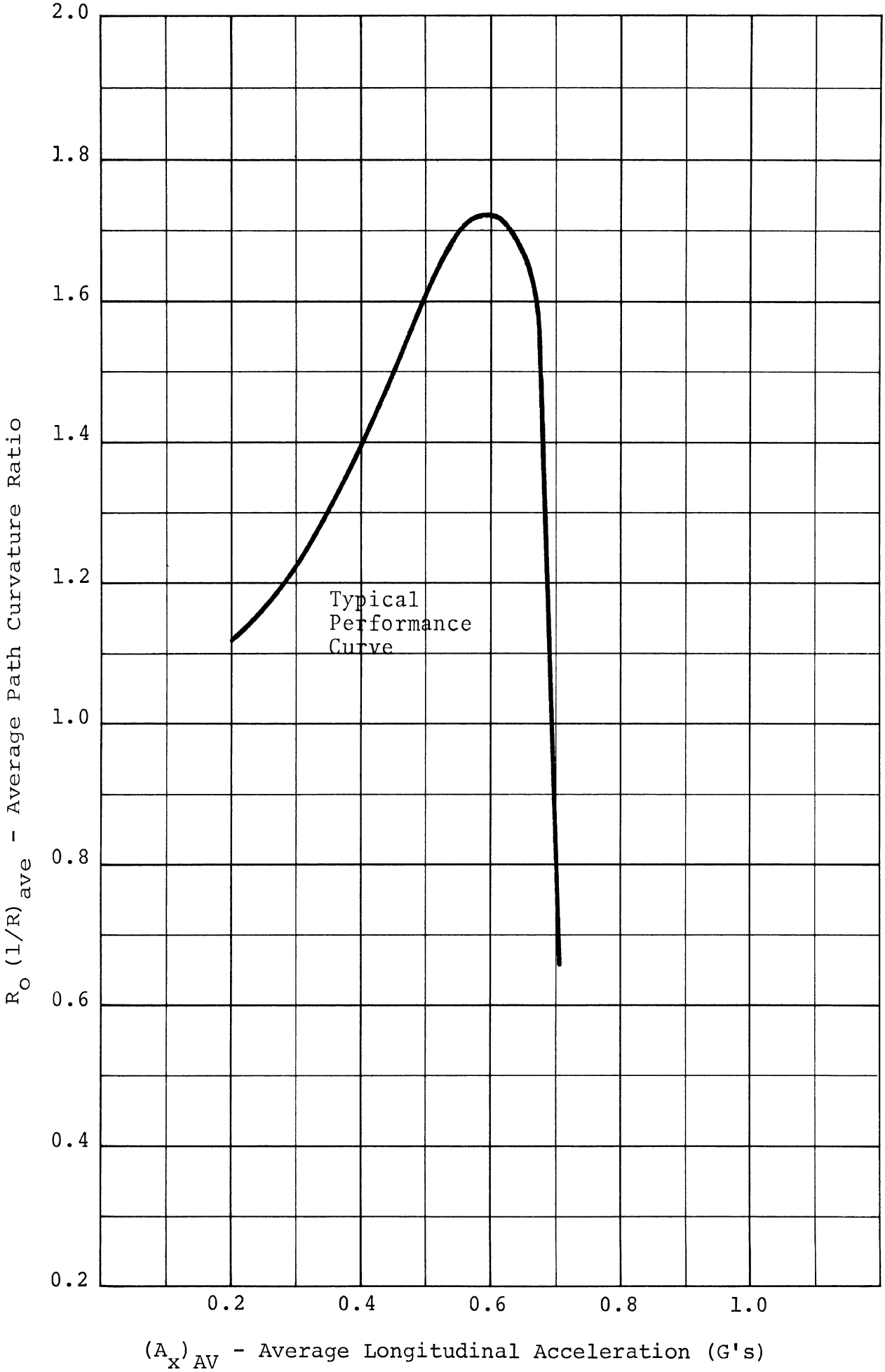

Figure 21. Braking in a turn plot format

represent turning response evaluations that have been made possible through the determination of vehicle sideslip and path-curvature time histories by computer processing.

Note that the subject maneuver involves an initially curved path whose curvature can change as a result of braking. It is argued that drivers do not apply braking with the intention of effecting a change in directional response. Consequently, an interpretation scheme is needed which comprehensively describes the properties of a turn such that deviations from the initial turn can be recognized and evaluated. Thus, the data presentation is structured to detect deviations or changes from the initial condition, which change drivers would have to recognize and accompany with a steering correction.

An ideal directional response is defined for this maneuver to be a constant path radius (or curvature) trajectory, over which the vehicle maintains a zero value of sideslip angle. (These response variables are diagrammed in Figure 22.) It is postulated that the ideal turn definition, expressed in these terms, represents a comprehensive manner of viewing directional response in this or any turning maneuver.

The sideslip response, β, is felt to be of major safety significance. It is argued that excessive sideslip responses, as occur under limit maneuvering conditions, disorient the driver with respect to the normal view of his vehicle's path, and cause the vehicle to project a larger target for collision in the roadway. The rarity of emergency maneuvering events suggests that driver adaptability under such circumstances must derive from talents other than those attainable from learning (trial and error) experience. Thus the analog or continuous measurement of sideslip angle and sideslip rate is looked upon as representing an error quantity which imposes

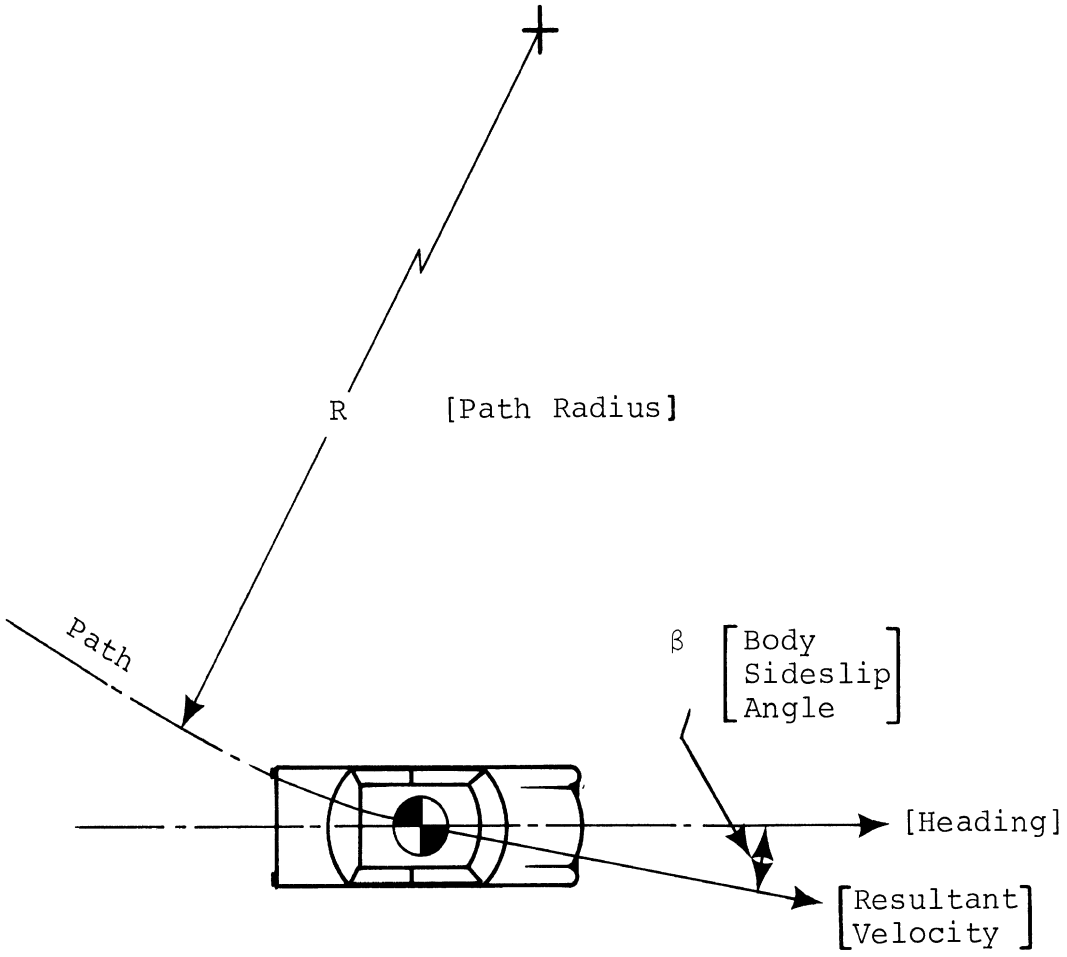

FIGURE 22
The Sideslipping Vehicle in a Curved Path

a monotonically increasing challenge to the human controller to close the loop. Note that the path curvature measure provides a single quantity characterizing the curvilinear trajectory without introducing any ambiguities in the measure due to a simultaneous sideslip response. In the VHTP study, yaw rate and lateral acceleration measures were used, with these variables becoming uninterpretable under conditions of severe sideslip response.

Figure 20 presents the peak rate of change of sideslip angle that obtains when braking in a turn as a function of average deceleration. Although peak sideslip angle also would be of interest here, poor accuracy is obtained in computing sideslip as velocity goes to zero. Nevertheless, in this shortlived maneuver, it is felt that both β and $\dot{\beta}$ each reflect the same phenomenon, with $\dot{\beta}$ being a substantially more sensitive measure. This measure will readily characterize the limit performance of vehicles which exhibit lockup of rear wheels prior to lockup of front wheels.

Conversely, locking of front wheels prior to rear wheels is characterized by a loss of path curvature which loss is indicated by a sharp decrease in 1/R in Figure 21. The ideal value of normalized path curvature response, defined as the average value of path curvature ratioed to the initial steady turn value, would be 1.0, indicating that no directional adjustment would be required due to braking.

2.5.3 ROADHOLDING IN A TURN. In the VHTP study, the roadholding performance of a vehicle traversing a simulated road disturbance was characterized in terms of yaw rate and lateral acceleration change ratioed to the initial turn values. Since this experiment has a direct analogy to the braking-in-a-turn test, it was determined that a comparably refined data presentation be employed. The encounter of a road

disturbance in an initially steady turn can be viewed in the same terms as was brake application in a turn, with directional response variables, sideslip angle and path curvature, constituting comprehensive descriptors of vehicle turning behavior. Figures 23 and 24 show these directional response variables plotted versus the test index variable—road roughness frequency. Specifically, Figure 23 presents a normalized average path curvature, defined as the average value of 1/R (computed over the 1 second traversal of the disturbance grid) ratioed to the initial value of 1/R. For vehicles which suffer a heavy loss in tire side forces, this quantity will indicate a tangential departure from the hypothetical roadway by registering values of normalized path curvature near zero.

Figure 24 presents peak sideslip rate plotted versus disturbance frequency. In both the roadholding maneuver and the braking-in-a-turn test, the $\dot{\beta}$ measure is used for its ease of computation and in recognition of its sensitivity as an indicator of directionally unstable responses. For vehicles which become heavily destabilized, with a large yaw moment imbalance relative to yaw moment of inertia, an excursion in $\dot{\beta}$ will be seen very quickly, whereas the sideslip response (the integral of $\dot{\beta}$) is slower. Thus the crucial question "has the vehicle reached a limit of performance?" can be best anticipated through examination of the sideslip rate.

These reflections are the basis for making certain choices in data presentation of vehicle response properties, but they do not address the more difficult matters of driver sensitivity to sideslip response. It is not suggested here that further research will find drivers to be equally sensitive to sideslip acceleration, rate, and angle. On the contrary, it is suspected that quite different driver response

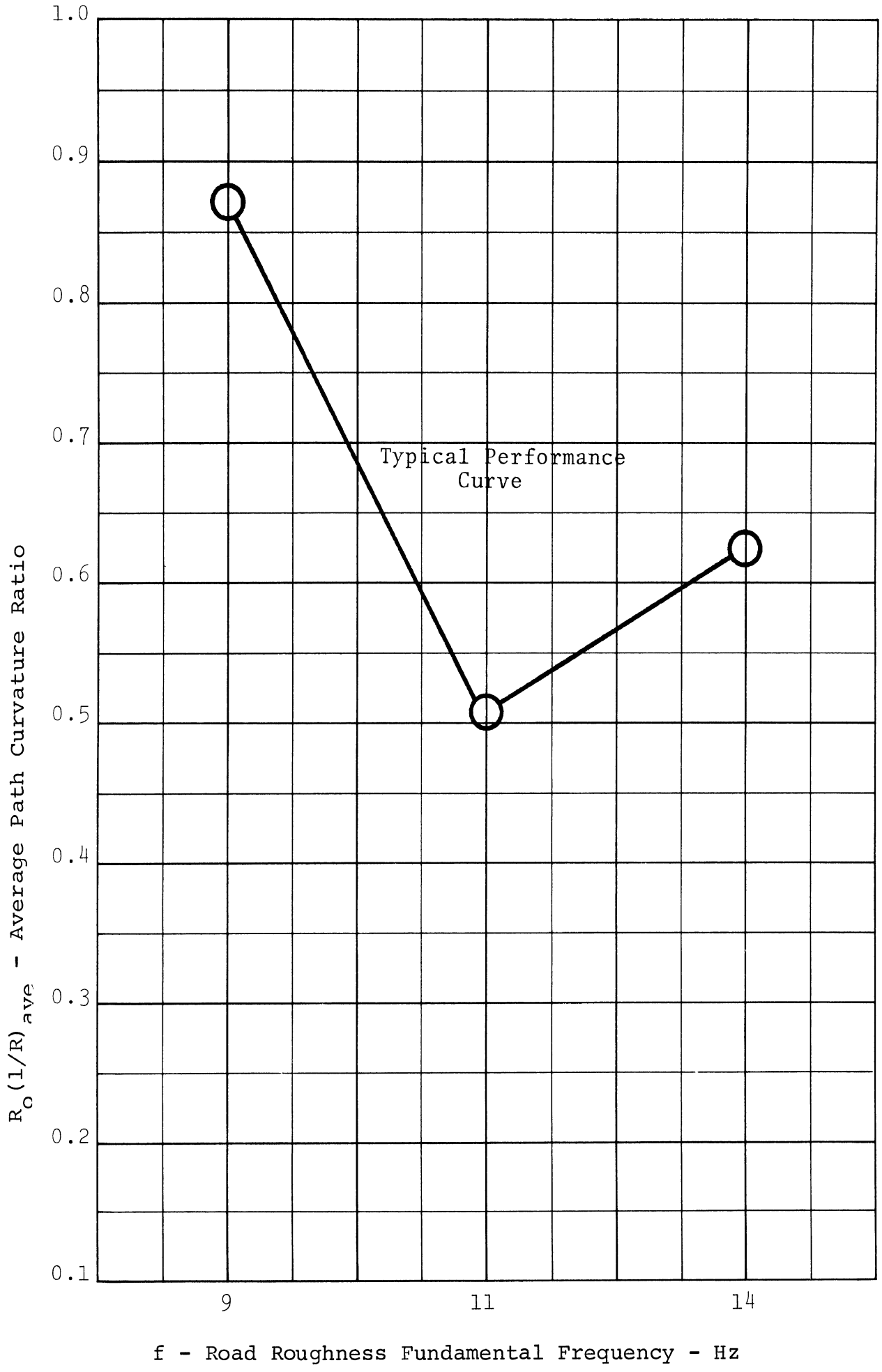

Figure 23. Roadhonding in a turn plot format

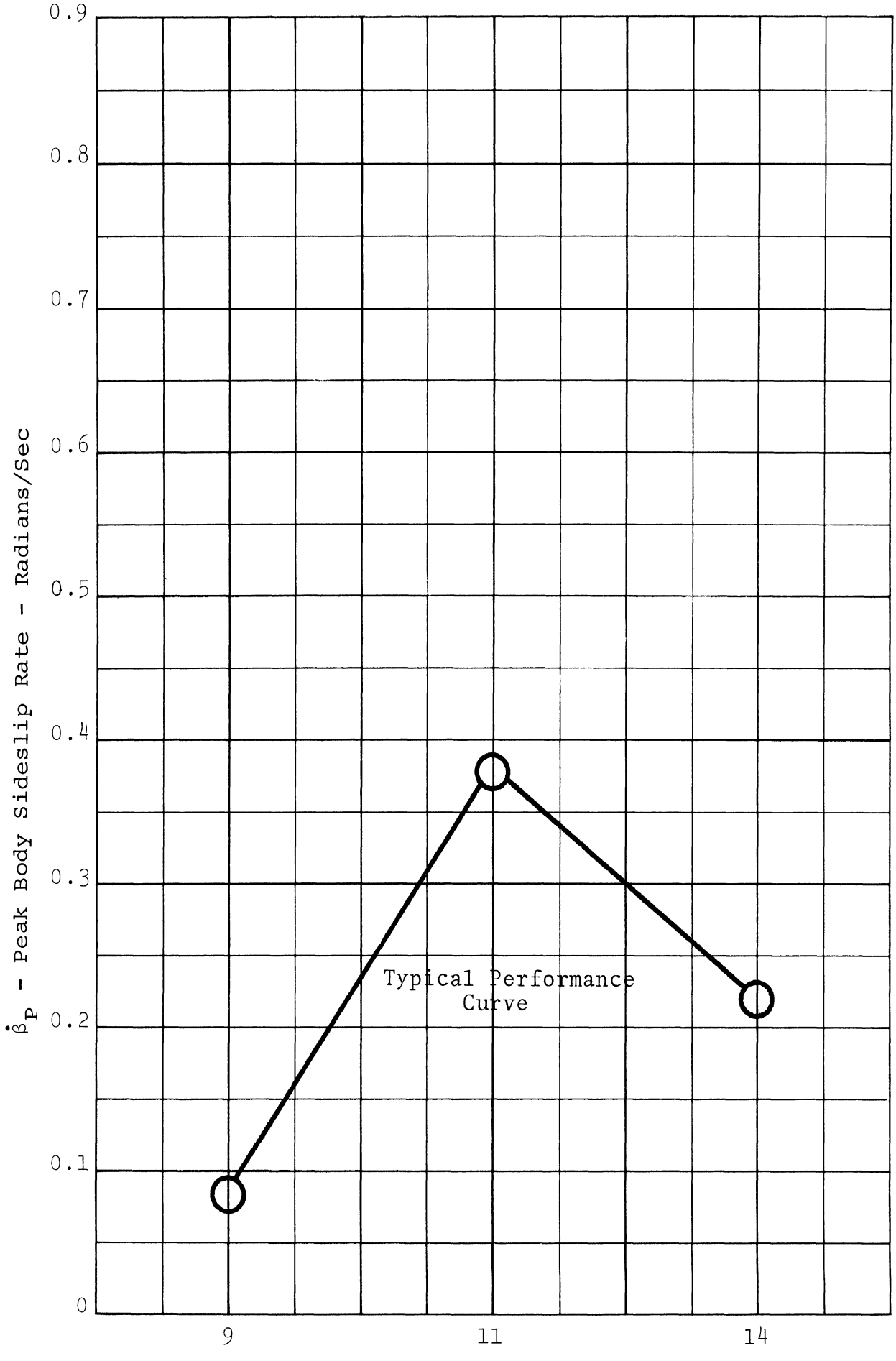

Figure 24. Roadholding in a turn plot format

mechanisms may apply to each derivative. Nevertheless, we submit that an equal treatment of each derivative can be useful, if one will accept that the various driver sensitivities to sideslip will at least be monotonic, i.e., "more is worse" in a safety sense. For example, in the Figure 24 presentation of peak $\dot{\beta}$ response to road roughness, the supposition is that large $\dot{\beta}$ is indicative of a vehicle property which imposes more challenge to the driver (than less), and that large β's could be expected to follow if the destabilized condition were allowed to persist.

2.5.4 TRAPEZOIDAL STEER. This maneuver results in a J-turn trajectory which is not representative of any realistic highway maneuver but does, nevertheless, provide the conditions appropriate for examination of the transition from straight-line motion to limit turning, such as may occur in the initial phase of an obstacle avoidance maneuver. The effectiveness with which a vehicle performs an obstacle avoidance task in an emergency, as a result of a steering input, would seem to be determined by the ability of the vehicle to achieve lateral displacement in a controllable manner. As a consequence of having non-steerable rear wheels, the motor vehicle achieves lateral displacement only by means of a curvilinear trajectory. It follows that a characterization of the curvilinear path produced by a rapid steering input can serve as a measure of the obstacle avoidance capability of a motor vehicle.

In the VHTP study, data obtained from the so-called "step steer" test were presented in the form of peak values of lateral acceleration and normalized yaw rate. It appears that a better measure of turning performance is given in Figure 25. Normalized path curvature, $R_s(1/R)_{ave}$ is obtained from a digital averaging of the path curvature time history over a 2-second period following the initiation of the steer trapezoid. By the averaging process, the measure combines

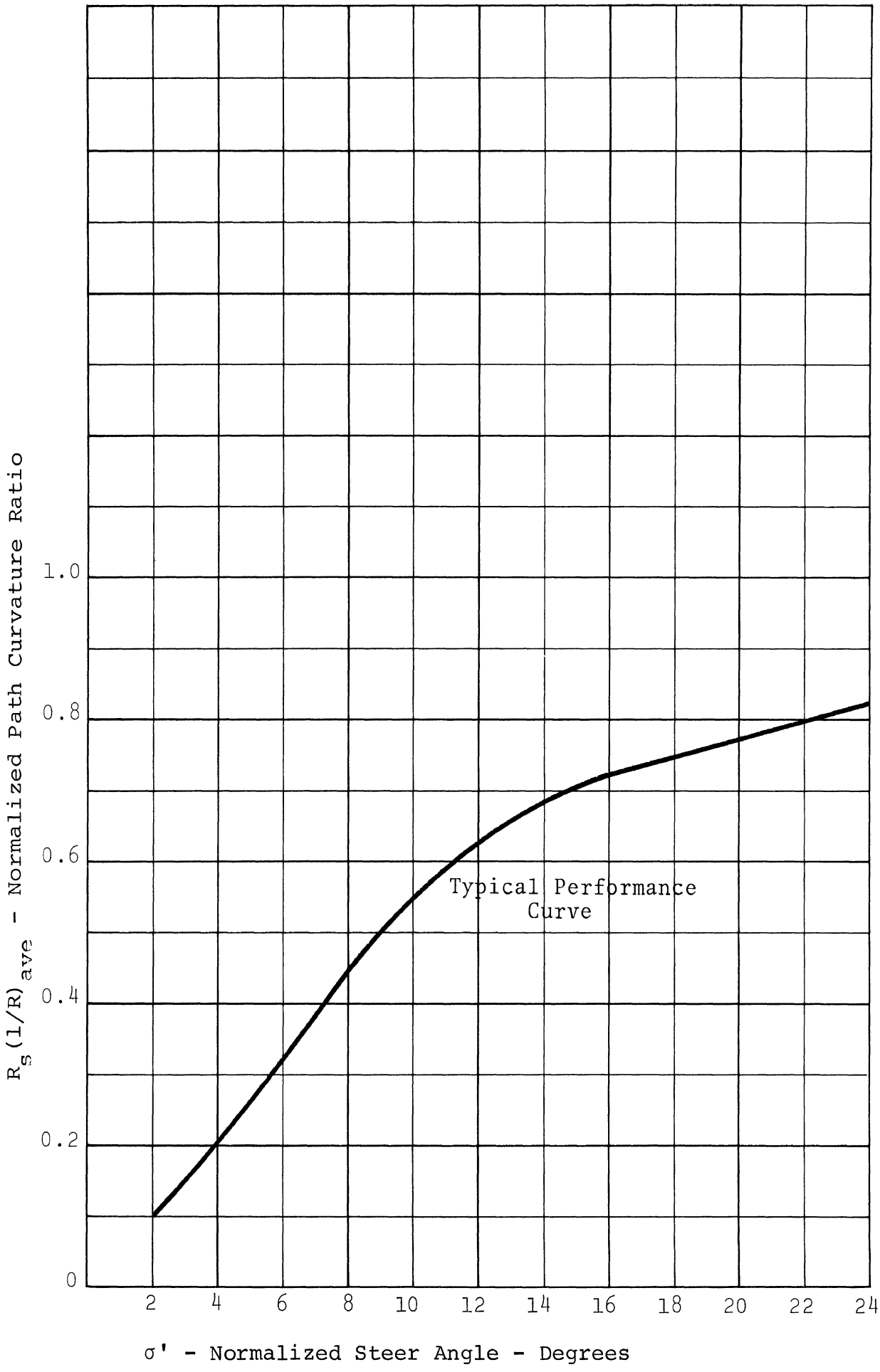

Figure 25. Trapezoidal steer plot format

the dynamic delay together with the achieved level of path curvature. The normalizing term, R_s, is the value of path curvature deriving from a steady 1g turn at 40 mph, and is used simply to obtain a convenient scale.

The sideslip response to trapezoidal steer input, as presented in Figure 26, is again seen as a driver challenge factor. The measure presents the peak value of β observed within the first 2 seconds of the maneuver. Figure 26 plots the peak sideslip response encountered over the range of steer levels, while Figure 27 indicates the "price" in terms of sideslip angle "paid" for the level of path curvature that is achieved. It is hypothesized that obstacle avoidance capability is maximized in those vehicles which provide high path curvature without exhibiting significant sideslip.

2.5.5 SINUSOIDAL STEERING. The sinusoidal steer test is designed to examine the effectiveness with which steering control can produce a lane change, in a limit sense. Whereas, in actual driving, the trajectories required during emergencies obtain from closure of the control loop by the driver, in this test the intent is to evaluate the resulting loop-closure challenge on the basis of findings obtained in an open-loop testing procedure. Implicit in the use of the sinusoidal steer input is the proposition that, in normal driving, symmetric steering inputs are found to be appropriate for producing lane change trajectories. In an emergency it is hypothesized that the driver loop-closure burden is least when a lane change can be achieved in response to control inputs which are directly extrapolated from normal driving.

The response to sinusoidal steering was evaluated in the VHTP study in terms of the deviation in heading angle, a measure that quantified the non-parallelism of the trajectory. The measure, as developed, provided no basis for

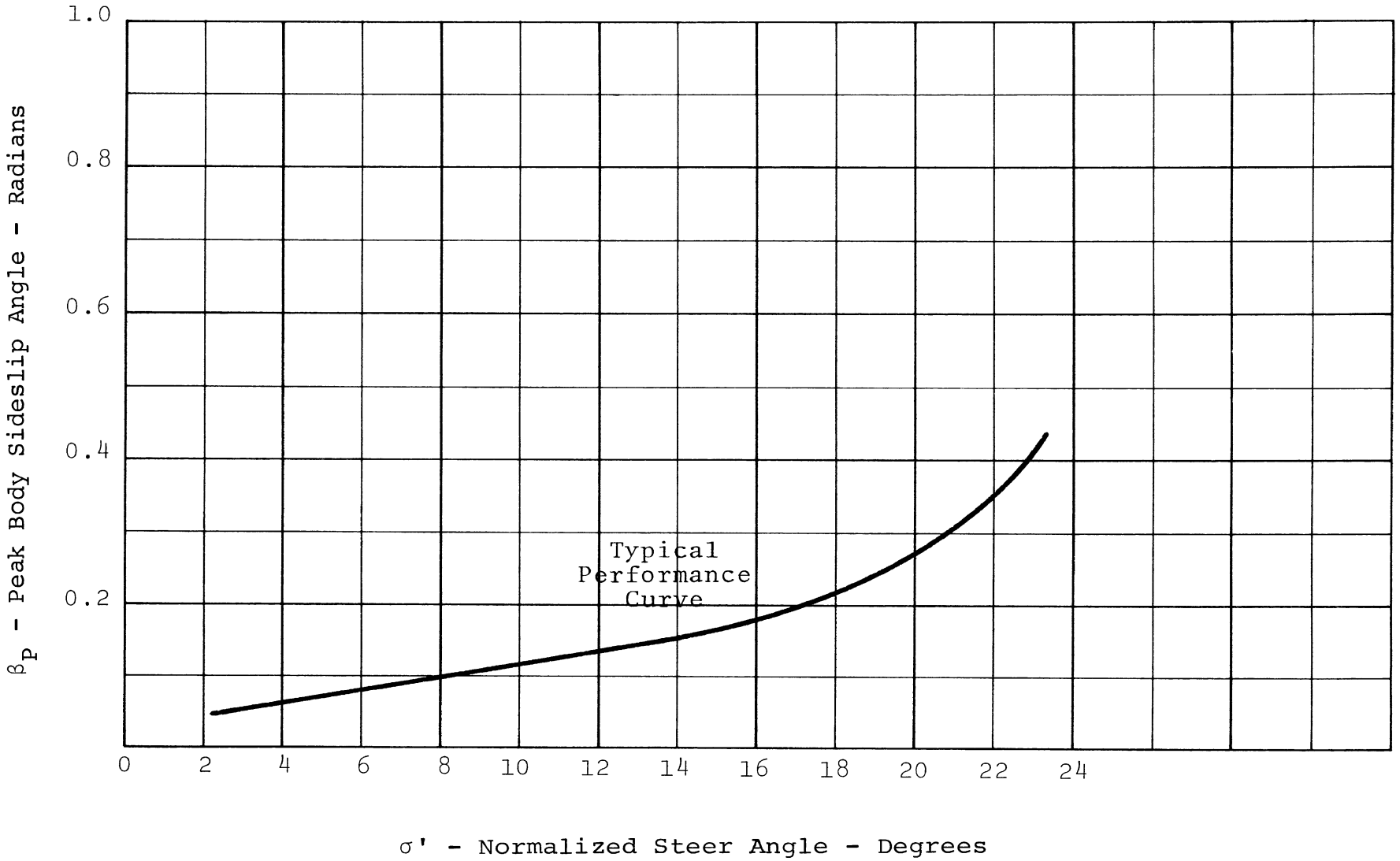

Figure 26. Trapezoidal steer plot format

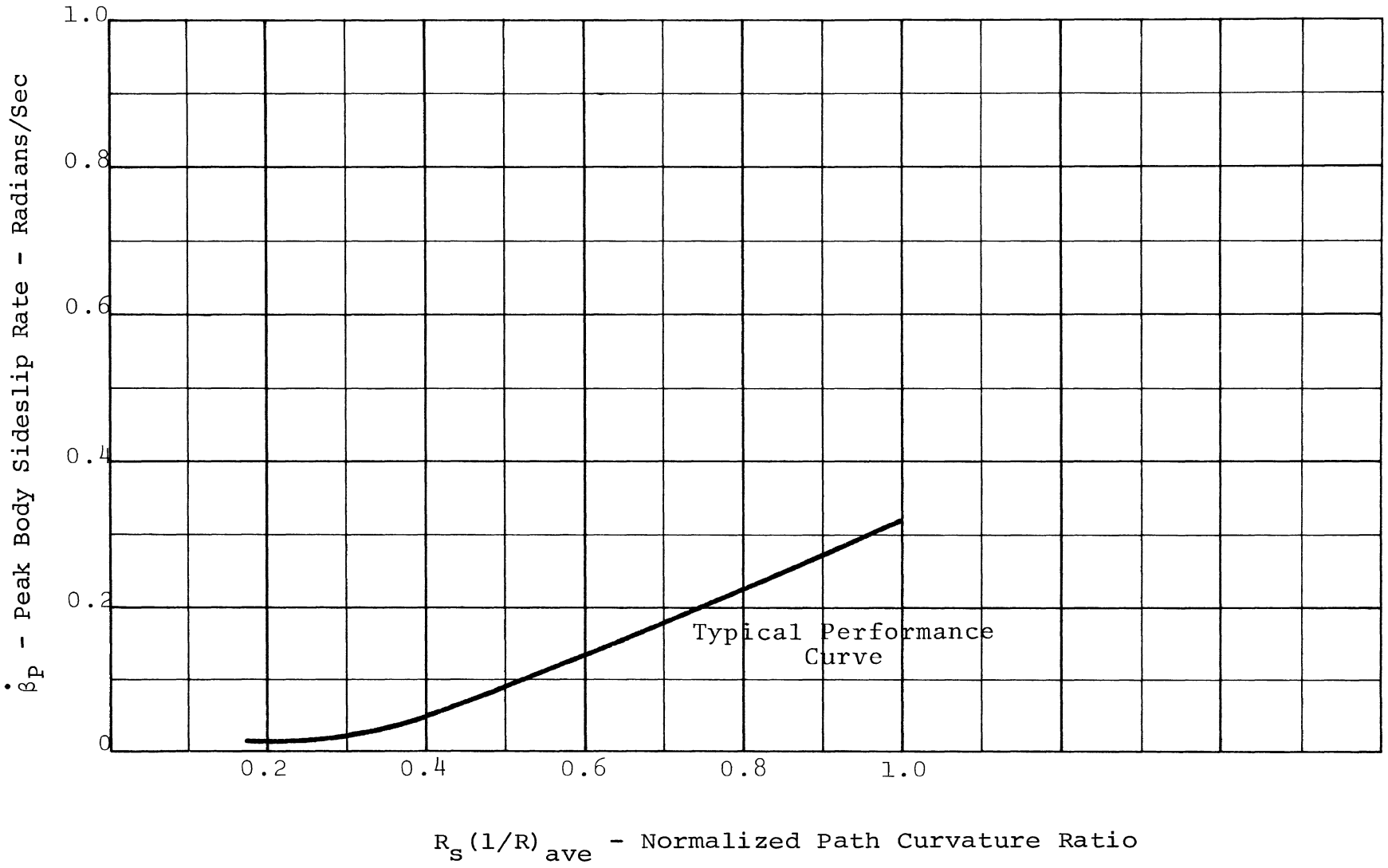

Figure 27. Trapezoidal steer plot format

comparing the attained lateral displacement response to the nominal width of a highway lane. It was concluded that a refined measure should be developed to evaluate the response trajectory directly, by computation of a "lane change deviation" measure.

This measure, Δ, is defined as an integral error term operating on the lateral displacement time history, $y(t)$, Figure 28, and is expressed by the following relationship:

$$\Delta = \frac{\int_0^{3.4} |12-y|\,dt}{3.4}$$

Note that the measure has units of feet, representing an average deviation from the desired lateral displacement of 12 feet as determined over the computation time, 3.4 seconds. The "ideal" value would be zero, indicating a step change in lateral displacement of precisely 12 feet. This measure, Δ, is plotted in Figure 29, as a function of the amplitude of the sinusoidal steer input. As defined, $\Delta = 12$ for a zero value of steer displacement.

Further data presentation refinements are provided by computing the sideslip response and plotting versus steer input, as shown in Figure 30. Peak sideslip angle can also be cross-plotted with the lane change deviation measure, Δ, as shown in Figure 31. It is hypothesized that the driver loop-closure burden is monotonic with both of the variables plotted in Figure 31 such that desirable performance is constituted by data points clustered near the origin.

2.5.6 DRASTIC STEER AND BRAKE. The drastic steer and brake procedure produces a variety of response conditions; however, the maneuver is designed only to evaluate the rollover tendency. In the VHTP study, the findings were presented to either show that the vehicle rolled over or did not. A small refinement has been added in this study wherein the peak roll

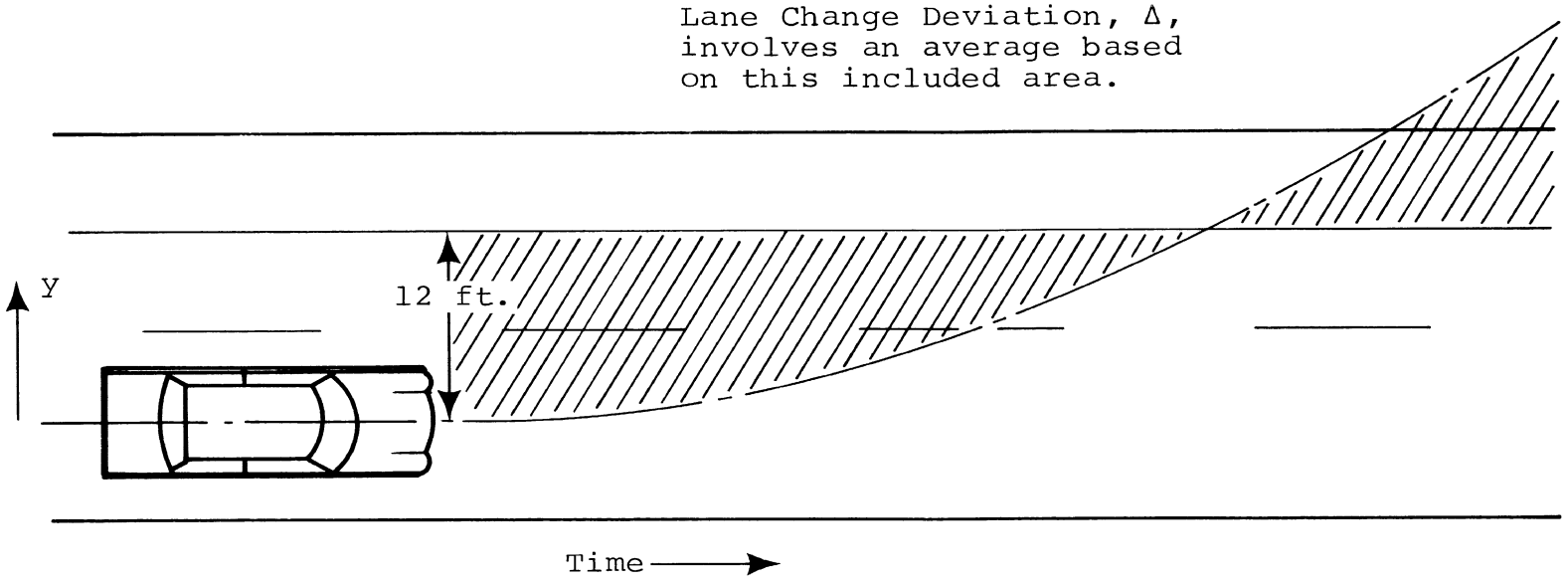

FIGURE 28
Open Loop y(t) Time History to Sine Steer Input

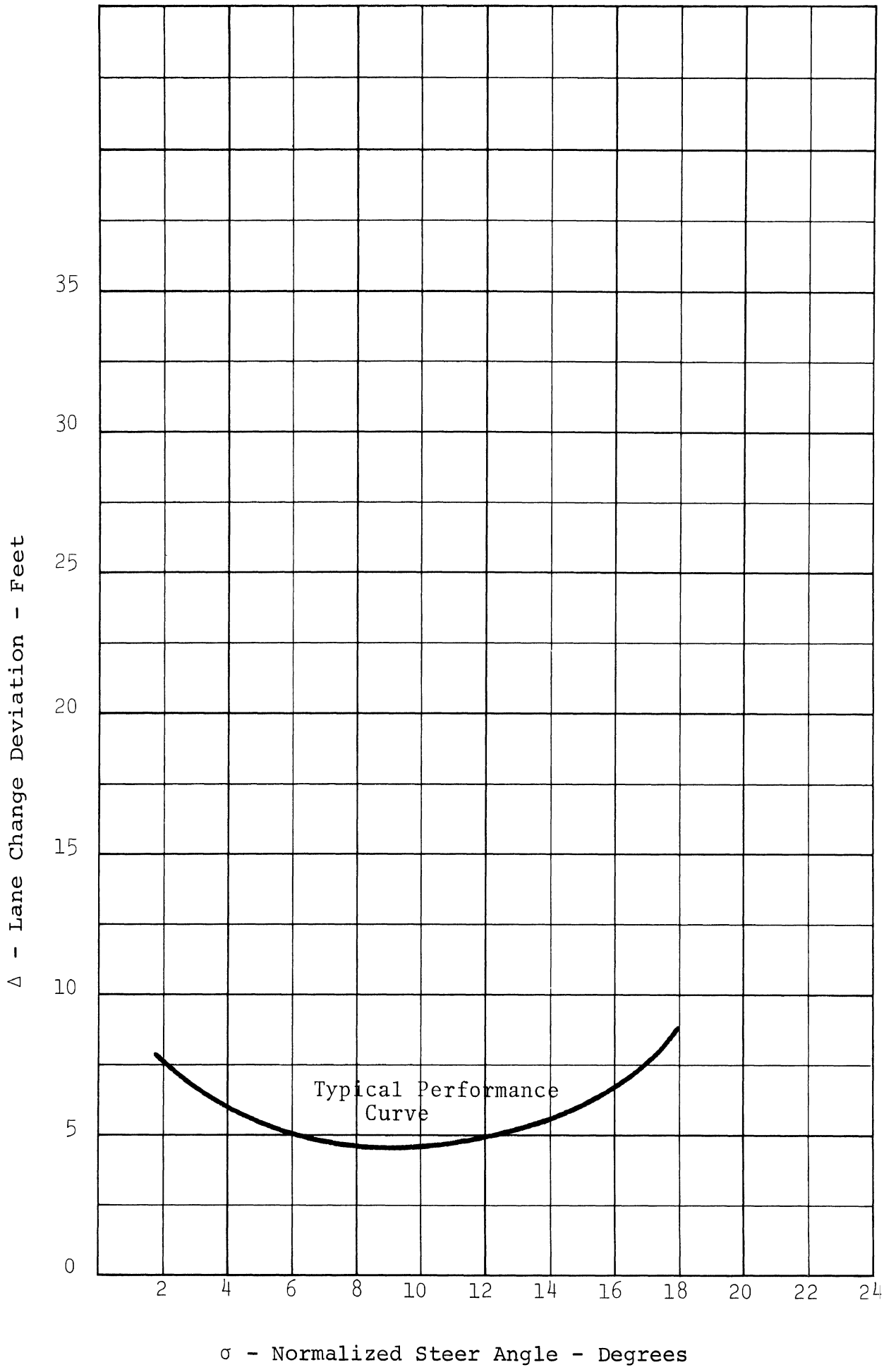

Figure 29. Sinusoidal steer plot format

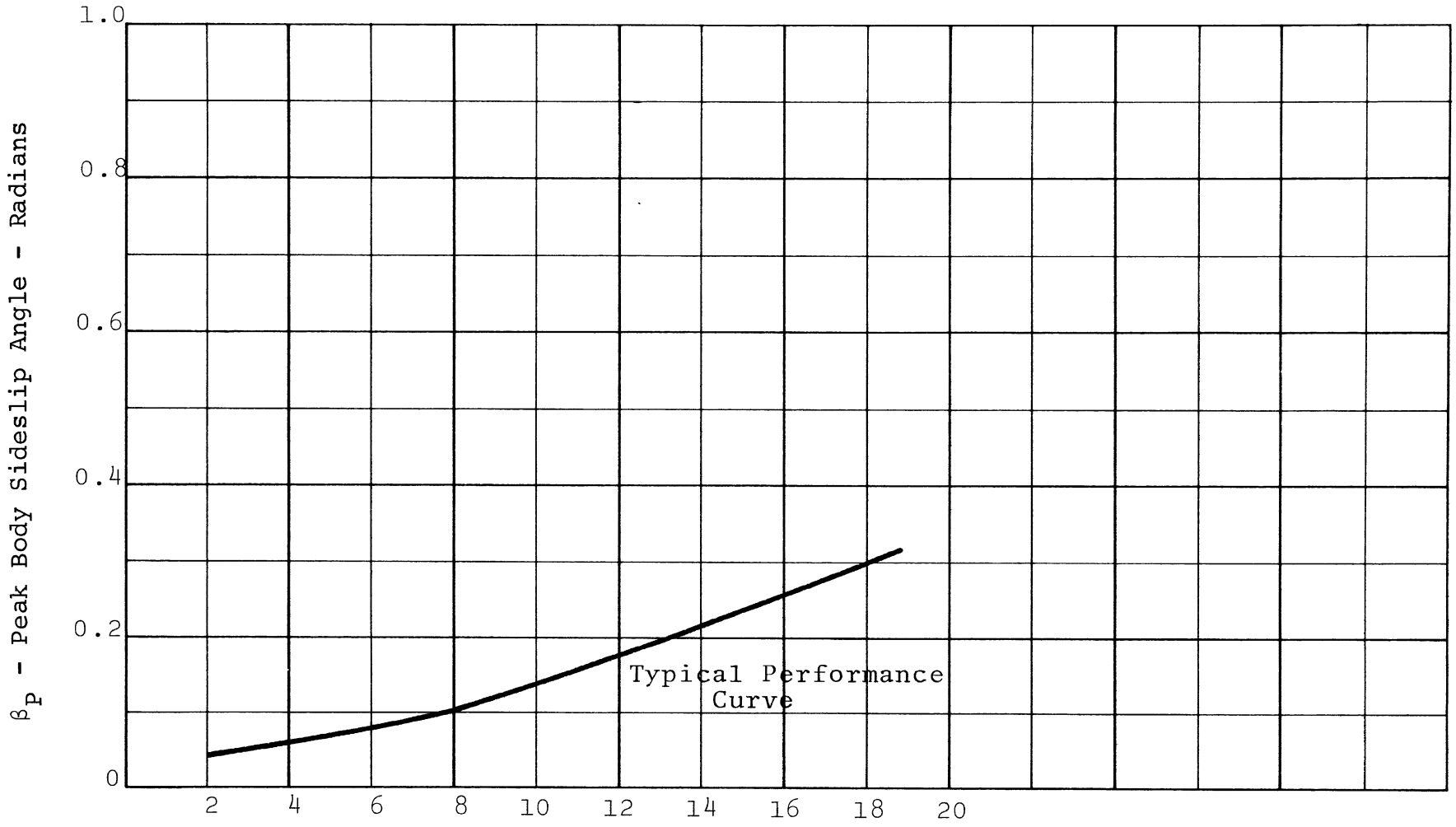

Figure 30. Sinusoidal steer plot format

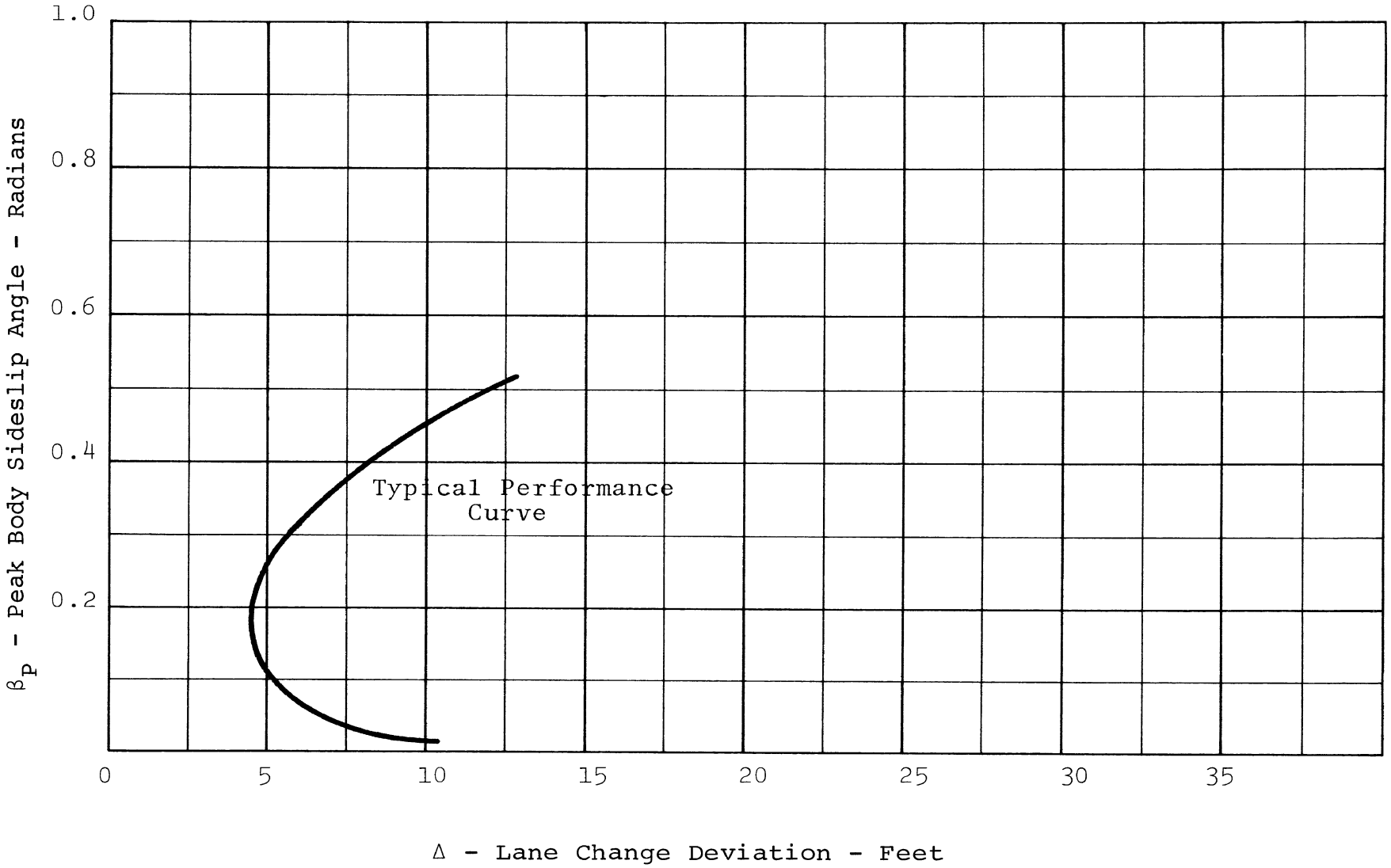

Figure 31. Sinusoidal steer plot format

angle attained by each vehicle in a drastic steer and brake maneuver is determined and plotted (see Fig. 32). Vehicle rollover, as restrained by the outriggers, would register on Figure 32 as a peak roll angle of 20° or larger.

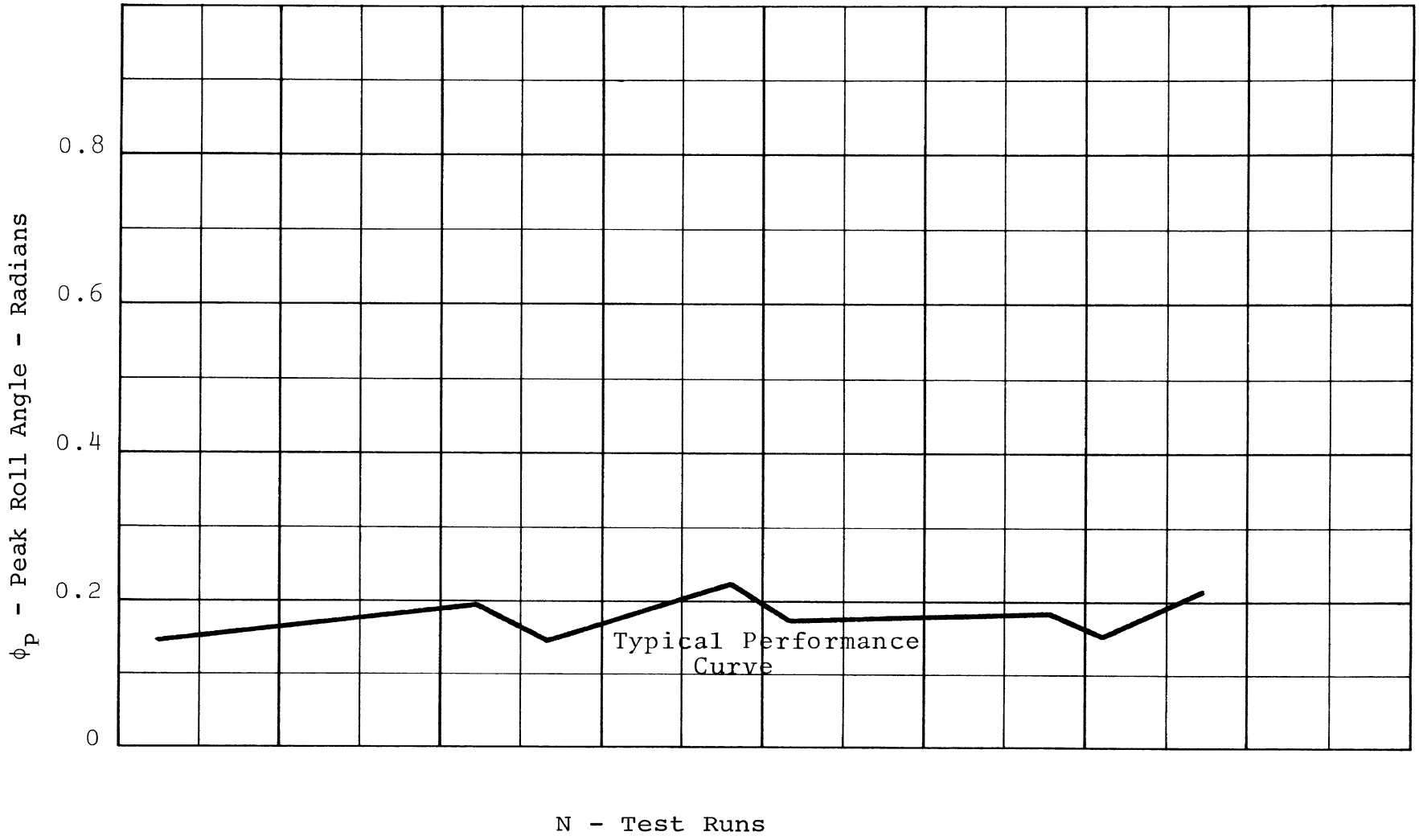

Figure 32. Drastic steer/brake plot format

3. FULL-SCALE TEST PROGRAM: EXECUTION AND FINDINGS

This section of the report is concerned primarily with presenting the experimental findings that were produced in the major test program mandated by the requirements of this study. Specifically, the objective was that of applying the six open-loop, limit maneuver measures, discussed in Section 2, to a test sample of twelve contemporary passenger vehicles. Since it was requested that the vehicle test sample be representative of the domestic and foreign vehicles available for purchase in the U.S. and that the sample further span the spectrum of handling qualities possessed by present day passenger cars, the process used to select the test sample is briefly indicated below and summarized, in further detail, in Appendix IV. A listing follows of (1) the vehicles that were actually tested in this program, and (2) the many procedures and test practices that were observed and used throughout the full-scale test activity. In an effort to give the report maximum readability, the reader should note that the detailed test findings have been gathered into a separate appendix, the body of the text being limited to a highly compact summary which constitutes an overview of the data base that was established in the course of this project.

3.1 SELECTION OF THE VEHICLE TEST SAMPLE

Two distinct analyses were conducted to select a test vehicle sample that would span the range of limit handling properties representative of the passenger vehicle population. These analyses included:

a) a characterization of the vehicle population in terms of design differences, mechanical characteristics, and performance levels;

b) an examination of accident data to detect over-involvement attributable to vehicle performance characteristics.

Appendix IV documents these analyses and presents the rationale that was used to select a fifteen-vehicle test sample. For budgetary reasons, this sample was reduced to eleven with another vehicle being added from a companion study, resulting in an actual test sample of 12 vehicles. It should be noted that the following major design differences and/or vehicle categories were represented:

- 4 vehicles were imported cars
- 1 vehicle had a rear engine location
- 1 vehicle had a mid-engine location
- 2 vehicles applied drive thrust through the front wheels
- 1 vehicle was equipped with a four-wheel antilock system
- 3 vehicles weighed less than 2000 pounds
- 4 vehicles weighed more than 4000 pounds
- 4 vehicles had 4-wheel independent suspension

In addition, a large number of suspension designs were represented. An itemized list of vehicle properties possessed by the sample is given in Table VII of Appendix IV. The actual test sample consisted of the following vehicles (all were 1971 models):

1. Volkswagen Super Beetle
2. Chrysler Imperial
3. Mercedes 300 SEL
4. Lotus Europa
5. Austin America
6. AMC Gremlin
7. Pontiac Firebird Trans Am
8. Ford Galaxie

9. Oldsmobile Toronado
10. Dodge Coronet
11. Chevrolet Brookwood station wagon
12. AMC Ambassador

In addition, a Toyota Corolla 1200 was outfitted for testing but later removed from the sample when repeated outrigger-restrained rollover responses during tire break-in runs resulted in the failure of a large number of suspension components. This response anomaly is, however, included in the discussion of the test results (see Section 3.3). Photographs of the twelve vehicles are shown in Figure 33.

3.2 TEST PRACTICE EMPLOYED IN THE FULL-SCALE TEST PROGRAM

Vehicle test progress was facilitated by conducting two parallel series of experiments, with the equipment required to perform the driver and automatic series of tests being sequentially installed and utilized in each of the test vehicles. To facilitate the installation of the test equipment in the field, a number of vehicle modifications were made. These modifications included the following permanent installations fitted to each vehicle:

1. a fifth wheel mount bracket
2. brake lining thermocouples at left front and right rear wheels
3. a plywood platform for mounting test instrumentation
4. a steering limiter mount bracket
5. brake limiter connection tubing
6. painted black/white masks on each wheel
7. front-wheel spindle mounts for front-wheel rotation detectors
8. rear-wheel rotation detector mounts
9. outrigger-tie-cable bolts in the front and rear bumpers

AMC Ambassador

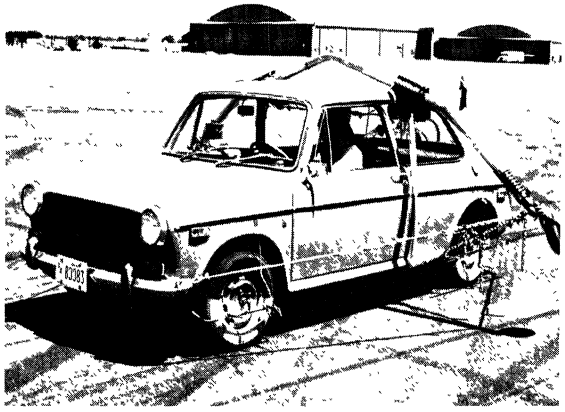

Austin America

Chevrolet Brookwood

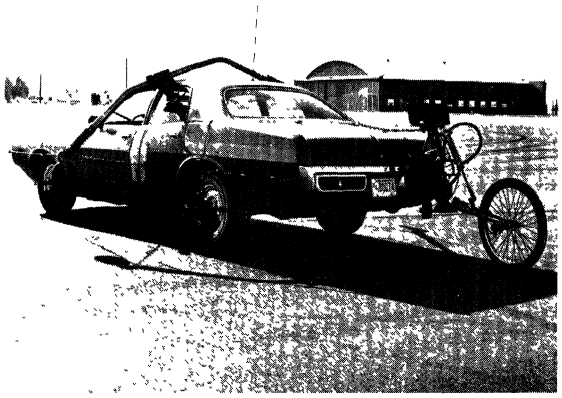

Dodge Coronet

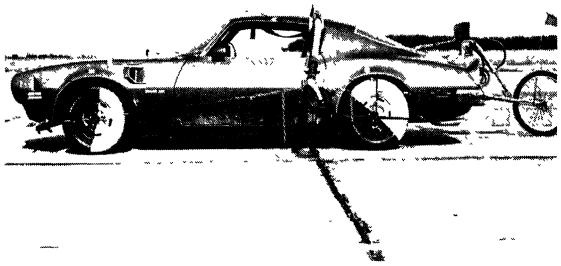

Pontiac Firebird TransAm

Ford Galaxie

Figure 33. Test vehicle sample

AMC Gremlin

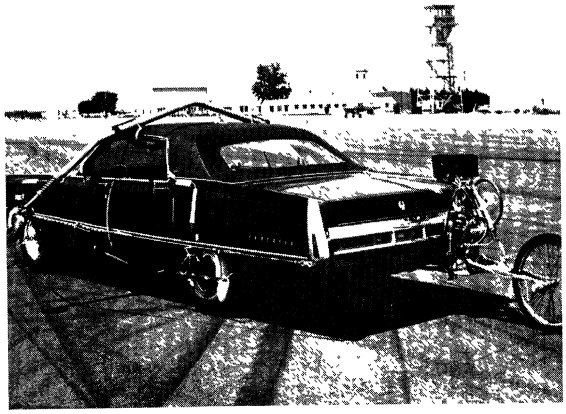

Chrysler Imperial

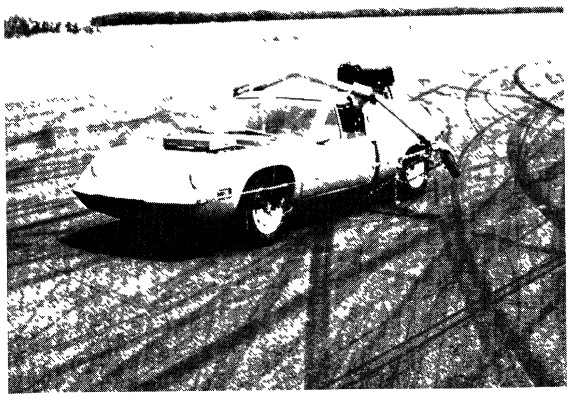

Lotus Europa

Mercedes 300 SEL

Oldsmobile Toronado

Volkswagen Super Beetle

Figure 33. (con't)

10. hydraulic pump mount and drive pulley on the engine
11. 12-volt fuse block and terminal

As a standard procedural practice prior to test, each vehicle was subjected to the SAE brake burnishing procedure (J843a) and was driven a minimum of 500 miles in a normal traffic environment. Tires for all vehicles were purchased directly from the manufacturers such that all experiments on any vehicle were run with tires obtained from a common lot. Tires were "broken in" on each vehicle by subjecting them to normal driving over 100 to 200 miles.

Prior to initiating either the driver or automatic series tests on each vehicle, the following practices were observed:

1. The vehicle was weighed prior to installation of the instrumentation package.
2. While the vehicle remained in its empty state, the front-end alignment (and in the case of independent rear suspensions, the rear alignment) was adjusted to be within the original equipment manufacturer's specification.
3. A physical calibration was performed on all data transducers.
4. The instrument package was installed and functional checks were made.
5. The instrument-laden vehicle was weighed.
6. Measurements of wheel alignment were made on the instrument-laden vehicle.
7. The steering ratio, N_G, was measured statically. This ratio was determined as the average ratio for both wheels turned 12° left and right:

$$N_G = \frac{\delta_{sw_1} + \delta_{sw_2} + \delta_{sw_3} + \delta_{sw_4}}{48}$$

where: δ_{sw_1} = steering wheel angle for 12° left turn on left front wheel

δ_{sw_2} = steering wheel angle for 12° right turn on left front wheel

δ_{sw_3} = steering wheel angle for 12° left turn on right front wheel

δ_{sw_4} = steering wheel angle for 12° right turn on right front wheel.

The value of N_G was used to compute the control input levels of steering per the procedures outlined in Appendix II.

8. Next, trial runs were conducted, with sample data taken and checked.
9. New tires which had been "broken in" by at least 100 miles of driving were installed prior to conducting the side-force stabilization tests.
10. During these stabilization tests, tire inflation pressures were maintained at the manufacturer's recommended cold inflation pressure and the fuel tank was maintained between half full and full.
11. The tire side-force stabilization tests were stopped after 20 runs and the tires were transferred to an opposite diagonal position. Further runs were conducted as dictated by the wear-in scheme outlined in Appendix III.
12. Prior to all data-taking sequences, the vehicle was driven over a 3-mile paved course, and inflation pressure were adjusted as necessary. An electrical calibration sequence was conducted as outlined in Appendix V.
13. Test procedures were conducted, with electrical calibrations repeated whenever a run sequence

exceeded 25 samples. A sample number was assigned to each test run and to each mode of the electrical zero and gain-set calibration sequence. Each sample was recorded in a data log book as well as being identified on the voice channel of the tape recorder.

14. Following all tests in a series (driver or automatic) a post-calibration sequence was conducted and the physical gains of all transducers compared with the values taken prior to the series. If any of the critical response variables were seen to have varied more than the amounts indicated below, the entire test series was repeated.

Variable	Allowed Calibration Variation
A_x	1 1/2%
A_y	1 1/2%
r	2%
ϕ	2%
V_5	1 1/2%

15. Front-end alignment was measured following each test series to record the alteration in static wheel positions resulting from testing.

16. Recordings were obtained of environmental conditions throughout the test program, even though it was recognized that no basis currently exists for utilizing these data to apply corrections to the test results.

17. The test pad was swept periodically with a scrubbing sweeper to minimize the deterioration of friction properties caused by surface contamination.

18. Skid trailer measurements were made on the test surface, indicating average dry pavement ASTM skid numbers of 76-82.

19. All response data gathered during the test program was stored and transported in magnetically shielded containers. When tape data canisters were manually carried onto commercial airline flights, the airlines were requested to deactivate whatever high gauss metal detectors may have been operational.

Height of the installed instruments in the automatic test series were measured on each vehicle to enable estimates to be made of the elevation of the center of mass of the installed load. A table of these calculated values is given below. The installed gear weighed 515 pounds. In each vehicle, however, seats were removed, such that the net load compares faborably with a nominal two passenger-no luggage condition. In comparing estimated c.g. heights of a vehicle loaded with two passengers and no luggage, it would appear that no vehicle suffered a net c.g. height relocation as large as one inch. For the Chevrolet station wagon, whose c.g. height was measured in the laboratory, the tested condition involved a net c.g. height approximately .010 inches below that of the nominal two passenger-no luggage condition.

Table of C.G. Heights
of the Installed 515 lb. Load
Used in the ACV Tests

Vehicle	h	Vehicle	h
Mercedes	25.6	Gremlin	26.9
Austin	24.8	Firebird	26.6
Volkswagen	26.6	Toyota	25.2
Imperial	27.4	Chevrolet	26.6
Lotus	24.1	Dodge	23.6
Galaxie	26.6	Ambassador	26.1
Toronado	27.4		

3.3. VHP FINDINGS

The VHP response data gathered during the full-scale test program are presented below in summary form. (A complete

catalog of the data plots produced for each vehicle will be found in Appendix VII.) Each limit response maneuver is considered and discussed in turn, with the objective of identifying the typical response categories produced by the sample. Both raw data reproductions and condensed data plots are employed to illustrate the various categories of response behavior. Specifically, the condensed data plots are presented in a form which consolidates the data from the entire sample, indicating, also, the range and the distribution of performance. These consolidated plots were obtained by graphical overlay methods. It appears that a rigorous statistical treatment of the data base might be advisable in any future processing of these data.

3.3.1 STRAIGHT-LINE BRAKING. Three categories of limit response can be defined among the data collected:

a) front wheels lock up first, as typified by the Lotus Europa
b) rear wheels lock up first, as typified by the AMC Ambassador
c) 4-wheel antilock performance as represented in the sample by the Chrysler Imperial.

Typcial raw data time histories are shown in Figure 34. Except for the case of rear-wheel lockup, in which a yaw divergency may result, all raw data from straight-line braking resembles the example in Figure 34. Figure 35 presents the distribution of performance for the test vehicle sample, by means of an overlay of the three response categories typified by the Lotus, Ambassador, and Imperial. This plot defines the range of A_x vs. P_B as represented by the individual plots presented in Appendix VII. The plot was constructed by approximating each vehicle's mean performance by six discrete points, although the plots in Appendix VII

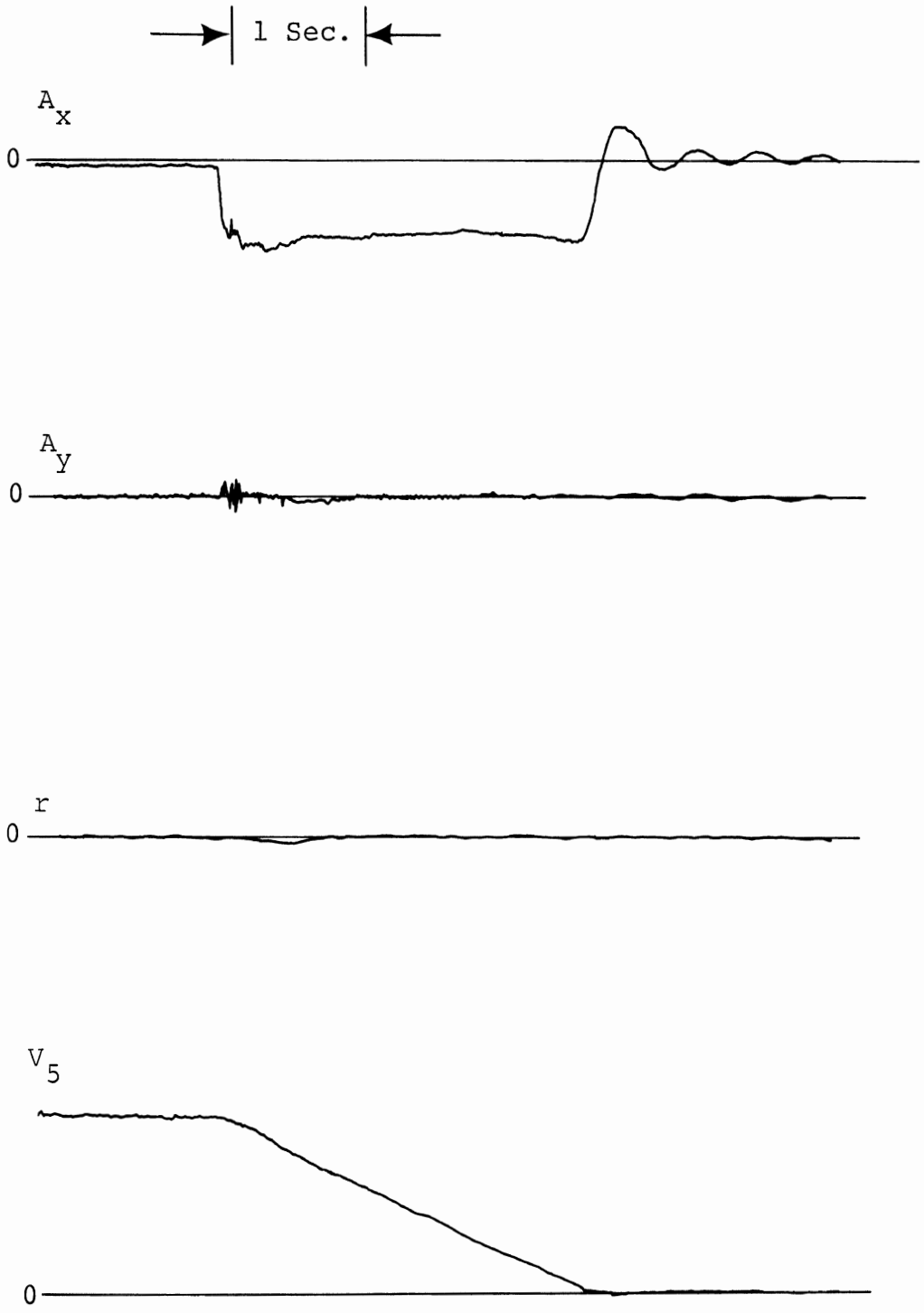

FIGURE 34

Straight Line Braking Raw Data Time Histories

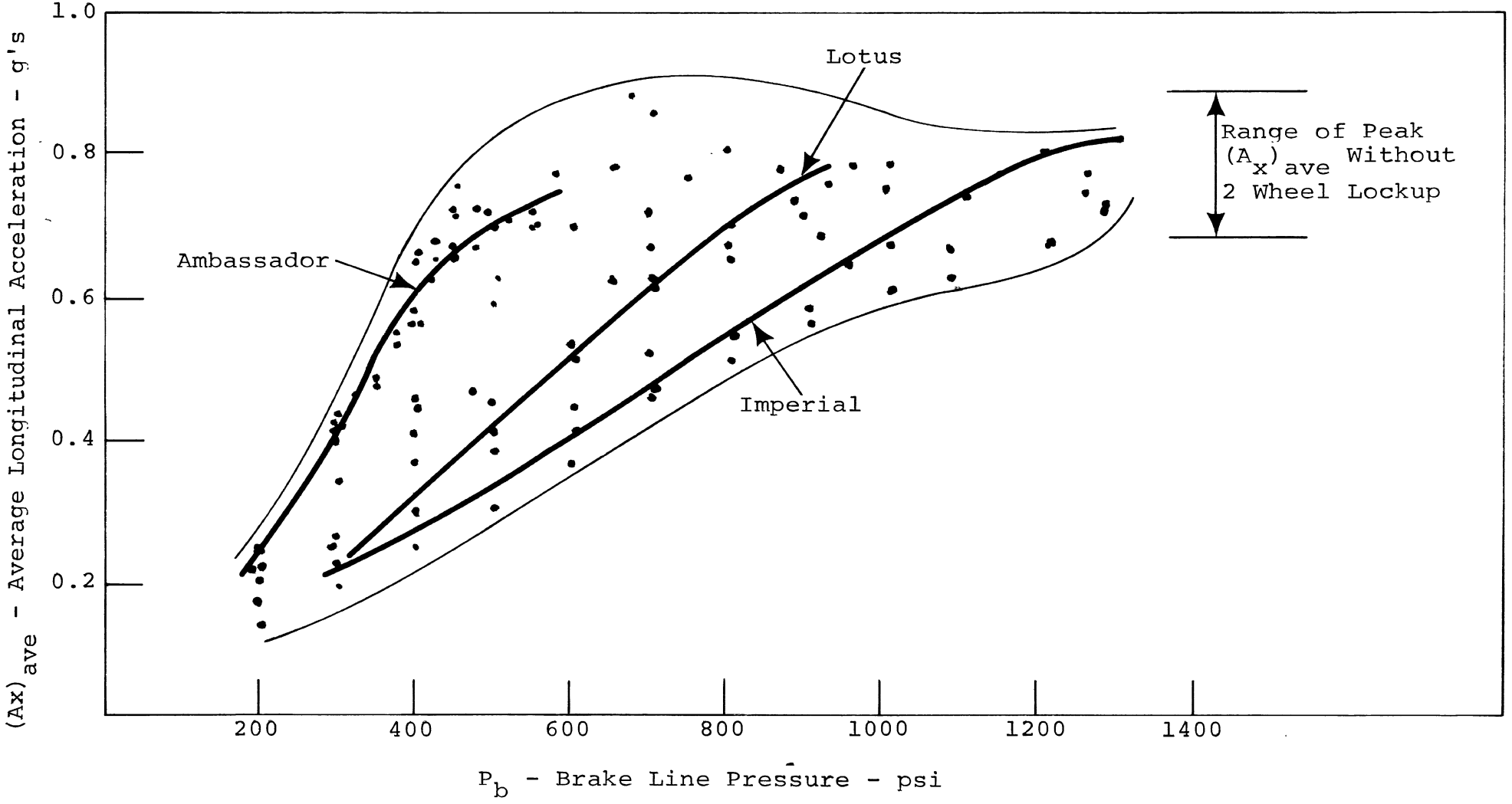

FIGURE 35
Summary Plot - Straight Line Braking

indicate far larger numbers of samples for certain vehicles.

Clearly, the range of vehicle performance on this plot is determined both by differences in gain (A_x/P_B) and by differences in the peak longitudinal acceleration achieved without locking two wheels on the same axle. The spread of peak acceleration performance is indicated in the figure to be 0.22g.

3.3.2 BRAKING-IN-A-TURN. As with straight-line braking, the significant limit response categories are

a) front-wheel lockup, as with the Mercedes
b) rear-wheel lockup, as with the AMC Gremlin
c) 4-wheel antilock performance, Imperial.

Figure 36 presents time histories produced in a typical sublimit condition, with no wheels locking. The longitudinal acceleration is seen to rise abruptly following brake application in the steady turn. Path curvature increases from its initial value, in this case, as the vehicle slows to a stop.

Figure 37 presents a raw data sample of the limit response to braking-in-a-turn characterized by lockup of the front wheels. Characteristically, this limit is indicated by an immediate drop in the A_y and r time histories, with negligible sideslip ($\tan\beta$) and a decrease in path curvature to zero. The divergent end condition of the b and 1/R time histories reflects the computational instability that results when the forward velocity appearing in the denominator of both variables goes to zero. This nominal response also typifies the performance exhibited by vehicles with 4-wheel antilock systems.

In Figure 38, raw data are presented for the rear-wheel lockup case, clearly indicating the unstable directional response that typifies this limit category.

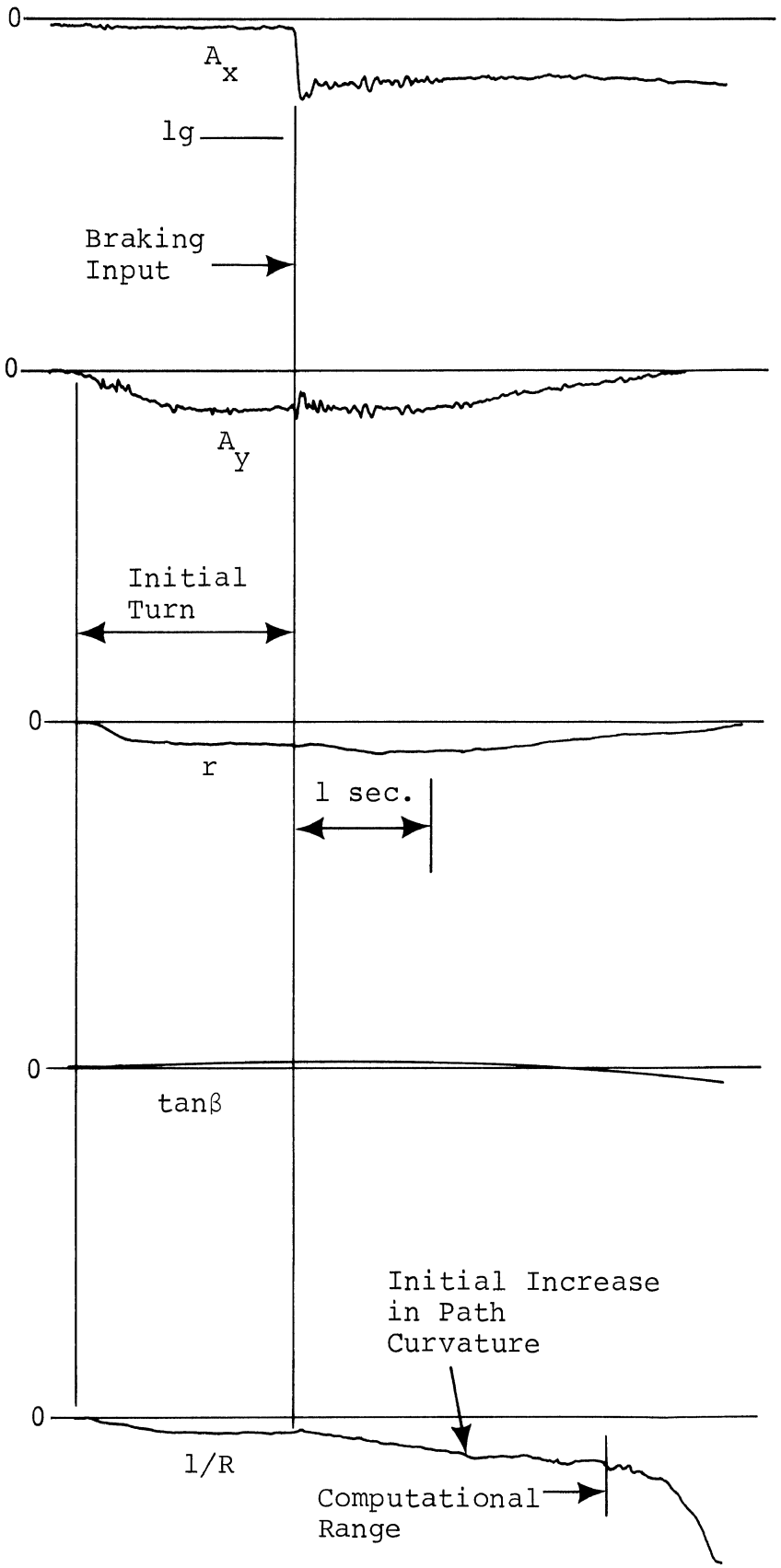

Figure 36.
Braking In A Turn - No Wheels Locked

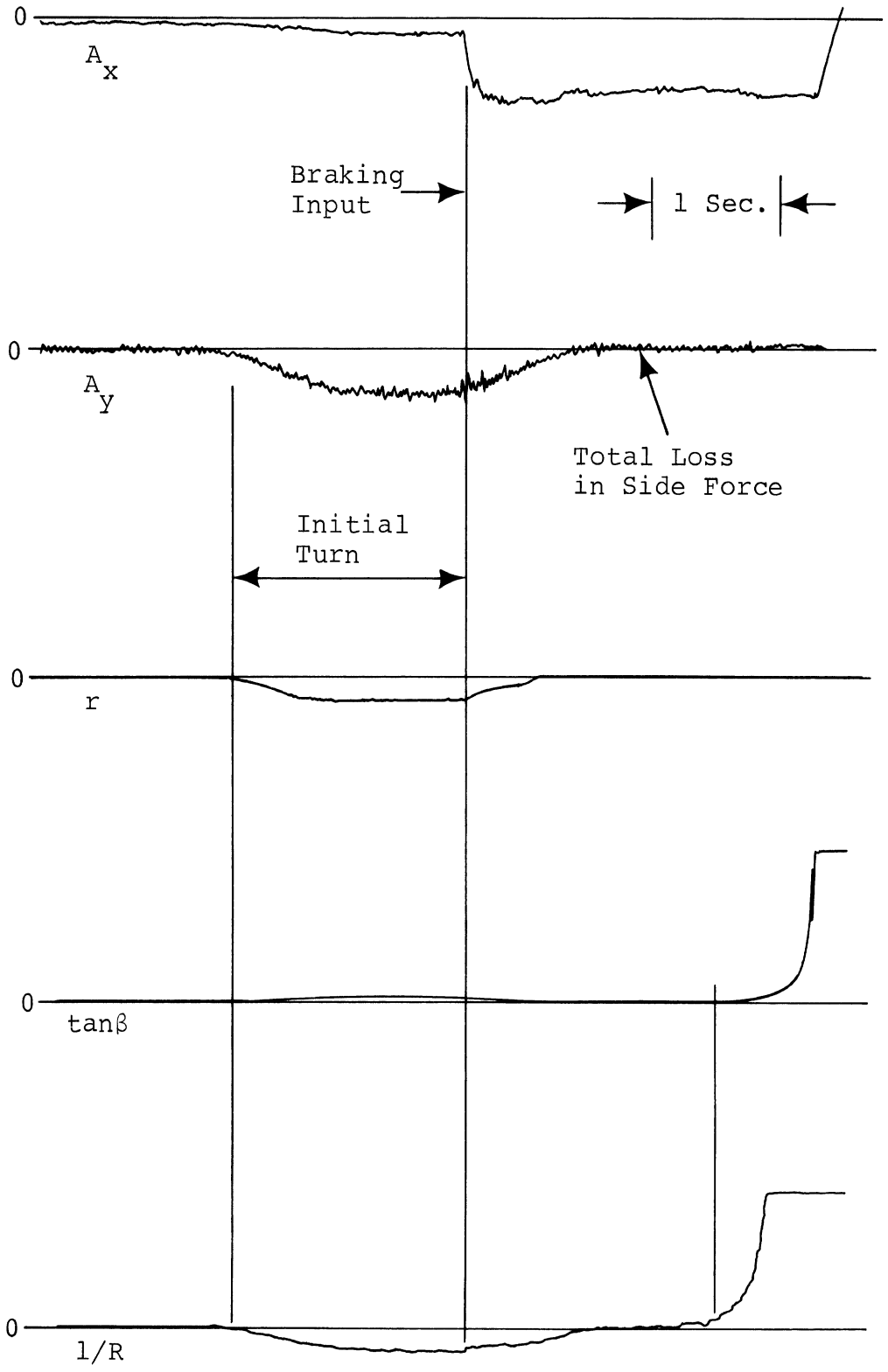

FIGURE 37

Braking In A Turn - Front Wheels Lockup

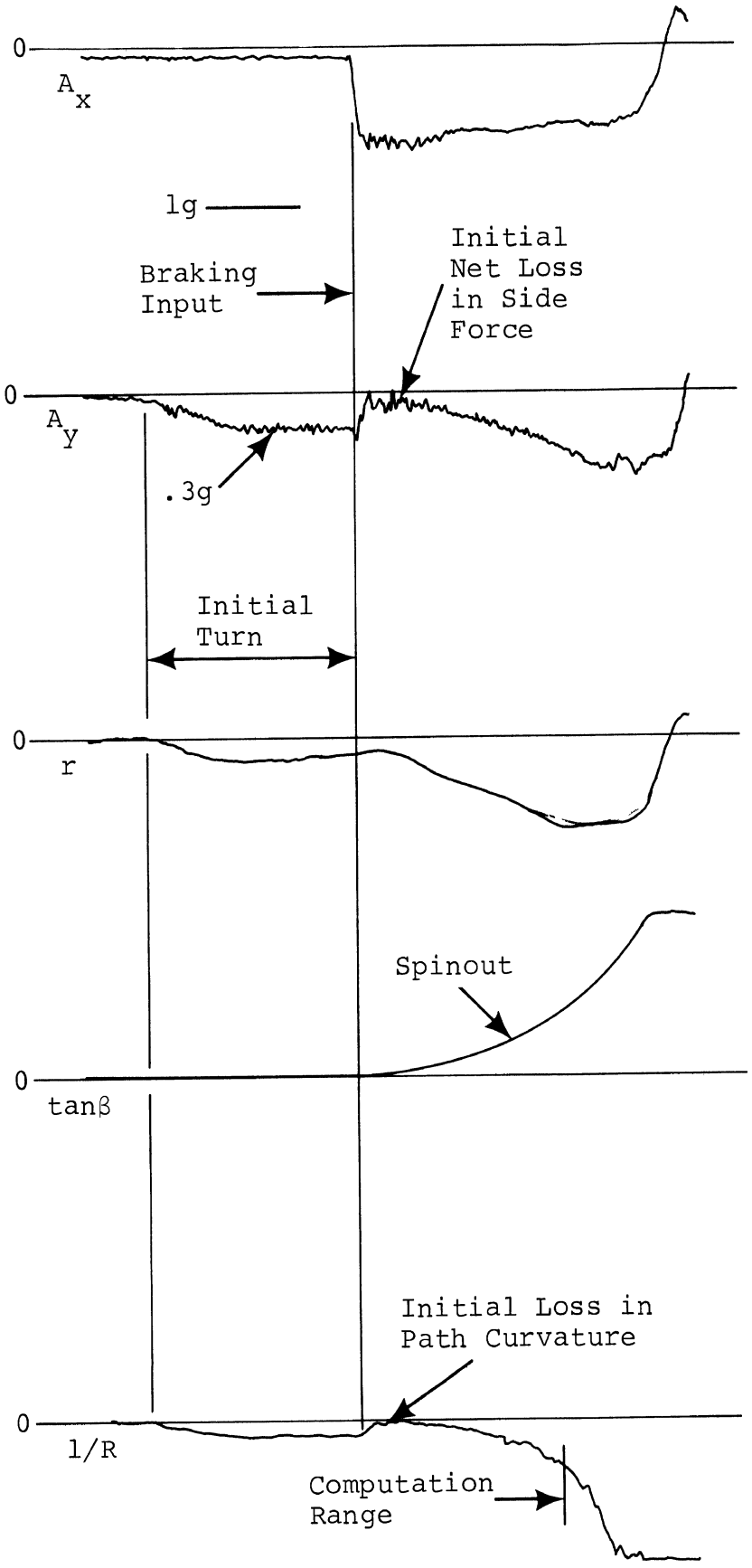

Figure 38.

Braking In A Turn - Rear Wheels Lockup

Sideslip-rate and path-curvature responses are presented in Figures 39 and 40 for the test vehicle sample. These plots indicate the range and distribution of braking-in-a-turn performance, together with lines representing the approximate mean performance of the vehicles typified by front-wheel lock, rear-wheel lock, and no wheel locking limit performance. It is clear that the only vehicles exhibiting substantial sideslip are those which exhibit rear-wheel lockup, while either front- or rear-wheel lockup can cause a dramatic loss in path-curvature response at the limit.

Interesting features of the path curvature data presented in Figure 40 include the generally increasing trend in normalized 1/R with increased braking, as well as the predominance of sublimit points showing values greater than 1.0. An explanation of these characteristics is provided by reflection upon the understeer contribution to path curvature that accompanies a decreasing velocity with constant steer angle. As the understeer vehicle slows down, even in the absence of braking, path curvature gain increases. Thus the results plotted in Figure 40 indicate the summation of two path-curvature responses; one deriving simply from understeer effects, and another deriving from factors related to the braking process. It would appear, then, that this plot indicates a response property representing an undesirable effect of understeer, at least per the safety hypothesis expressed earlier. Such an observation runs counter to conventional judgement which holds that the positive benefits of understeer far outweigh this hypothetically negative property.

Clearly, a broad range in path-curvature response was measured while the sideslip responses are rather confined. The apparent spread in any of these measures, however, is heavily dependent upon the scale chosen for data presentation.

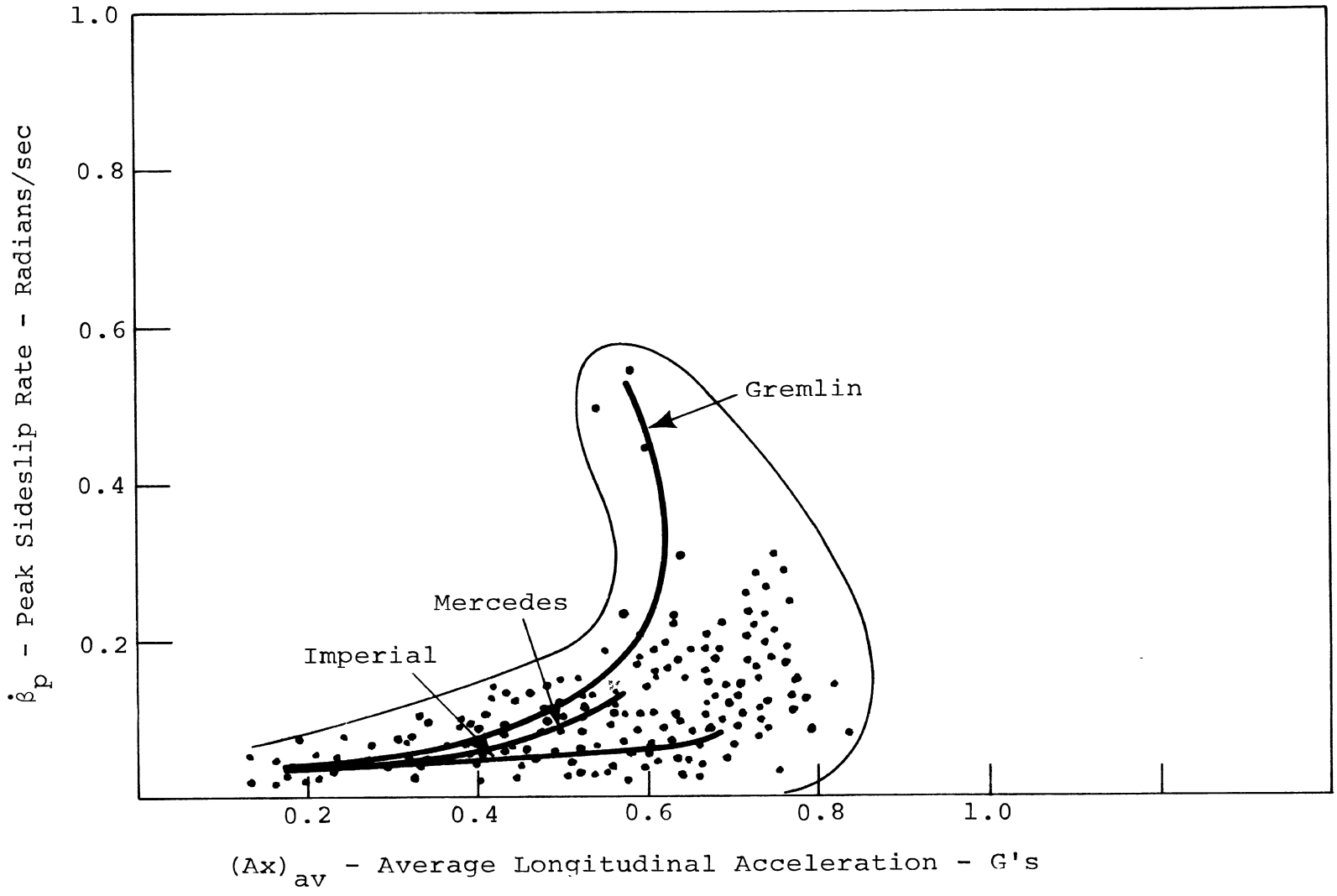

FIGURE 39

Summary Plot - Braking In A Turn

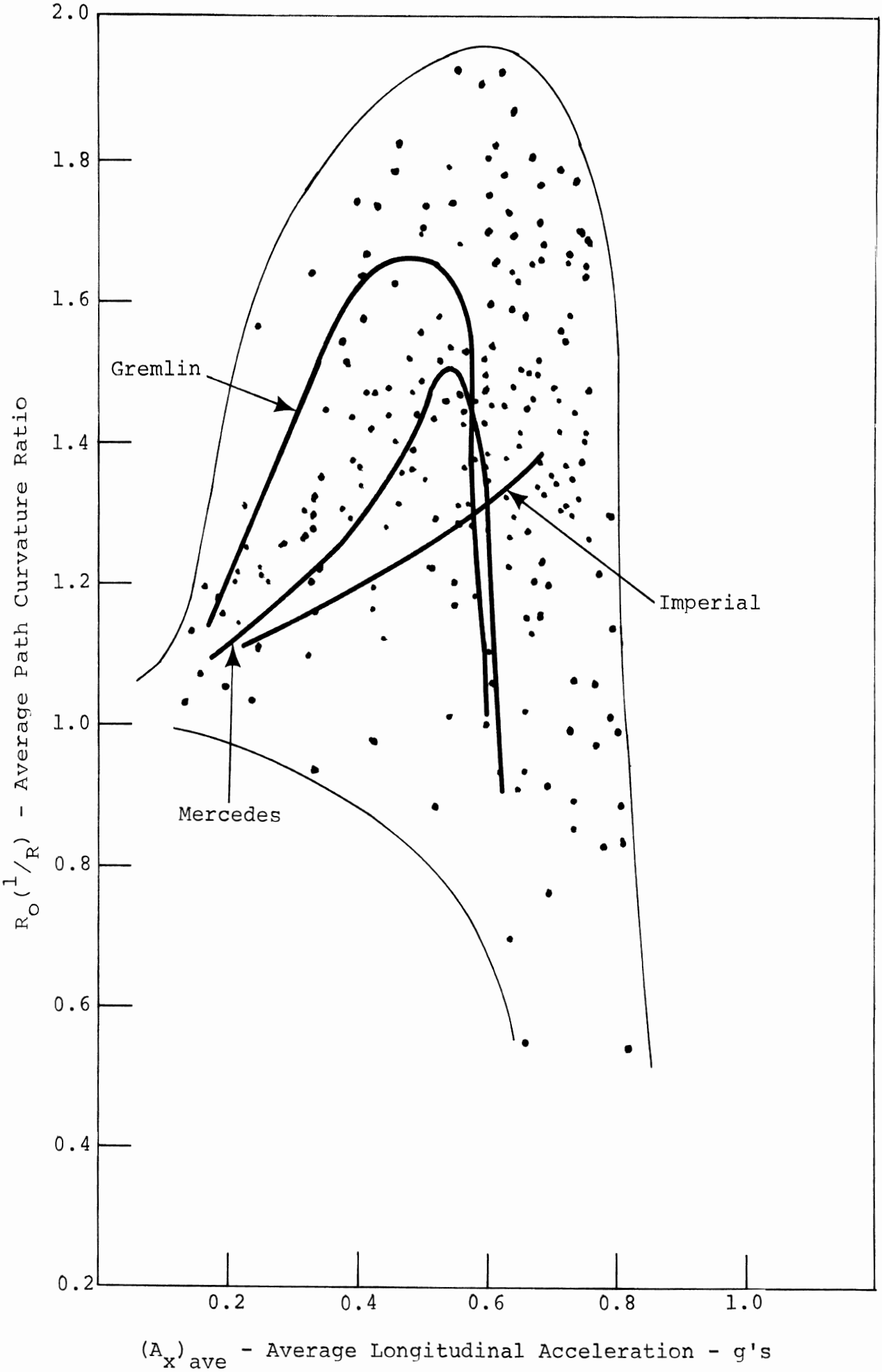

FIGURE 40
Summary Plot - Braking In A Turn

The increasing trend in normalized path curvature, with increasing A_x, is partially due to an anomaly in the data presentation scheme. Since $(1/R)_{ave}$ is computed only over the first one second of response, following brake application, the level of deceleration directly determines the velocity decrement within which the one-second average is evaluated. Because path-curvature gain is inversely related to vehicle velocity for the understeer vehicle, and because certain mechanisms in the braking process can disturb the lateral-force balance, an increase in 1/R with increasing levels of A_x is generally observed.

Certain vehicles were seen to illustrate marked asymmetry in response to right vs. left turn braking. Of particular notice, the Lotus Europa indicated dramatically differing path-curvature responses between right and left turns.

3.3.3 ROADHOLDING IN A TURN. Two categories of limit response are observed in the data produced by the roadholding in a turn maneuver:

1. predominant wheel-hop resonance of front suspension is exhibited, resulting in significant loss in path curvature without large sideslip;
2. rear wheel-hop resonance dominates, causing a destabilizing yaw moment and a resulting sideslip excursion.

Example time histories characteristic of the response caused by dominant wheel-hop resonance of the front wheels are given in Figure 41. Note that the yaw-rate response decreases quickly, when the vehicle contacts the disturbance grid, causing the computed path-curvature response, 1/R, to drop.

Dominant resonance at the rear wheels yields the time histories shown in Figure 42. With a substantial loss in

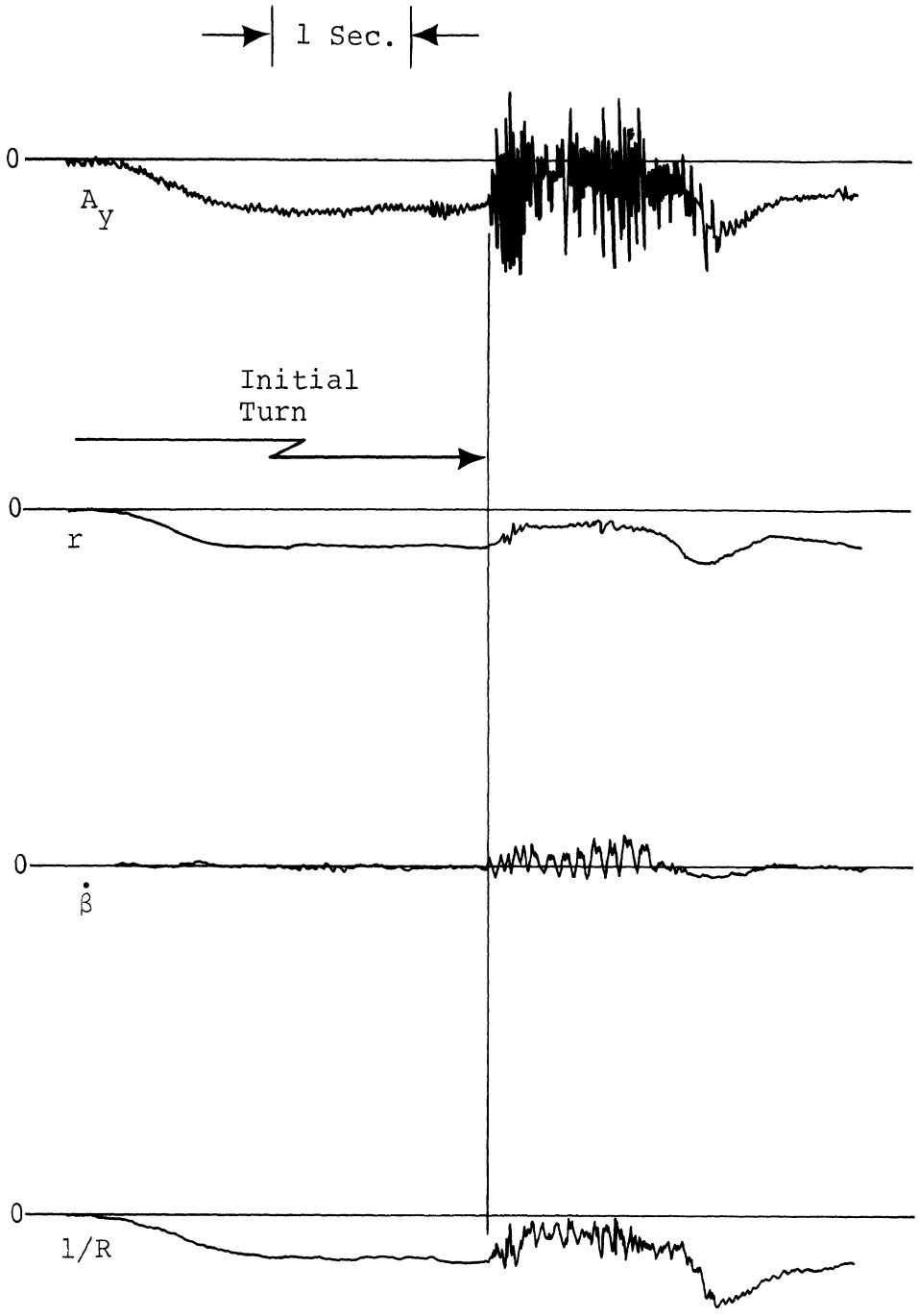

Figure 41.

Roadholding In A Turn -
Dominant Front Wheel Resonance

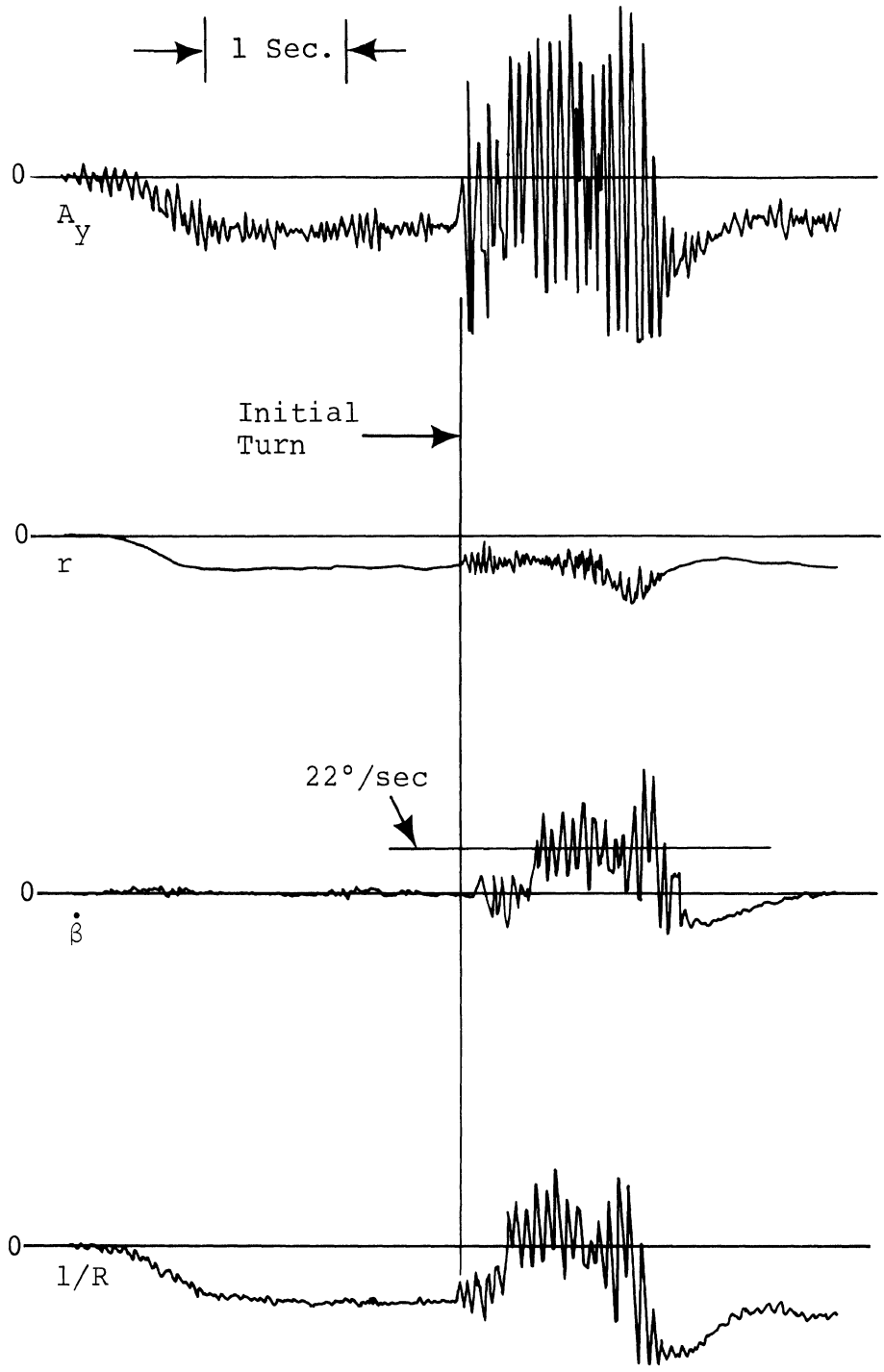

Figure 42.

Roadholding In A Turn -
Dominant Rear Wheel Resonance

rear-tire side force, $\dot{\beta}$ rises to a rather large level, and the path curvature decreases toward zero. It is interesting to note that the $\dot{\beta}$ and 1/R measures indicate a dramatically altered directional response while the yaw rate signal remains remarkably steady. This phenomenon, deriving from the inability of the yaw rate gyro to distinguish the rotational rate of the velocity vector which contributes to turning from the rotation accompanying sideslip rate, illustrates the utter inadequacy of yaw rate as a measure of performance in this maneuver.

Data presented in Appendix VII for each vehicle are summarized in Figures 43 and 44, illustrating the range and distribution of performance in the test vehicle sample. As indicated in Figure 43, the range of normalized path-curvature data essentially covers all conceptual possibilities. While certain vehicles showed rather slight loss in path curvature, upon encountering the road roughness grid, others exhibited an essentially tangential, zero-curvature, response.

It should be noted that Figure 43 was constructed without including the data produced by testing either the Mercedes, or Lotus. The omission of these vehicles from the summary plot derives from the observation of response anomalies which are not explainable by means of basic kinematic principles. Figure 45 shows an example of raw data taken with the Mercedes which shows lateral acceleration not only decreasing during the traversal of the disturbance grid, but also making a large excurison of polarity opposite to that of the initial turn. As a result, the computed path-curvature response indicates a change in polarity, suggesting a trajectory which is further out of the initial path than would be the case for a nominal tangential trajectory. No mechanism has been defined by which this response can be understood. However, no major data

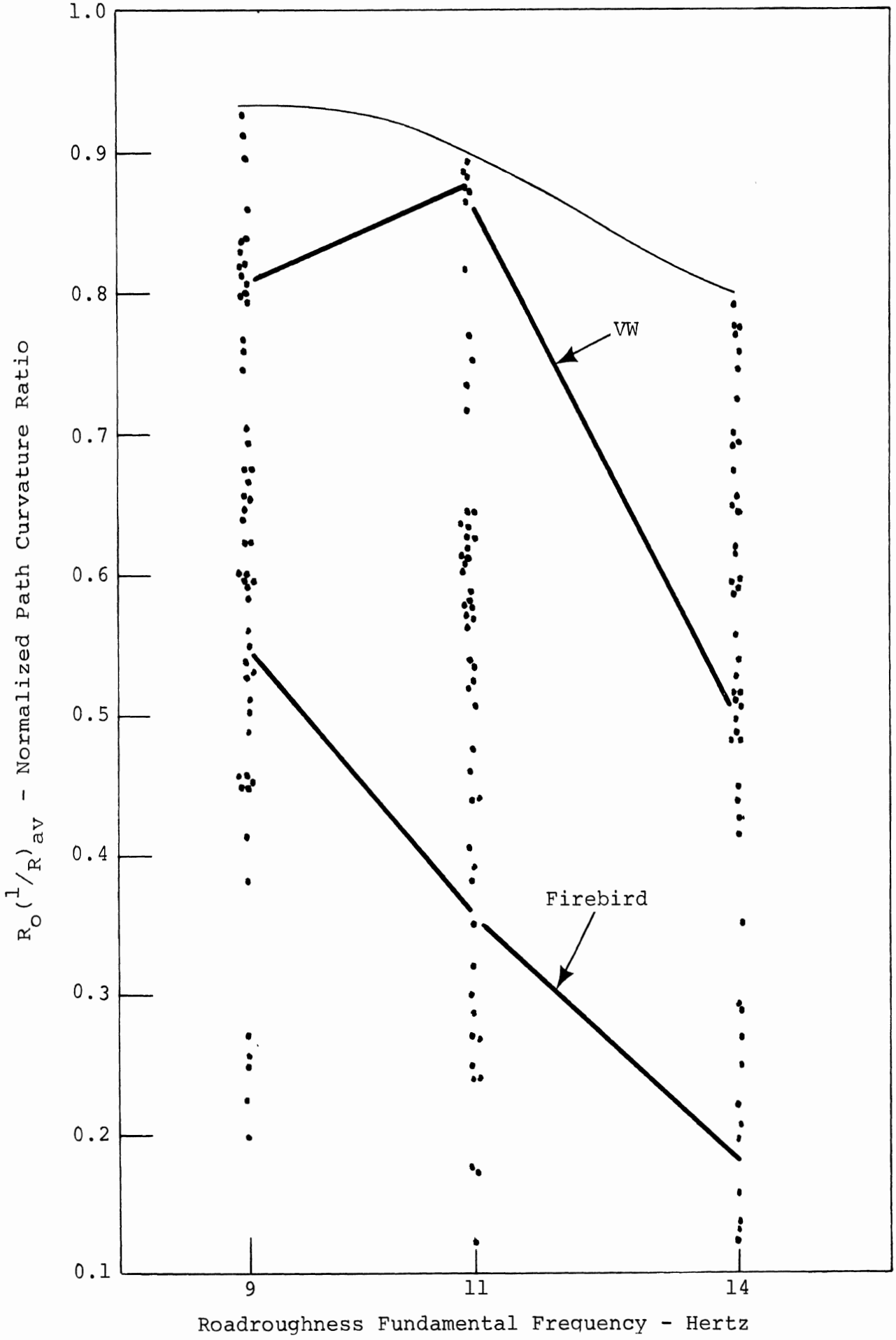

FIGURE 43
Summary Plot - Roadholding In A Turn

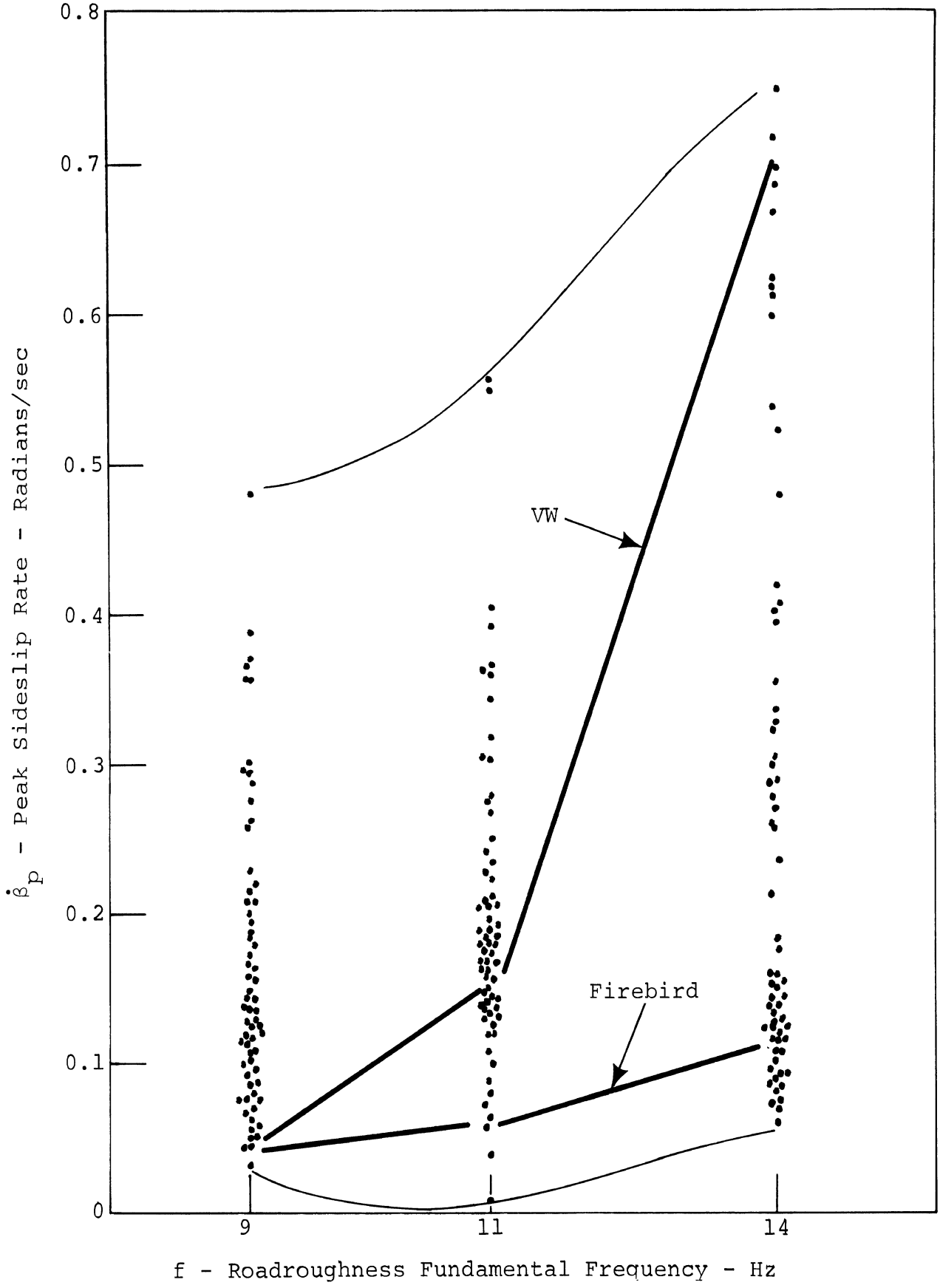

FIGURE 44

Summary Plot - Roadholding In A Turn

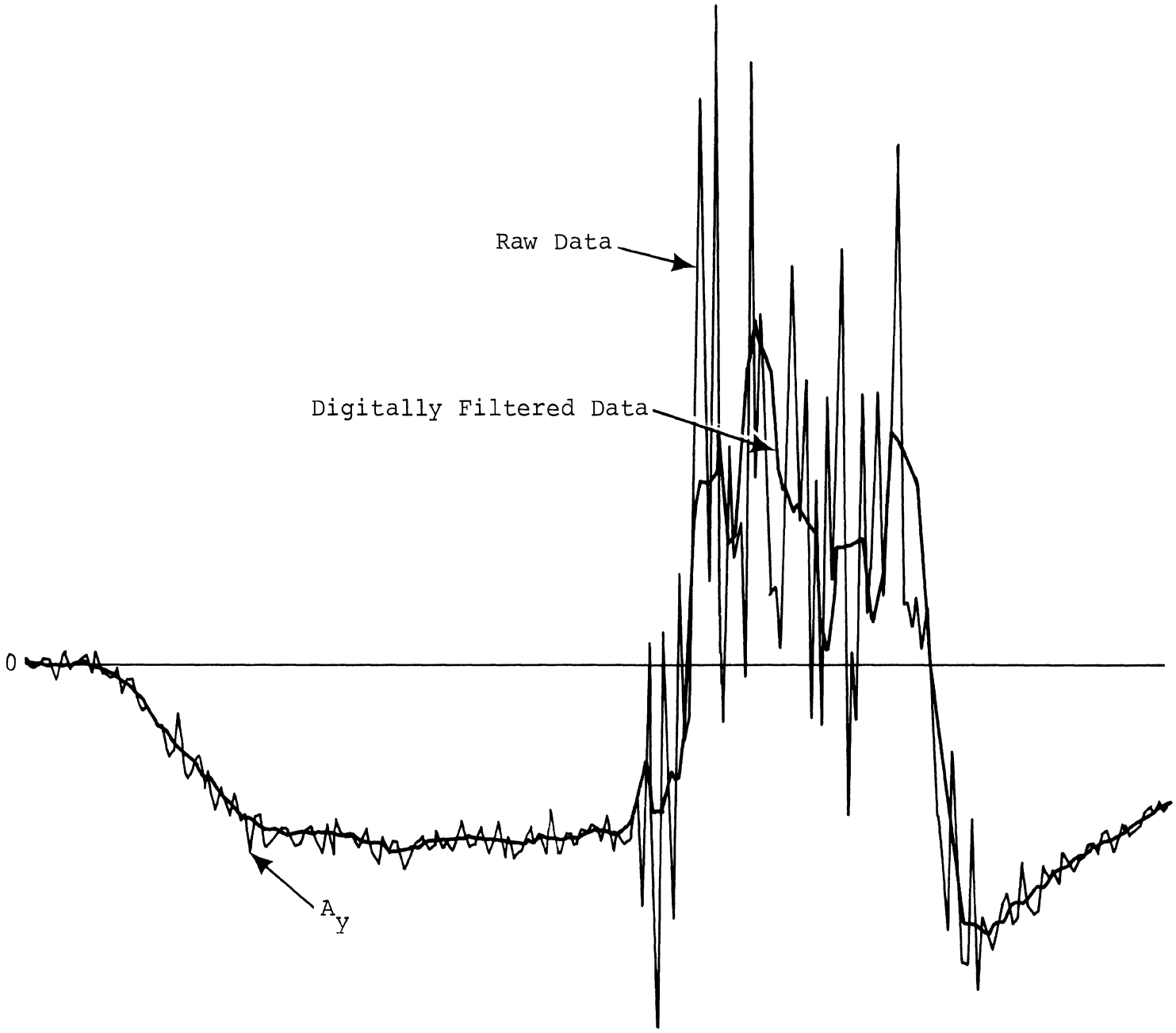

FIGURE 45

Raw A_y Data - Roadholding In A Turn - Mercedes 300 SEL

acquisition problem could be identified which would suggest that the data be discarded as invalid. This conclusion of validity is maintained, despite the observation of a high level of high frequency noise in the lateral acceleration signal on most vehicles. Lateral acceleration signals in excess of 4g peak-to-peak amplitude at 40 Hz resulted in this maneuver, which signal the physical range of the transducers, and thus were clipped. This vibration level, which is completely unknown in ride oscillation spectra [5], was unexpected and remains to be fully understood.

Accordingly, a cautionary note is attached to the data plots for this maneuver (see Appendix VII) indicating that certain distortions, believed to be small, may exist in these data.

3.3.4 TRAPEZOIDAL STEER. In the execution of the trapezoidal steer test procedure, a sequence of steer levels is executed, by which increasing levels of lateral acceleration result, eventually saturating the lateral force capability of specific tires. Test findings fall into three categories, distinguished by the manner in which side-force saturation of the tires is achieved. These categories of behavior are:

1. A "spinout" limit response is achieved, by which a dramatic yaw divergence is experienced as a result of side-force saturation being incurred on the rear tires at an input level which still leaves considerable side force capability on the front tires.
2. A driftout limit is achieved in which the front tires saturate in side force prior to rear tires, resulting in residual unrealized side force capability on the rear, such that any perturbations of vehicle sideslip beyond this nominal trim condition

result in increased side force on the rear tires, thus accounting for the stabilizing yaw moment which prevents any further accrual of rear tire side force.

3. A rollover response can be exhibited due to the large moment arising during the high lateral acceleration turn as aggravated by dynamic factors in the transient portion of the test. The contact of the wheel rim with the test surface can further contribute to a rollover response.

The two directional-response limits, categories 1 and 2, respectively, result in time histories such as are presented in Figures 46 and 47. In Figure 46 the spinout limit is depicted by a divergency in sideslip response. In Figure 47, the driftout limit is represented by a stable directional response. This driftout limit defines a boundary in turning performance which the vehicle is incapable of exceeding, but which generally is accompanied by a small sideslip response. The driftout condition is thus representative of a certain inefficiency in vehicle turning performance but does not involve the controllability challenge of the spinout limit.

It should be noted that the vehicle whose turning is limited by driftout is indistinguishable in the data, from a vehicle which is perfectly balanced to accrue lateral-force saturations on the front and rear tires simultaneously. Thus the trapezoidal-steer performance exhibited across the sample is not reduced into spinout and driftout categories, but rather is summarized in a general form, as shown in Figure 48. This presentation suggests that, improved or more efficient turning is associated with the maximum path curvature attainable with minimum sideslip. Figure 48 represents a cross-plot of the sideslip-rate

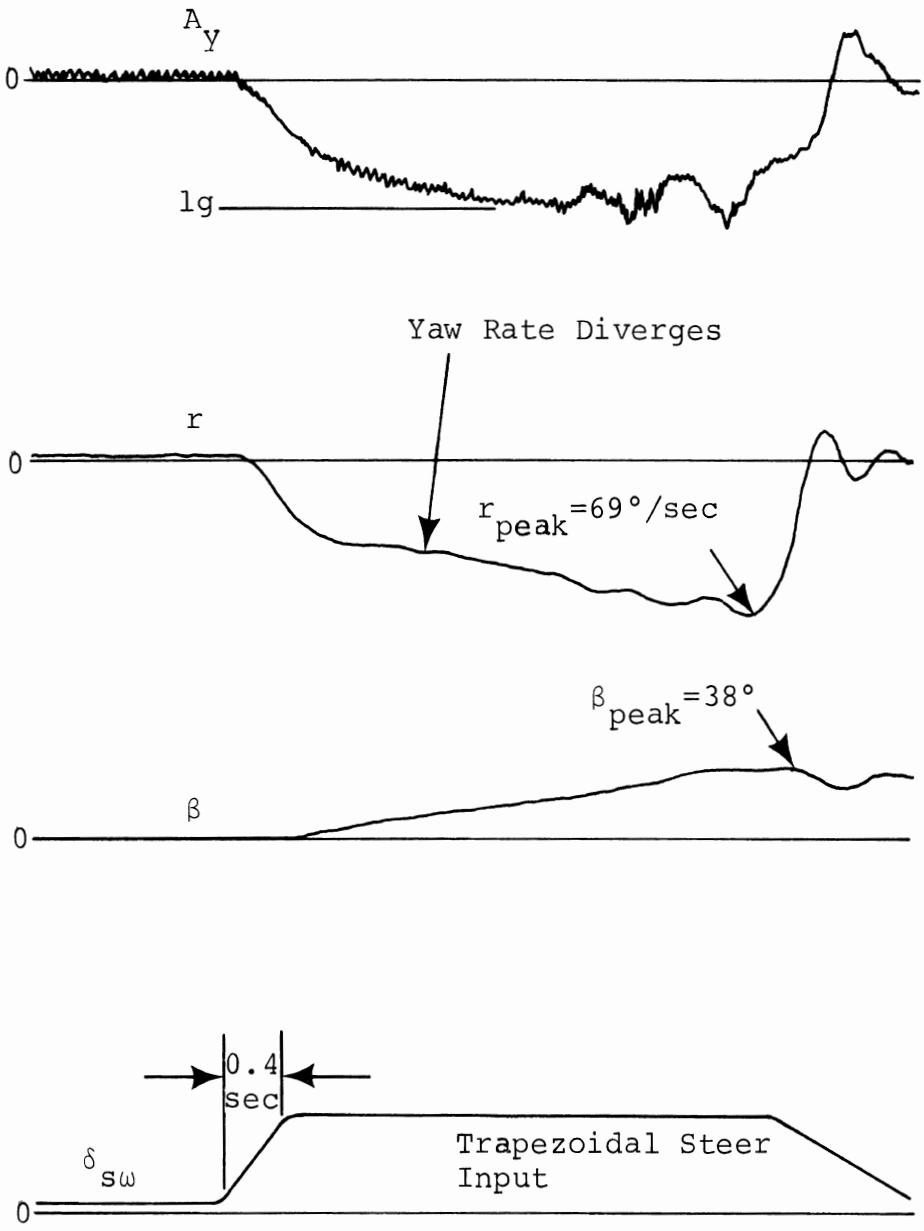

FIGURE 46

Trapezoidal Steer Rear Tire
Saturation - Spinout

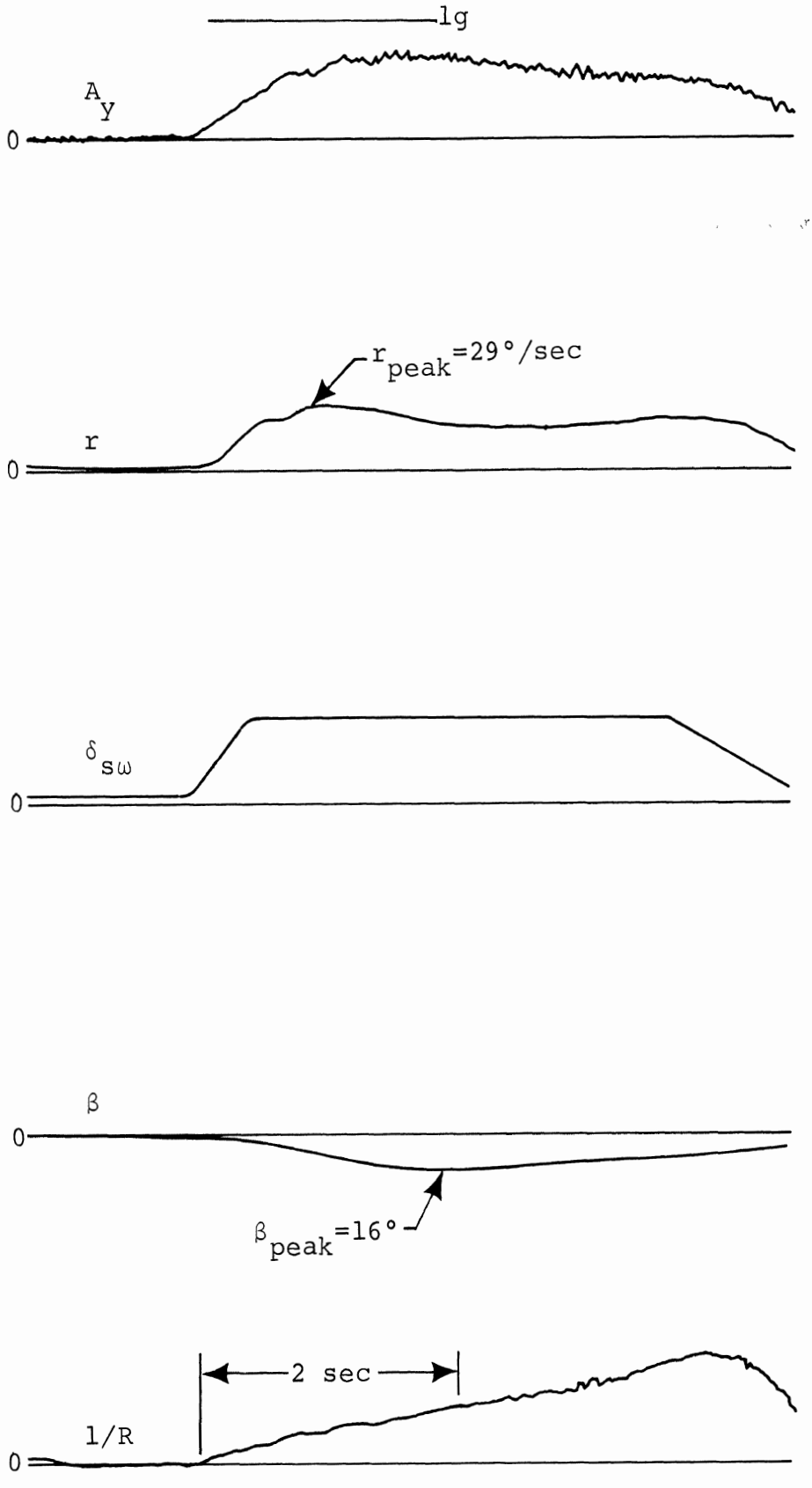

FIGURE 47

Trapezoidal Steer Front Tire
Saturation - Driftout

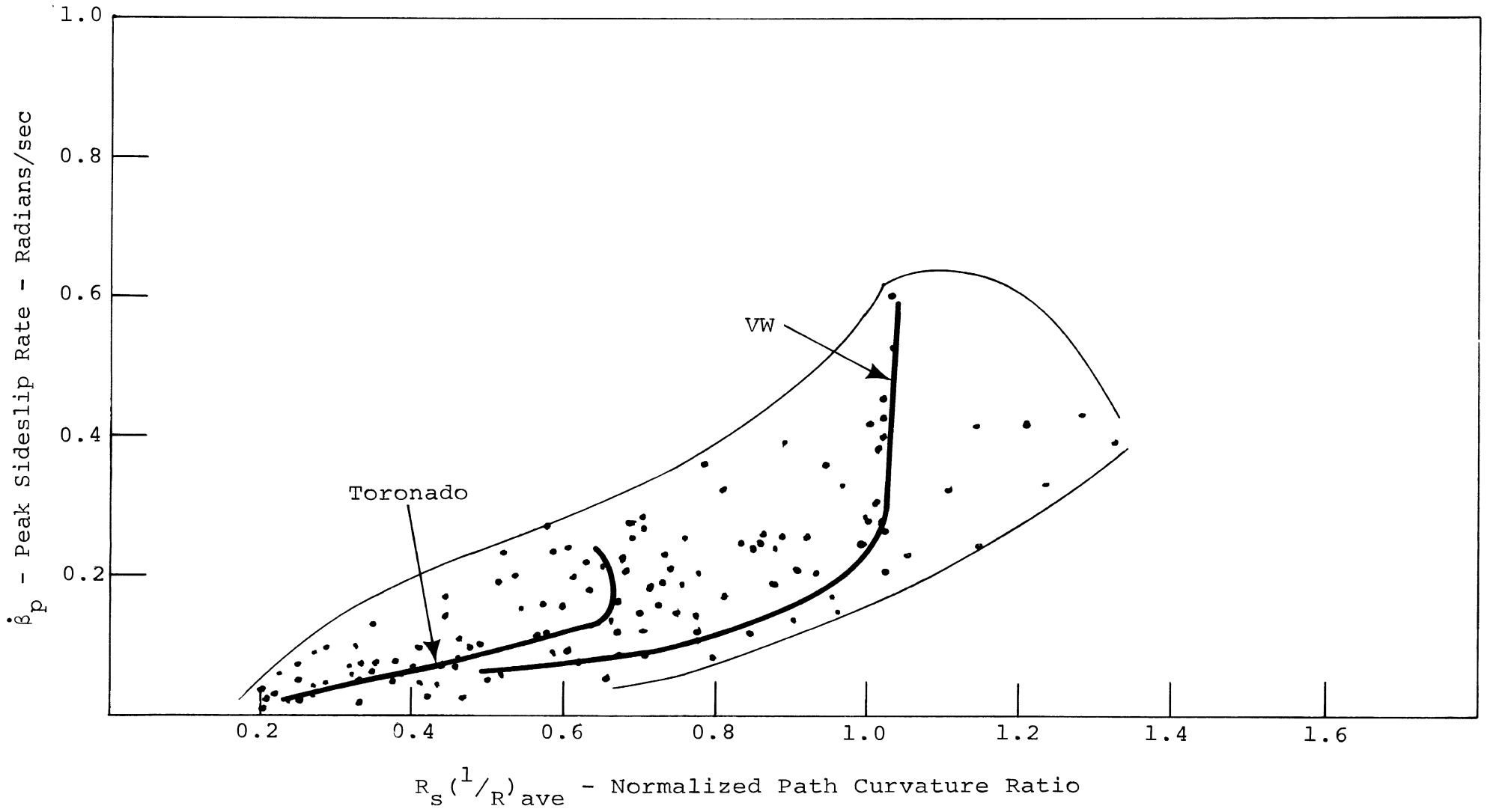

FIGURE 48
Summary Plot - Trapezoidal Steer

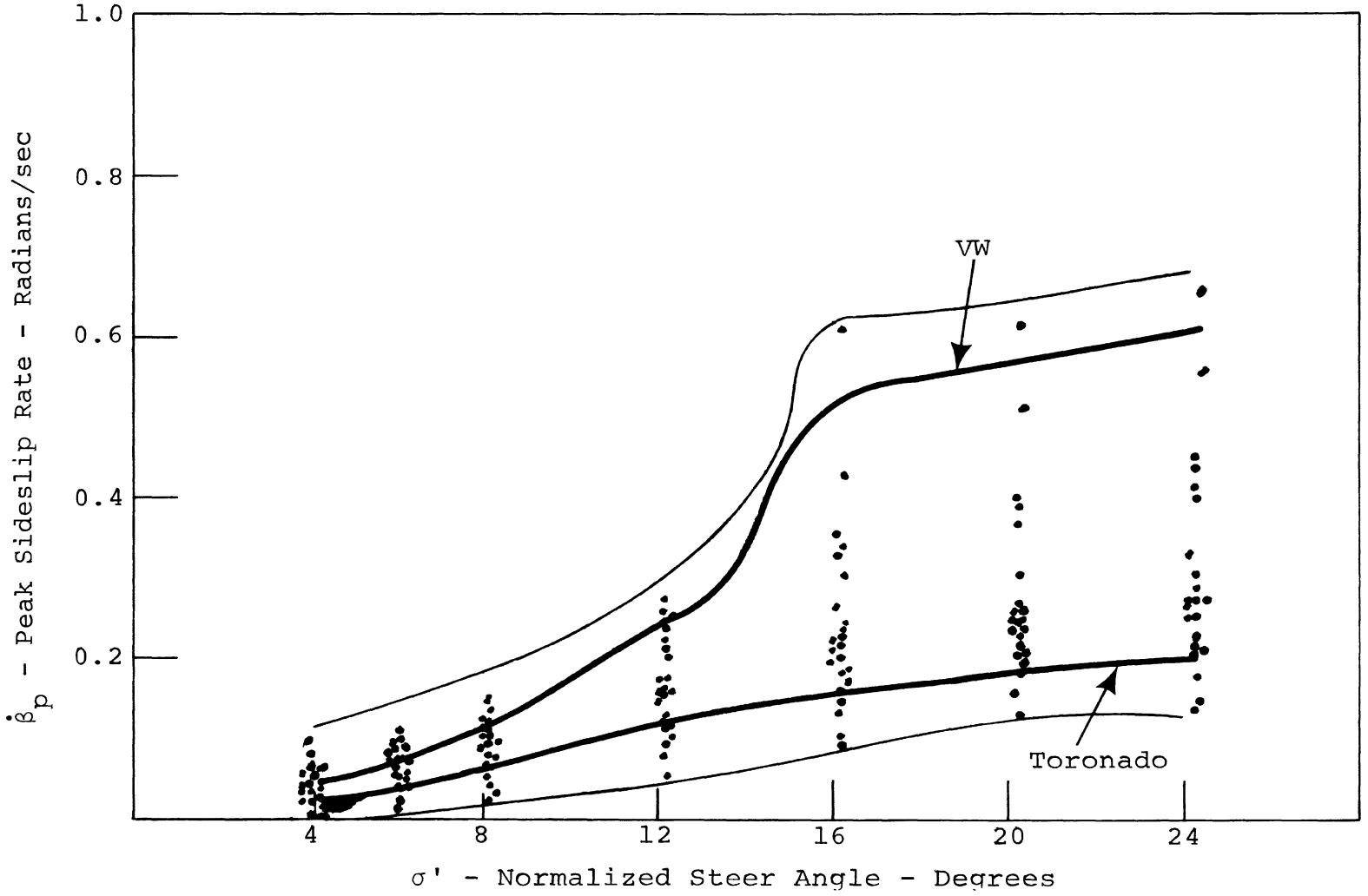

FIGURE 49
Summary Plot - Trapezoidal Steer

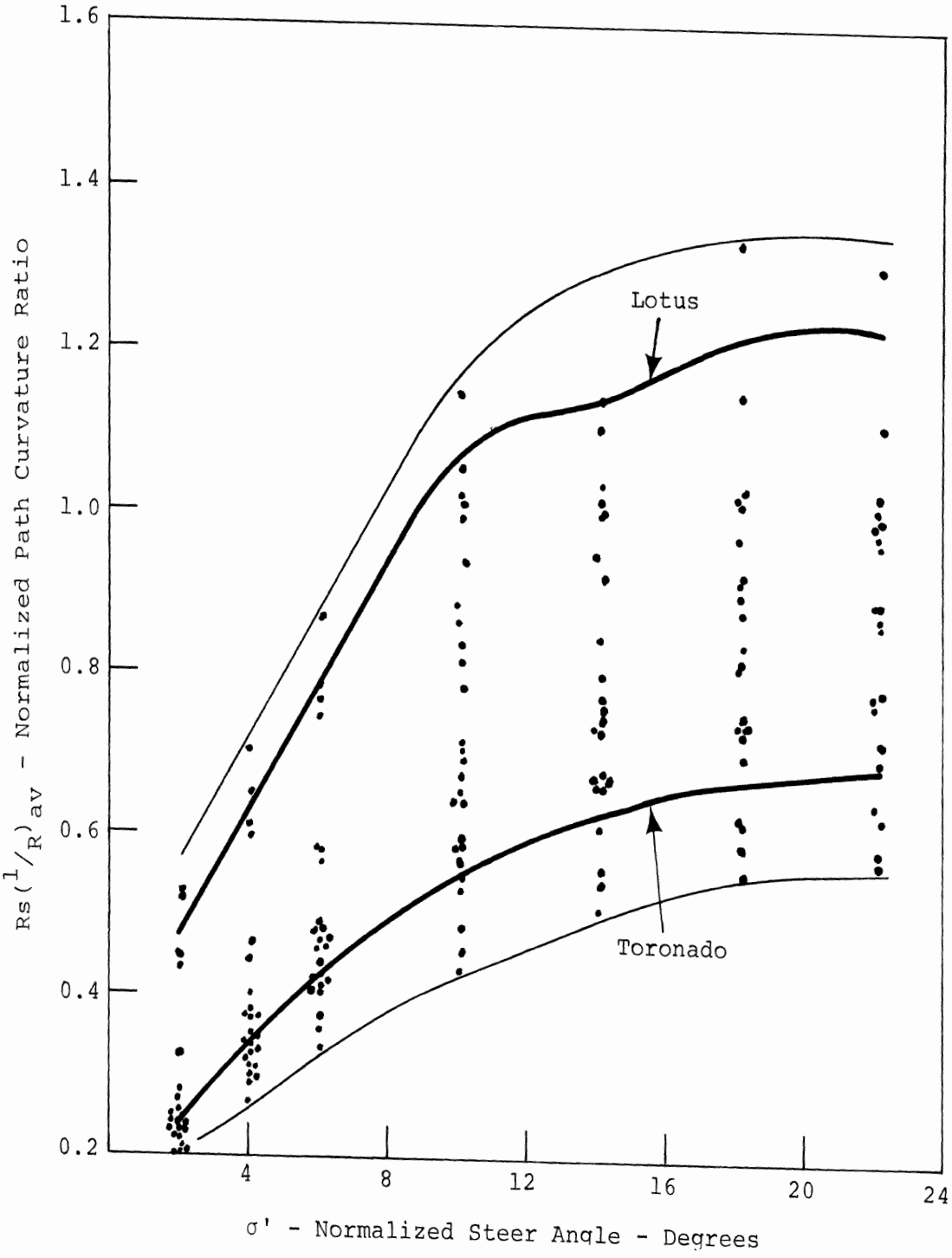

FIGURE 50
Summary Plot - Trapezoidal Steer

and path-curvature data shown in Figures 49 and 50. Example data from a spinout-limited vehicle (e.g., the VW) and an apparently driftout-limited vehicle (Toronado) are presented as overlays on each of these plots. Whereas Figure 48 is useful for categorizing overall limit performance in terms of path curvature without excessive sideslip, the data in Figures 49 and 50 provide a clear view of the manner in which turning properties change as steer level is increased. It would seem reasonable to expect that these transitions are also relevant as determinants of vehicle controllability.

The tremendous spread in the average path-curvature measures shown in Figure 50 derives from three factors which are evident in the time history data.

1. Certain vehicles indicate a large delay in yaw response, thus minimizing the average value which is computed over a two-second period.
2. Certain vehicles accrue such a large velocity loss over two seconds that they can exhibit a tightly curved path later in the run; thus biasing the average value upward.
3. Large differences in path-curvature capability exist, simply because of the differences in the normalized side-force capability of their installed tires. This fact is illustrated by the range of lateral acceleration levels shown in Figure 51.

The data in Figure 51 represents the range and distribution of the peak lateral accelerations exhibited during the tire shoulder break-in experiments. Clearly, a significant sensitivity to shoulder wear is the rule. Thus, it can be concluded that contemporary vehicles exhibit large differences in lateral acceleration capability, both when tires are unworn and when their tires have been lateral-force stabilized.

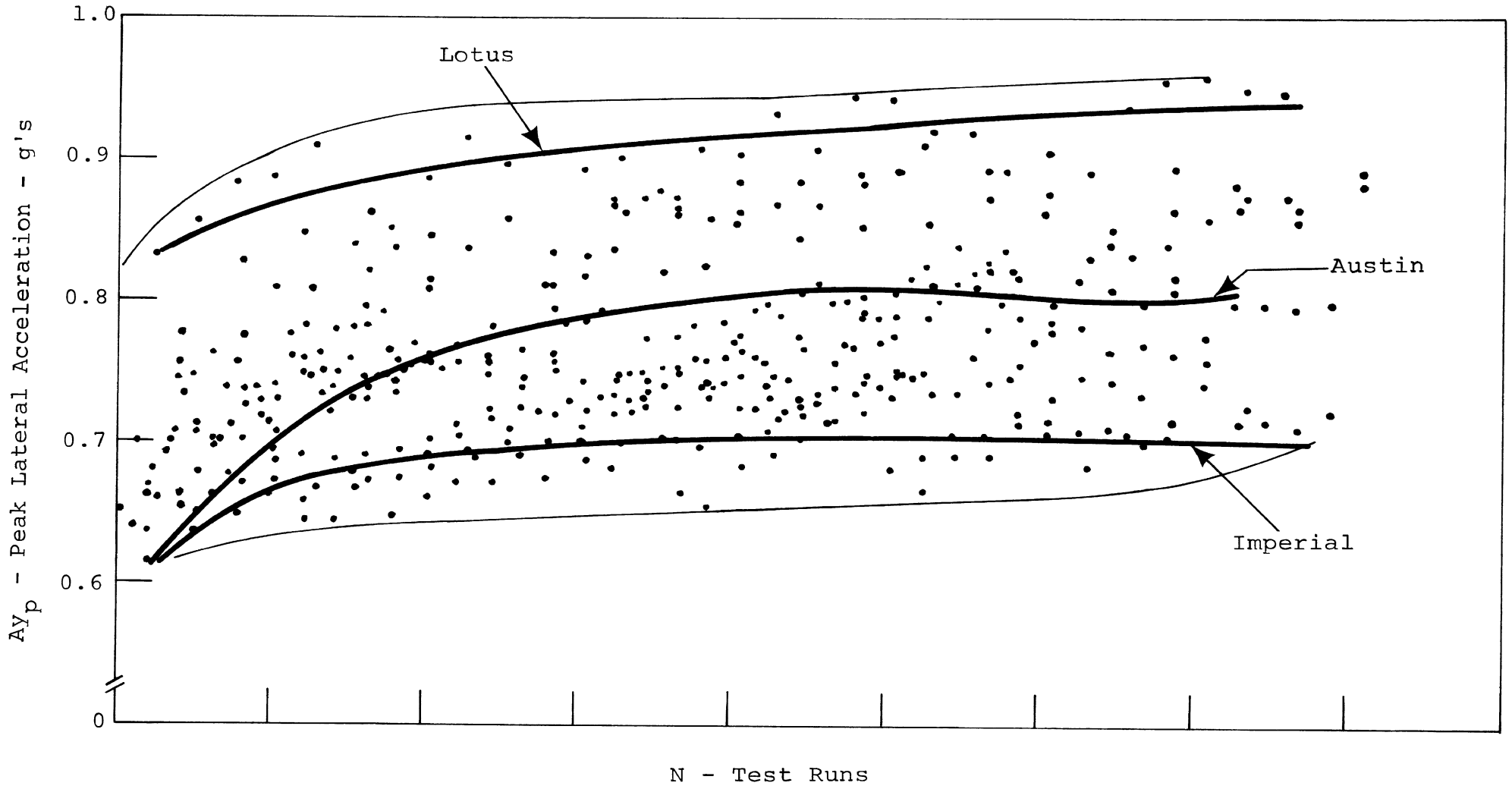

FIGURE 51

Summary Plot - Trapezoidal Steer - Tire Break-In Data

The following additional plots are presented in Appendix VII:

- Peak A_y vs. normalized steer level
- Peak r vs. normalized steer level
- Peak β vs. normalized steer level

Note that these plots of peak A_y and r are presented for comparison with earlier test findings even though each plot represents an inconclusive view of the turning response of a sideslipping vehicle.

It was seen that certain amounts of asymmetry are exhibited in the response plots of each of the indicated variables. Since these right to left differences are substantial in certain vehicles, the extra test burden of measuring both polarities of response seems to have been warranted.

Both the Volkswagen and Mercedes vehicles were observed to rollover in response to a trapezoidal steer input. The Volkswagen, which was the first vehicle to be tested in the automatic series, was rolled completely over onto its roof (Figure 52). This unexpected result made it clear that outriggers should be used in conducting this maneuver.

Substantially more damage was incurred on the Mercedes 300 SEL, when this vehicle exhibited a rollover response of such severity that a complete transfer of vehicle weight to the outrigger occurred, with all four wheels rising off the pavement. The ensuing oscillation, in which the vehicle mounted the outrigger and fell three times, caused major suspension failures. The costly repair of these extensive failures suggested that, in certain cases, less damage might be incurred by permitting complete follover rather than by restraining it.

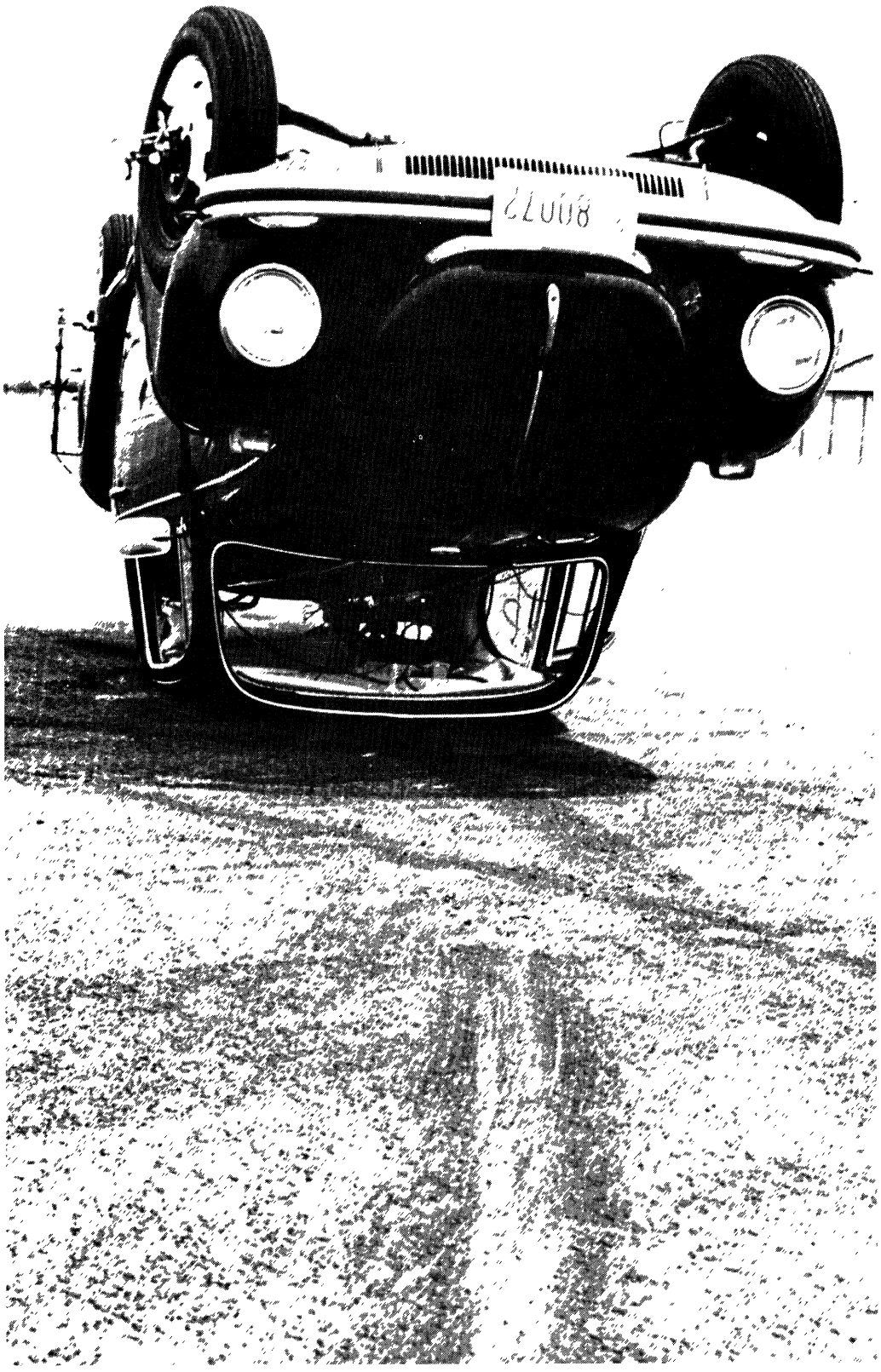

Figure 52.

Rollover resulting from trapezoidal steer input.

3.3.5 SINUSOIDAL STEER TEST. In this maneuver, vehicles can exhibit a wide range of responses which are patently unlike a lane change. Most commonly, increasing the steer amplitude simply results in lateral displacements which are in excess of the nominal dimensions of the roadway. Thus, with regard to a lateral displacement response, the concept of a defineable limit would not seem to apply. Certain vehicles in the sample, however, indicated a remarkable propensity for achieving near-perfect lane change trajectories over the entire range of steering amplitudes. Thus a lateral displacement "saturation" or limit was exhibited, but the mechanisms by which certain vehicles achieved this limit involve very complex motions, for which no generalized understanding has been developed.

Two categories of yaw response limit have been identified, however, which can be characterized as asymmetries of directional gain in response to the leading and trailing half-waves of the sinusoidal steer input. These limit responses have been grouped into "undercorrective" and "overcorrective" yawing motions in which the 2nd half of the sine wave is viewed as the corrective or recovery stage, during which the driver is attempting to reestablish his initial heading.

In the undercorrective response, the vehicle accumulates a large sideslip angle early in the maneuver, such that the recovery half of the steer input is essentially nullified. A raw data sample typical of this condition is shown in Figure 53. The vehicle's front tires, during the second half wave of steering input, experience an insufficient sideslip angle of the recovery polarity to effect sufficient restoring yaw moment. Carried to the extreme, a spinout is initiated with the first half wave of steering, which spinout the

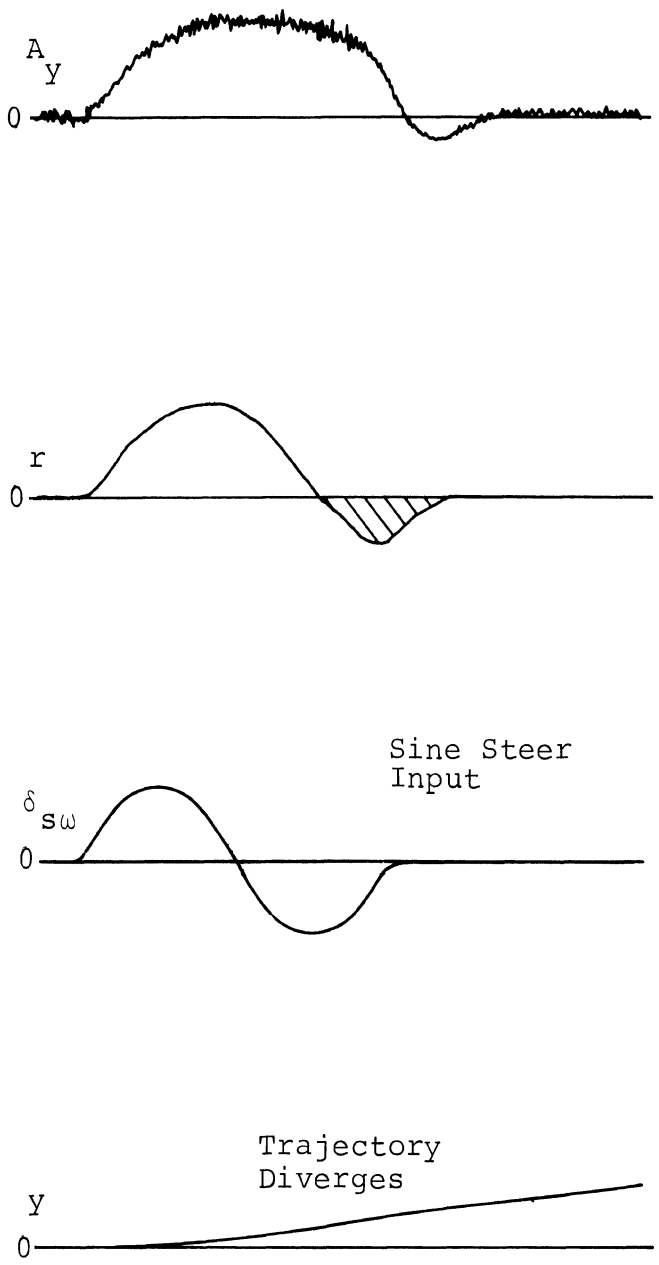

FIGURE 53

Sinusoidal Steer
"Undercorrective" Response

second half of the symmetric steer input is incapable of arresting.

The overcorrective response, as typified by the time histories shown in Figure 54, results in a terminal heading which is directed back toward the original lane from which the maneuver began—the recovery half of the steering input being more effective than the initial steering input. The physical mechanism underlying this phenomenon remains to be fully identified.

Six summary plots are presented in Figures 55 through 60, indicating the range and distributions of:

1. Peak sideslip response vs. steer level at 45 and 60 mph (Figures 55 and 56);
2. Lane change deviation vs. steer level at 45 and 60 mph (Figures 57 and 58);
3. Sideslip response vs. lane change deviation at 45 and 60 mph (Figures 59 and 60).

In Figures 55 and 56, the peak sideslip angle exhibits a monotonic upward trend for all vehicles, and clearly indicates a narrow performance range for the sample. Figures 57 and 58 clearly illustrate that certain vehicles manifest a reasonable approximation of a lane-change trajectory over a wide band of steer inputs, while others exhibit lateral displacements of substantially larger dimension.

The basic trend observed for all vehicles is a minimum value of Δ occurring at some value of steer level, σ, between 4 and 10. Below these values of σ, the steering amplitude is not sufficiently large to result in a lateral displacement near 12 feet, (when $\sigma=0$, the value of Δ must be 12, because the vehicle will run a straight course 12 feet away from the adjacent lane). It was observed that the vehicles which exhibit the largest values of Δ at higher steer levels also

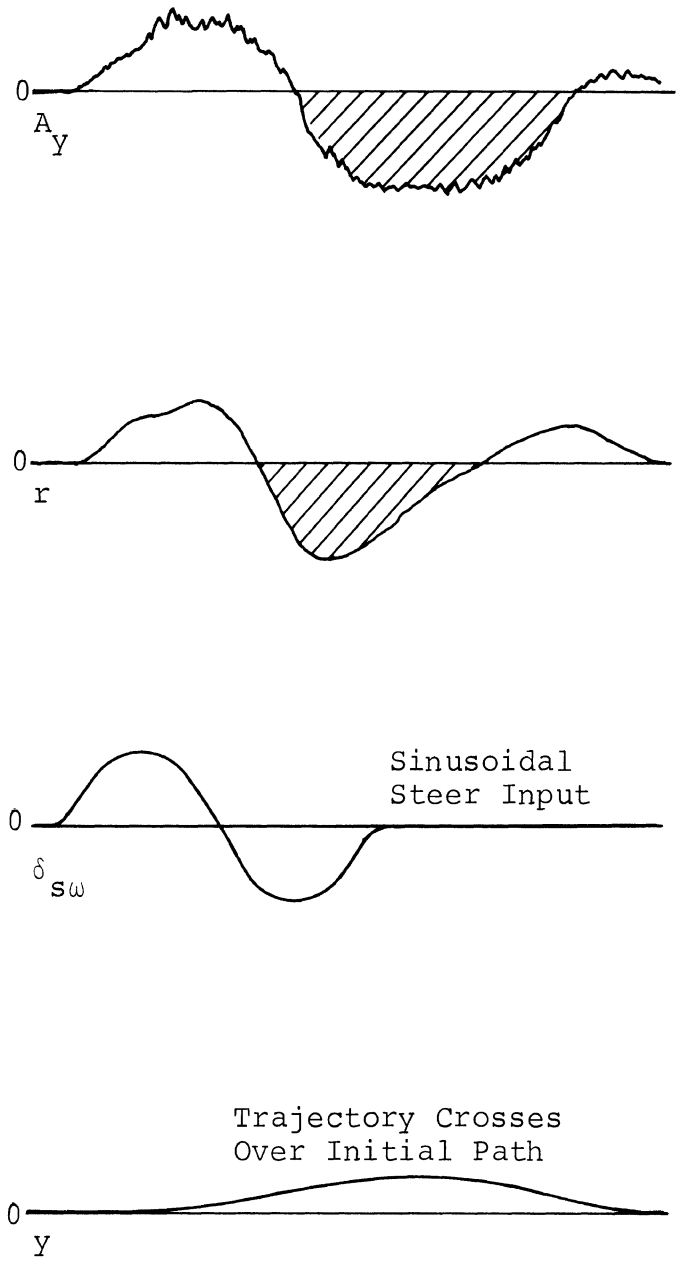

FIGURE 54

Sinusoidal Steer
"Overcorrective" Response

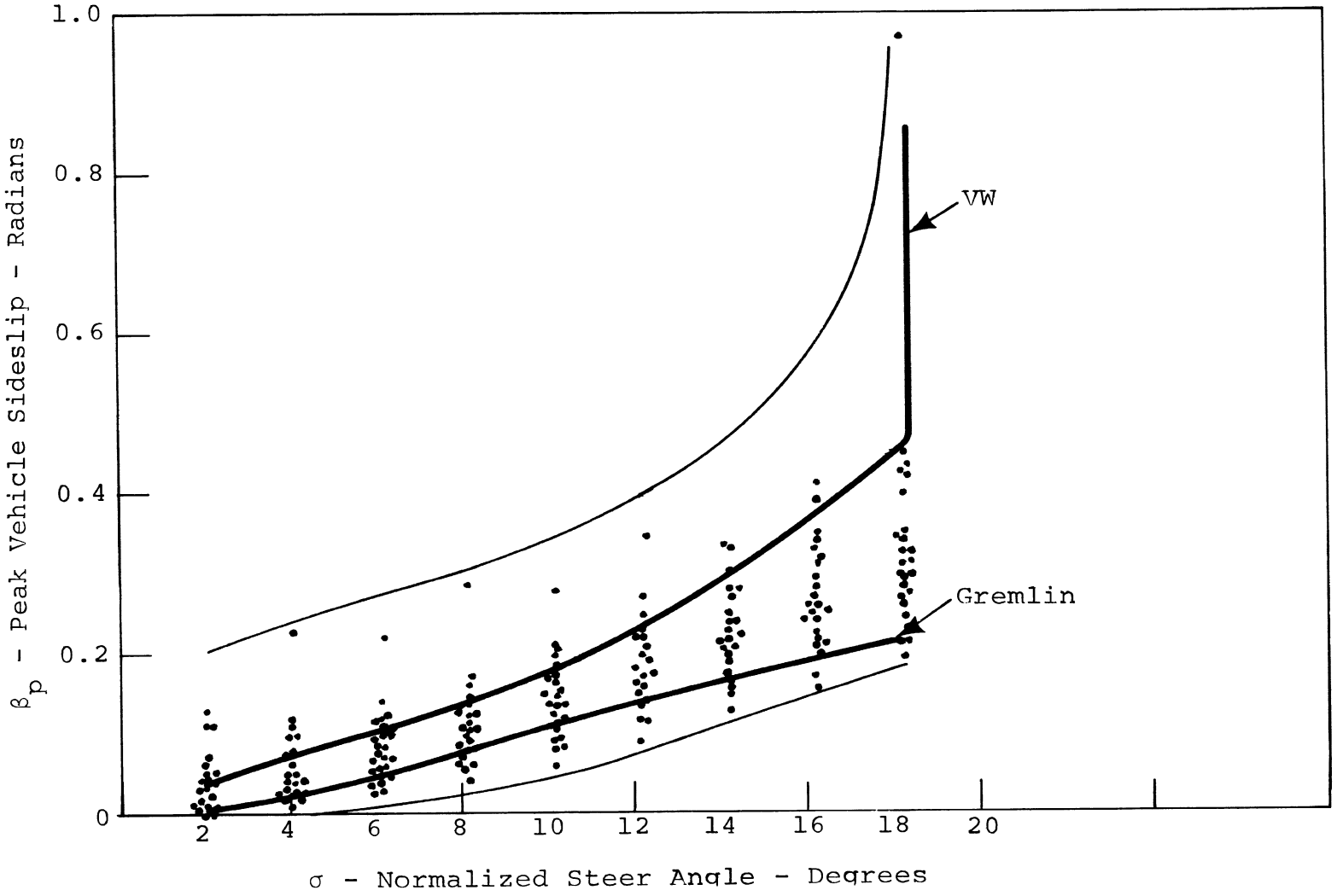

FIGURE 55
Summary Plot - Sinusoidal Steer - 45 mph

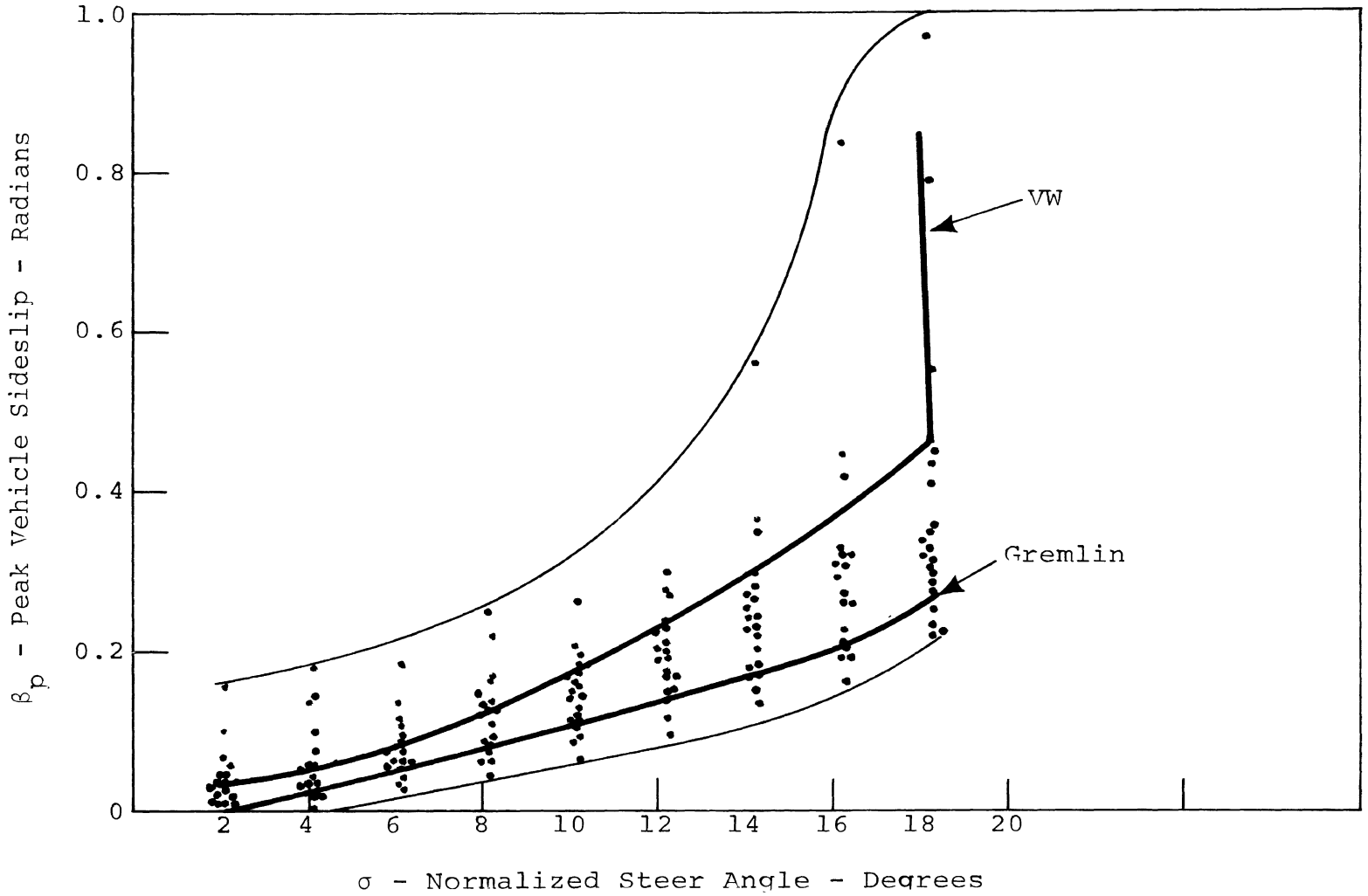

FIGURE 56

Summary Plot - Sinusoidal Steer - 60 mph

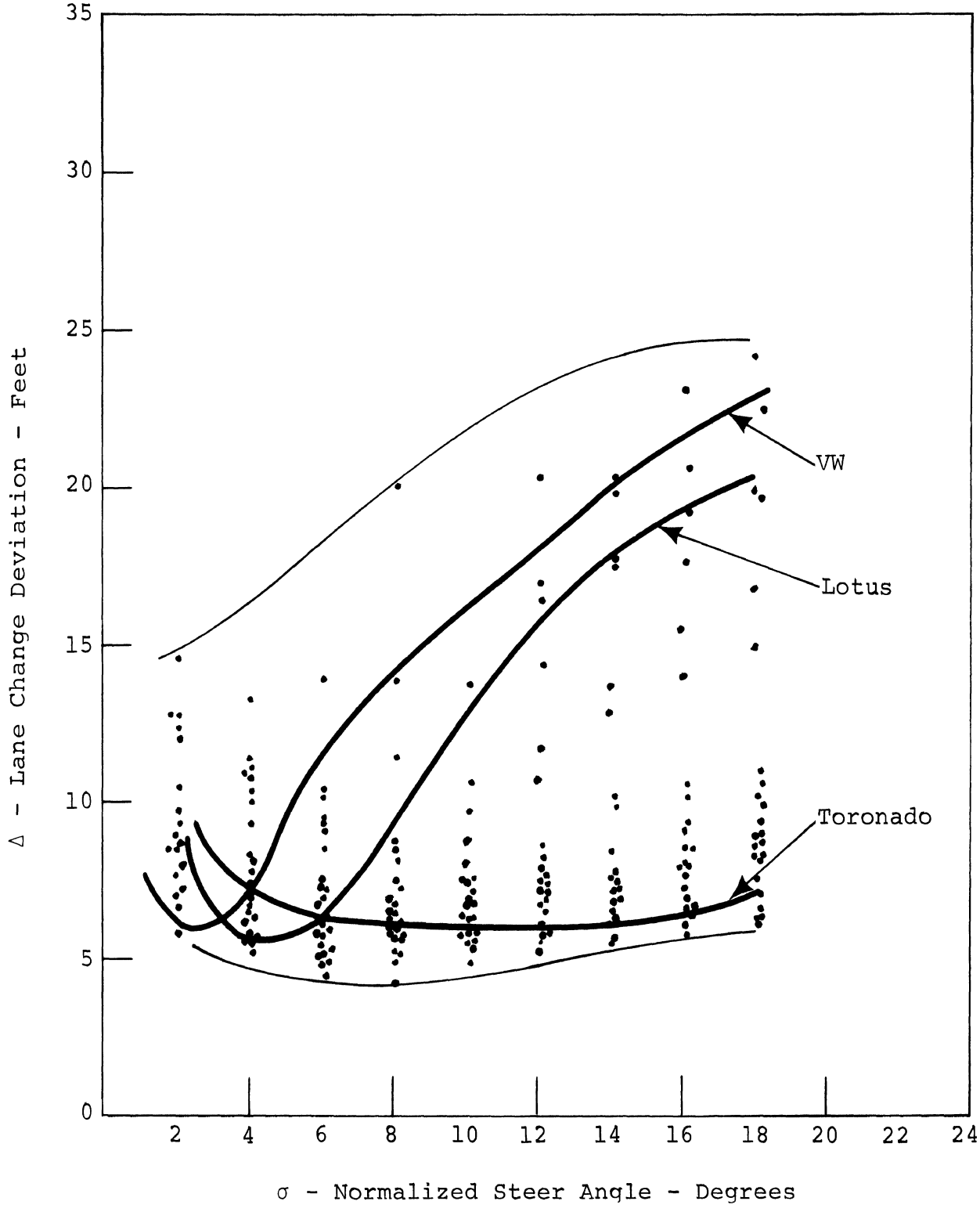

FIGURE 57

Summary Plot - Sinusoidal Steer - 45 mph

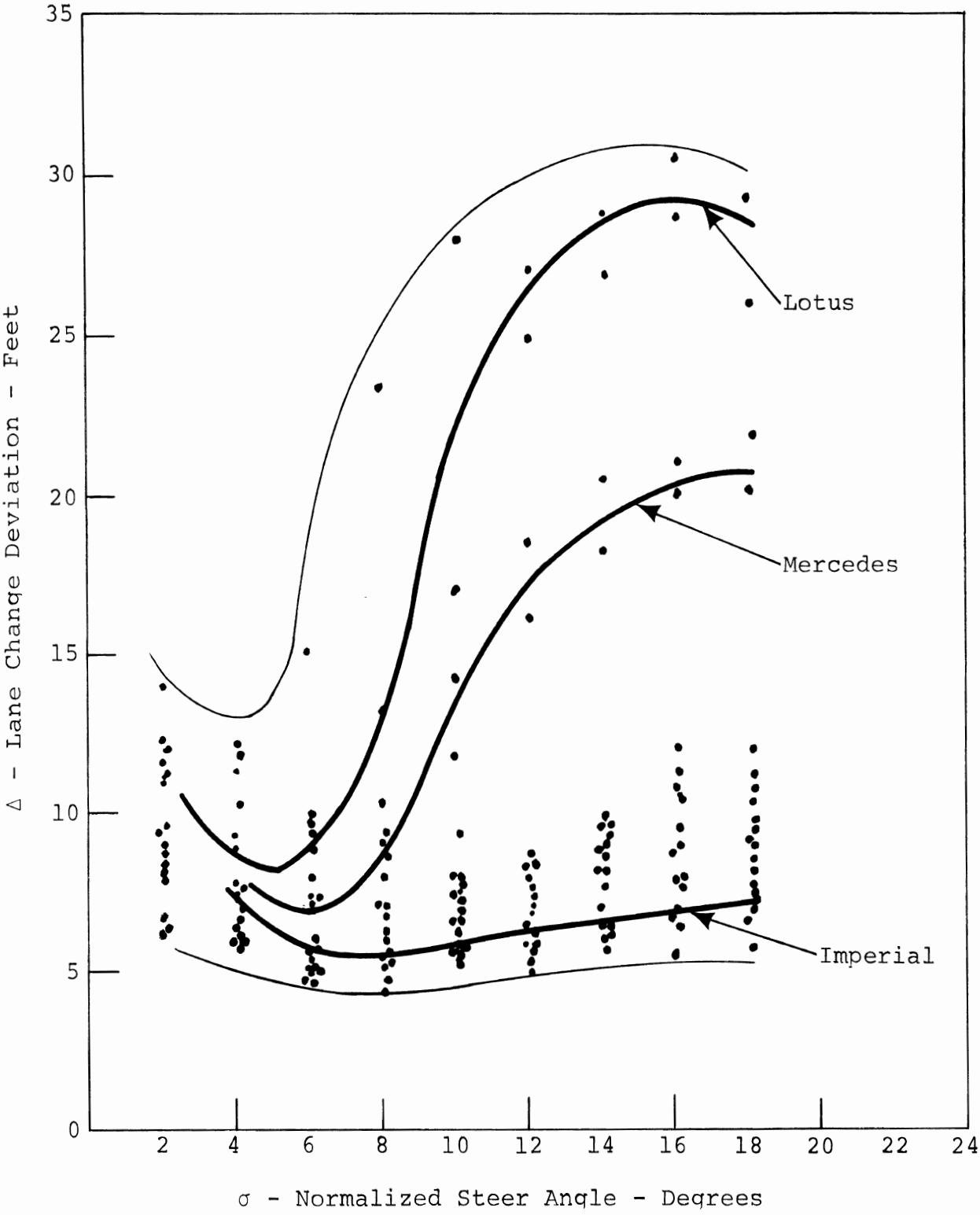

FIGURE 58

Summary Plot - Sinusoidal Steer - 60 mph

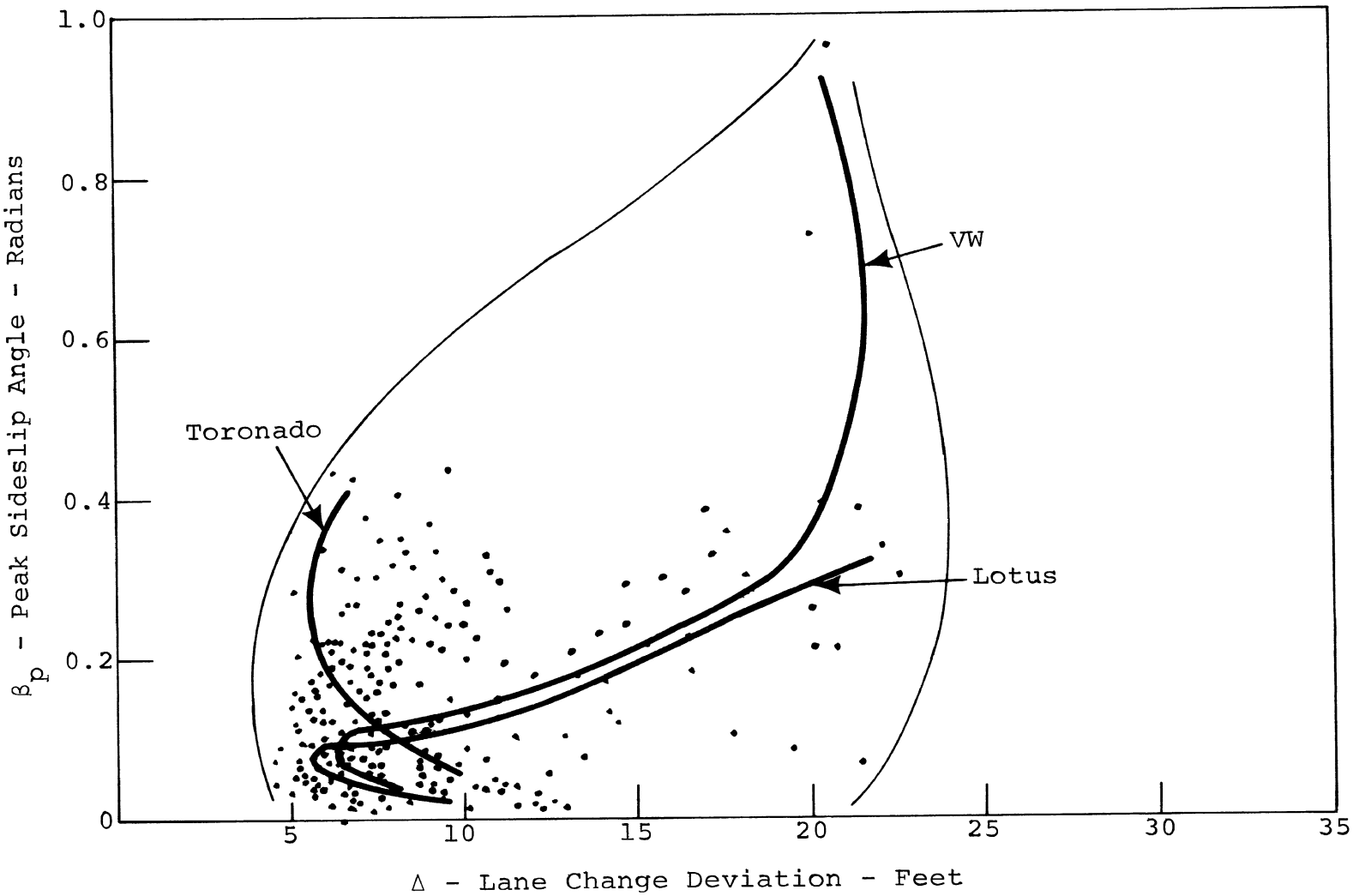

FIGURE 59
Summary Plot - Sinusoidal Steer - 45 mph

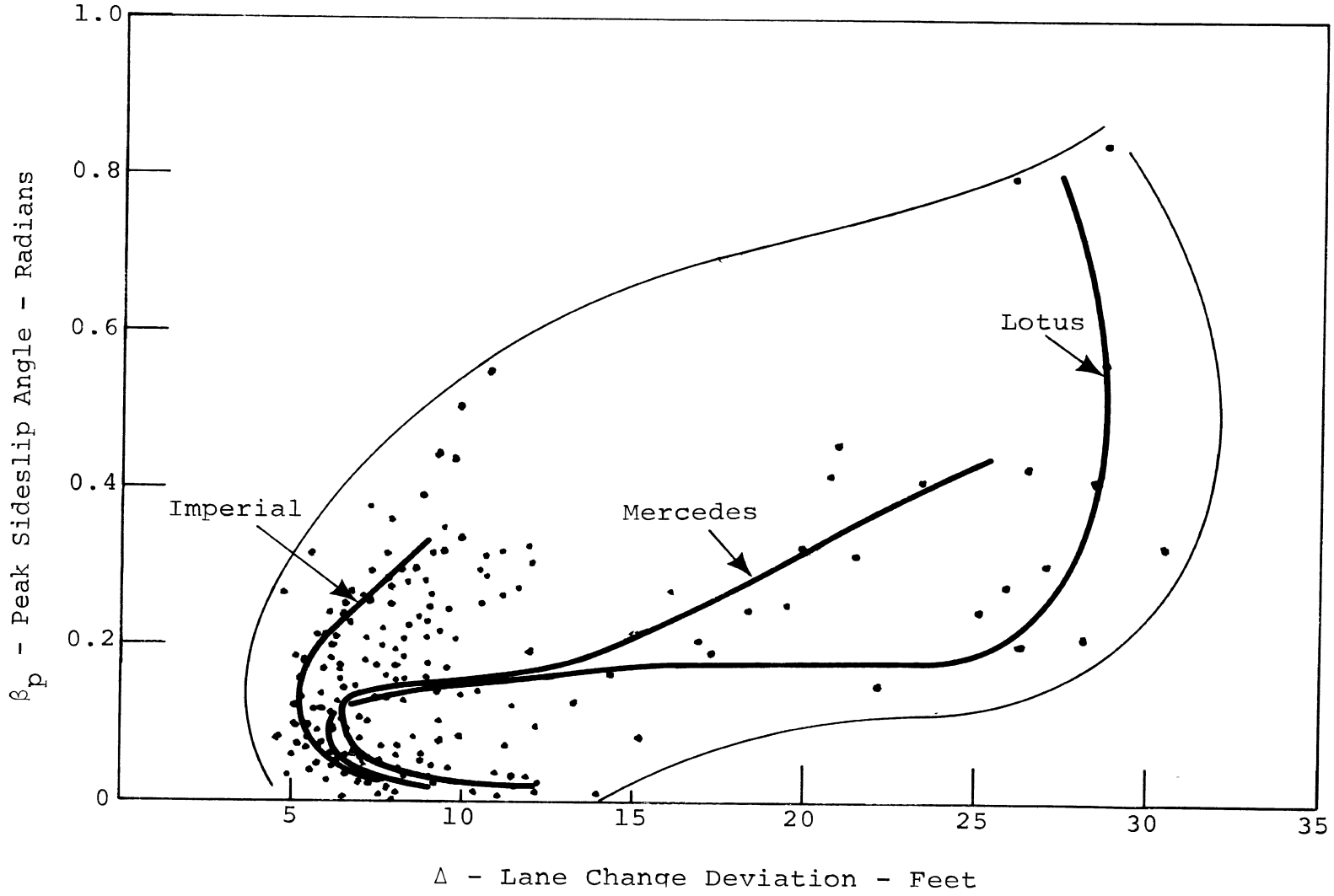

FIGURE 60
Summary Plot - Sinusoidal Steer - 60 mph

manifest an undercorrective yaw response. Additionally, many of the vehicles exhibited significant amounts of asymmetry in this measure, when lane changing to the left compared with lane changing to the right.

Figures 59 and 60 summarize the Δ/β responses for the sample. Whereas certain vehicles cluster their responses near the origin, others appear to define the range for both the Δ and the β variables.

3.3.6 DRASTIC STEER AND BRAKE. The only limit response of interest in this maneuver is the manifestation of an unstable roll motion. Sample time histories obtained for a vehicle exhibiting a limiting roll response are shown in Figure 61. Following release of the brake, a dramatic increase in lateral acceleration is observed, accompanied by a roll moment imbalance which rapidly increases the roll angle up to the point of outrigger contact. Only the Volkswagen and Mercedes exhibited such a limit response with peak roll angles exceeding 0.4 radians, prior to the motion being arrested by the outriggers, Figures 62 and 63.

A summary of the range and distribution of peak roll angles exhibited by the sample are presented in Figure 64, showing a range of stable responses falling within an 0.2 radian band.

3.3.7 OTHER FINDINGS OF THE FULL-SCALE TEST PROGRAM. In the course of conducting the full-scale test activity, certain observations were made relating to vehicle performance and test methodology. These items will be discussed below.

1. On many vehicles, mechanical failure of steering and suspension system components was observed to result from repeated limit-maneuver testing. In limit-turning maneuvers, failures were experienced

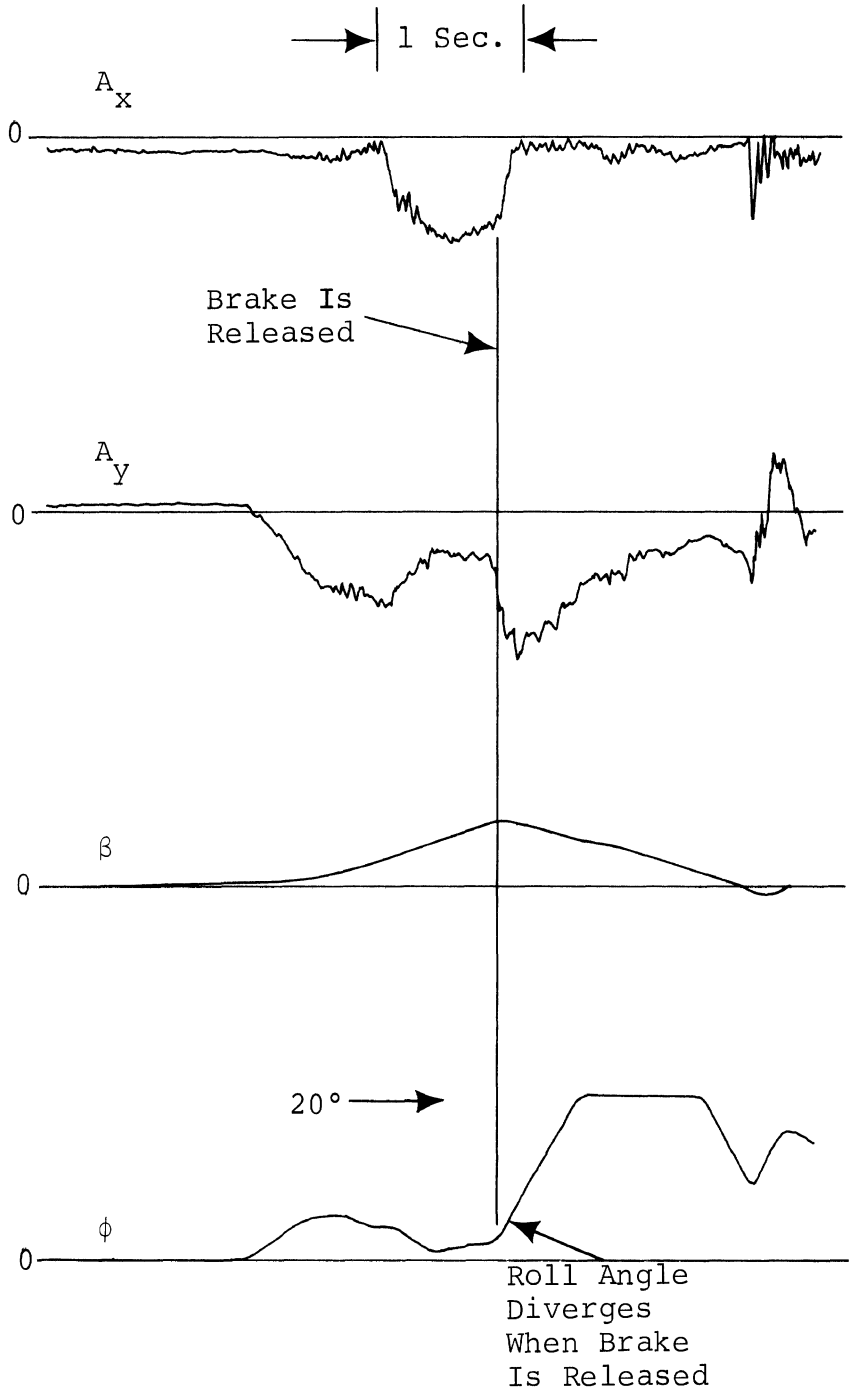

FIGURE 61

Drastic Steer and Brake
Divergent Roll Response

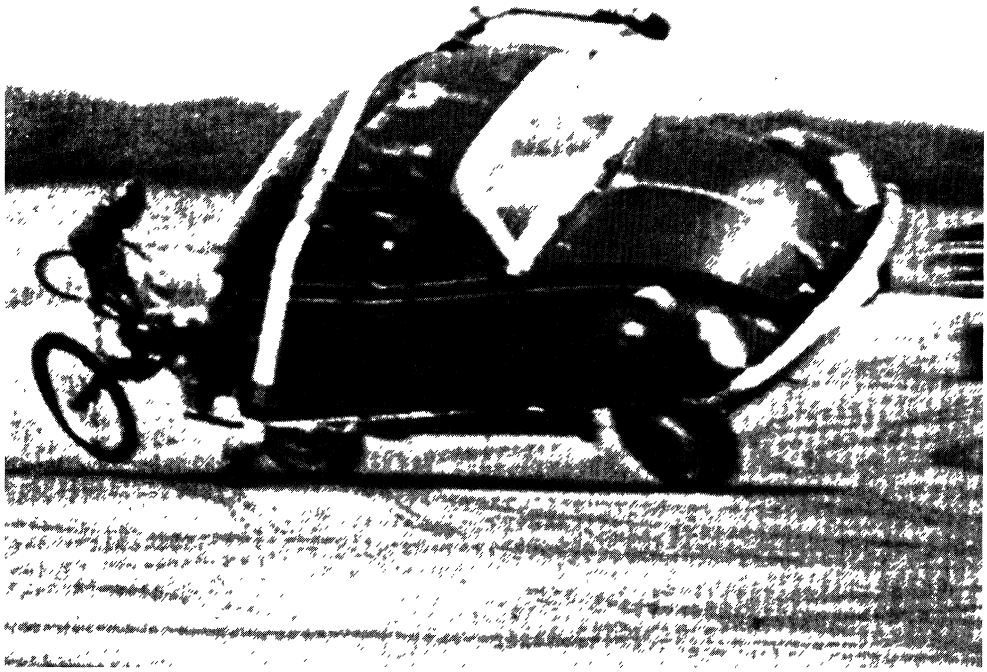

Figure 62.

Roll response to drastic steer and brake input.

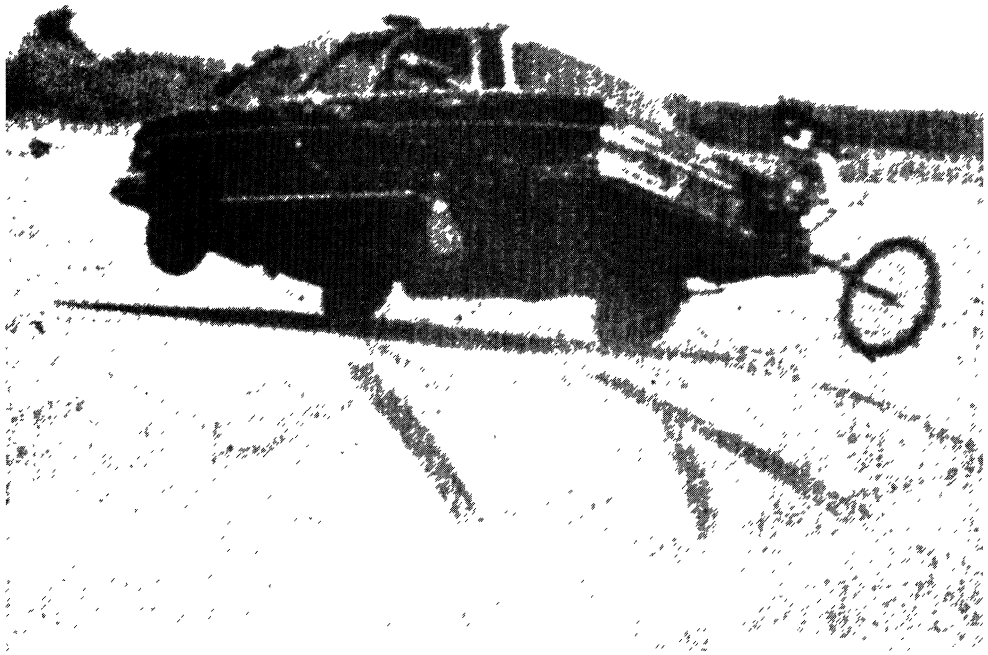

Figure 63.

Roll response to drastic steer and brake input.

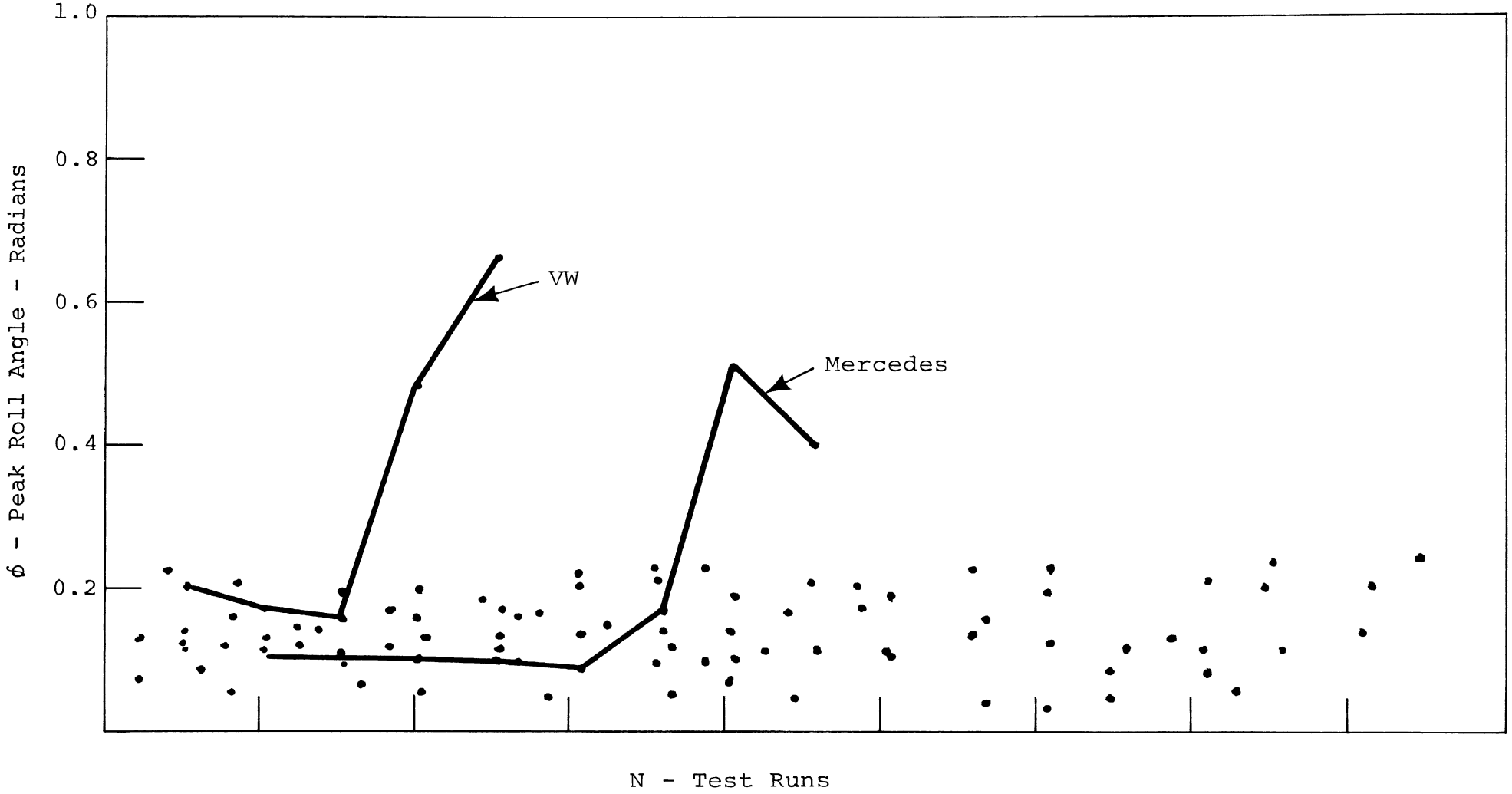

FIGURE 64

Summary Plot - Drastic Steer/Brake

with control arms, wheel spindles, wheels, and rear-axle inner fluid seals. Various brake system components failed during repeated limit braking, including brake shoes, back-up plate, master cylinder, and, in certain vehicles, brake-limiting valves. As mentioned earlier, the restraint of rollover response with outriggers was observed to cause massive failures in suspension components as a result of the violent energy exchanges accompanying the roll-hopping phenomenon.

2. Deflation of the outside front tire during limit turning was observed with certain of the heavier test vehicles. These occurrences generally resulted in wheel failure, excavation of the test surface, and severe distortions in front-end alignment.

   Tire deflation due to bead unseating, as well as wheel rim contact without tire deflation, were felt to be somewhat aggravated by the maintenance of "cold" inflation pressure as a test practice. Although the procedure of maintaining the cold inflation level appears warranted on safety grounds, it is clear that tire structural properties are sufficiently sensitive to inflation pressure that this practice can result in response anomalies which may not occur at higher inclation levels.

3. The Toyota Corolla exhibited repeated rollover responses during a large number of driver-executed limit-turn experiments. These tests were being performed to obtain side-force stabilization of a set of tires prior to performing the driver-series tests. After experiencing numerous suspension

failures as a result of a violent rolling response, (Figure 65) the vehicle was removed from the test sample to preserve test schedules.

4. While being operated in the automatic test series, the Austin America was heavily damaged in a collision with a pole. This event occurred when the engine failed while the vehicle was being negotiated through a confined section of the test facility. Hydraulic power loss occurred and was followed by an abort brake application but substantial velocity existed prior to impact resulting in major damage (Figure 66). This experience emphasizes the need for sufficient operating clearance while guiding vehicles remotely. Destruction of the vehicle occurred prior to completing the 60 mph sinusoidal-steer tests and the drastic steer brake tests.

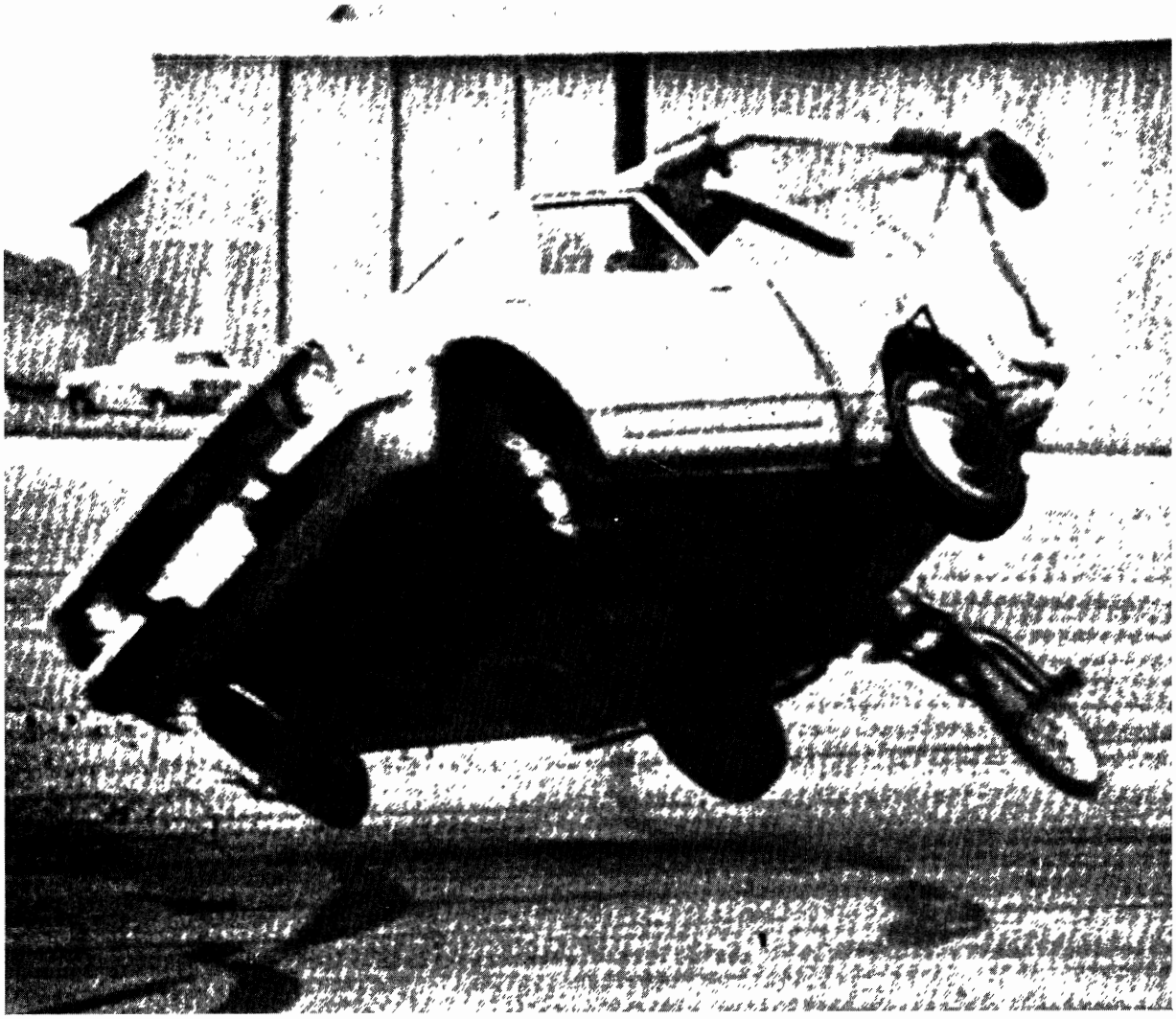

Figure 65.

Response to trapezoidal steer input—applied by a driver, during tire wear-in tests.

Figure 66.

Impact damage incurred following loss of controller power.

4. CONCLUSIONS AND RECOMMENDATIONS

4.1 CONCLUSIONS

The most significant single finding of the program bearing on the conduct of open-loop performance testing is that tire side-force capability is a first-order function of the shoulder wear resulting from limit turning maneuvers. Five specific conclusions result from this finding:

1. It appears that adequate measurements of "O.E." limit cornering performance cannot be made for certain tire-vehicle systems by a testing method that utilizes repetitive runs as a means of searching for the limit, since the testing process acts to alter the O.E. condition.
2. The rate of change of side-force capability with test runs is so large with many tire-vehicle systems as to render any compensating tire change procedure impractical.
3. It is apparent that the limit cornering capability of some vehicles will be substantially lower in the O.E. condition than the theoretical level that would occur from either
   a) different tire selection, or
   b) the same basic O.E. tire, manifesting (by some modification of design) its full potential as indicated by the performance exhibited with a worn shoulder.
4. Indiscriminate changing of tires at any of the wheels of a vehicle subjected to severe cornering maneuvers may result in a wide scattering of its directional response properties. A similar conclusion is presented in a GM document [6] which states

that "...mixing of worn and new tires on the front and rear of a car can substantially alter the balance of tire properties that affect vehicle handling performance."

5. Those tires that indicate a substantial sensitivity to shoulder wear also illustrate a stable performance regime which is established at a sufficiently low level of wear that tire structural integrity is not yet compromised. Thus, certain performance envelopes can be obtained, although admittedly non-O.E. performance, on vehicles equipped with shoulder-worn (i.e., side-force stabilized) tires.

Support for these conclusions derive from the data presented in Appendix IV.

Two other basic conclusions derive from the side-force variation experiments that were performed with the tires used on the test vehicle sample:

6. No systematic variations in tire side-force capability were seen to accompany asphalt pavement temperatures ranging from 83° to 119°F.
7. An asphalt surface which has been wetted with water (only) can be presumed to have recovered its dry friction properties as soon as the surface "appears dry," (i.e., no residual discoloration).

Six major conclusions have been reached from the findings produced in the full-scale test program:

8. In general, modern vehicles vary widely in their limit maneuvering properties.
9. Certain modern passenger vehicles can be caused to roll over on a smooth surface, as a result of steer inputs alone.

10. Certain vehicles exhibit tire deflation due to bead unseating while maneuvering on a smooth surface.
11. Certain vehicles will provide very nearly a lane change trajectory in response to sinusoidal steer inputs which span almost the entire ergonomically achievable range of steer amplitudes.
12. Certain vehicles can roll over so violently, as a result of maneuvering on a smooth surface, that the use of outriggers to arrest such motion will not necessarily result in minimum damage being incurred.
13. Existing reduced-friction test technology is inadequate for conducting limit maneuver (open-loop) testing, at elevated velocities.

The use of the automatic controller in this program yields a number of observations which permit the reasonability of its application to handling studies to be assessed:

14. The application of automatic controllers to the open-loop measurement of limit responses appears to be a practical experimental method. (Whereas an assessment of "practicality" is subjective in nature, further observations are made in support of this judgment.)
15. It has been found that installation of the system is possible on any passenger vehicle if certain minor alterations are allowed, for example, modifications to obtain clearance and mounting support for an automatic lift fifth wheel, the steer, brake, and accelerator servos, and an engine-mounted hydraulic pump. The installation of the automatic controller package is usually achievable with 3 man-days of technician effort, once the required modifications have been made to the vehicle.

16. A level of reliability has been achieved which is comparable to other complex experimental apparatus, such as tape recorders, stable platforms, etc.. On the average, one hour is spent in maintenance for every ten hours spent in running. Set-up time is required with each vehicle installation for gain calibration and zero setting.
17. The quality of the automatically-controlled tests is such that an overall precision (initial velocity, input wave shapes, and input timing) within 2% is consistently achieved.
18. The apparatus has been found sufficiently rugged as to suffer no ill effects from actual rollover occurrences, although such experiences have been so infrequent as to discourage generalization.
19. The safety hazards associated with operation of an unmanned vehicle in the proximity of other vehicles, personnel, and buildings deserves serious attention, but through the observance of certain precautions a high level of operational safety can be assured.
20. The drone-mode operation is sufficiently straightforward such that no difficulty has been experienced in tracking a lane at speeds up to 60 mph with any of the vehicles tested to date. The versatility of operation provided by drone control, compared with rail or wire-path guidance or other schemes for delivering the vehicle to the point at which the maneuver should be initiated, has great benefit, especially when a variety of test facilities must be used.
21. The automatic controller is a complicated system of mechanical, electrical and hydraulic assemblies which, in the event of breakdowns, does require the

attention of a competently trained technical staff. Despite its high level of reliability and the ease of drone control, this equipment should be used only on a test facility of sufficiently generous dimensions as to permit a spatial margin for operator judgment and reaction.

4.2 RECOMMENDATIONS

It is evident that substantial progress has been made in refining the open-loop test methodology which was originally proposed and developed in the Vehicle Handling Test Procedures study. The discovery of the tire side-force sensitivity to shoulder wear has seriously challenged the viability of the limit test concept, however, and much research needs to be done to address the following related matters:

1. The physical mechanism must be identified by which small amounts of shoulder wear can produce first-order changes in peak side force.
2. There should be a review of tire design practice, upon identifying the above mechanism, such that the design variations required to assure reasonable side force stability are determined and recognized in the trade off with other desirable tire properties.
3. Tire properties research should be conducted to determine the range of shear force performance which accompanies tread wear under normal usage. It should be determined whether the shoulder wear produced during limit turning represents a performance state which the tire will naturally exhibit in the course of normal wearing.

Much research is needed to provide an understanding of those factors which determine driver-vehicle performance under

emergency conditions. Specifically, experiments must be conducted which can demonstrate the relationship between driver-vehicle system performance and the open-loop properties of vehicles, such as have been measured in this study. The sensitivity of drivers to the sideslip response of the motor vehicle should be evaluated to determine whether a monotonic degradation in driver control performance derives from increasing sideslip response.

With regard to the data base which has been generated, considerable further use of the data library should be made. Studies should be conducted to examine alternative response evaluation schemes. Various correlation studies could be conducted to evaluate the relationship between various design properties and the measured performance characteristics. Since the time history data exists intact in a tape library, computer simulations intending to model limit performance can be validated for a host of vehicle configurations and maneuver conditions.

As was made evident frequently in the test, the need for a broadened understanding of the mechanics of limit response is a major problem. Quite often, the test engineer finds himself in a position in which certain data is discarded because the indicated response is known to be counter to some physical principle. In some limit maneuver testing, this process fails because the motions are so complex that they deny any simple evaluation or challenge of validity. It appears that the only sure method for gaining this understanding is to undertake well-structured research directed towards improving the mathematical models of tire-vehicle systems. Efforts must be concentrated initially on the identification of those mechanisms in which the real nonlinear vehicle differs from existing models.

Basic research is needed to provide an accident reporting approach which will contribute toward the identification of the role played by handling factors in accidents. For example, the heavily sideslipping vehicle will frequently leave a visible pavement marking which can actually be reduced to a sideslip angle measure, knowing vehicle wheelbase and track. Such information as can give evidence of the extent to which corrective actions were attempted would also be most valuable.

5. REFERENCES

1. Dugoff, H., Ervin, R.D., Segel, L., Vehicle Handling Test Procedures, Final Report, NHSB Contract FH-11-7297, Highway Safety Research Institute, The University of Michigan, Ann Arbor, November 1970.

2. Bird, K.D., Belsdorf, M.R., Rice, R.S., Effects of Steering and Suspension Component Degradation on Automobile Stability and Control, Final Report, NHTSA Contract FH-11-7384, Cornell Aeronautical Laborabory, Inc., January 1971.

3. Gengenbach, W., "Experimentelle Untersuchung von Reifen auf nasser Fahrbahn (Experimental Investigation of Tires on Wet Tracks)," Automobiltechnische Zeitschrift, Vol. 70, 1968, pp. 310-316.

4. Harned, J.L., Johnston, L.E., and Scharpf, G., "Measurement of Tire Brake Force Characteristics as Related to Wheel Slip (Anti-lock) Control System Design," SAE Paper No. 690214, 1969.

5. Butkunas, A.A., "Random Vibration Analysis and Vehicle Development," SAE Paper No. 690109, January 1969.

6. Rasmussen, R.E. and Cortese, A.D., "The Effect of Certain Tire-Road Interface Parameters on Force and Moment Performance," General Motors Proving Ground, Engineering Publication A-2526, July 1969.

APPENDIX I

AUTOMATIC VEHICLE CONTROLLER

THE REQUIREMENT FOR AN AUTOMATIC CONTROLLER

Open-loop test procedures are designed to evaluate the properties of a vehicle minus the driver. Consequently, a requirement exists for minimizing driver influence in test execution. Despite the ability of many test drivers to apply control inputs in an open-loop manner without regard for vehicle response, there reside certain limitations on input fidelity which the driver is incapable of improving.

Driver control is, in general, deemed to be an acceptable method in those test procedures in which the observed lack of driver precision is known to have a negligible effect on vehicle response or in which the influence of imprecise inputs are significant but can be tolerated by virtue of data interpretation schemes which focus on specific aspects of the overall response.

In certain open-loop limit performance test procedures, however, control input functions are required which place unreasonable demands upon a test driver for their adequate application. Imprecision of driver control input poses problems in the provision of:

1. initial velocity
2. steering function shape
3. braking function shape
4. phase relationship between steering, braking and accelerator inputs.

In the sinusoidal steer procedure, for example, the requirement for accuracy of the steering function shape, as well as level, automatically eliminates the unaided driver as a viable controller. Certain mechanical measures can be employed as aids in executing simple inputs, such that the driver is enabled to act simply as a power element (such as the application of a quasi-constant rotational rate of steering displacement until contacting a mechanical stop, for provision of a trapezoidal steer function). Where feasible, simple devices are generally desirable to insure control input fidelity without requiring an excessive hardware burden.

In test maneuvers involving complex inputs, e.g., combined applications of steering and braking, servo actuation becomes attractive. Moreover, in the research context, the versatility and precision of a programmable automatic control system is required. Only by the use of such a system can a vast regime of potential test procedures be considered in an efficient manner. Further, by virtue of the precision that an automatic controller provides, the effects of imprecision can be systematically studied to determine the extent to which simplified methods might be acceptable.

THE HSRI AUTOMATIC VEHICLE CONTROLLER

An Automatic Vehicle Controller has been developed at HSRI which replaces the driver with servomechanisms that provide control actuation to the steering shaft, brake and accelerator pedals. By way of a radio control transmitter (Figure I-1), operated from a "chase" vehicle, continuous control of steering, braking and acceleration is achieved

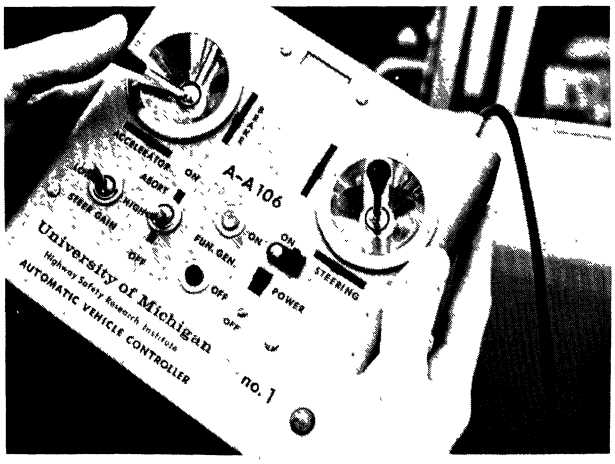

Figure I-1.
Radio control transmitter.

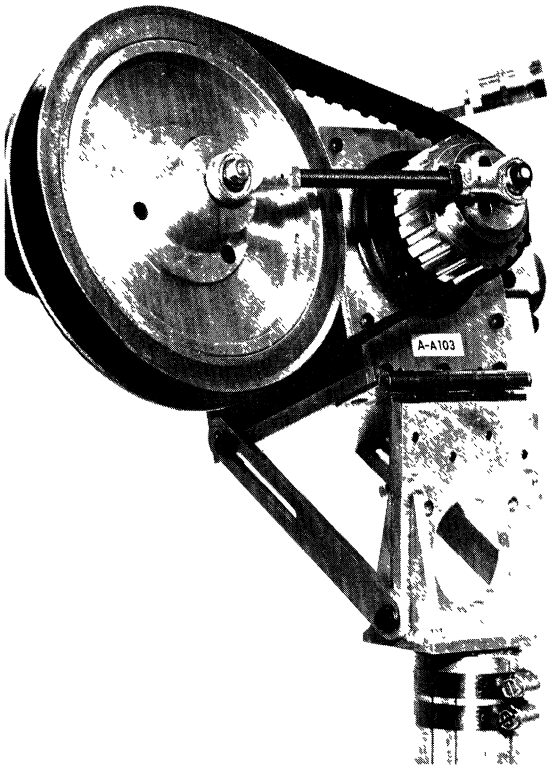

Figure I-2.
Steering servo.

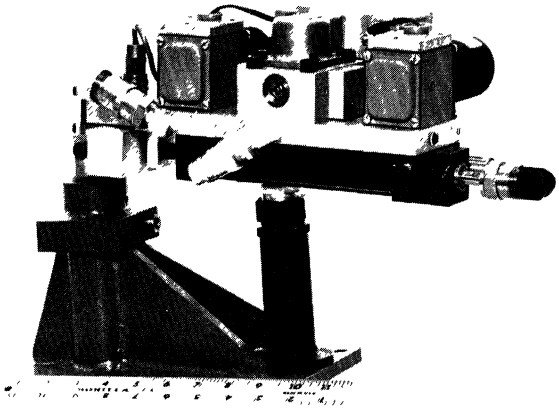

Figure I-3.
Brake servo.

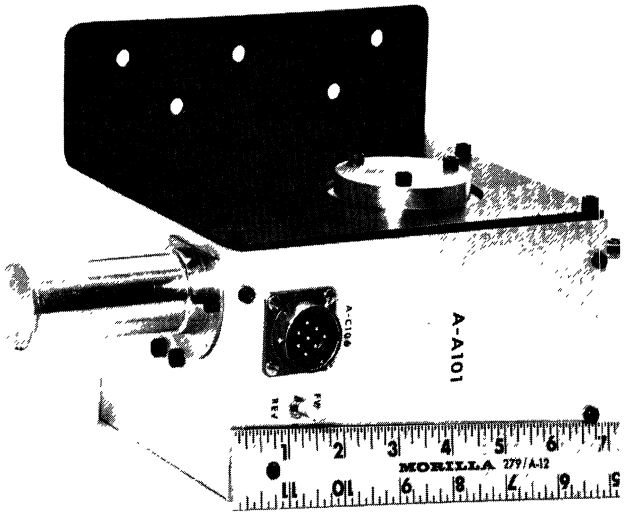

Figure I-4.
Accelerator servo.

while the test vehicle is being guided as a drone. Upon command from the transmitter operator, the drone mode is interrupted to permit a pre-programmed set of control input time histories to be generated by the installed servos. The desired program of control inputs is generated from circuitry constituting an on-board function generator.

The time at which the stored program is initiated is determined by a circuit which compares the actual velocity of the vehicle with the programmed level, thereby providing precise control of the initial velocity desired for a given test.

It is desirable that the performance of the steer and brake servomechanisms have a relatively broad bandwidth compared to the low frequency content of possible control inputs in order to assure a high level of precision in input time histories. Steer and brake servos have been designed to provide linear operation over a bandwidth in excess of 30 Hz. The steer servo (Figure I-2) has a torque capability of 50 ft/lbs at the steering shaft which torque can be achieved at its design rotational velocity, 1300 deg/sec. The brake servo (Figure I-3) has a peak force capability of 400 lbs, which force can be achieved at its peak translational rate, 130 in/sec.

The accelerator actuator (Figure I-4) is a relatively low performance servo, with a 12 Hz bandwidth, and a 16 lb force capability.

The function generator (Figure I-5) operates with a single master clock which controls the timing of the program events over a maximum program term of 10 seconds.

Steer function inputs can assume either a sinusoidal or trapezoidal waveshape, or any superposition of the two. Single sine waves are initiated at a time, t_1, and if

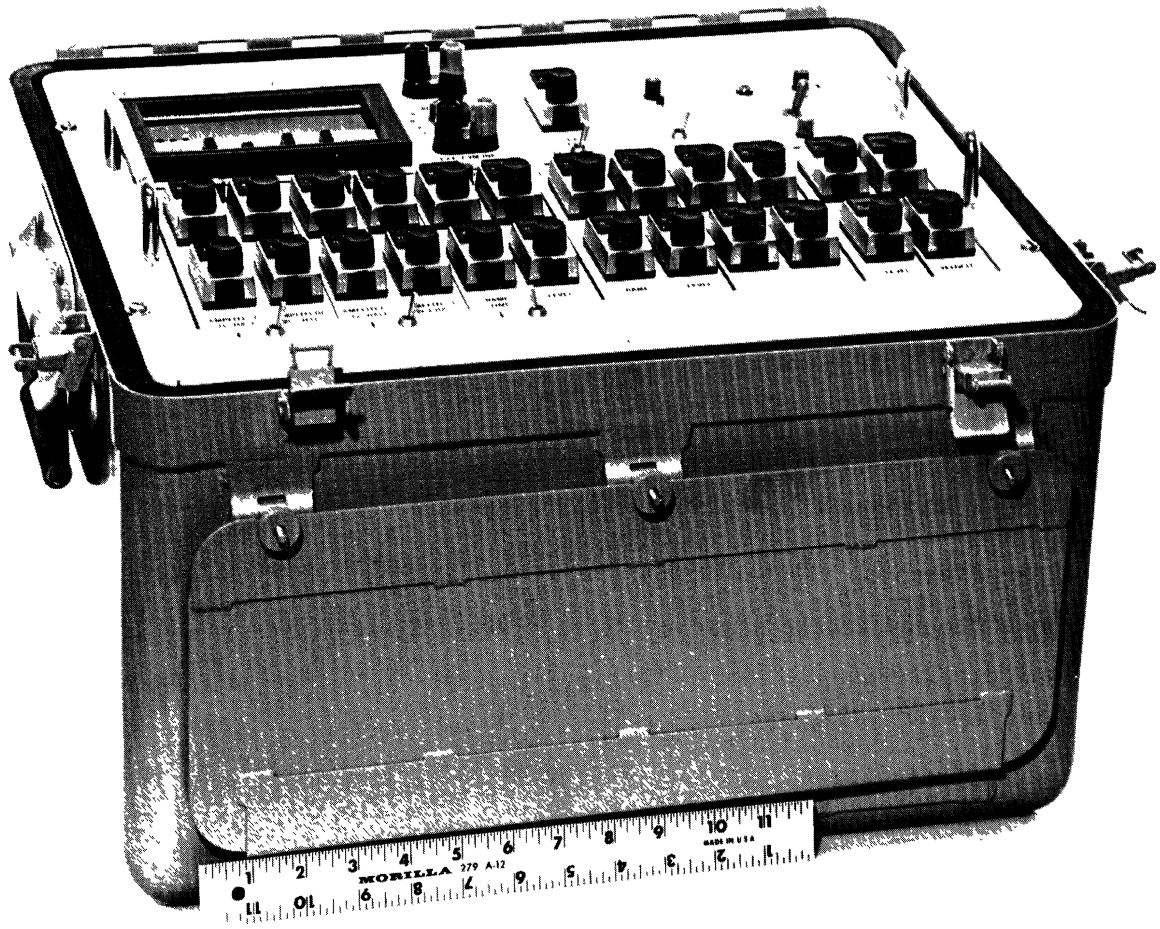

Figure I-5a.
Programmed function generator.

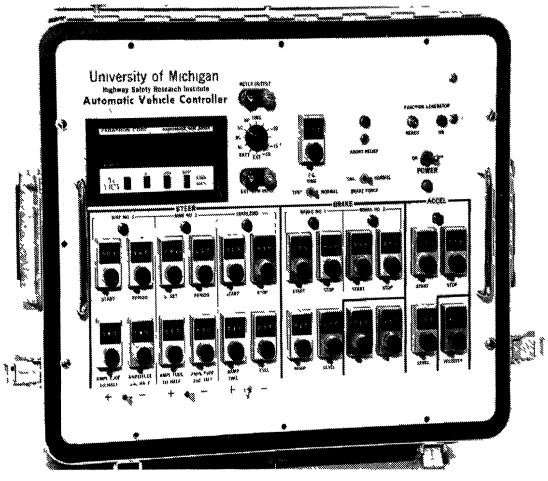

Figure I-5b.
Function generator control panel.

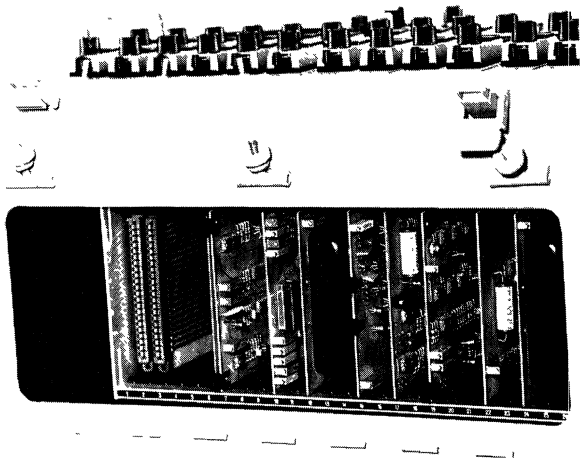

Figure I-5c.
Function generator circuit cards.

desired, a second sine wave can be initiated in the same program at t_2 (see Figure I-6). The period, T_1 and T_2, of each wave is adjustable, as is the amplitude of each "half wave," A_1, A_2, A_3, and A_4. Either wave may be inverted independently of the other. A half sine wave is obtained merely by selecting a single wave whose A_2 amplitude is set to zero.

Steering trapezoids can be produced having the general configuration shown in Figure I-7, with adjustable parameters, t_3, t_4, A_5, and S_1. This wave shape can also be inverted.

Braking inputs can be generated with trapezoidal wave shapes as in Figure I-8. Two successive trapezoids are available with selectable parameters, t_5, t_6, t_7, t_8, S_3, and A_6. A brake application or release can be selected to occur at any time in the program, but the obvious logical conflicts must be avoided (t_6 must be greater than t_5, etc.).

Accelerator inputs can be programmed into a maneuver as step functions only. Both the on/off times and level are adjustable.

The power requirements for the controller are provided by the test vehicle's engine. A pressure compensated variable displacement pump is driven by the engine through a V belt, Figure I-9. The pump draws fluid from a reservoir Figure I-10, delivering a maximum of 5 gpm at 1500 psi to a circuit package, Figure I-11, which stores fluid for use during the peak flow requirements of the steer and brake servos, and for application of the abort brake.

Electrical power is derived from the vehicle's 12 volt charging system, driving a 115 volt square wave inverter, Figure I-12, which in turn powers DC supply modules. The

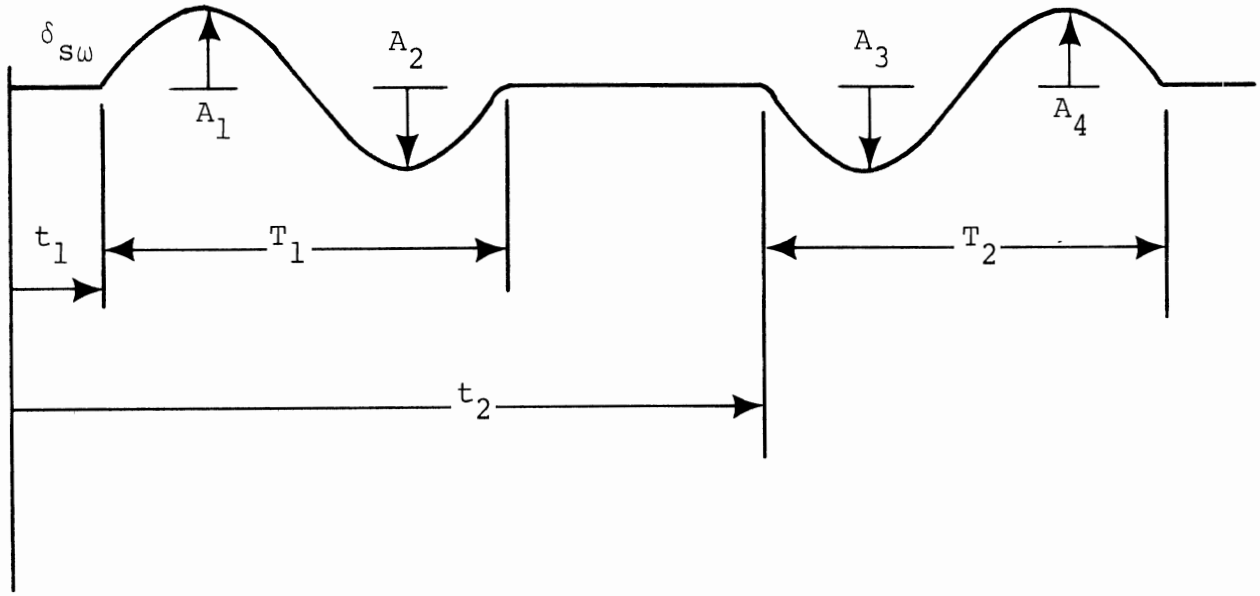

FIGURE I-6

Programmable Steering Command
One or Two Sine Waves of Steering Displacement

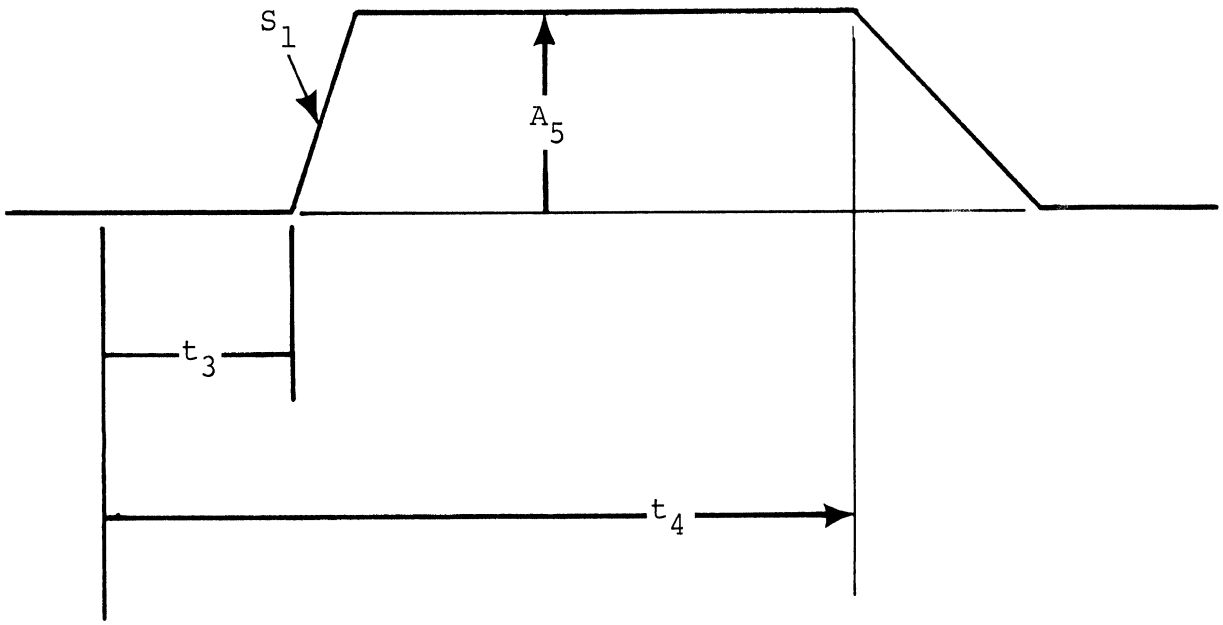

FIGURE I-7

Programmable Steering Command
One Trapezoid of Steering Displacement

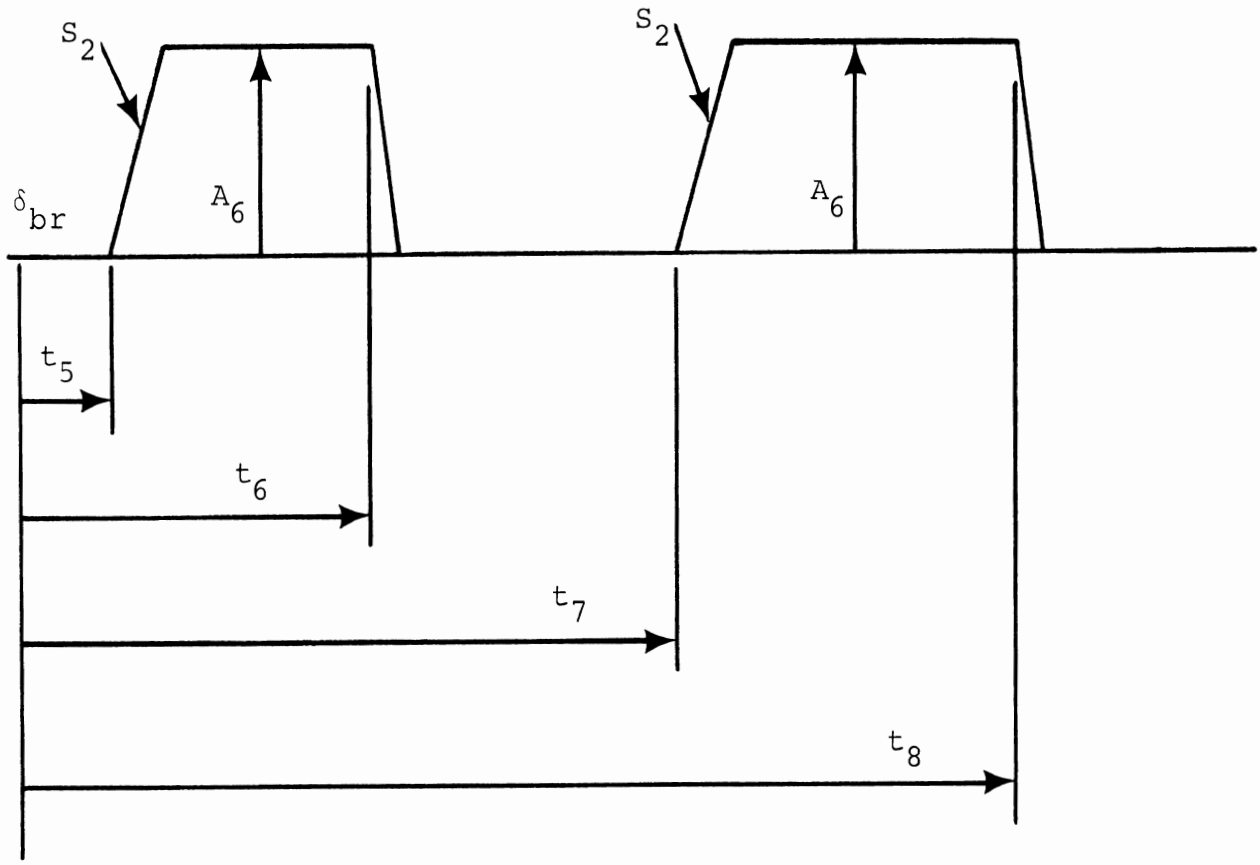

FIGURE I-8

Programmable Brake Commands
One or Two Trapezoids of Pedal Displacement
(or Force)

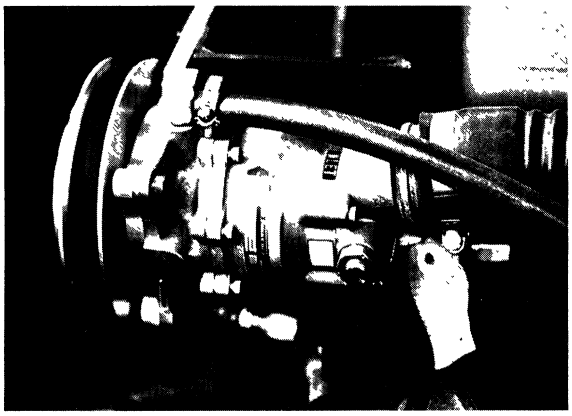

Figure I-9.
Hydraulic pump.

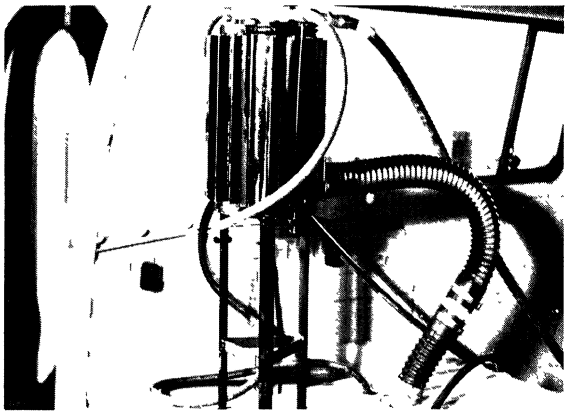

Figure I-10.
Hydraulic system reservoir.

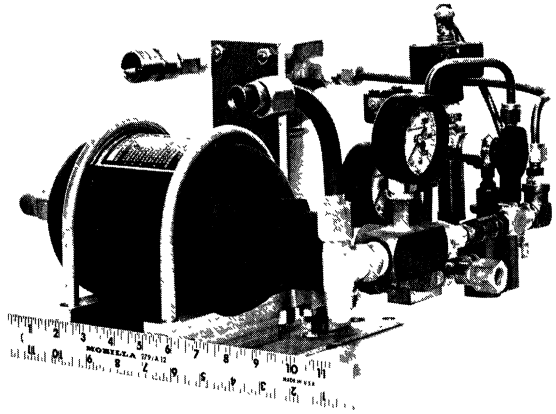

Figure I-11.
Hydraulic circuit assembly.

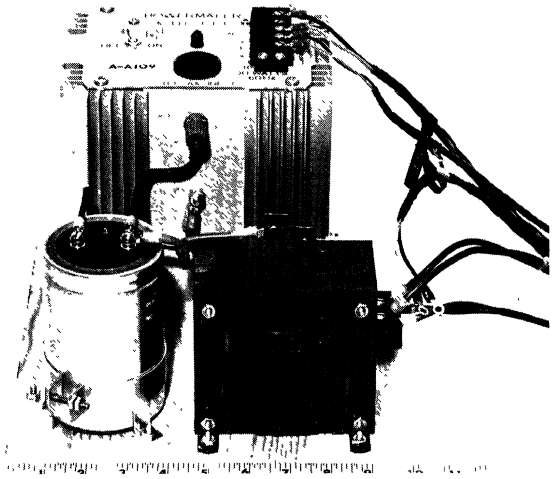

Figure I-12.
Power inverter with filter.

electrical power consumption is less than 150 watts, while at times of peak hydraulic flow requirement, the pump draws 6 Hp from the engine.

The total automatic vehicle controller system weighs 257 lbs.

The operation of this system in manual transmission vehicles has been accomplished for the simple case of one selected gear. A clutch actuator is provided to apply or release the clutch pedal in response to a transmitted command. With the vehicle initially at rest, the clutch is depressed and the proper gear is selected manually, with the engine running. The vehicle is pushed by the chase vehicle (Figure I-13) until a velocity of 20 mph is achieved. The chase vehicle is then backed away and the clutch released. Over 400 test runs were executed on the Lotus test vehicle by this procedure.

Approximately 6000 test runs were executed with three automatic vehicle controllers in twelve automobiles, over the course of this study. Certain observations deriving from this experience are presented in the Conclusions section (5.1).

Figure I-13.
Operation of the automatic controller in
a vehicle with manual transmission.

APPENDIX II

TEST PROCEDURE SPECIFICATIONS

In this appendix, the specific procedures used in conducting the full scale tests are presented. For each of the six maneuvers the following items are identified:

1. "Initial Conditions" indicate the steady-state conditions from which the limit maneuver portion of the test begins.
2. "Incremental Controls" identifies the index variables with which the test is sequenced.
3. "General Constraints" specify the preliminary steps to be observed prior to test initiation, as well as certain constraints to be observed during the test sequence.
4. "Minimum Signals Required" lists those input and response variables which are critical to the proper interpretation of the experimental results, and thus must be recorded.
5. "Procedure" specifies the sequence of steps to be observed during the execution of the test maneuvers.

Note that the procedures involve certain specifications which assume that the tests are being conducted with the use of the test apparatus identified in this report.

VHTP #1 - STRAIGHT-LINE BRAKING

Initial Conditions: V_o = 40 mph

δ_{sw} = 0°

Incremental Controls: P_B-- Brake Line Pressure

General Constraints:

1) All brake lines are to be controlled by one pressure limiter assembly.

2) Brake lining temperatures are not to exceed 250°F, prior to any run.

Minimum Signals Required: A_x, V_5, W_1, W_2, W_3, W_4, MC

Procedure:

1. Set initial brake line pressure level to 200 psi.
2. Approach test pad above initial velocity.
3. Manually initiate test mode.
4. Coast down to initial velocity.
5. Rapidly depress brake pedal to the physical limit of its stroke, holding steering wheel fixed.
6. Allow vehicle to decelerate to a complete stop and hold for 2 seconds minimum after any pitch motion has settled out.
7. Terminate test mode.
8. Increase brake line pressure by 100 psi increments and repeat steps 2 through 7 until a positive wheel lockup is detected, above 10 mph.

9. Decrease brake line pressure by 100 psi and execute steps 2 through 7 twice.

10. Increase brake line pressure by 25 psi increments and repeat steps 2 through 7 twice at each pressure setting until two wheels indicate positive wheel lockup above 10 mph.

VHTP #2 - BRAKING IN A TURN

Initial Condition: V_o = 40 mph

δ_{sw} = angle required for initial lateral acceleration to be 0.3g.

Incremental Controls: P_B-- Brake Line Pressure

General Constraints:

1) All brake lines are to be controlled by one pressure limiter assembly.

2) Brake lining temperatures are not to exceed 250°F, prior to any test run.

3) Perform trial tests to determine steering wheel angle required to obtain initial lateral acceleration of 0.3g at 40 mph.

Minimum Signals Required: A_x, A_y, r, V_5, W_1, W_2, W_3, W_4, MC

Procedure:

1. Set initial brake line pressure to 200 psi.

2. Approach test pad above initial velocity.

3. Manually initiate test mode.

4. Rapidly apply steering input to limit stop.
5. Coast down to initial velocity.
6. Rapidly depress brake pedal to the physical limit of its stroke, holding steering wheel fixed.
7. Allow vehicle to decelerate to a complete stop and hold for 2 seconds minimum after any pitch motion has settled out.
8. Terminate test mode.
9. Repeat steps 2 through 8 for opposite polarity steering input.
10. Increasing brake line pressure in 100 psi increments, repeat steps 2 through 9 until a positive wheel lockup is detected above 10 mph.
11. Decrease brake line pressure 100 psi and repeat steps 2 through 8 twice for each steering polarity until 2 wheels on a single axle indicate positive wheel lockup above 10 mph.

VHTP #3 - TURNING ON A ROUGH ROAD

Initial Condition: V_o = 30 mph

δ_{sw} = Angle required for initial lateral acceleration to be 0.4g.

Incremental Controls: Three road disturbance grids fundamental frequencies of 9, 11, and 14 Hz.

General Constraints:

1) Perform trial tests to determine steering wheel angle required to obtain initial lateral acceleration of 0.4g at 30 mph.

2) Velocity and lateral acceleration initial conditions are to be achieved upon initial contact with the disturbance grid.

3) Road disturbance grids are to be laid out as in Figure II-1.

Minimum Signals Required: A_x, A_y, r, V_5, MC

Procedure:

1. Approach the test area above the initial velocity.
2. Manually initiate test mode.
3. Apply steering input to limit stop, timed to aim the vehicle at the center of the first grid.
4. Manually lift fifth wheel prior to traversing grids.
5. Terminate test mode after exiting from the grid and prior to changing the steering angle.
6. Each of the three grids (of 9, 11, and 14 Hz construction) is to be successfully traversed five times. A successful traversal requires that all four wheels contact all grid elements.

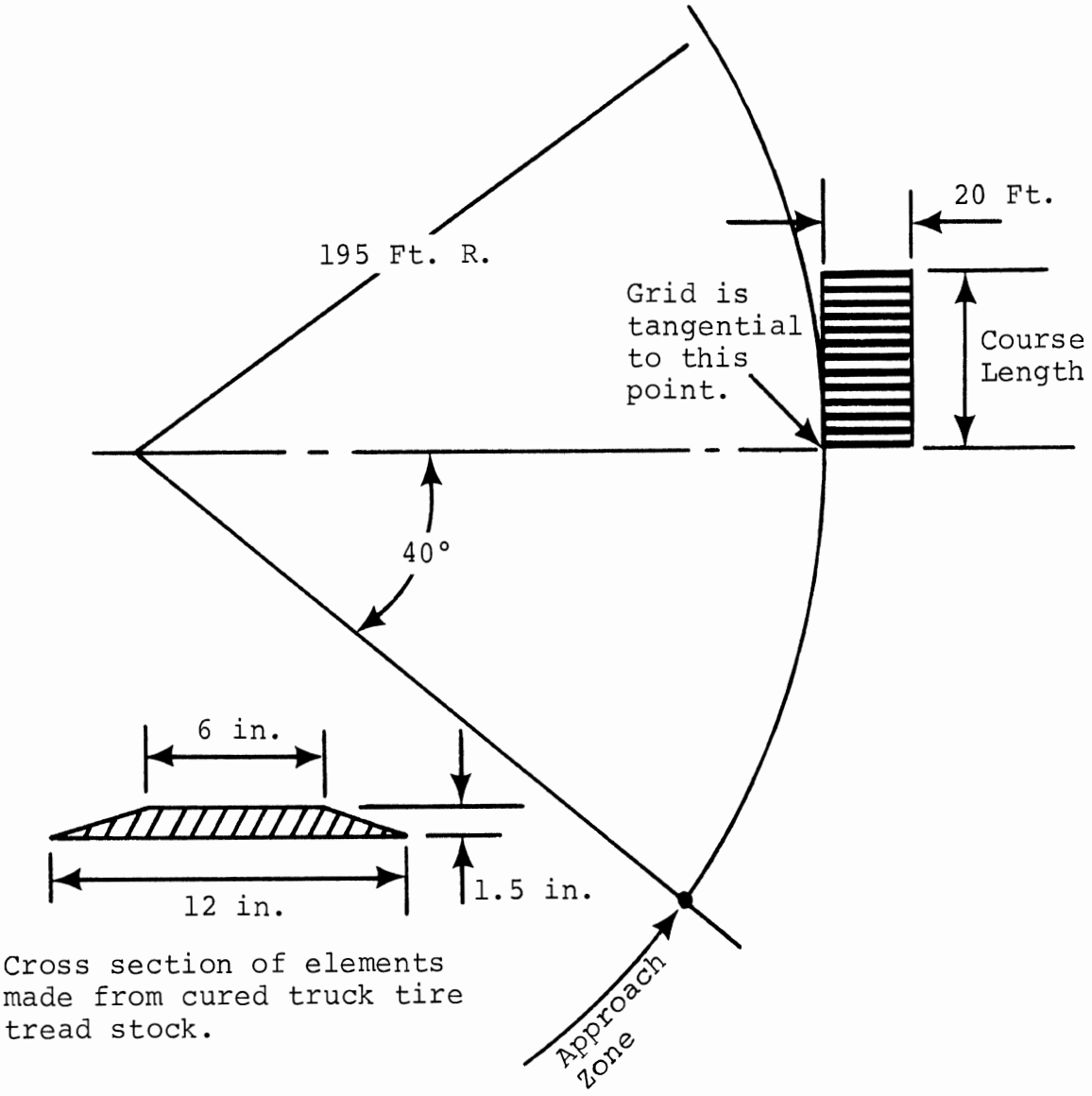

Cross section of elements made from cured truck tire tread stock.

Fundamental Frequency	9 Hz	11 Hz	14 Hz
Center Spacing - Feet	4.8	4.0	3.14
Course Length - Feet	38.4	40	40.8

FIGURE II-1

Road Disturbance Course Layout

VHTP #4 - TRAPEZOIDAL STEER

Initial Conditions: V_o = 40 mph

$\delta_{sw} = 0°$

Incremental Controls: $\delta_{sw} = N_g \frac{\ell}{10} \sigma'$

for σ' = 4,6,8,12,16,20,24

where ℓ = wheel base in feet

N_g = overall steering ratio

General Constraints:

1) All function generator time settings are fixed for all vehicles.

Steer Trapezoid Start = 1.00 sec (100)
Ramp Time = .40 sec (40)
Steer Trapezoid Stop = 4.50 sec (450)
Total Time = 5.50 sec (550)

} Note: Controller settings refer to the HSRI Automatic Vehicle Controller

2) All unused function generator controls are to be set at zero magnitude, with start times set at values greater than 9.00 sec (900).

Minimum Signals Required: A_x, A_y, r, V_5, MC

Procedure:

1. Knowing the overall steering ratio, compute δ_{sw} for first σ value, and set trapezoid level accordingly.
2. Set steering trapezoid controls for 0.4 second ramp time, with δ_{sw} polarity to "left turn."
3. Maneuver vehicle with drone controls into approach path above initial velocity criterion.

4. Initiate function generator cycle. (Tape recorder, test mode and maneuver execution cycle automatically.)

5. Execute maneuver twice (steps 3 and 4) for a left turn and twice for a right turn.

6. Compute δ_{sw} value for the next σ' value and execute steps 2 through 5 until all σ' values have been executed.

VHTP #5 - SINUSOIDAL STEER

Initial Conditions: V_o = 45 mph (1 complete run set)

V_o = 60 mph (1 complete run set)

$\delta_{sw} = 0°$

Incremental Controls: 1) V_o = 45, 60 mph

2) $\delta_{sw} = \frac{66}{V} \frac{\ell}{10} \sigma \ N_g$

for σ = 2,4,6,8,10,12,14,16,18

where V = Initial velocity in ft/sec

ℓ = wheel base in ft.

N_g = overall steering ratio

General Constraints:

1) All function generator time settings are fixed for all vehicles:

Steer Start = 1.00 sec (100)
Sine Period = 2.00 sec (200)
Total Time = 5.00 sec (500)

2) All unused function generator controls are to be set at zero magnitude with start times set at calues greater than 9.00 sec (900).

3) Each initial velocity threshold is a separate test sequence.

4) This test is not to be executed when wind velocity normal to the initial path exceeds 15 mph.

Minimum Signals Required: A_x, A_y, r, V_5, MC

Procedure:

1. Knowing the steering gear ratio and vehicle wheel base, compute δ_{sw} for the first velocity and first σ value.
2. Set first initial velocity threshold on function generator.
3. Set steering sinusoid controls for 2.0 sec. period, sinusoid amplitudes equal to the calculated δ_{sw}, and "left turn" polarity.
4. Maneuver vehicle with drone controls into approach path.
5. Initiate function generator cycle. (Tape recorder, test mode and maneuver execution cycle automatically.)
6. Execute maneuver twice (steps 4 and 5) for both polarities of sinusoidal control.
7. Repeat steps 3 through 6 for each σ' value.
8. Repeat steps 2 through 7 for each V_o value.

VHTP #6 - DRASTIC STEER AND BRAKE

Initial Conditions: V_o = 50 mph (1 complete set)

V_o = 60 mph (1 complete set)

$\delta_{sw} = 0°$

Incremental Controls: 1) V_o = 50, 60 mph

2) $\delta_{sw} = \delta_{sw}^* \gamma$

for $\gamma = 0.75, 1.00$

and $\delta_{sw}^* = 360(\frac{N_g}{22.5})\ (\frac{\ell}{10})$

3) Brake release times, selected after viewing response data in procedure steps #9 and #16

General Constraints:

1) These function generator time settings are fixed for all vehicles:

Steer Start = 1.00 sec (100)
Sine Period = 2.00 sec (200)
Total Time = 5.00 sec (500)
Brake Ramp = 0.05 sec (005)

2) Brake application and release times are "tuned" to the vehicle response.

3) All unused function generator controls are to be set at zero magnitude with start times set at values greater than 9.00 sec (900).

4) The brake force should be large enough to lock all four wheels but shall not exceed 250 lbs.

Minimum Signals Required: A_x, A_y, r, V_5, $\dot{\phi}$, MC

Procedure:

1. Set first initial velocity threshold.
2. Knowing the overall steering ratio and vehicle wheel base (see Table I-3), compute δ_{sw}*.
3. Set steering sinusoidal controls for a 2.0 second period with first half amplitude set to (δ_{sw}* times first γ value) and second half amplitude set to zero.
4. Set δ_{br} controls to zero.
5. Maneuver vehicle with drone controls into approach path above initial velocity criterion.
6. Initiate function generator cycle.
7. Repeat steps 5 and 6.
8. Examine the response data from the previous two runs, determining the time at which the yaw rate time history was seen to have reached 95% of its peak value.
9. Select brake application time, t_5, to coincide with timing of 95% peak yaw rate value, and brake release time, t_6, equal to (t_5+2.0).
10. Set brake ramp time to 0.050 sec.
11. Set brake level for amplitude of full brake pedal stroke, with force not to exceed 250 lbs.
12. Maneuver vehicle with drone controls into approach path above initial velocity criterion.
13. Initiate function generator cycle.
14. Repeat steps 12 and 13.

15. Play back tape recorder signal of roll rate, ϕ, onto the pen recorder, along with function generator time base, t_{ac}.

16. Examine the response data from the previous two runs, determining the values for brake release time, t_6, from the roll rate response. Two release timings are to be selected, t_p and t_z, coinciding with 2nd sympathetic polarity peak and 3rd zero crossing, respectively.

17. Set brake release time, t_6 to t_p; repeat steps 5 and 6 twice for each value of γ.

18. Set brake release time, t_6 to t_z; repeat steps 5 and 6 twice for each value of γ.

19. Repeat steps 17 and 18 for second velocity threshold.

20. A rollover is counted and logged if an outrigger wheel touches the test surface. A rollover occurrence terminates the test sequence.

APPENDIX III

TIRE LATERAL FORCE INVESTIGATION

BACKGROUND

In the pilot test phase of the VHP and S/SS programs, vehicle response data from trapezoidal steer tests were gathered which indicated a large variation in peak lateral acceleration capability over a two-week period. A later set of tests on another vehicle operated over a three-week period confirmed the previous response variations. Since this variability seriously degrades the viability of the limit performance measurement procedures, a research study was undertaken to identify the causative factors contributing to the non-repeatable response. It was hypothesized that the magnitude of the variability could only be explained by a major change in conditions at the tire-road interface. Thus, the research effort was designed to investigate the relationship between peak lateral force capability of the tire and each of three potential test variables: tire wear, surface wetness, and pavement temperature. Experiments directed toward the investigation of each factor will be treated here individually.

INVESTIGATION INTO THE RELATIONSHIP BEWTEEN TIRE SIDE FORCE CAPABILITY AND TIRE TREAD WEAR

Since the trapezoidal steer maneuver and both other automatically controlled vehicle handling test procedures involve repetitive testing with the tires experiencing large sideslip angles, a considerable degree of tire wear is

incurred as a result of the test process. The character of this type of wear is quite different from that obtained in normal driving. The most rapid changes in tread profile take place at the outside shoulder and sometimes further up the sidewall.

In recognition of the multi-variable character of vehicle testing, it was determined that specific findings on tire properties could only be obtained through experiments with tight control on condition variables. The HSRI Mobile Tire Tester was used as the experimental apparatus for a) providing, in a controlled fashion, a vertical load and slip angle to a tire such that it could be incrementally worn in a manner analogous to that obtained in testing the vehicle, and b) for gathering tire side force data concurrent with the wearing process.

The first two tires subjected to this experiment were a Uniroyal L78-15 Fastrak and a Goodyear F78-14 Polyglas. These tires were provided as original equipment on the two test vehicles with which variability in trapezoidal steer data had been first observed. Each tire was subjected to a sequence of runs over both concrete and asphalt by which the Mobile Tire Tester, travelling at 40 mph, lowers the tire onto the pavement at a 20° slip angle and a selected large vertical load. Tire tread profiles were measured by use of a contour copying device and reproduced versus average side forces for each data sample, in Figure III-1. Data sets were gathered in groups of 4 runs each, designated as a "lap" of the Mobile Tire Tester involving a path over the TTI facility as shown in Figure III-2. The very first piece of data with the new tire, then, is on concrete, followed by two runs on asphalt, and one more on concrete.

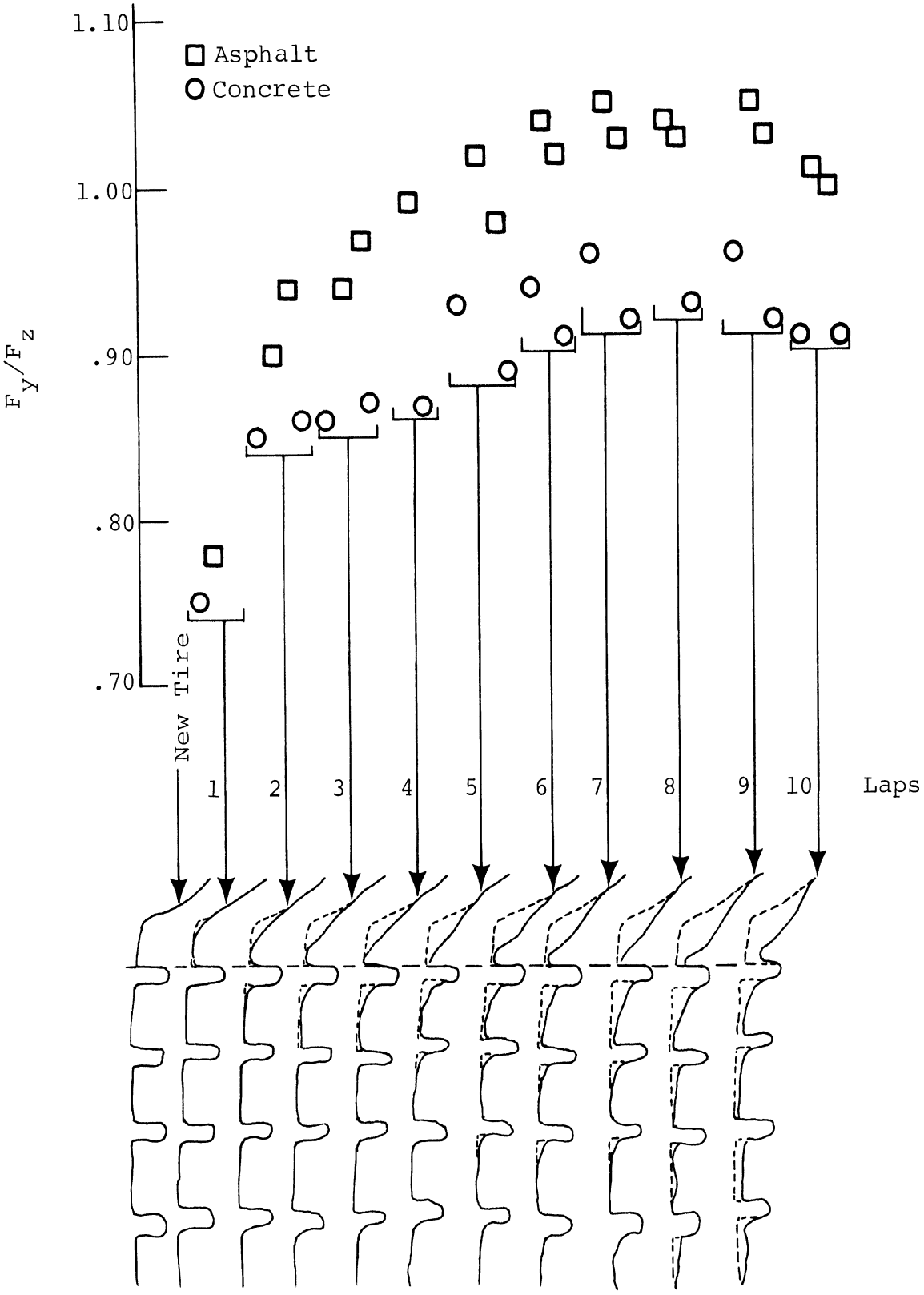

Tread Profile - Outside Shoulder

α=20° F_z=1550 Uniroyal L78-15 Fastrak

Tire Sample No. 1

FIGURE III-1

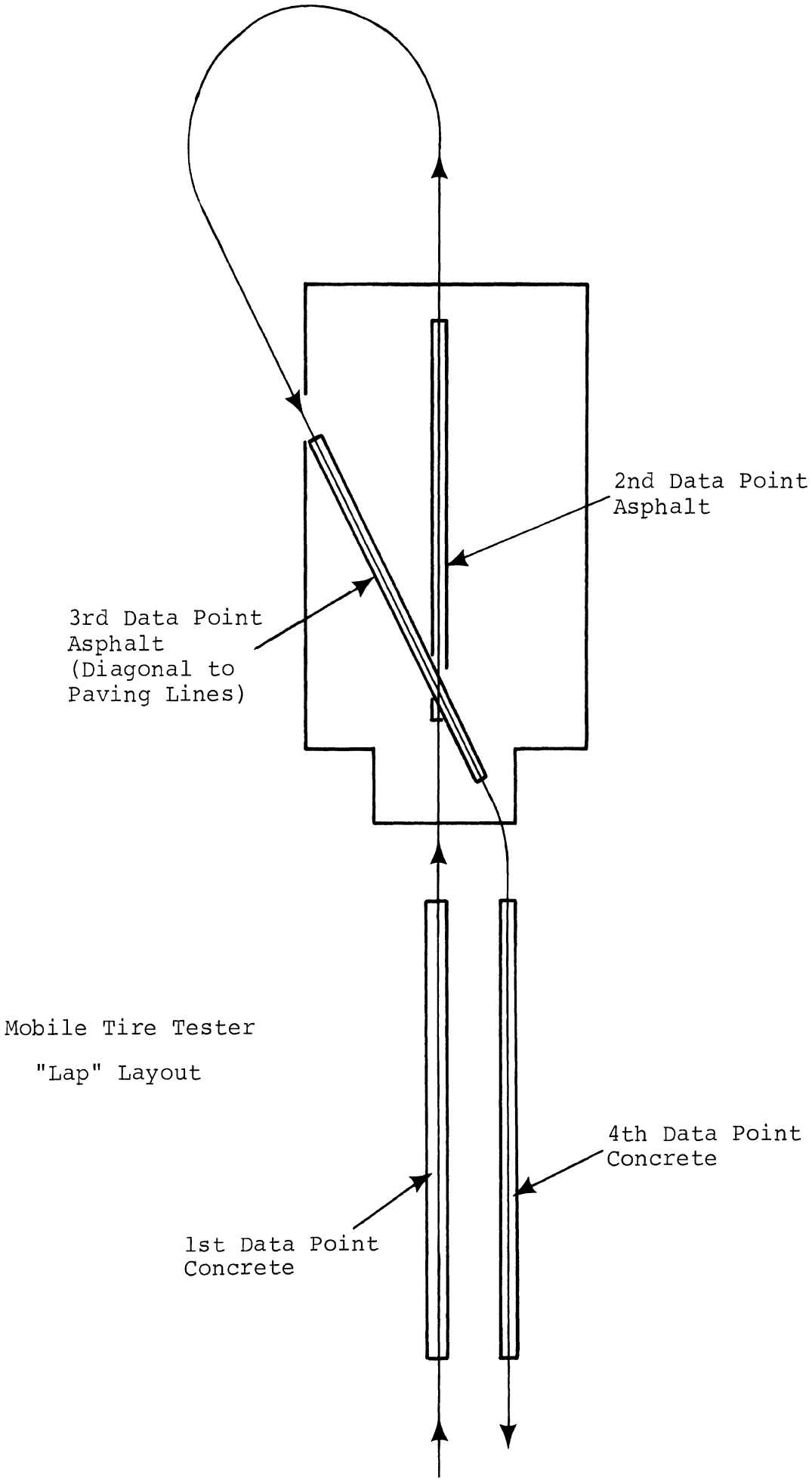
2nd Data Point
Asphalt
3rd Data Point
Asphalt
(Diagonal to
Paving Lines)
Mobile Tire Tester
"Lap" Layout
4th Data Point
Concrete
1st Data Point
Concrete

FIGURE III-2

The tire data shown in Figure III-1 thus indicates a significant rise in side force capability with increased wear. It is apparent that the first data point, on concrete, represents a condition whereby a significant improvement in the tire's lateral force capability is taking place, even as the run progresses over 9 seconds, see Figure III-3. Note in Figure III-3 that the force is increasing as runs progress on both concrete and asphalt.

This remarkable result was confirmed with a second Uniroyal L78-15 Fastrak to assure that the general finding was not, for some reason, atypical. (See Figure III-4.) A similar wear sensitivity (force increase) characteristic was then obtained with the Goodyear F78-14 Polyglas tire. (Figure III-5) It is presumed that, although the first concrete data point is consistently the lowest force on Figures III-1, 4, and 5, the wearing process is the dominant influence. If the first run had been over asphalt, the lowest force would be expected to have been observed there also.

Additional force data was taken on asphalt for these two tire types, at slip angles of α = 5, 10, 15, 20°, after they had been worn. This data was needed to determine the adequacy of the α = 20° choice in representing peak force capability during the wear experiments. In Figure III-6, both tires are seen to be operating at approximately peak side force at α = 20°.

CORRELATION OF MOBILE TIRE TESTER RESULTS WITH VEHICLE TESTS

Trapezoidal steer tests were conducted to determine the extent to which vehicle test results could be shown to correlate with the Mobile Tire Tester data (concerning

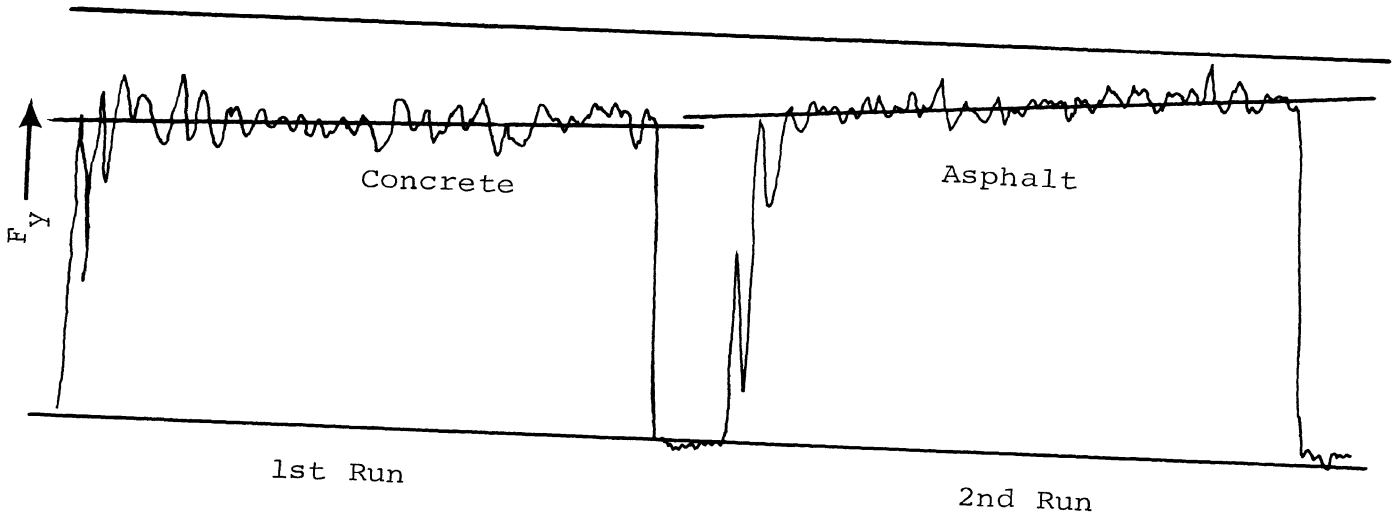

Uniroyal L78-15
Fastrak

FIGURE III-3

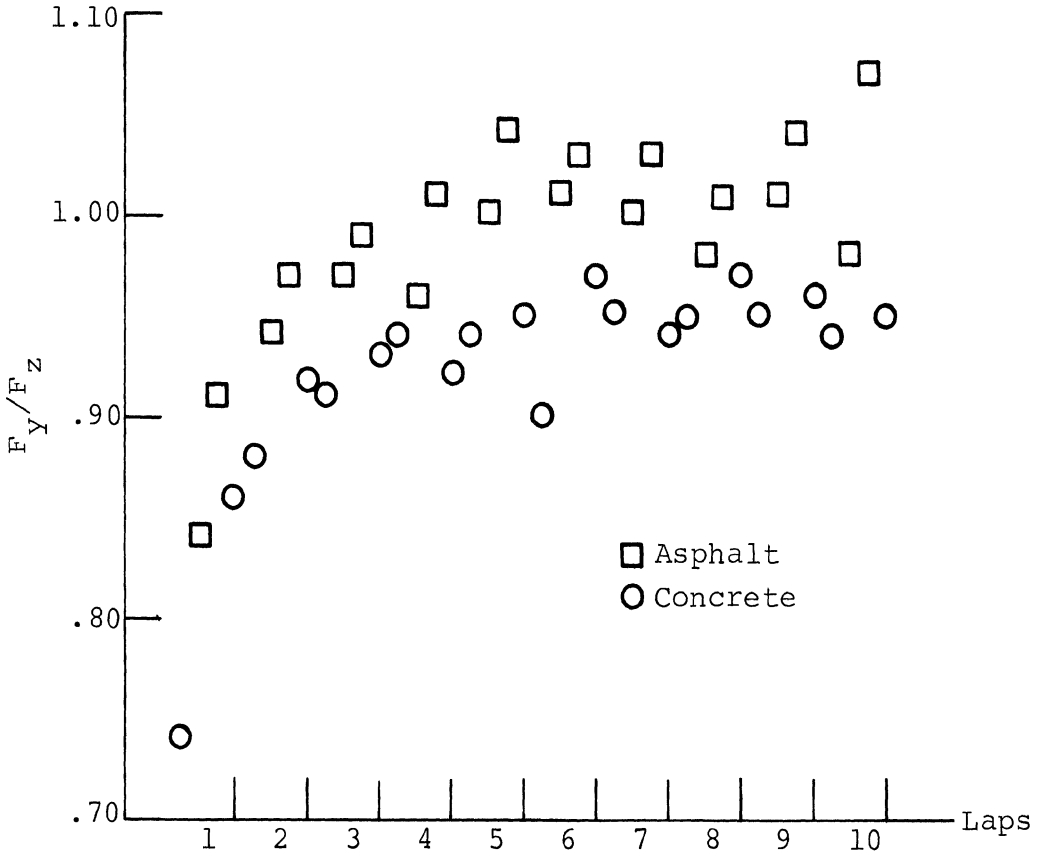

Lateral Force/Wear Data
Mobile Tire Tester
α=20° F_z=1550 lbs. 27 psi 40 mph
Uniroyal L78-15 Fastrak
Tire Sample No. 2
Chevrolet

FIGURE III-4

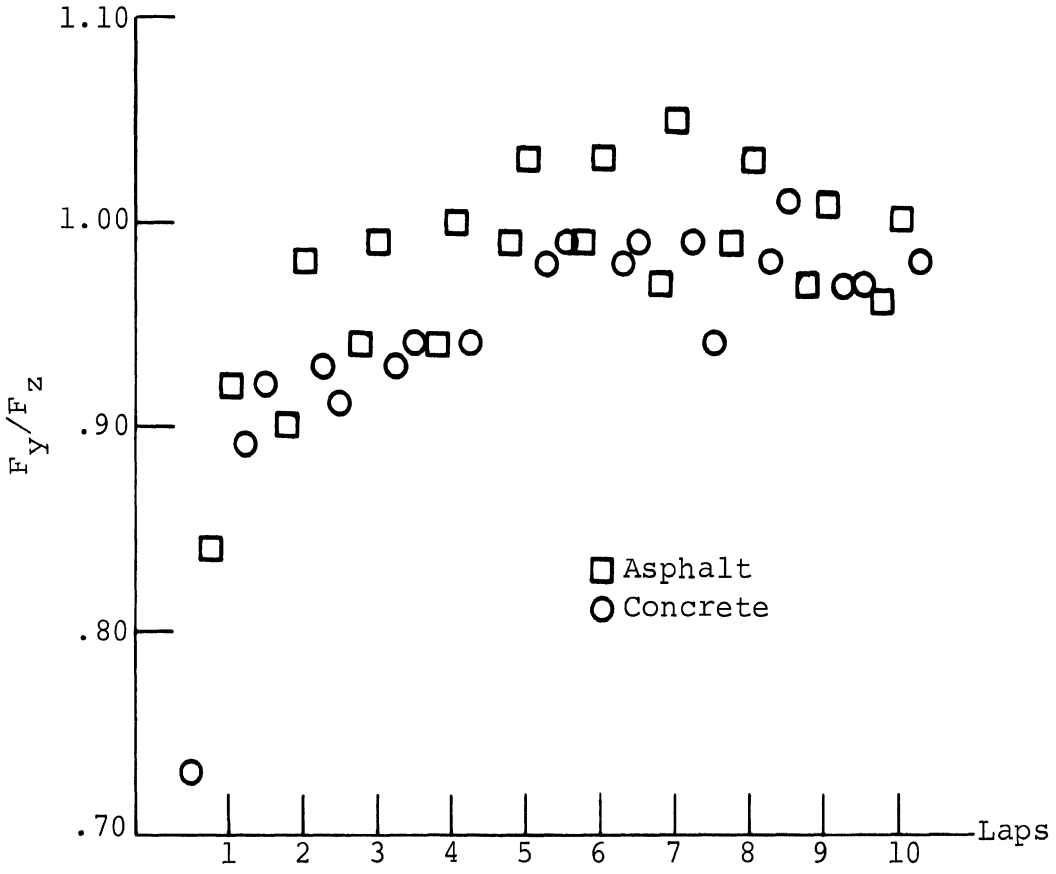

Lateral Force/Wear Data

Mobile Tire Tester

α=20° F_z=1200 lbs. 26 psi 40 mph

Goodyear F78-14 Polyglas

Coronet

FIGURE III-5

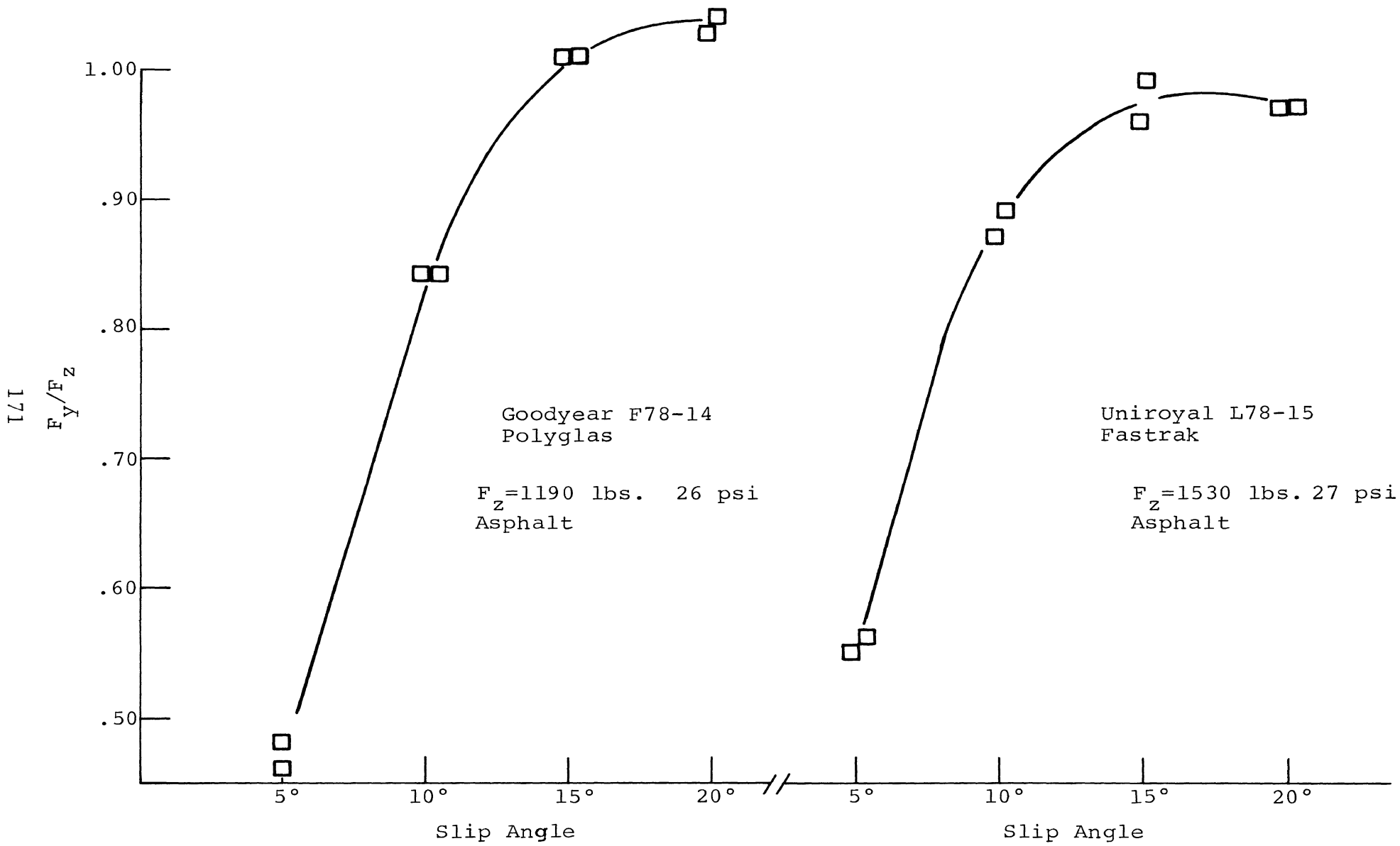
1.00
.90
.80
.70
.60
.50
F_y/F_z
Goodyear F78-14
Polyglas
F_z=1190 lbs. 26 psi
Asphalt
Uniroyal L78-15
Fastrak
F_z=1530 lbs. 27 psi
Asphalt
5°
10°
15°
20°
Slip Angle
5°
10°
15°
20°
Slip Angle

FIGURE III-6

tire wear sensitivity). A trapezoidal steer sequence was performed on a Dodge Coronet with Goodyear F78-14 Polyglas tires that had been heavily worn due to previous testing, followed by a sequence with worn rear but new front tires (the term "new tires" always refers to tires that have been broken in with 100 or 200 miles of "normal" driving). Peak lateral accelerations achieved are plotted versus steer angle in Figure III-7. The worn tire sequence was run going up in steer level and the new-front, worn-rear tire condition was run starting with the highest steer level and going down. The first two (left turn) runs with 2 new tires show a .23g lower acceleration response than was obtained at the highest steer level with all worn tires. The slight increase in lateral acceleration at the next lower steer level with 2 new tires appears to indicate the increased force potential of the new tires with cumulative wear. At the conclusion of this sequence a significant alteration in tire properties was evident from the elevated performance obtained in six more runs at the highest steering level. (These six runs are shown in the hexagon in Figure III-7.)

The wear/side force data from the Mobile Tire Tester was more directly correlated with data gathered using a Chevrolet Station Wagon, equipped with a set of (4) new Uniroyal L78-15 Fastrak tires. Trapezoidal steer responses were obtained at the highest level of steering used in the procedure (i.e., $\delta_{SW} = 400°$) employing alternating sets of three left and three right turns on both asphalt and concrete. These data are plotted in Figure III-8 and show that the tire wearing process is accompanied by large changes in the value of peak lateral acceleration.

A degradation in directional stability appears to result from the wearing process as quantified by the data in Figure III-9, depicting an increasing spin-type response on

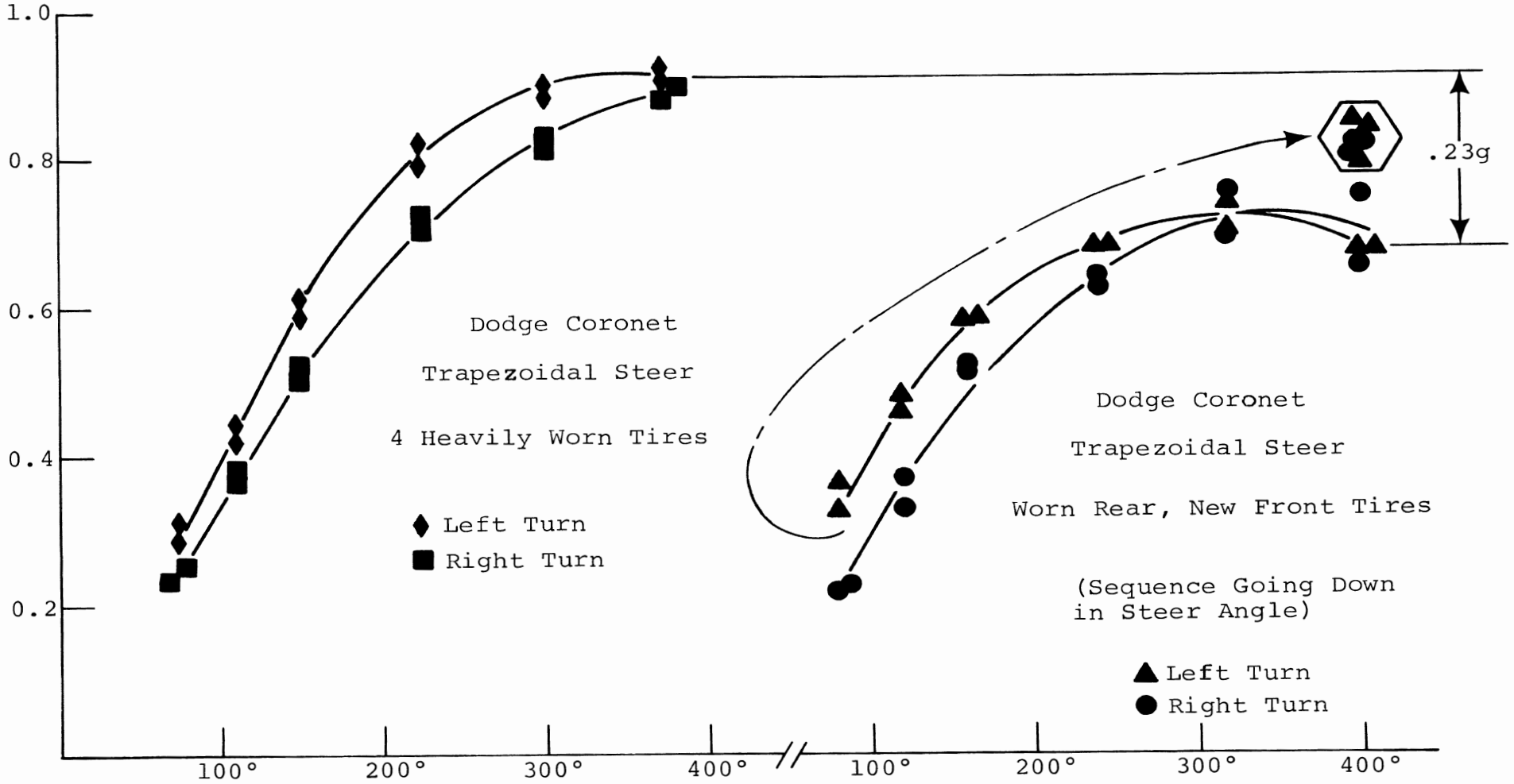
1.0
0.8
0.6
0.4
0.2
$A_{y_{peak}}$
Dodge Coronet
Trapezoidal Steer
4 Heavily Worn Tires
Left Turn
Right Turn
.23g
Dodge Coronet
Trapezoidal Steer
Worn Rear, New Front Tires
(Sequence Going Down
in Steer Angle)
Left Turn
Right Turn
100°
200°
300°
400°
100°
200°
300°
400°
Steering Wheel Displacement (Degrees)

FIGURE III-7

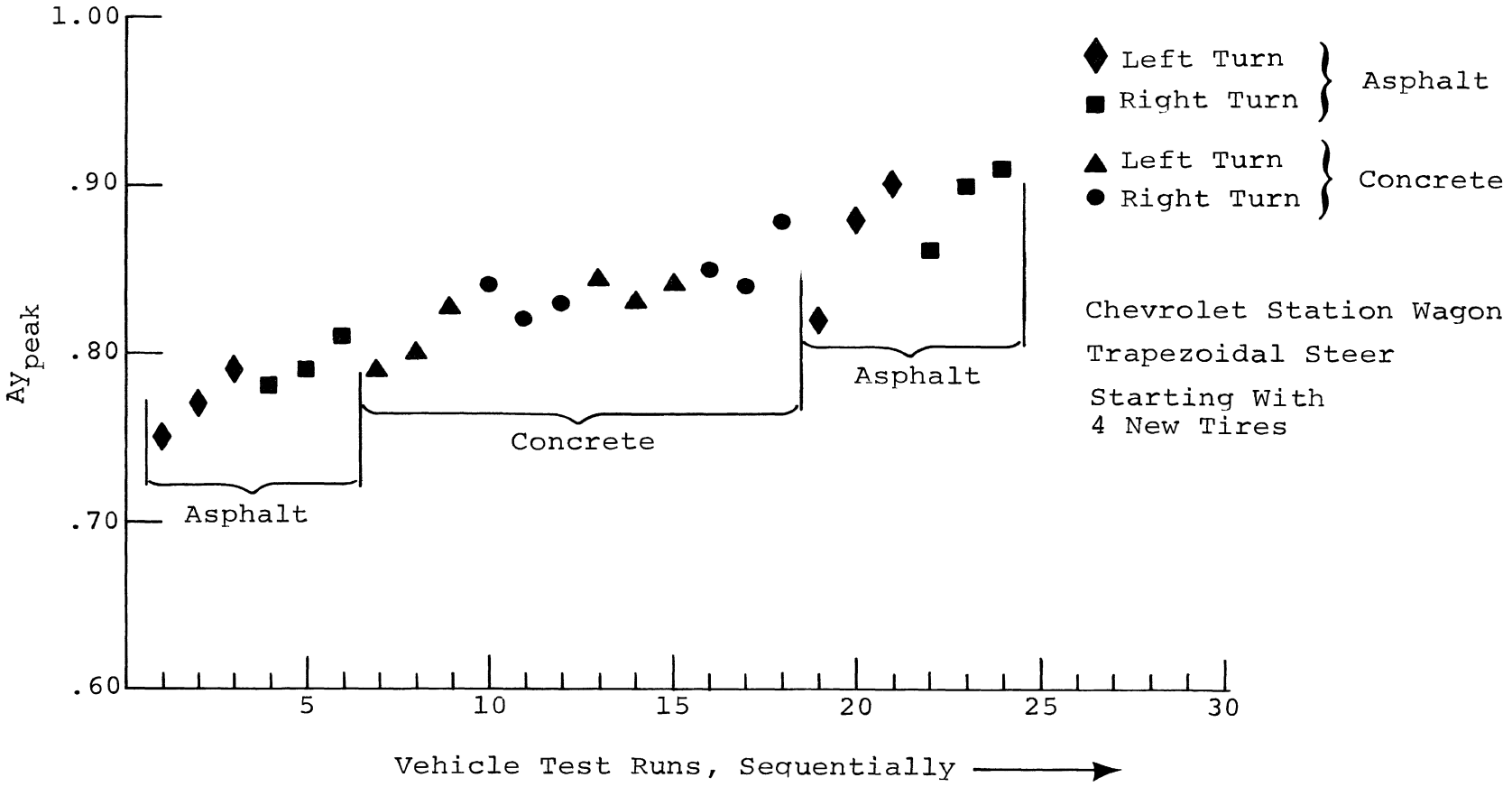
1.00
.90
.80
.70
.60
Ay_{peak}
Left Turn
Right Turn
Asphalt
Left Turn
Right Turn
Concrete
Chevrolet Station Wagon
Trapezoidal Steer
Starting With
4 New Tires
Asphalt
Concrete
Asphalt
5
10
15
20
25
30
Vehicle Test Runs, Sequentially

FIGURE III-8

asphalt (increasing peak value of vehicle sideslip angle). This result is attributed to the higher rate of wear occurring on the front tires resulting from the large load transfers caused by the roll stiffness of the front suspension. A similar manifestation of the effectiveness of tire wear distribution in destabilizing the limit turning response also appears in Figure III-9, where data is presented for tests performed with worn tires installed on the front wheels and new tires on the rear axle. After a few spin-out responses, the new rear tires show an apparent trend toward more wear, and thus greater vehicle stability.

The results obtained with the Mobile Tire Tester and the test results obtained with the Chevrolet and Dodge show very clearly that the tire wear produced in the trapezoidal steer maneuver has a very large influence on the maximum side forces produced by the tires and, consequently, has a large influence on the peak lateral accelerations that are attained, including the character of the total vehicle response.

Data obtained recently from the flat bed tire test machine at General Motors Proving Ground also indicate a significant change in lateral tire force capability as a function of wear. In the GM work, tire wear was achieved by shaving the tread surface and thus substantial wear of the tread face was incurred, in a manner more analogous to normal driving wear. Although the conditions are not the same and not directly comparable to the MTT results, the same trend is evident. Expressed in similar terms, the GM data shows an increase in F_y/F_z, normalized lateral force, from .69 to .81 over the full range of tire wear.

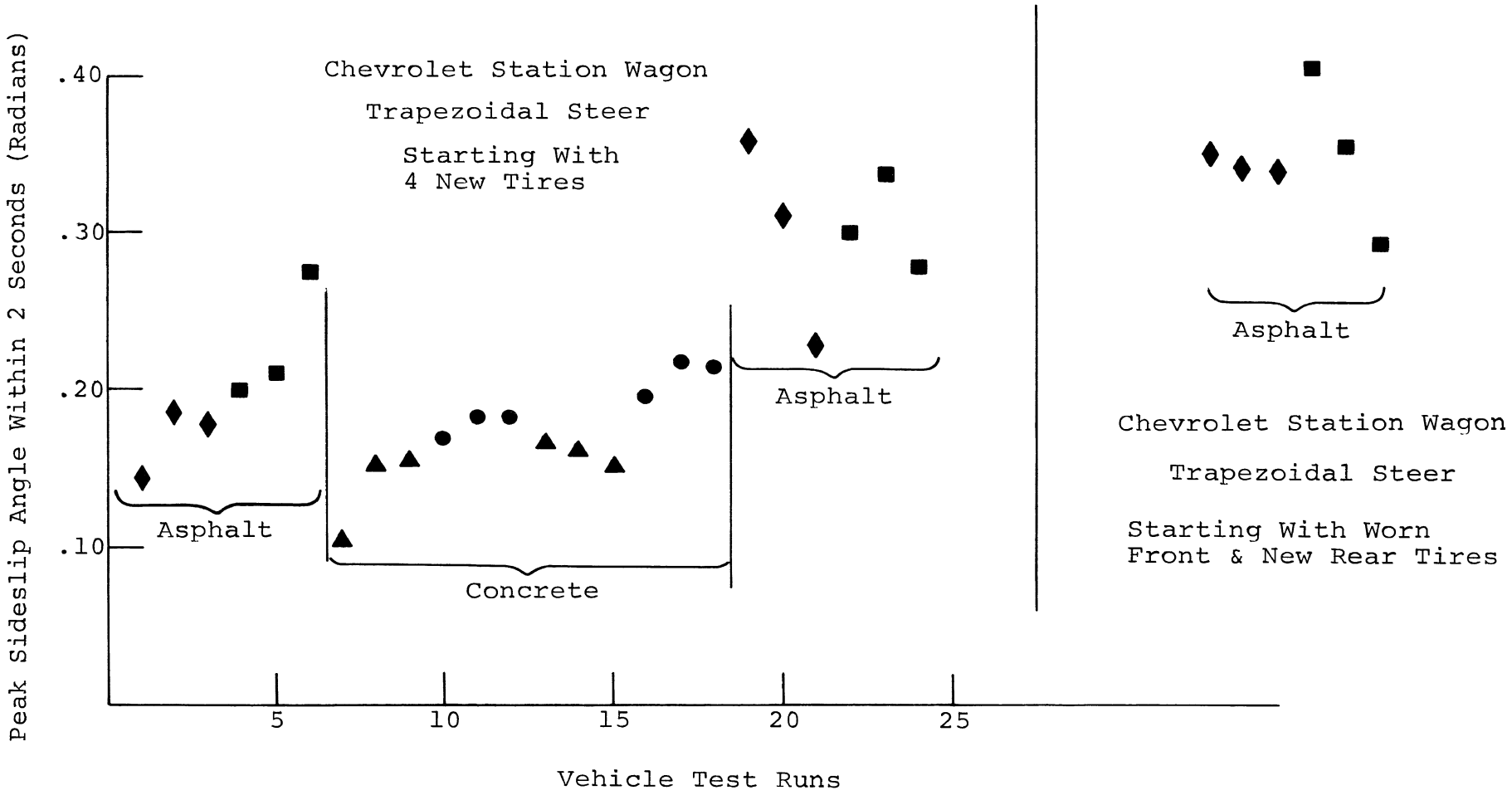
Peak Sideslip Angle Within 2 Seconds (Radians)
.40
.30
.20
.10
Chevrolet Station Wagon
Trapezoidal Steer
Starting With
4 New Tires
Asphalt
Concrete
Asphalt
Asphalt
Chevrolet Station Wagon
Trapezoidal Steer
Starting With Worn
Front & New Rear Tires
5
10
15
20
25
Vehicle Test Runs

FIGURE III-9

INVESTIGATION INTO THE RELATION BETWEEN TIRE SIDE FORCE CAPABILITY AND SURFACE DRYING TIME

The drying time experiment consisted of: (1) wetting one-half of the skid pad with a water truck, (2) measuring maximum normalized tire side force with the Mobile Tire Tester at several times and at several locations as the pad was drying and (3) measuring peak lateral acceleration obtained with the Chevrolet Station Wagon in a limit trapezoidal steer maneuver as the pad was drying.

The west (low side) of the asphalt test pad was heavily wetted by making a series of parallel passes over the length of the skid pad with the watering truck. The Mobile Tire Tester tests and the vehicle tests started as soon as possible after the water truck had finished. The water depth over the wetted portion of the skid pad varied considerably due to small unevenness in the pad surface caused by the asphalt laying process. Almost immediately after wetting there were areas of standing water and areas of asphalt which were discolored from wetting but over which no water was standing.

The Mobile Tire Tester was used to make side force measurements on areas of the asphalt skid pad with differing water conditions. Tests were made in areas of standing water, in areas discolored by wetting, and in areas which had never been wetted. The tests were made using a Chevrolet Station Wagon tire operated at 20° slip angle and 40 mph. The results are summarized in Table III-1. The normalized lateral force capability of the surface varied from 0.56 to 0.80 at two different locations on the surface just after it had been wetted. In just less than two hours after the surface had been wetted almost all of the standing water was gone. A section of asphalt which was still discolored from wetting had a normalized lateral force capability of

about 0.83. The asphalt which appeared dry after having been wetted had a normalized lateral force capability of 0.96 which was identical to the normalized lateral force capability of the portion of the skid pad which had never been wetted.

Simultaneously with these tire tests, trapezoidal steer maneuvers were conducted with the Chevrolet Wagon on the skid pad. The test results are presented in Figure III-10. Note that, before the pad was wetted, the maximum lateral acceleration obtained in a series of 6 trapezoidal steer maneuvers varied from 0.84 to 0.87g. After the pad was wetted, the maximum lateral acceleration obtained in 6 trapezoidal steer tests varied from 0.65 to 0.78g. (This spread in values demonstrates the variability in lateral force capability resulting from variations in water depth.) The maximum lateral acceleration obtained in tests performed approximately 2 hours after wetting the surface varied from 0.825 to 0.86g, indicating that the surface had essentially recovered its "dry" friction properties.

On the basis of these findings, it is concluded that vehicle testing can commence after a rain when the pavement appears to be dry, that is, the asphalt is no longer discolored from wetting.

TABLE III-1. SUMMARY OF MTT (MOBILE TIRE TESTER) WET TEST DATA, F_y/F_z

Time	Wet (Standing Water)	Discolored From Wetting (Partially Wet)	Appears Dry After Wetting	Not Wetted (Dry Surface)
0:00	0.56	0.80		0.98 0.98
0.15	0.60	0.81		0.98
0:55	0.56 0.59	0.86 0.84		
1:40		0.83 0.84	0.96 0.96	
1:50				0.96 0.96

Asphalt Skid Pad
40 mph
1550 lbs. Load, F_z
20° Slip Angle
"20%" Worn Chevy S.W. Tire, Tire #1

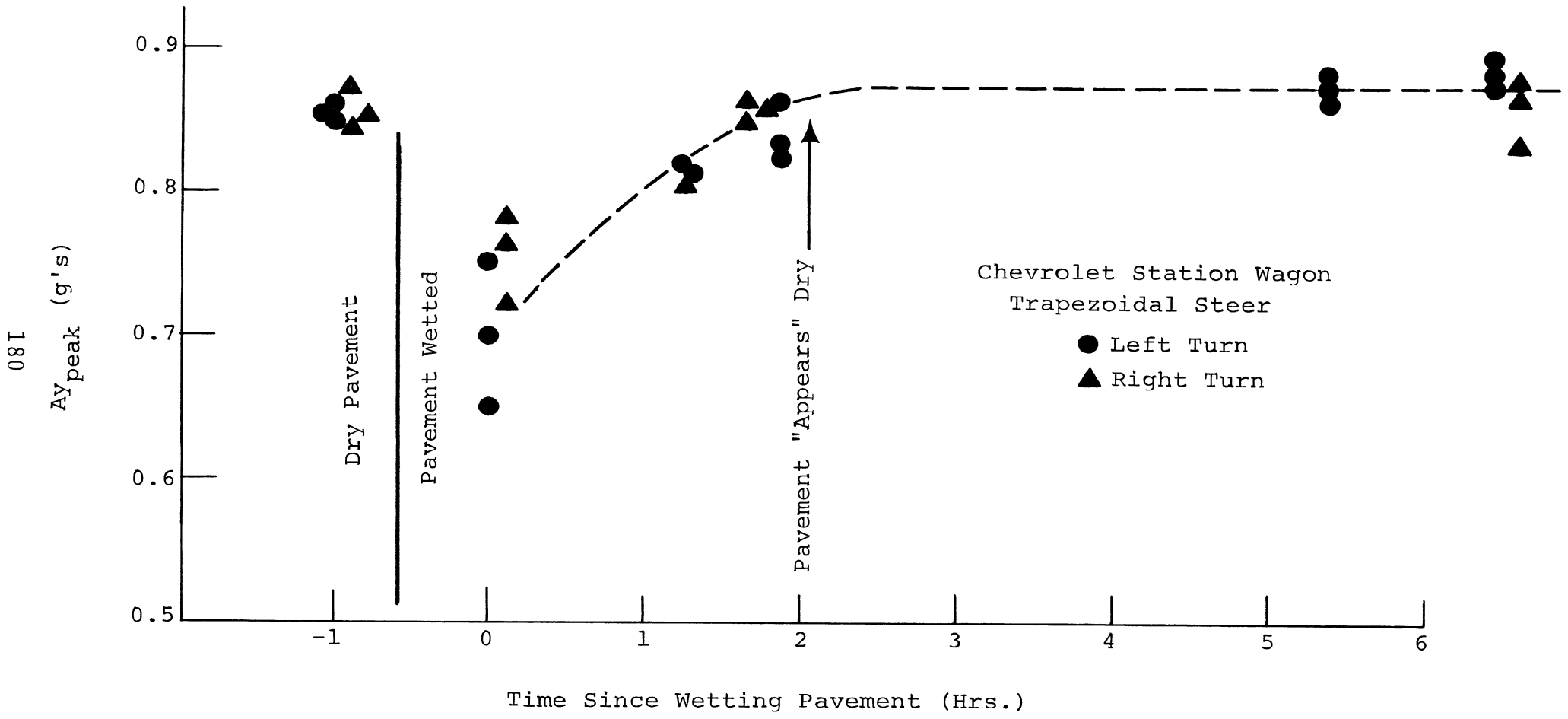

FIGURE III-10

INVESTIGATION INTO THE RELATION BETWEEN TIRE LATERAL FORCE CAPABILITY AND PAVEMENT SURFACE TEMPERATURE

To obtain test data over a wide range of asphalt pad temperatures, tire force measurements and trapezoidal steer maneuvers were performed with the Chevrolet Wagon over a period of 7 days, morning and afternoon. It is clear that this experiment involved uncontrolled variables since environmental factors such as humidity and wind could have been changing over this period. However, all of the tires were well worn and thus tire wear is not believed to have been a significant factor in these tests. The pad was not wetted during this period.

The test results for the asphalt pad are shown on Figure III-11. Similar results are shown for the concrete pad in Figure III-12. It is seen that there is very little change in peak lateral acceleration produced in a trapezoidal steer maneuver when the asphalt pad temperature varied from 83°F to 119°F. On the basis of these data it is concluded that pad surface temperature does not have a significant influence on the peak lateral acceleration that can be attained by a vehicle. It can also be concluded that any other environmental factors such as humidity or wind which may have been varying to some extent over the seven-day-period did not have a significant effect on the test data. Thus no test constraint involving surface temperature was adopted.

LATERAL FORCE CAPABILITY AS EFFECTED BY TIRE WEAR AND TEMPERATURE EFFECTS AS RELATED TO PAVEMENT TYPE

The test results showing the influence of tire wear, as given in Figures III-1, 4, 5, and 14 through 23, were obtained on both concrete and asphalt surfaces. While the

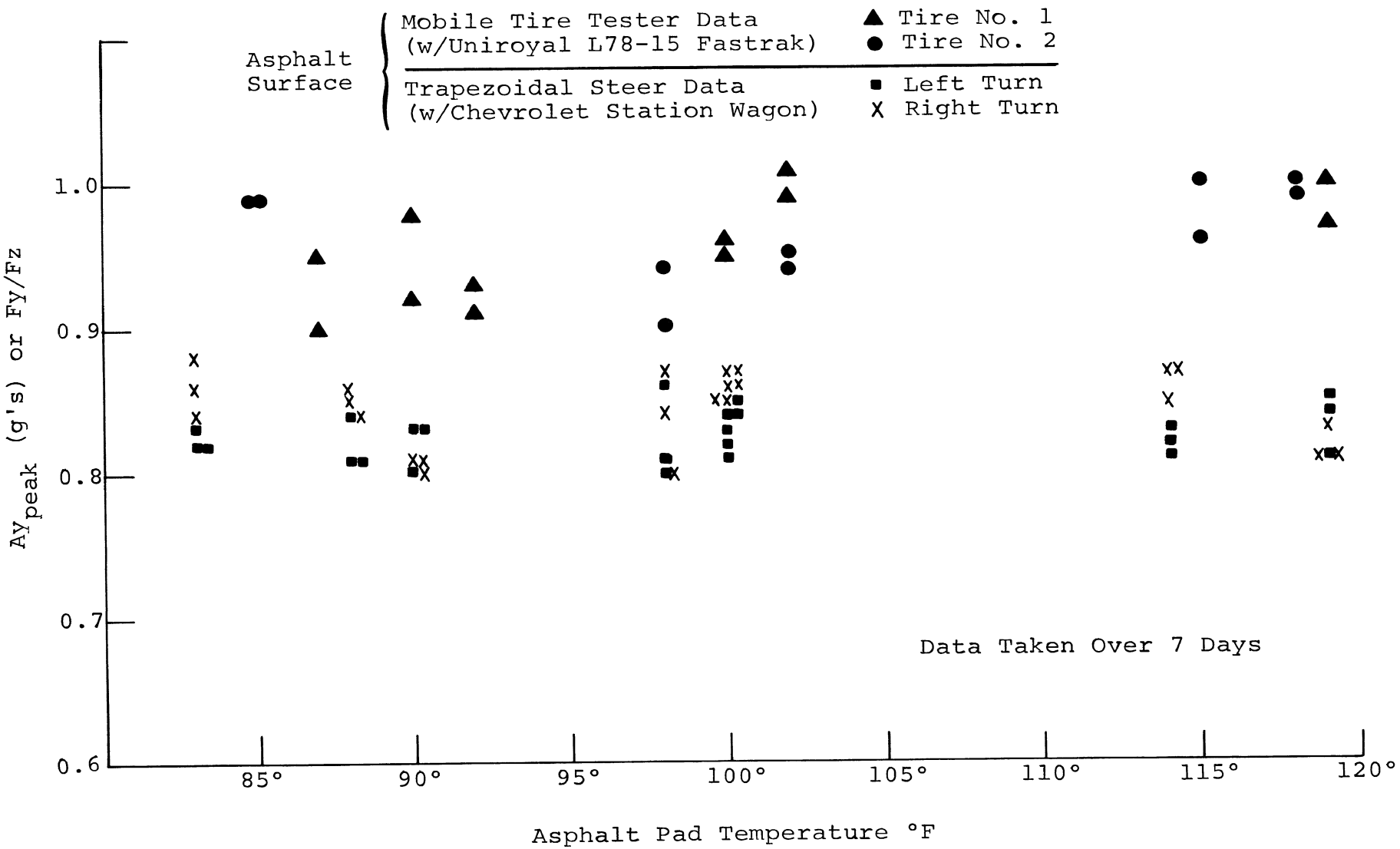

FIGURE III-11

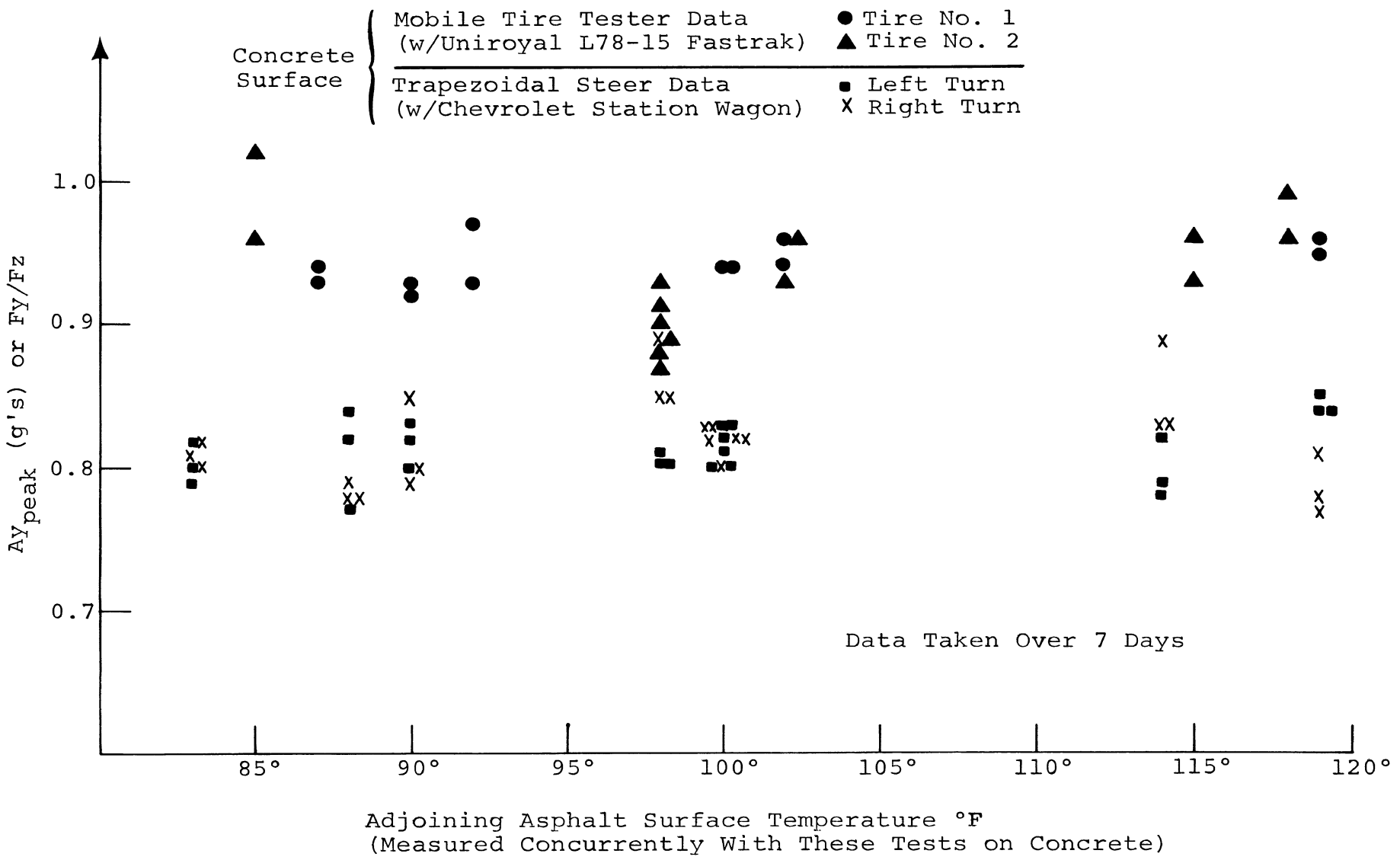

FIGURE III-12

asphalt produces a slightly higher lateral force than the concrete for almost all of the tires tested, there does not appear to be any significant difference between the two surfaces with respect to the manner in which tire wear progresses.

Pad temperature does not have a significant influence on lateral force capability of tires operating on the asphalt surface. Unfortunately, the temperature of the concrete surface was not measured directly. However, the results given in Figure III-13 indicate that temperature change was not a significant factor influencing the developed lateral force during the seven-day measurement period.

In summary, no tire wear or temperature factors have been identified as a basis for selecting a concrete surface over an asphalt surface for vehicle test purposes.

CONCLUSIONS BASED ON THE INVESTIGATION

The results obtained with the Mobile Tire Tester and the test results obtained with the Chevrolet and Dodge show very clearly that:

1. The tire wear produced in the trapezoidal steer maneuver has a very large influence on the maximum side forces produced by the tires and consequently has a large influence on the peak lateral accelerations that are attained. Additionally, the character of the limit response of the vehicle can alter markedly as dissimilar tire wear rates are accrued at front and rear.

2. The pad surface temperature varying over the range (83°F to 119°F) has no first order influence on peak side force.

3. The influence of surface wetness following a rainfall can be presumed negligible upon recovery of apparent dryness, i.e., no pavement discoloration.

APPLICATION OF LATERAL FORCE VERSUS WEAR FINDINGS

Since tire lateral force, and consequently vehicle lateral acceleration, has been shown to increase rapidly with severe cornering wear, it was necessary to establish a tire wearing procedure to eliminate large variations in vehicle test results. Based on Figures III-1 and III-8, it was estimated that the tire wear effects produced in 20 trapezoidal steer maneuvers is equivalent to the amount of tire wear produced during one "lap" of the MTT, as defined in Figure III-2. The resultant procedure was determined in a two step process.

The first step necessitated gathering the tire wear data for all of the vehicles in the sample in a controlled fashion with the MTT. Test conditions for each of 12 tires measured were:

1. 20° slip angle
2. 40 mph steady velocity
3. Tire inflation pressure set to average of front and rear values specified for the respective test vehicle
4. Normal load

$$F_z = .30[\text{Vehicle Weight} + 300] + 50 \text{ lbs.}$$

Under these conditions, lateral force data was collected for all sample tires over 10 "laps" of the MTT. The range of this data is summarized in Figure III-13. The bars indicate the range of data collected for each test tire. The separate data points collected during each run for all tires are shown in Figures III-14 to III-23.

This data was then analyzed and tabulated to determine the number of laps required for the ratio, F_y/F_z, to stabilize within 5% of its long-term average value. Based on the correlation data taken with the Chevrolet Brookwood, this yields an equivalent number of limit trapezoidal steer maneuvers required. Table III-2 presents a listing of the pertinent tire wear-in values for each of the measured tires.

TABLE III-2. TIRE WEAR-IN DATA

Vehicle	Tire	Asphalt Long-Term F_y/F_z	No. Laps To Wear In To Within 0.05	Equivalent Limit Trapezoidal Steer Maneuver
VW	Continental 560-15	1.07	1.0	20
Imperial	Goodyear L84-15	0.99	2.0	40
Mercedes	Firestone 735-14	1.00	0	20 (min.)
Lotus	Dunlop 144 HR13	0.81	0	20 (min.)
*Austin	Dunlop 595-12	0.59	1.5	30
Gremlin	Goodyear F60-15	1.08	2.0	40
Trans-Am	Goodyear F60-15	0.88	1.5	30
Toyota	Dunlop 155-13	0.81	0	20 (min.)
Galaxie	Uniroyal F78-15	1.07	2.0	40
Toronado	Firestone J78-15	0.99	1.5	30
Coronet	Goodyear F78-14	1.00	2.5	50
Brookwood	Uniroyal L78-15	1.02	2.5	50

It is interesting to note the wide variation in the number of runs required to wear-in these different types of tires. It is also interesting to note that these tires seem to divide into 4 ranges of lateral force capability. The VW, Gremlin, and Galaxie tires have very large lateral force capability ($F_y/F_{z_{max}} \doteq 1.07$). The Imperial, Mercedes, Toronado, Coronet, and Brookwood tires have large lateral force capability ($.99 \leqq F_y/F_z \leqq 1.02$). The Lotus, Trans-Am, and Toyota tires have relatively low lateral force capability ($0.81 \leqq F_y/F_z \leqq 0.88$). The Austin tire was measured to have an exceptionally low lateral force capability, although it is suspected that this property is indicative of a side force/slip angle relation which peaked at substantially below $\alpha = 20°$, such that the indicated force level does not represent "peak" side force.

The second phase of this procedure requires that the vehicle be tested with the number of "equivalent trapezoidal steer" runs shown in Table III-2 prior to collecting the limit performance data. The conduct of this preliminary set of trapezoidal steer tests, designated as tire break-in tests, was given additional constraints:

1. The minimum number of test runs was chosen to be 20, although MTT data showed no wear effect for certain tires.

2. Tires were cross-rotated after 20 runs if additional limit break-in tests were required.

3. Vehicle response data was recorded during the break-in tests for all vehicles with the automatic test package instruments.

4. All test tires were originally broken in with a minimum of 100 miles of standard driving, prior to initiating any of the wear-in tests.

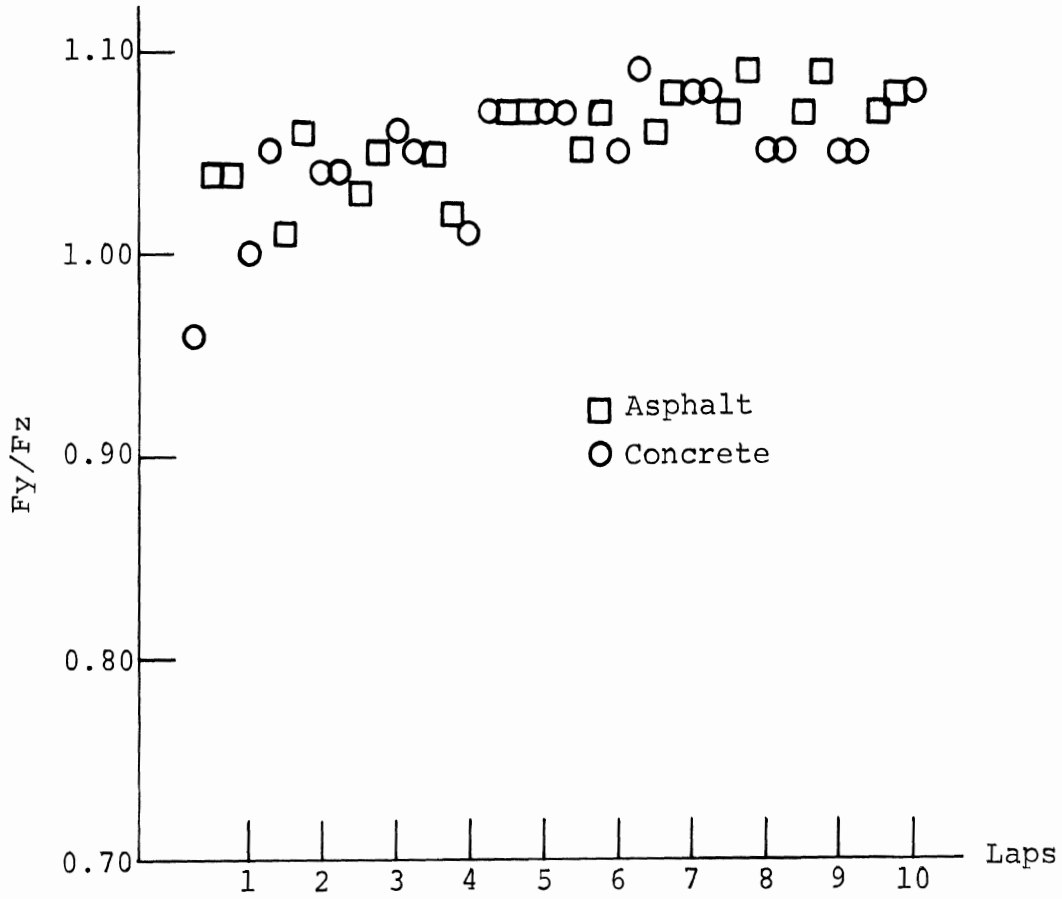

Lateral Force/Wear Data, Mobile Tire Tester, Continental 560-15 (VW).

α=20°, F_z=730, 22 psi, 40 mph

FIGURE III-14.

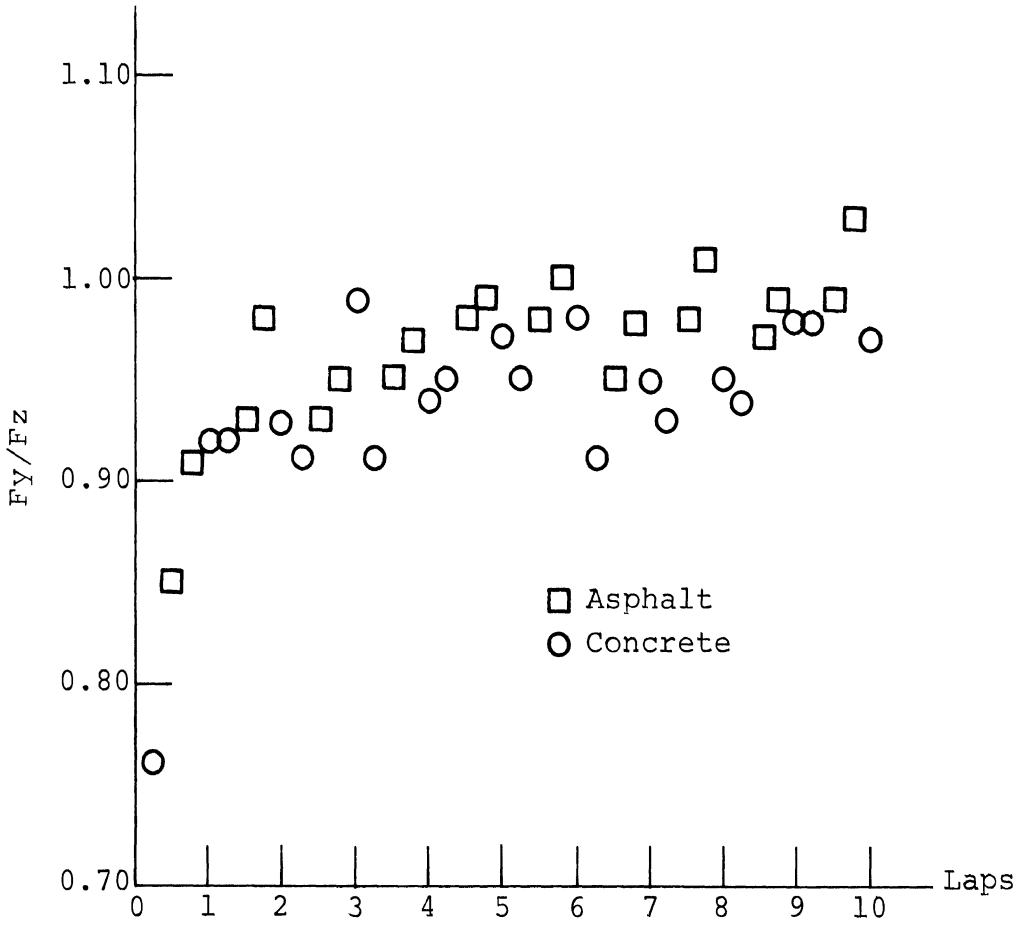

Lateral Force/Wear Data, Mobile Tire Tester, Goodyear L84-15 (Imperial).

α=20°, F_z=1580, 23 psi, 40 mph

FIGURE III-15.

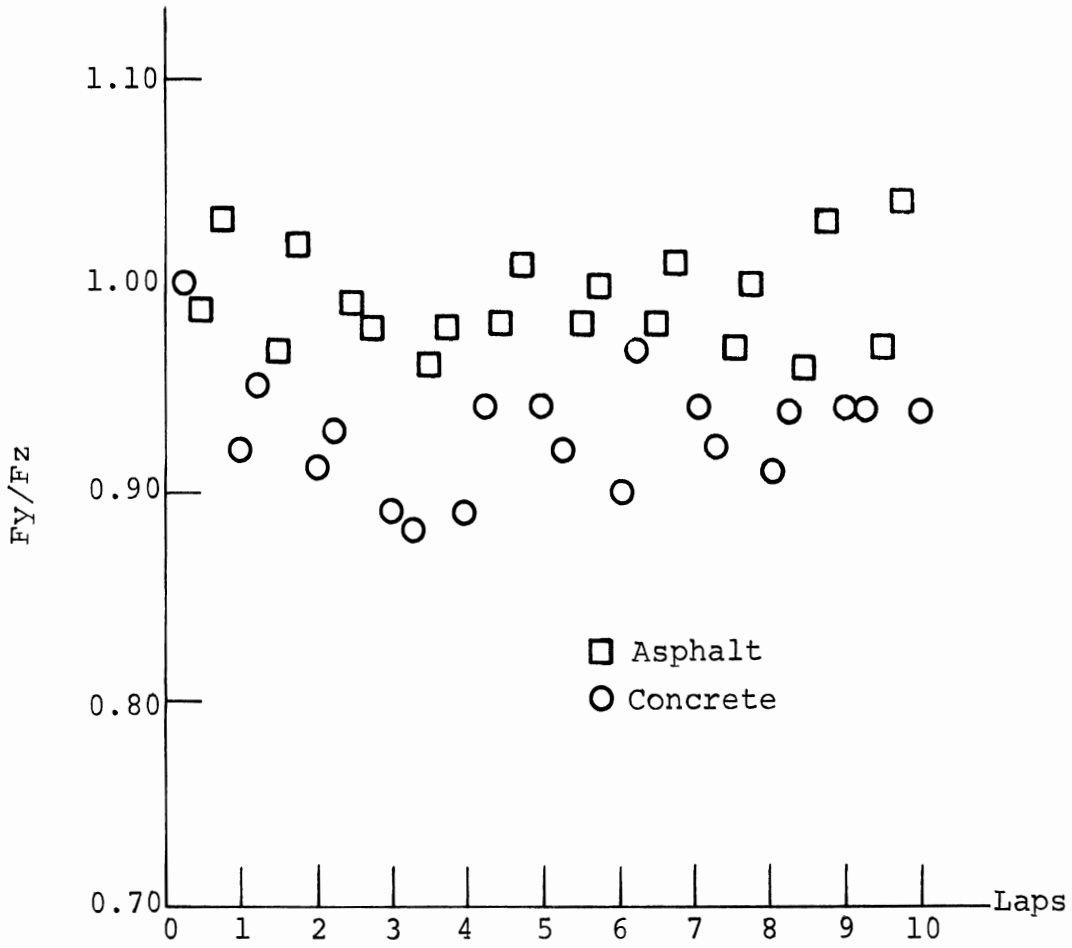

Lateral Force/Wear Data, Mobile Tire Tester, Firestone 735-14 (Mercedes).

α=20°, F_z=1300, 32 psi, 40 mph

FIGURE III-16.

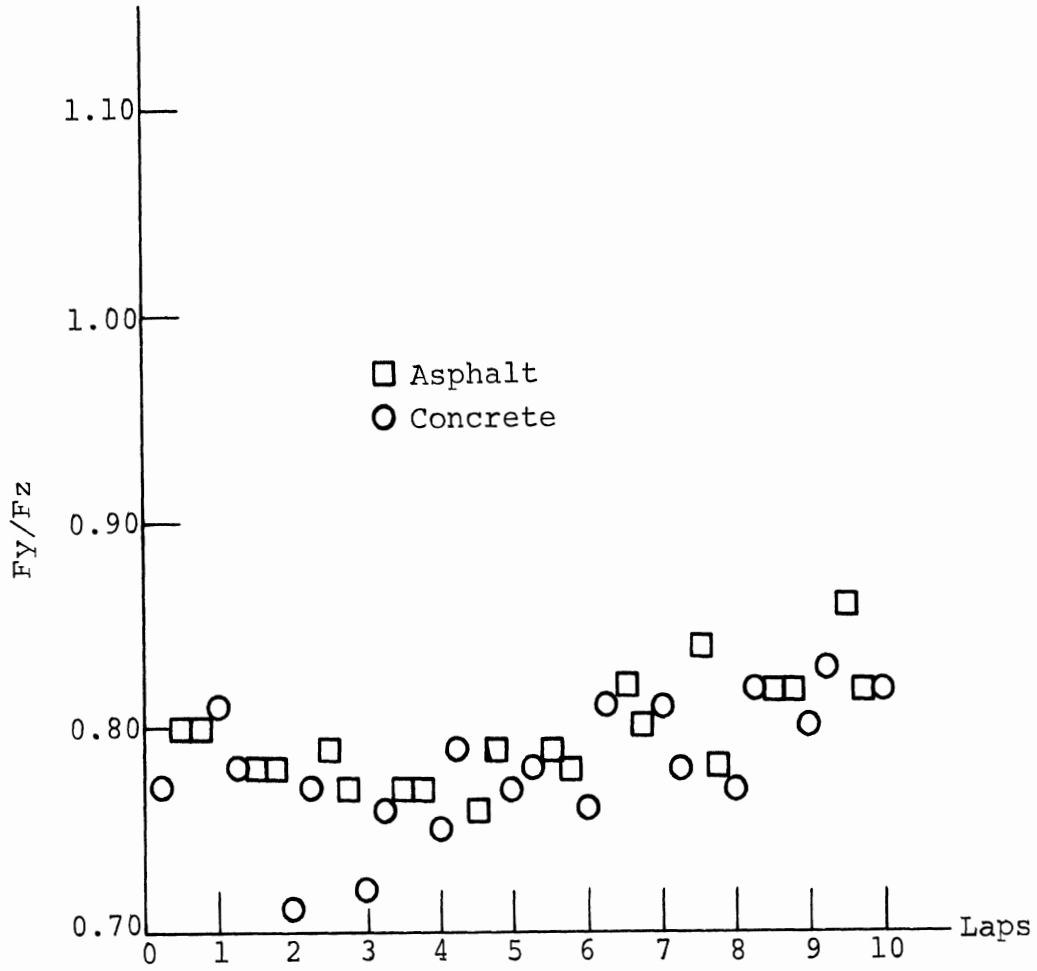

Lateral Force/Wear Data, Mobile Tire Tester, Dunlop 155 HR13 (Lotus).

α=20°, F_z=630, 22 psi, 40 mph

FIGURE III-17.

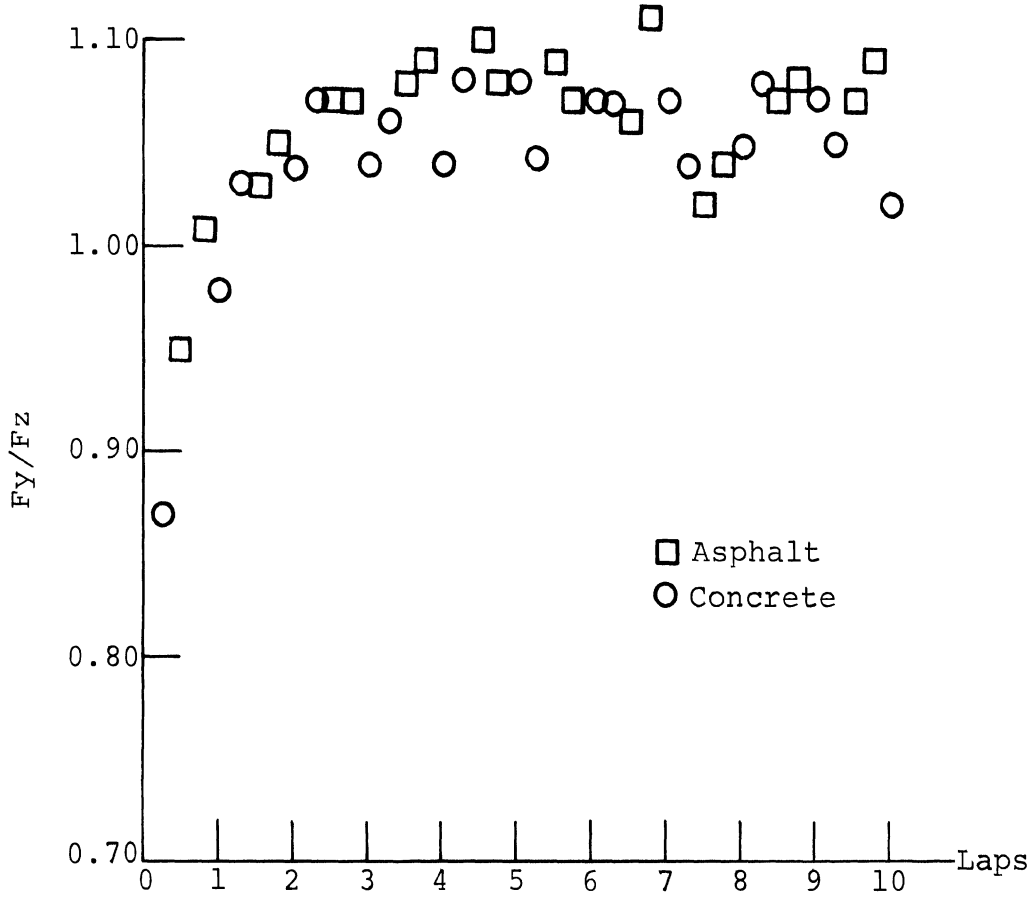

Lateral Force/Wear Data, Mobile Tire Tester, Goodyear 645-14 (Gremlin).

α=20°, F_z=900, 28 psi, 40 mph

FIGURE III-18.

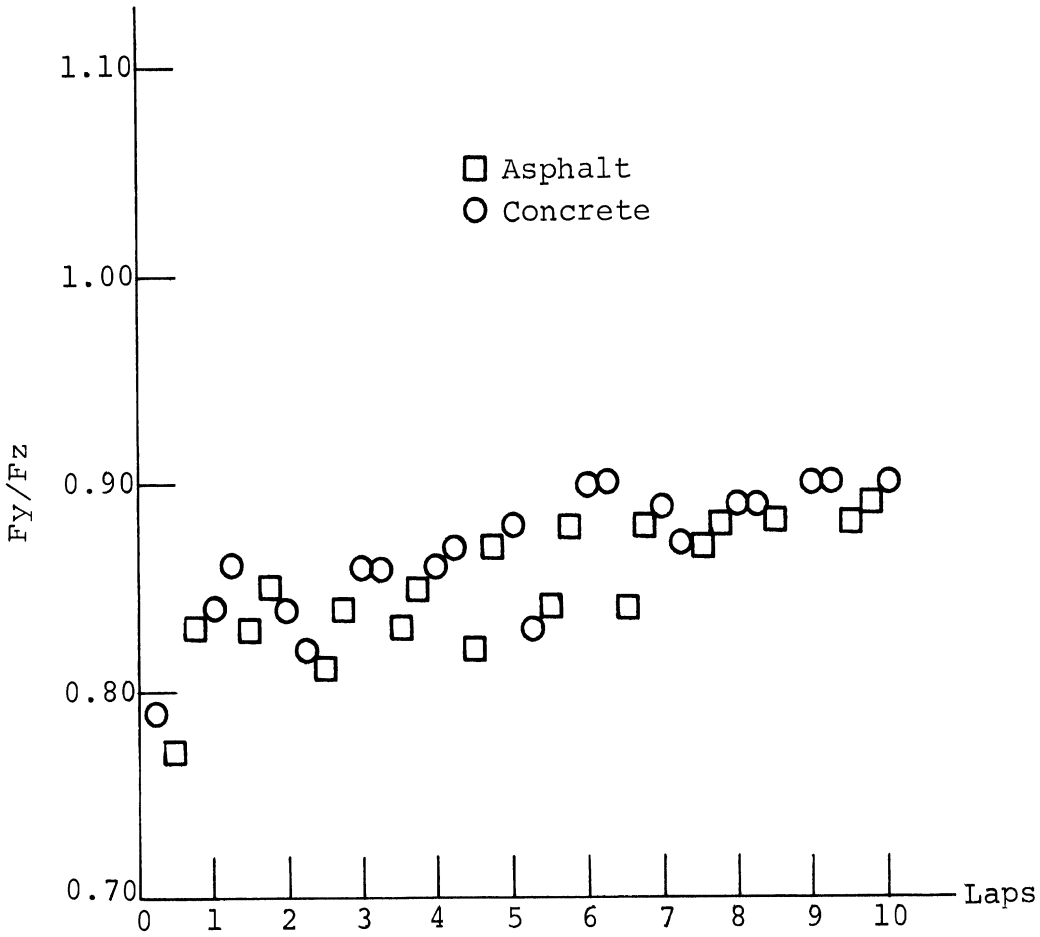

Lateral Force/Wear Data, Mobile Tire Tester, Goodyear F60-15 (Trans Am).

α=20°, F_z=630, 22 psi, 40 mph

FIGURE III-19.

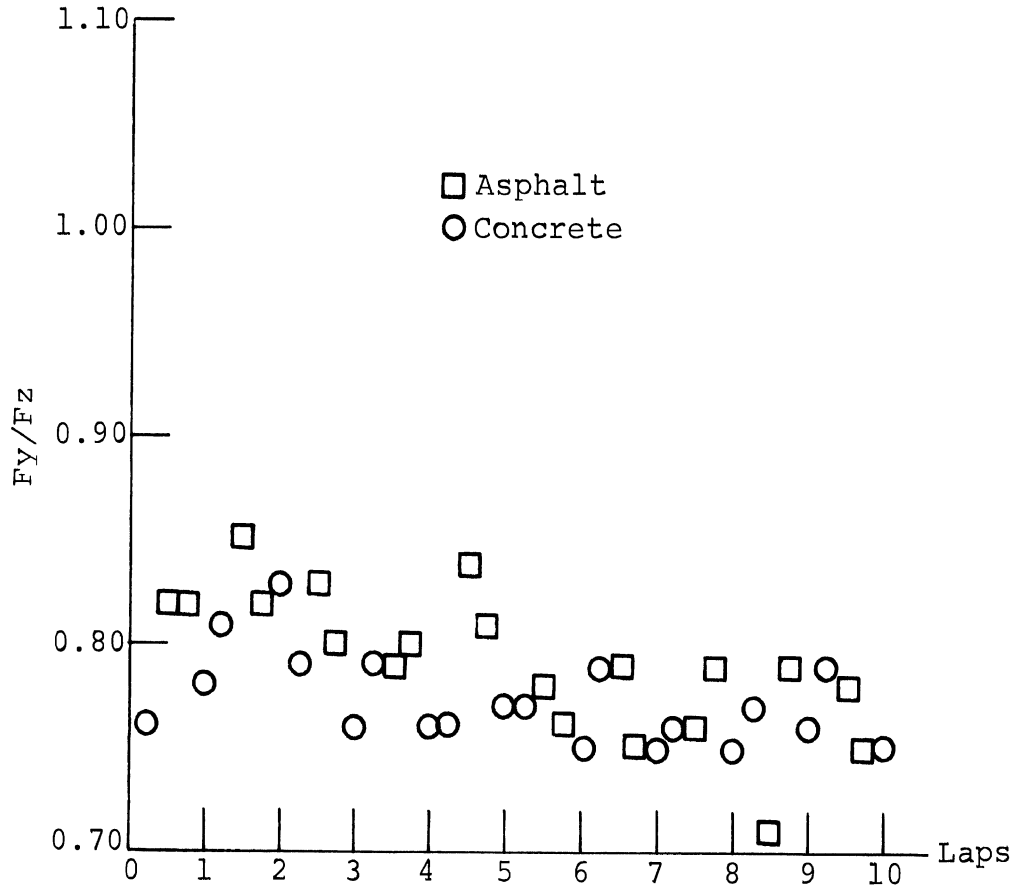

Lateral Force/Wear Data, Mobile Tire Tester, Dunlop 155-13 (Toyota).

α=20°, F_z=710, 22 psi, 40 mph

FIGURE III-20.

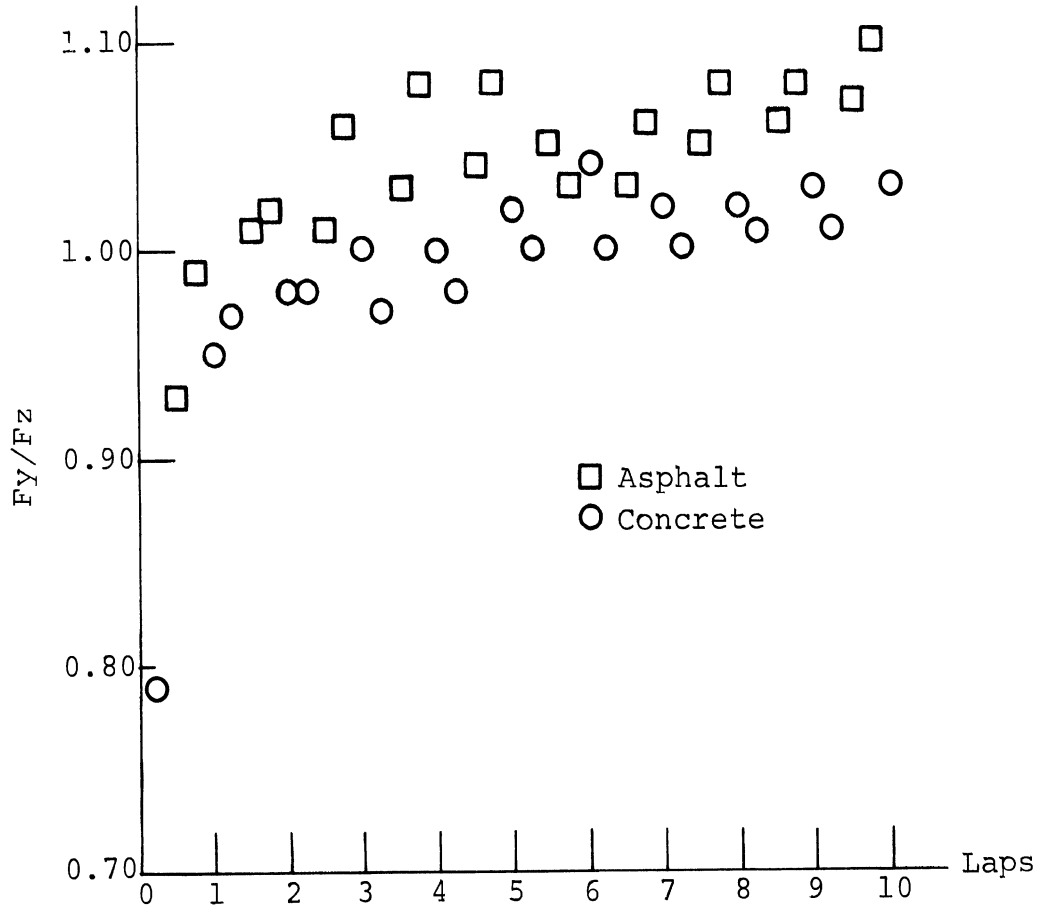

Lateral Force/Wear Data, Mobile Tire Tester, Uniroyal F78-15 (Galaxie).

α=20°, F_z=1310, 28 psi, 40 mph

FIGURE III-21.

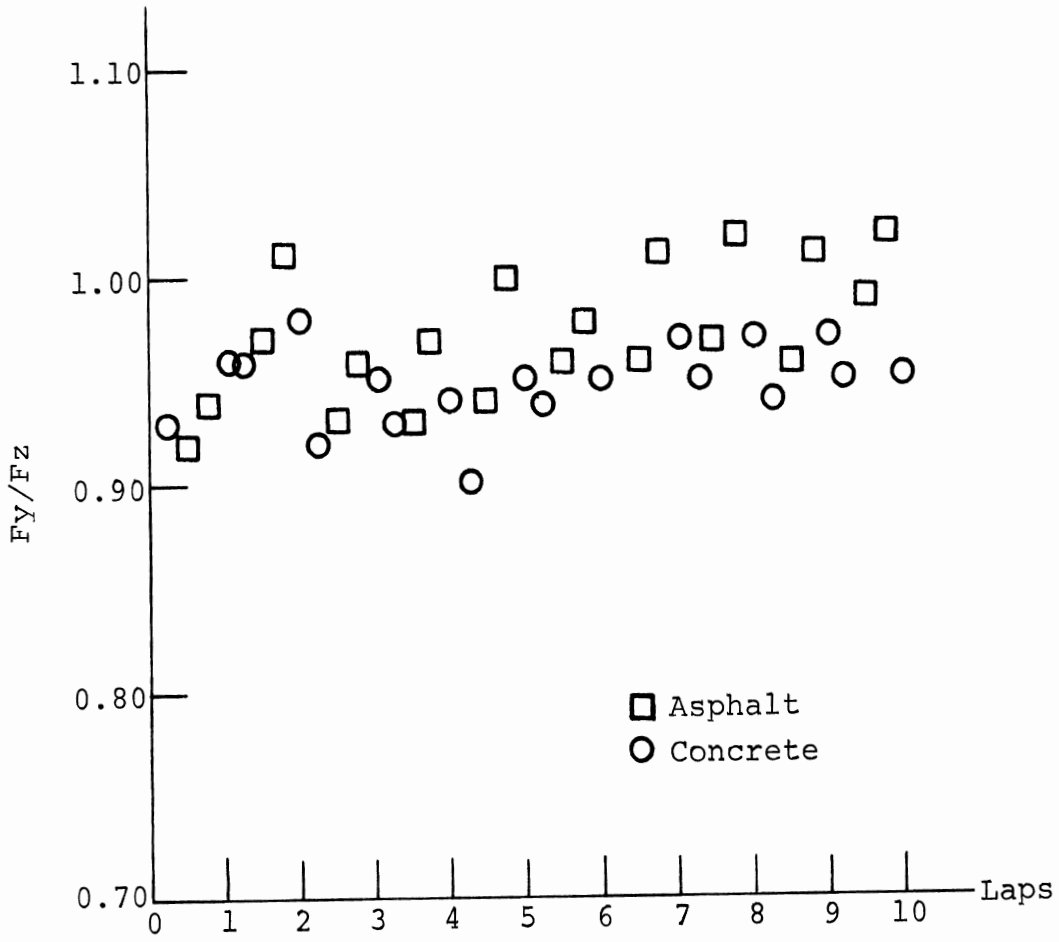

Lateral Force/Wear Data, Mobile Tire Tester, Firestone J78-15 (Toronado).

α=20°, F_z=1570, 24 psi, 40 mph

FIGURE III-22.

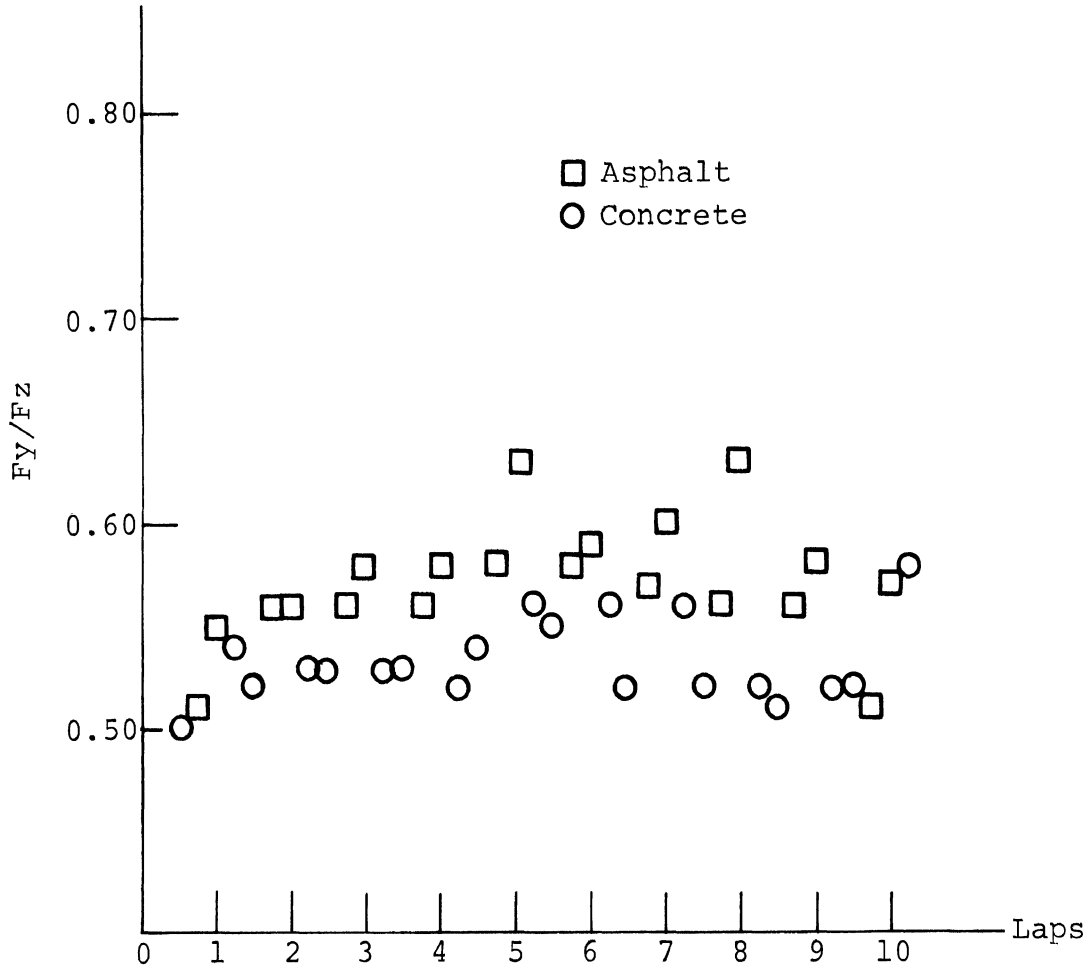

Lateral Force/Wear Data
Mobile Tire Tester
Dunlop 5.95-12 (Austin)
α=20°, F_z=750, 28 psi, 40 mph

FIGURE III-23

APPENDIX IV

SAMPLE VEHICLE SELECTION

This appendix contains the findings and rationale for the selection of 15 vehicles as a test sample. These vehicles were selected on a technical basis, utilizing data available in the literature and in HSRI Accident Data files, to be representative of the population of domestic and foreign passenger cars and multi-purpose passenger vehicles. Due to time and money constraints arising from technical difficulties during the course of the project, only 11 of these vehicles were tested during the full scale test activities. The Toyota Corolla, Ford Bronco, VW Microbus, and Ford Mustang were deleted.

Wherever possible, the vehicle sample is characterized by various parameters and specifications pertinent to vehicle handling performance. Two distinct analyses were conducted:

1. A characterization of the vehicle population in terms of design differences, mechanical characteristics and performance levels.
2. An analysis of accident data to detect over-involvements attributable to vehicle performance characteristics.

All of the required information was not available in the appropriate format. Additional sources of data, such as vehicle testing as performed by independent groups with regular trade publications, were reviewed and utilized as necessary. The final result is a vehicle sample derived from a blend of pragmatism, vehicle mechanics analysis, and accident data analysis.

ACCIDENT DATA ANALYSIS

The first area of analysis utilized accident data files to identify (1) specific vehicle models, or (2) specific vehicle design characteristics which are over-represented in the total accident population. Eighteen data banks of mass accident data are available at HSRI, each covering a specific area or accident type. For this analysis, HSRI selected the Oakland County, Michigan accident file for the calendar year 1969. This file lists crashes in a county with a population of nearly one million people and which has a wide cross-section of rural and urban areas. The primary reason for using this file is the additional encoding introduced over and above the standard police reports. The file contains 29,265 accident cases with 179 variables each. By means of the Vehicle Identification Number (VIN), positive identification can be made as to vehicle model, body style, manufacturer, and year of manufacture for a subset of cases.

A two-fold analysis was performed on the available data. It appears reasonable to assume rollover accidents and single-vehicle accidents form a logical basis for detecting potential handling difficulties. Hence the analysis attempted to determine which vehicle types are overinvolved or under-involved in these two types of accidents.

It is clear that the question of whether or not other factors are involved in the cause of these types of accidents must be considered in an analysis of this nature. Accordingly, an attempt was made to construct a statistical model to normalize other possible causative factors, such as driver age, the condition of the road surface, and drinking involvement.

These efforts led to a negative finding, namely, very little variance in rollover accidents can be attributed

to factors such as those cited above. On the other hand, about ten percent of the variance in single-vehicle accidents can be attributed to driver age, road surface condition, etc. Notwithstanding this finding, application of these correction statistics to the single-vehicle accident analysis did not appear warranted after the raw data were tabulated.

In contrast with other accident files, Oakland County police code vehicles as the "number one" and "two" vehicles without making judgments as to culpability. Consequently, we cannot assume that the vehicle coded as #1 is a "striking" vehicle rather than a "struck" vehicle. This fact places certain limitations on the depth of the various analyses that can be performed.

If the entire file is examined, rather than the subset in which the VIN numbers can be used to identify a specific model, we obtain Table IV-1 in which vehicles are identified only by the name of the manufacturer. The table tabulates the number of single-vehicle accidents and rollovers for each make and the ratio of rollovers to single-vehicle accidents (given as a percentage). It is apparent that Volkswagens have a tendency to roll relative to their number of single-vehicle accidents that is at least three times greater than any other make listed.

If we assume that vehicles coded as vehicle #1 reflect the distribution by make in the total accident population, we can construct Table IV-2, producing a ranking that reflects rollover involvement with respect to the total accident population in Oakland County. Again the Volkswagen stands out as a make having a greater tendency to roll than any other brand of car. A table similar to Table IV-2 can also be constructed to establish the ratio of single-vehicle accidents

TABLE IV-1

Vehicle Make	Number of Rollover Accidents	Number of Single Vehicle Accidents	Rollovers as a Percent of Single Vehicle Accidents
Volkswagen	30	96	31.2
American Motors	5	46	10.9
Chrysler	4	37	10.8
Plymouth	13	139	9.4
Ford	37	497	7.4
Pontiac	28	397	7.1
Chevrolet	42	627	6.7
Cadillac	2	32	6.3
Mercury	5	91	5.5
Buick	7	130	5.4
Dodge	4	117	3.4
Oldsmobile	4	143	2.8

TABLE IV-2

Vehicle Make	Rollovers as a Percent of the #1 Vehicle Population
Volkswagen	7.9
American Motors	2.3
Chrysler	2.3
Plymouth	2.2
Ford	1.8
Pontiac	1.7
Chevrolet	1.7
Buick	1.2
Mercury	1.2
Cadillac	1.1
Dodge	0.8
Oldsmobile	0.6

to the distribution of vehicles in the accident population. Table IV-3 results and, not surprisingly, shows that there is only a small differentiation between makes (i.e., brands) in their tendency to become involved in a single-vehicle accident.

A more meaningful analysis would, in theory, be obtained if the population were broken down in groupings representing either particular vehicle models or design similarities. The problem always exists, however, in that the greater the number of vehicle groupings, the smaller the number of cases in each cell producing a lesser statistical significance for the finding. Accordingly, an effort was made to group vehicles in a manner that would single out design features and, in certain instances, specific models without defining a category that would result in so few vehicles that it would not be possible to compute statistically significant overinvolvements. These considerations led to the groupings that are defined in Table IV-4, which grouping has been used in the analyses to be reviewed below.

The accident file subset (with the VIN data encoded therein) produces the raw data tabulated in Table IV-5. It will be noted that the two American front-wheel-drive automobiles (Group D) yield the smallest number of accident cases reflecting their small percentage of the total motor vehicle population. It should also be noted that the vehicles, as grouped, produce a distribution that is approximately the same irrespective of whether this distribution is computed on the basis of vehicles coded as #1 or #2. The only marked difference in the table between the percentage of #1 and #2 vehicles in the accident population is Group M (all vehicles manufactured by Volkswagen) where it is seen that significantly more Volkswagens are coded #1 than #2 in the accident reports. In this subset of 1969 Oakland County accidents, we

TABLE IV-3

Vehicle Make	No. of Veh. Coded #1	No. of Single Vehicle Accidents	Single Veh. Accidents as a % of the #1 Vehicle Population
Oldsmobile	950	143	15.2
Volkswagen	672	96	14.3
Chevrolet	4956	627	12.7
Ford	4466	497	11.1
Dodge	1064	117	11.0
Pontiac	3632	397	10.9
American Motors	435	46	10.6
Plymouth	1363	139	10.2
Buick	1450	130	8.95
Chrysler	459	37	8.1
Cadillac	458	32	7.0

TABLE IV-4

Group	Manufacturer	Body Size	Years
A	American Motors	all except mini & sport compact	all
B	General Motors	intermediates	1968-
	Chevrolet	personal luxury	1969-
	Pontiac	personal luxury	1969-
C	General Motors	full-sized	1969-
	Buick	personal luxury	all
D	Cadillac	personal luxury	all
	Oldsmobile	personal luxury	all
E	Chevrolet	sport compact	all
	Pontiac	sport compact	all
	Plymouth	sport compact	all
	Dodge	sport compact	all
F	American Motors	mini	all
	Chevrolet	mini	all
	Dodge	mini	all
	Ford	mini	all
	Plymouth	mini	all
G	Chrysler	full-sized	1967-
	Dodge	full-sized	1967-
	Imperial	full-sized	1967-
	Plymouth	full-sized	1967-
H	Dodge	intermediate	1967-1970
	Plymouth	intermediate	1967-1970
I	Chevrolet	compact	all
	Ford	compact	all
	Dodge	compact	all
	Mercury	compact	all
	Plymouth	compact	all
J	Ford Motor Co.	full-sized	1969-
	Ford Motor Co.	personal luxury	1969-
K	Ford and Mercury	intermediate	1968-
L	Ford and Mercury	sport compacts	all
M	Volkswagen	all	all
O	all	station wagon	all
*N2	all	van type (VW Microbus, etc.)	all

*This group was added later and is not included in the totals used in computing percentages for groups A through O.

find that there are 1080 single-vehicle accidents and 93 rollover accidents.

The data in Table IV-5 have been used to compute for each grouping involvement ratios defined as:

$$\frac{\text{percentage of rollovers}}{\text{percentage of all accidents}}$$

or

$$\frac{\text{percentage of single-vehicle accidents}}{\text{percentage of all accidents}}$$

These involvement ratios are tabulated in Table IV-6 where a number of greater than one can be interpreted as an over-involvement and a number less than one is an underinvolvement. Note that the vehicle groups are ordered in the table in accordance with their rollover involvement ratio. The ranking with respect to single-vehicle accident involvement is also shown.

Examination of Table IV-6 shows that two groups (all Volkswagens and all van-type vehicles) are heavily over-involved in rollover accidents. A second clear finding is that station wagons (Group O) are markedly underinvolved in rollover accidents. Thirdly, it is seen that the Volkswagens and the vans are also markedly overinvolved in single-vehicle accidents. In general, there appears to be a strong correlation between rollover and single-vehicle accident involvement ratios. For purposes of guiding the selection of the 15 vehicle sample, the conclusion was drawn that one specific vehicle make and one design category should be included to represent vehicles that are presumed to be handling deficient. It is less clear whether there is a design grouping that can be reliably assessed as making a smaller than normal contribution to the accident records as a result of its good performance characteristics.

TABLE IV-5

Vehicle Group	Number of Rollovers (%)	Number of S.V.A. (%)	Number of #1 Veh. (%)	Number of #2 Veh. (%)	Veh. #1 + Veh. #2 (%)
A	2(2.2)	32(3.0)	241(2.95)	297(3.1)	(3.0)
B	8(8.8)	131(12.3)	1009(12.4)	1268(13.2)	(12.8)
C	9(9.9)	133(12.5)	1142(14.0)	1438(15.0)	(14.5)
D	0(0.0)	4(0.4)	67(.8)	64(.7)	(.7)
E	5(5.5)	71(6.7)	462(5.7)	543(5.6)	(5.65)
F	2(2.2)	26(2.4)	164(2.0)	213(2.2)	(2.1)
G	1(1.1)	50(4.7)	605(7.4)	736(7.7)	(7.55)
H	5(5.5)	79(7.4)	429(5.3)	525(5.5)	(5.4)
I	7(7.7)	66(6.2)	496(6.1)	648(6.7)	(6.4)
J	4(4.39)	51(4.8)	482(5.9)	581(6.0)	(6.0)
K	1(1.1)	32(3.0)	315(3.9)	359(3.7)	(3.8)
L	11(12.1)	130(12.2)	895(11.0)	1100(11.4)	(11.2)
M	33(36.3)	133(12.5)	722(8.9)	532(5.5)	(7.1)
O	3(3.3)	126(11.8)	1117(13.7)	1311(13.6)	(13.7)
N2	2(2.2)	16(1.5)	74(.4)*	NA	NA
TOTAL	91	1064	8146	9615	

*This figure is the sum of vehicles coded #1 and #2

TABLE IV-6

Vehicle Group	Number of Rollovers	Rollover Involvement	No. of Sing. Vehicle Acci.	S.V.A. Involvement	S.V.A. Ranking
N2	2	5.214	16	3.571	1
M	33	5.136	133	1.771	2
I	7	1.194	66	.963	8
L	11	1.076	130	1.087	6
F	2	1.028	26	1.146	5
H	5	1.022	79	1.382	3
E	5	.972	71	1.181	4
J	4	.734	51	.801	12
A	2	.725	32	.993	7
B	8	.686	131	.960	9
C	9	.681	133	.860	11
K	1	.288	32	.792	13
O	3	.241	126	.866	10
G	1	.144	50	.621	14
D	0	0	4	.507	15

VEHICLE DESIGN AND PERFORMANCE ANALYSIS

The problems and difficulties that are inherent to the task of predicting variance in limit maneuver performance has been previously discussed in HSRI's response to RFP-NHTSA-1-A517. To summarize briefly, the major difficulties are the inability to obtain information on (1) the mechanics of tires and (2) data that define the distribution of loadings on the tires in steady-state or transient maneuvers. Recognizing that there are very little published data by which it is possible to make a reliable prediction of limit maneuver performance, HSRI suggested to DOT that we would utilize performance data to the degree that these data were available. Subsequently, it was determined that the majority of the objective performance data collected on behalf of the "Motoring Which" publication in Great Britain apply to vehicles which are not exported to the U.S. for sale. Fortunately, additional sources of objective data were found, primarily from magazines published on behalf of the motor vehicle enthusiast. Given that there is no basis for judging the accuracy of the published information, the prevailing attitude has been one of "making do."

Vehicle response to steering and braking inputs depends on a large variety of vehicle and tire parameters. Absolute values of these parameters do not, however, serve to indicate response or performance differences. Rather it is proper to compare tire and vehicle parameters after they have been reduced to an appropriate nondimensional form. Some of these nondimensional forms are readily derived from the linearized equations of motion describing a motor vehicle and others may be deduced both from physical reasoning and mathematical descriptions of the nonlinear tire-vehicle system.

Although many nondimensional parameters were originally advanced by HSRI to serve as a basis for characterizing the motor vehicle population from a performance point of view, it did not prove to be possible to generate all of the desired tabulations. Certain data could be generated for domestic vehicles which could not be generated for foreign vehicles, and vice versa. Ultimately, it proved necessary to accept the following eight variables as meaningful predictors of performance in some of the limit maneuvers developed earlier by HSRI:

(1) nondimensional value of yawing moment of inertia

(2) distribution of weight between front and rear axles

(3) brake torque distribution between front and rear axles (normalized by the weight distribution)

(4) path curvature generated at zero speed by a unit displacement of the steering wheel

(5) minimum value of tire reserve load (percent)

(6) height of c.g. to average track

(7) peak braking capability (wheels unlocked)

(8) peak cornering capability

The first quantity provides a measure of the nondimensional yaw damping possessed by a vehicle and the yawing acceleration created by a steering input, if the cornering coefficient of the tires can be assumed to be the same for all members of the vehicle population. This latter assumption is obviously not valid. Consequently, item (1) can only be an indicator of the aforementioned vehicle properties. Although efforts were made to develop a rough predictor of the

cornering coefficient of tires, as installed on a given vehicle, the attempt had to be abandoned.

A more important tire property, with respect to limit maneuver performance, is the maximum traction that can be generated on a given surface. Since traction data are not available for the multitude of tires that are used on vehicles today, tire traction levels may be partially deduced from maximum acceleration measurements, items (7) and (8), with some evidence of traction performance deriving from item (5)--tire reserve load.

Weight distributions, per se, is not a clear-cut indicator of the manner in which a vehicle will perform at the limit. It is a property, however, which a designer must take into careful account in order to achieve a design that behaves satisfactorily in the hands of the average driver. To the degree that weight distribution becomes further biased when a vehicle is loaded to its maximum capacity, the potential for change in limit performance is significantly increased. Designs that produce a large shift in c.g. location as a result of carrying a maximum payload provide a convenient means to evaluate the influence of weight bias and suspension static trim on the mechanical properties of tires and suspension and the resulting impact on limit maneuver performance.

Brake torque distribution clearly influences the maximum braking performance as a function of loading and tire-roadway friction coefficient. This design parameter also influences the order of wheel lock-up and lock-up tendencies in maneuvers involving combined turning and braking. Accordingly, it appears that this nondimensional variable, as adjusted by weight bias, should be taken into consideration in selecting a vehicle test sample.

Clearly, the understeer level of a vehicle and the change in this level as a function of lateral acceleration are performance characteristics constituting a substantive means for discriminating among the elements of the vehicle population. Unfortunately, such data are not in the public domain. Nevertheless, it is possible to establish the basic steering response gain which understeer modifies as a function of speed and level of lateral acceleration. Given that steering-wheel imputs in emergency maneuvers are ultimately displacement limited, it appears that the zero-speed value of path curvature gain (the inverse of the product of overall steering ratio and wheelbase) is a factor of interest.

The ratio of c.g. height to average track should, in theory, be a valid indicator of rollover potential, provided the tire population has a peak lateral traction capability which is relatively constant. Other design features, however, play a significant role and, in certain cases, suspension geometry may constitute the critical factor. Notwithstanding the variability in tire traction properties and the complexities involved in predicting a potential for rollover, it appears advisable that the test sample include some extreme values of c.g. height to average track.

All of the design variables or vehicle parameters discussed above were tabulated for a large number of models and, where possible, for foreign vehicles sold in the U.S. (The overall task was complicated considerably by the myriad of choices available to the consumer in the domestic vehicle market.) These tabulations together with test findings of maximum acceleration plotted as shown in Figure IV-1 constituted the raw material for the selection process.

The final selection of the test sample was based on these findings with the aid of a pragmatic and somewhat arbitrary method for interrogating the summarized data. The final selection process and the results are summarized below.

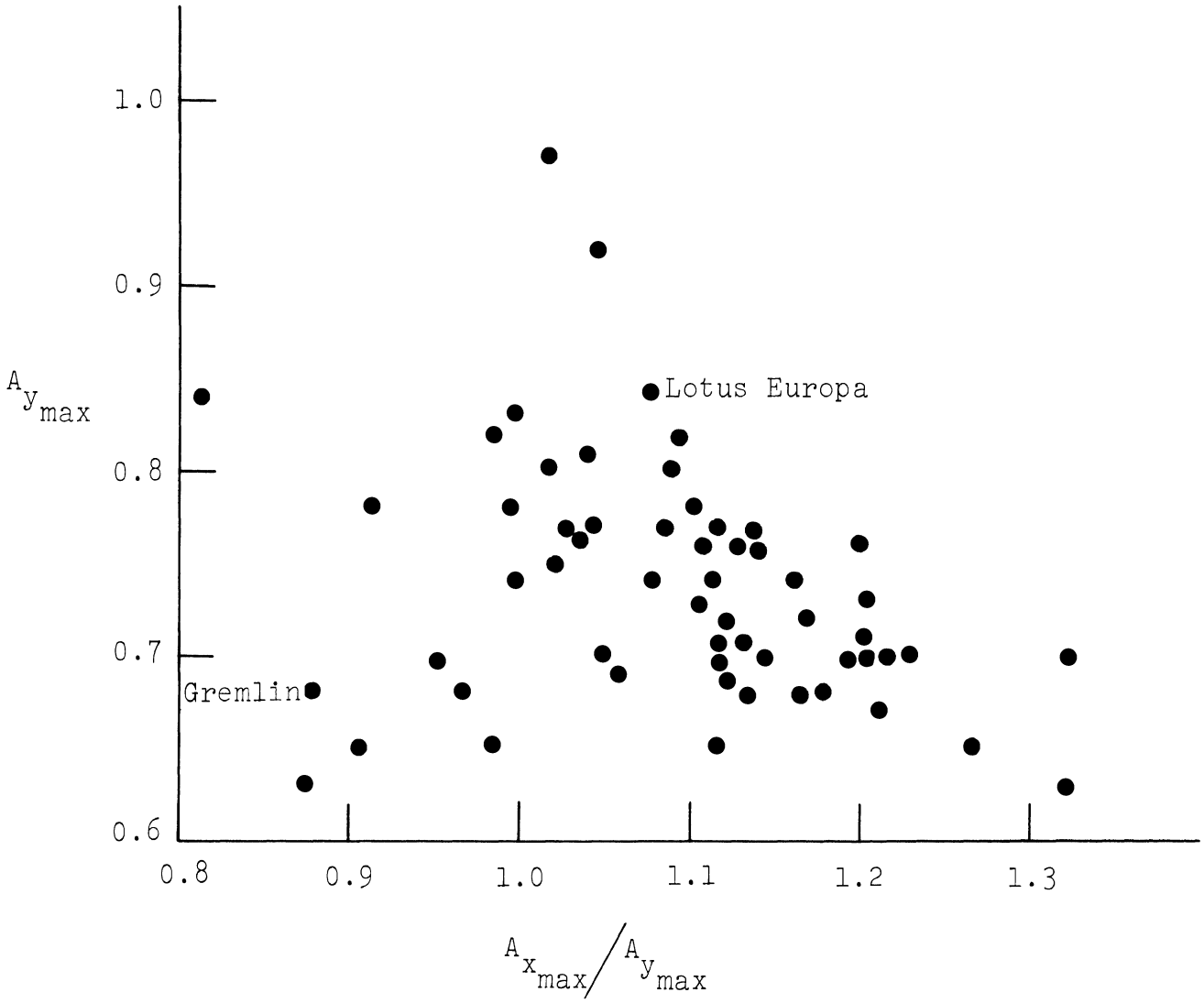

Figure IV-1.

Maximum Steady Accelerations
(Cornering and Braking)

Achieved by 57 Vehicles Tested
by Sports Car Graphic on the Digitek Skid Pad

SUMMARY OF THE FINAL SELECTION PROCEDURE

In general, the criterion used for vehicle selection involved:

(a) a search for an extreme value along a continuum of a single variable or parameter,

(b) a search for vehicles that are located near the edge of the maneuvering space defined in Figure IV-1,

(c) consideration of the findings of the accident analysis,

(d) consideration of other factors, both technical and pragmatic in nature.

Among the latter factors, HSRI identified:

(a) overall size and weight

(b) vehicle cost as a reflection of component quality and engineering investment

(c) location of driving wheels

(d) c.g. shift due to loading

(e) high power to weight ratio as, for example, exists in a so-called "muscle" car

(f) presence of a wheel antilock system.

In addition to these considerations, some test data were available on the amount of chassis roll per unit of steady lateral acceleration (degrees per g). Although rolling compliance was not discussed as a variable serving to differentiate among the elements of the vehicle population, it appears that this dimensional parameter has a variation in excess of 100 percent (i.e., two to one). It proved

possible to factor this variable into the sample determination without requiring a vehicle to be chosen that otherwise would not be selected.

In the following outline of the selection process, we give the rationale and pragmatic basis for arriving at the vehicle sample. As each vehicle is identified it is given a number (in parentheses). At the conclusion of the discussion, the pertinent data are tabulated for all 15 vehicles listed in Table IV-7.

In addition to being a vehicle that represents a high initial cost, the Mercedes 300SEL (1) is designed with a load-sensitive air suspension that keeps the suspension deflection fixed for all loading conditions. The Mercedes constitutes a rather large vehicle in the import population (curb weight is 3920 pounds) and for purposes of contrasting its performance with a large luxury domestic vehicle, it appears logical to select a Chrysler Imperial (2) (a 2-door sedan weighing 4795 pounds), which vehicle further provides the opportunity to evaluate the influence of a four-wheel antilock system on limit-maneuver performance.

Consider next the desirability of having front, rear, and four-wheel drive vehicles in the sample. Three vehicles, other than conventional rear drive vehicles, were selected. The Oldsmobile Toronado (3) is a large size luxury car possessing front-wheel drive which can further be compared with the Chrysler Imperial (2) and the Mercedes 300 SEL (1). The Austin America (4)* is a small front-wheel drive car whose performance can and should be compared with the small rear-drive vehicles. In order to cover all wheel drive configurations, a Ford Bronco (5), with the four-wheel drive option, was added to the vehicle sample.

---

*All vehicles marked with an asterisk are part of the five-vehicle sample shared with the Component Wear and Degradation Study.

At this point, we chose to consider vehicles that represent two extremes in the nondimensional value of yawing moment of inertia. The Chrysler Imperial (2) appears to rank very high on this scale (i_x = .294) with the Lotus Europa (6) (i_x = .142) ranking among the lowest in this regard due to its mid-engine design. A second reason for selecting the Lotus Europa (6) is its relatively high value of maximum lateral acceleration ($A_{y_{max}}$ = .84) as reported in tests performed by Sports Car Graphic. At the low end of the maximum lateral acceleration scale we find the Austin America (4)* ($A_{y_{max}}$ = .624), a choice that thus serves on two counts.

With respect to weight distribution, the Toronado (3) appears to be well up among cars with a large forward weight bias (W_f/W = .602). A vehicle serving to represent a large rearward weight bias is the VW Super Beetle (7)*. (W_f/W = .44). Of course, the accident record, as analyzed above, provides further ground for selecting the VW Super Beetle (7)*, although it must be recognized that this vehicle has a suspension that differs from the VW's that were involved in the single-vehicle accident and rollover study. A second reason for selecting the VW Super Beetle (7)* is its large value of estimated c.g. height to average track (.604). On the other hand, one of the lowest values of this parameter is possessed by the Ford Mustang (8)* (.453). A vehicle possessing an estimated c.g. height to average track that is even higher than the VW Super Beetle is the Toyota Corolla 1200 (9) (.618) and it is included in the sample for additional reasons of (a) representing the Japanese imports and (b) being a second vehicle with a low value of measured maximum lateral acceleration ($A_{y_{max}}$ = .65).

A station wagon is the vehicle configuration that suffers the largest change in fore and aft weight distribution as a result of loading. Although it may be anticipated that an intermediate wagon with a six-cylinder engine might suffer the most in this respect, the Chevrolet Brookwood Wagon (10)* was included in order to take advantage of its presence in the five vehicles being shared with the Suspension and Steering System Wear and Degradation Study. It should be noted that the rearward weight bias of the Brookwood (10)* (W_f/W = .452) is almost as large as the VW Super Beetle.

A vehicle is added to the sample by considering the space of maximum maneuvering capability represented by Figure IV-1. It is clear from examining this figure that motor vehicles, on the average, are able to brake at higher accelerations than they can corner, a test result that certainly is in agreement with theoretical expectations. With the exception of the bonafide racing vehicles included in this test sample, the vehicles that were tested appeared to be able to corner at accelerations ranging from 0.63 to 0.84g. The ratio of maximum longitudinal acceleration to maximum lateral acceleration ranges from 0.875 to 1.32. It is clear that the Lotus Europa (6) represents a vehicle with a high value of cornering capability with comparable braking capability. At the low end of the cornering and braking performance scale we identify the Gremlin (11) ($A_{y_{max}}$ = .68; $A_{x_{max}}$ = .879), one of the U.S. mini-compacts. When chassis roll per unit of lateral acceleration is considered, we also find that the Gremlin (11) has large roll compliance (ϕ/A_y = 10.7 deg/g) relative to the Lotus Europa (6) (ϕ/A_y = 4.52). Only the Toyota Corolla (9) (ϕ/A_y = 11.5) and the Corona have larger roll compliance than the Gremlin.

With respect to tire reserve, it is found that the Lotus Europa (6) is representative of vehicles with large reserve load capacity (29.48 percent) whereas the Ford Mustang (8) has the lowest reserve load capacity (0.55 percent) of any of the vehicles proposed for the sample.

Only two parameters remain for consideration. With respect to the zero-speed value of path curvature gain, we find that the Gremlin (11) with a manual steering gear possesses a very small value (.00429 ft^{-1}/rad) notwithstanding its small wheelbase. The VW Super Beetle (7)* has a path curvature gain (.00877 ft^{-1}/rad) that is twice that of the Gremlin (11) and possesses the largest value of this parameter of any of the vehicles. With respect to brake torque distribution, no data were readily available for vehicles of foreign manufacture and consequently this parameter has not been weighed in developing the sample.

The accident analysis suggests that a van-type vehicle be included in the sample. The VW Microbus (12) was selected for reasons of its popularity and its low price. It follows that it possesses the highest value of estimated c.g. height to average track of any of the vehicles in the sample.

The "muscle" car in the sample is the Firebird Trans Am (13). Finally, a consideration of the percentage of the market still accounted for by the full-size standard automobile leads to the inclusion of a Ford Galaxie (14). The last vehicle in the sample was taken from the seven passenger vehicles that are being tested for the wear and degradation study and is the Dodge Coronet (15), an intermediate size vehicle.

A breakdown of the sample shows that five of the vehicles are imported cars. It should be clear that each of these were selected to implement the technical portion of the rationale. Of the ten remaining domestic vehicles, four are

General Motors products, three are produced by Ford, two by Chrysler, and one by American Motors. It would appear that the sample is roughly representative of the relative contribution made by each major producer to the domestic market. This result is a by-product of the selection procedure and was not considered to be an important or necessary feature of the selection process.

TABLE IV-7

TABULATION OF VEHICLE PROPERTIES FOR THE SAMPLE OF FIFTEEN VEHICLES

	Wheelbase (ft.)	I_z	Curb Weight (lbs.)	$I_z/M(W.B.)^2$	Wt. Distribution W_f/W	$(W_f/W)^{-1} \cdot T_f/T$	$\frac{1}{(G)(W.B.)10^{-5}}$	Min. Tire Reserve Load (%)	$\frac{h - g.c.}{\frac{2}{\text{Average Track}}}$
Chrysler Imp. (2-dr.)	10.57[1]	4290[1]	4795[1]	.2582[1]	.547[1]	1.095[1]	496[1]	3.3[15]	.501[1]
Mercedes 300 SEL 3.5	9.35[3]	3190[1]	3920[4]	.2995[3]			472[5]	2.4[17]	.535[6]
Oldsmobile Toronado	10.24[1]	4017[1]	4577[1]	.2721[1]	.602[1]	1.188	548[1]	6.6[15]	.471[1]
Lotus Europa	7.58[2]	370[2]	1455[2]	.1424[2]	.460[2]			29.48[2]	.462[2]
Firebird Trans. Am.	9.00[1]	2905[1]	3695[1]	.3127[1]	.578[10]	1.084[1]	670 to 777	7.6[2]	.453[1]
Toyota Corolla 1200	7.65[12]	909[2]	1755[12]	.3079[2]	.560[2]		727[18]	5.6[2]	.618[18]
Am. Mtrs. Gremlin	8.00[1]	1590[2]	2614[1]	.3013[2]	.585[1]	1.062[1]	429[1]	9.2[2]	.495[1]
Ford Bronco	7.67[4]	1595[14]	3175[16]	.2750[16]	.575[16]		543[16]	17.22[16]	.653[13]
VW Microbus	7.87[5]	1912[14]	2904[11]	.1792[14]	.440[11]		820[5]	11.8[11]	.764[5]
VW Superbeetle *	7.95[5]	1173[2]	1970[2]	.3035[2]	.440[2]		877[2]	4.5[2]	.604[2]
Ford Mustang *	9.08[1]	2270[1]	3186[1]	.2782[1]	.575[1]	1.083[1]	498[1]	0.55[15]	.453[1]
Austin America *	7.79[7]	878[14]	1962[8]	.2705[14]	.630[9]			5.0[15]	.525[7]
Dodge Coronet *	9.83[1]	2715[1]	3541[1]	.2535[1]	.542[1]	1.105[1]	544[1]	2.4[15]	.484[1]
Chevy Brookwood Wagon *	10.42[1]	4185[1]	4709[1]	.2642[1]	.452[1]		555 to 685	2.5[15]	.498[1]
Ford Galaxie (4-dr.)	10.08[1]	3410[1]	4090[1]	.2640[1]	.563[1]	1.048[1]	439[1]	1.48[15]	.470[1]

*purchased for S/SS Wear & Degradation study

Symbols

I_z = total vehicle yaw moment of inertia

T_f/T = percent of total braking done by front wheels

$1/(G \times W.B.)$ = overall steering ratio × wheelbase

Data Sources used in Calculations

1 - Data taken from 1971 AMA Specs. -- I_z computed from GM model

2 - Data taken from tabulations developed by Andrew Gilberg

3 - Data taken from Mercedes sales literature -- I_z computed from GM model

4 - Data taken from Automotive Industries magazine with shipping weight corrected to curb weight

5 - Data taken from VW manual entitled "Service Without Guesswork"

6 - Data taken from Arcure Mercedes technical data

7 - Data taken from Austin sales literature

8 - Data taken from Austin owner's manual

9 - Data taken from actual weighing of vehicle

10 - Data taken from 1970 AMA specs.; 71 AMA specs. did not contain necessary data

11 - Data taken from Consumer Reports, August 1971, p. 501

12 - Data taken from Toyota sales booklet, January 1971

13 - Data taken from Bronco sales booklet

14 - Data calculated using $I_z = (1/12)M(L^2 + W^2)$

15 - Data taken from manufacturers' consumer information sheet with new vehicle

16 - Data taken from Ford Dealers truck sales manual

17 - Data calculated using tire size, tire pressure, and gross vehicle weight from manufacturers specs., and tire load rating 1971 Tire & Rim Assoc. Yearbook

18 - Data taken from Toyota Corolla 1200 sales brochure

APPENDIX V

DATA ACQUISITION AND ANALYSIS

TRANSDUCER CAPABILITIES AND CALIBRATION

The various signals recorded on the magnetic tape are listed in Table V-1 with their nominal ranges. These signals are also identified by vehicle test system. For many of these components, secondary or back-up hardware were available and utilized to cope with equipment breakdowns.

Each transducer signal was routed through circuits in the interface module to standardize the voltage calibration levels for both systems. The signal levels were adjusted to yield a full scale calibration level of 71% of the linear dynamic range of the tape recorders. The block diagrams of Figures V-1 and V-2 illustrate the complete systems used to record data.

All of the transducers were calibrated for physical units during vehicle change-overs. Each type of transducer required a separate calibration technique:

1. Accelerometers - The Humphrey Inertial Package was suspended on a "sine table" and incremented through several inclination angles. The appropriate component of the gravity vector was determined for each inclination angle and tabulated to provide the physical reference levels, in g's, for determination of each accelerometer gain.

2. Rate Gyros - Rate gyros were mounted on the sine table and allowed to oscillate in simple harmonic motion. A calibrated rotary potentiometer, providing the time history of angular displacement was recorded together with the rate gyro output on a light-beam oscillograph. The resulting displacement and rate

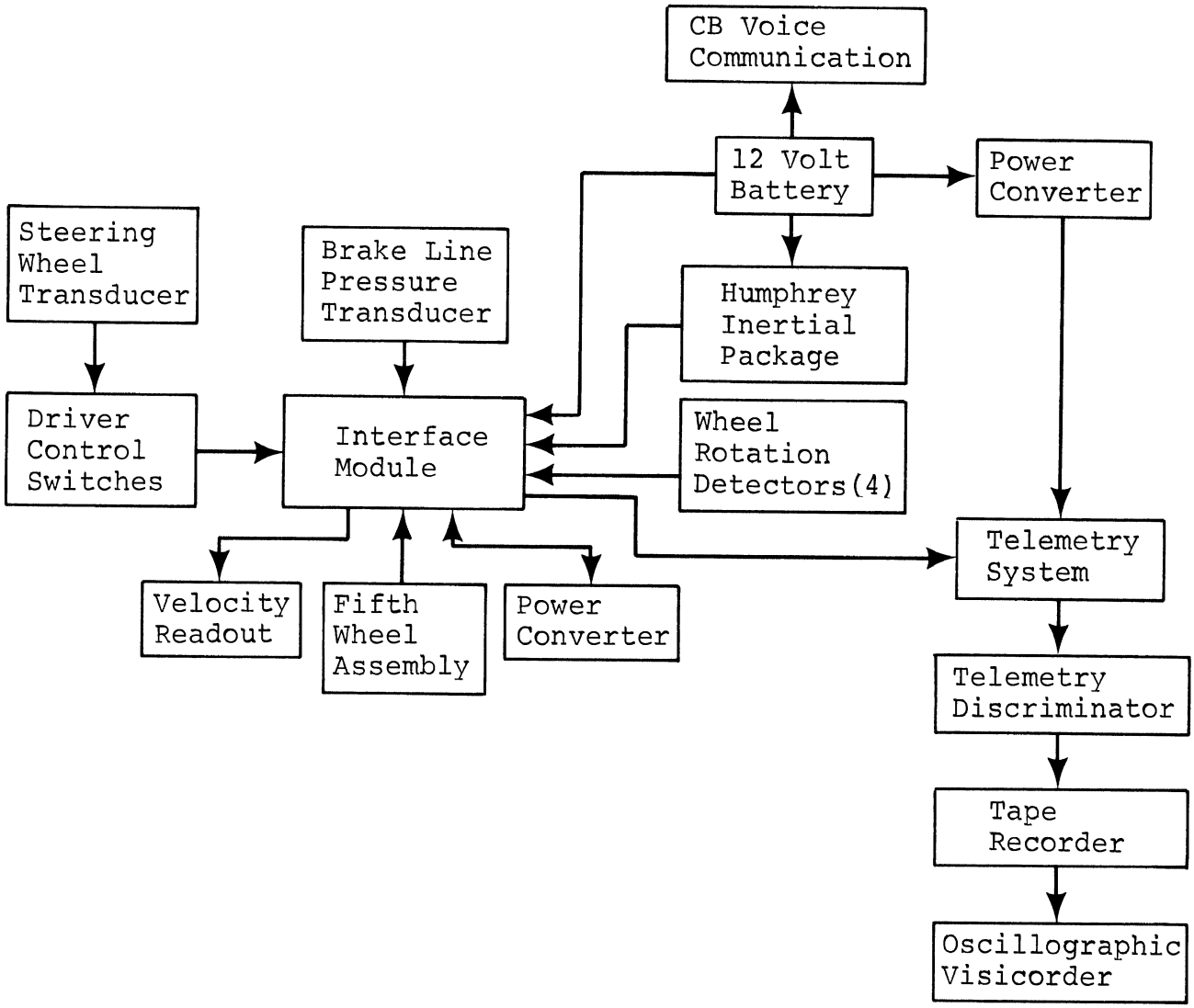

FIGURE V-1

Instrumentation Block Diagram - Driver System

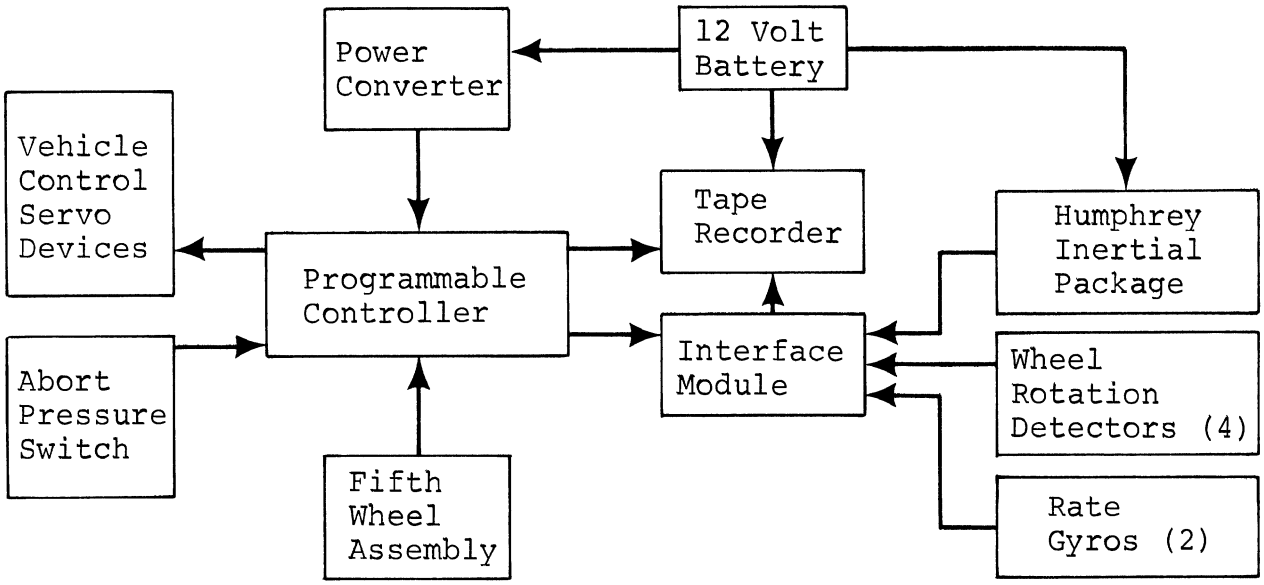

FIGURE V-2
Instrumentation Block Diagram - Automatic System

TABLE V-1

TRANSDUCER DESCRIPTION

Tape Channel	Signal Symbol	Transducer Device	Transducer Range	System	FSC Value
1	A_x	Humphrey Inertial Package	±2.0 g	AC-DR	1.00 g
2	A_y	Humphrey Inertial Package	±2.0 g	AC-DR	1.00 g
3	r	Humphrey Rate Gyro	±90 deg/sec	AC-DR	60.0 deg/sec
4	V_s	Tracktest Fifth Wheel	0-100 mph	AC-DR	50 mph
5	δ_{SW}	Geared Rotary Potentiometer	±900°	AC-DR	500 deg
6	W_1+W_2	Interface Wheel Rotation Circuit	N/A	AC-DR	4.0
7	W_3+W_4	Interface Wheel Rotation Circuit	N/A	AC-DR	4.0
8	P_b	Brake Line Pressure Potentiometer	1500 psi	DR	1000 psi
9	δ_{BR}	Linear Potentiometer	6" Extension	AC	5"
10	F_{BR}	Lebow Load Cell	500 lbs	AC	250 lbs
11	t_{AC}	Function Generator Time Ramp	0-10 sec	AC	10 sec
12	$\dot{\phi}$	AST Rate Gyro	±40 deg/sec	AC	40 deg/sec
13	ψ_H	Humphrey Inertial Package	360° Continuous	DR	360 deg.
14	Control	Interface Circuit	N/A	AC-DR	2.0

N/A Implies Not Applicable

sinusoids are related by the simple harmonic motion equations:

$$\theta = A \sin(\omega t)$$

$$\dot{\theta} = A\omega \cos\left(\omega t - \frac{\pi}{2}\right)$$

The oscillograph traces are then analyzed for period and amplitude of oscillation to determine the voltage calibration in deg/sec.

3. Fifth Wheel - A digital readout device is attached to a fifth wheel pulse-type tachometer. Driving over a measured mile, the fifth wheel tire inflation pressure is adjusted to yield 5280 pulses, or 1 pulse per foot. These pulses are compared against a crystal-controlled time base in a digital tachometer circuit to yield miles per hour. Then the analog tachometer voltage for the fifth wheel is measured at several steady velocity conditions, using the concurrent digital tachometer output as reference.

4. Control Inputs - The various potentiometer devices--steering wheel and brake pedal displacement--are simply calibrated against visual reference with a pointer or tape measure.

5. The Lebow Load Cell for brake force was provided with a shunt resistor for calibration. In this case, no physical load reference was effected at each recalibration of the device.

6. The wheel rotation circuit and control mode levels are functionally checked but are not calibrated.

Additional calibrations included periodic maintenance on the tape recorders and telemetry system according to the respective manufacturers' recommendations. All calibrations were performed with the equipment running in the test vehicle. Various calibrations were also performed as internal adjustments in the automatic controller: velocity threshold, sine period, radio drone gains, abort threshold levels, and calibration of the adjustable command levels on the programmable control. The final calibration activity prior to testing involved the precise setting of the full scale calibration voltage reference generated by the interface module.

TEST EXECUTION

During the test sequencing, the vehicle control inputs were incremented through the various levels as discussed in Appendix II. After recording the pre-calibration modes, the data was recorded for a typical sample:

1. Automatic System - The test operator maneuvers the vehicle into the approach lanes to the skid pad. The on-board tape recorder begins recording when the function generator is armed. This provides a run-up time prior to the maneuver initiation as the vehicle coasts down through the velocity threshold. The recorder automatically shuts off at the end of function generator time ramp.
2. Driver System - The test vehicle driver approaches the test pad in the same manner and he gives a verbal command on the citizen's band radio to the base station telemetry operator. The base tape recorder is thus started a few seconds

prior to test execution. Following the termination of test mode, controlled by a switch near the driver, the tape recorder is manually turned off.

Oscillograph traces of the raw data were created simultaneously with tape data recording during the driver tests. Data tapes from the automatic system tests were also "dumped" regularly on the base station equipment to verify the continued proper functioning of the system and transducers.

HYBRID ANALYSIS AND DIGITIZATION

HYBRID SYSTEM. The FM magnetic data tapes were processed on the HSRI Hybrid Computer facility. This facility consists of an Applied Dynamics AD-4 analog computer and an IBM 1800 digital computer. Various peripheral devices are associated with each basic computer as shown in Figure V-3.

1. Ampex FR 1900 FM 14-channel tape machine for reproducing data tapes.
2. Hewlett-Packard 101A Dual Beam Oscilloscope for monitoring tape data and validity checks.
3. Brush Mark 200 Recorder (2), total of 16 channels for plotting time history data.
4. Hewlett-Packard 2FA Dual Pen X-Y plotter for plotting trajectory data.
5. HSRI hybrid interface unit for hybrid communication signals and data transfer.
6. IBM 1442 card reader-punch for input data.
7. IBM 1443 line printer for listing edited tape files.
8. IBM 2401 Type I tape drive, 9 track, 800 BPI, for digitized data storage.

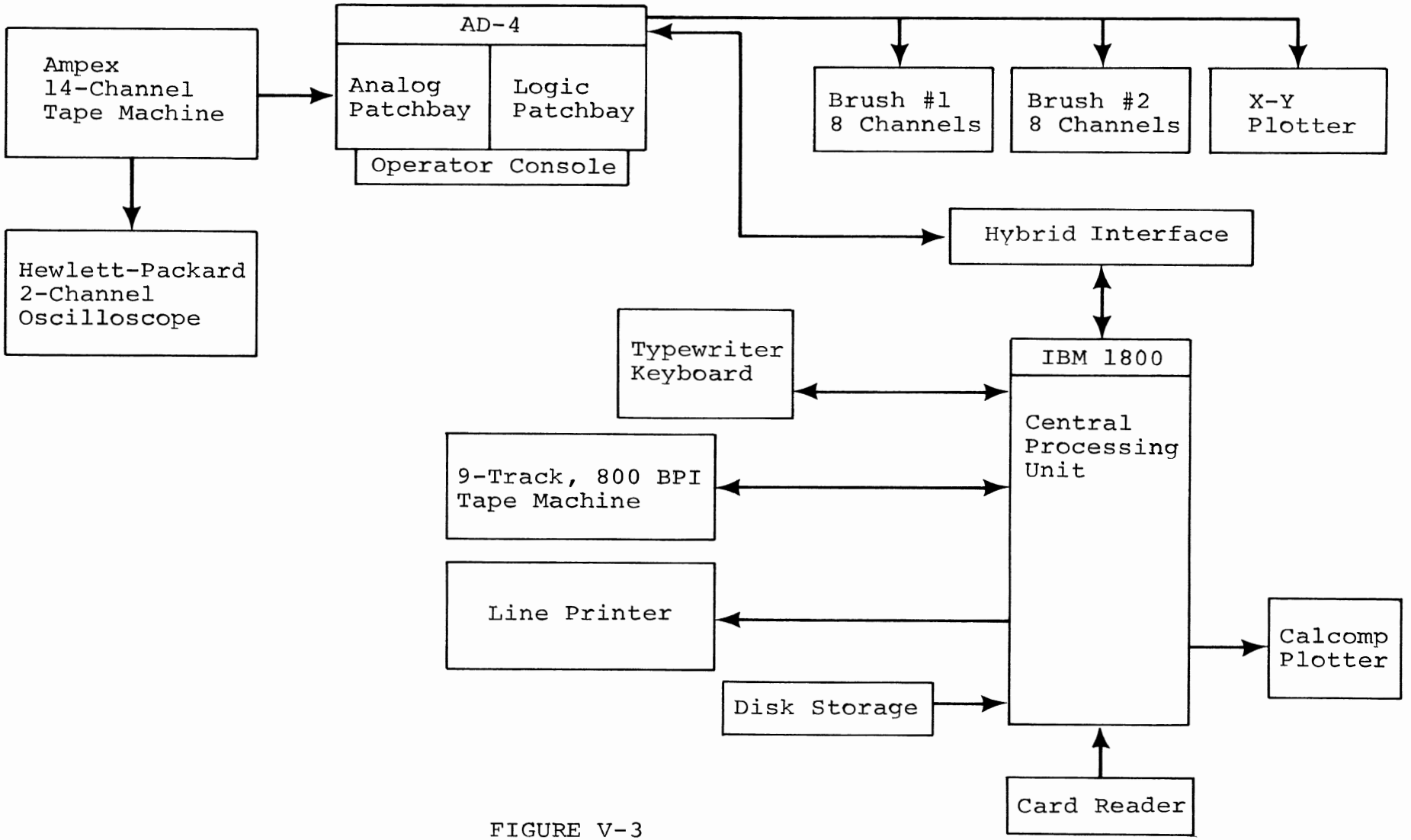

FIGURE V-3
Hybrid Data Processing Equipment

9. IBM 1810 disc drives for program storage.

10. IBM 1816 printer keyboard for operator interaction and control of the program sequence.

11. Calcomp 565 digital plotter for final analysis and validity checks.

The basic program is designed to be highly interactive. Each of these hardware devices is utilized at the appropriate times in the program sequence. The program sequence is directed by the operator and can be interrupted at any time.

TEST SEQUENCE MODE CONTROL

A test sequence is defined to be a single car executing a single maneuver in a single condition. Each test sequence, recorded on magnetic tape, was prefaced by initialize sequence (IS) mode and concluded by end of sequence (EOS) mode. In addition, the three calibration modes (Zero Calibration (ZC), Full Scale Calibration (FSC), and Zero Data (ZD)) were recorded immediately following IS mode. All vehicle test runs were recorded in "data" mode. These five modes are switch-selected on the interface module. A sixth mode, test mode, is generated uniquely in each vehicle series at a time immediately preceding the control input application. A typical test sequence would be recorded as follows:

1.	Initialize Sequence	30 seconds
2.	Zero Calibration	30 seconds
3.	Full Scale Calibration	60 seconds
4.	Data - Zero Data	30 seconds
5.	Data - Test Mode	as required
6.	End of Sequence	30 seconds

NOTES:

(1) Zero data is recorded while the vehicle is standing still on a level surface with all instrumentation activated.

(2) Test mode was initiated when the vehicle was traveling in a straight line above the initial velocity requirements, 2 seconds prior to control input execution.

(3) Every data sample recorded on the tape, including all sequencing and calibration modes, was assigned a unique sample number on the log sheets.

(4) All transducer calibrations are referenced as FSC equivalents. The transducer signals gathered and their calibration levels are listed in Table V-1.

A typical data sequence would be analyzed as shown in Figure V-4. During the initial phases of the program execution, the digital computer has main control over the analog; during the actual data analysis, the analog computer has main control. Modified sequencing or control mode selection can be selected at the operator's discretion by manually over-riding the automated logic sequencing during the data analysis phase. Several error recovery options are also included to aid in rapid trouble shooting of any unanticipated problems. Program-generated comments and operator control options are listed on the typewriter-keyboard to document the processing and catalog the digitized tapes.

ANALOG ANALYSIS

The data signals recorded on the magnetic tape fall into four basic categories:

BASIC DIGITAL BLOCK DIAGRAM
TYPICAL SEQUENCING

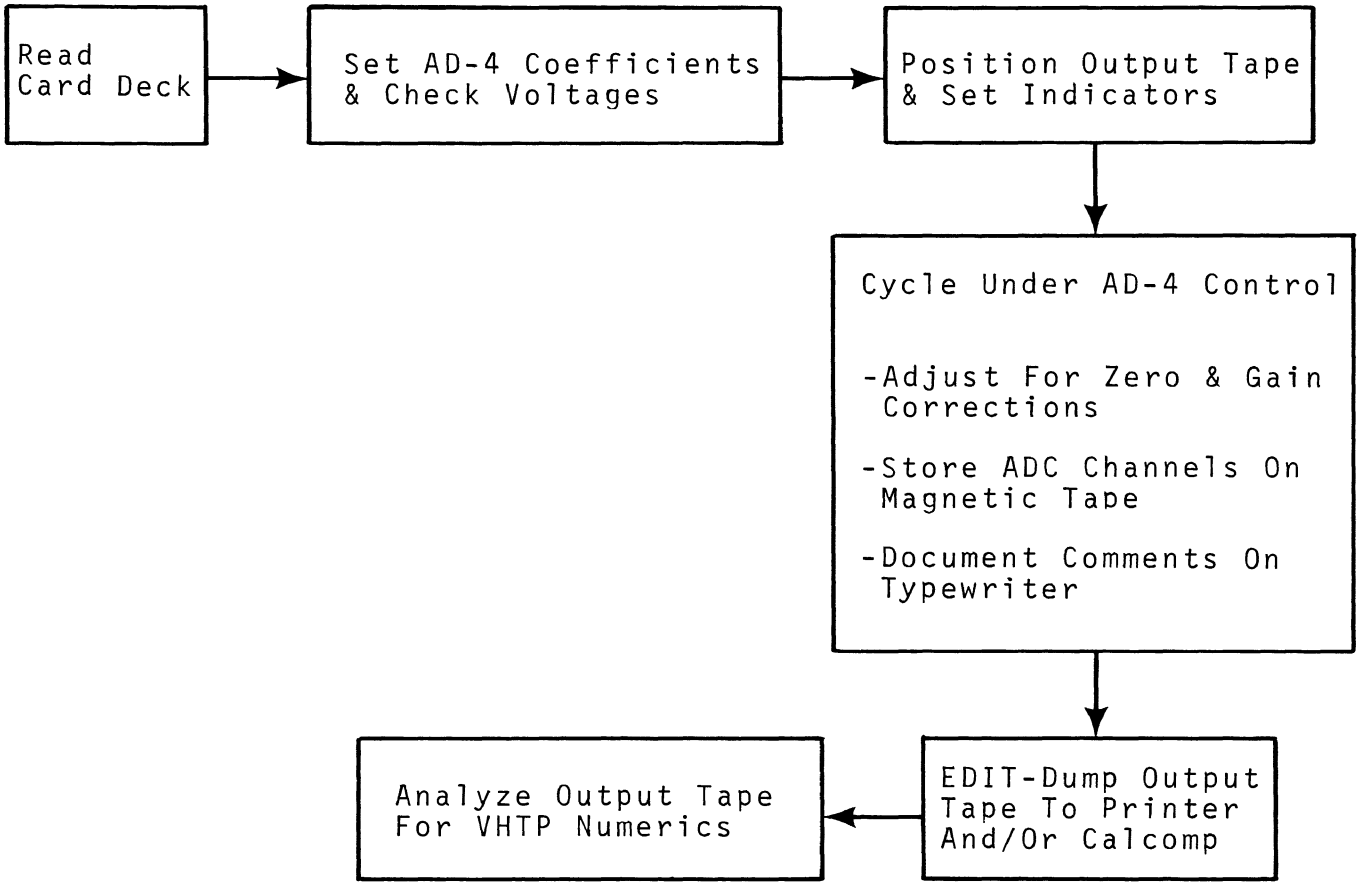

Figure V-4

1. Primary vehicle response data to be analyzed with basic kinematics equations.
2. Vehicle control inputs and informational data.
3. Analog multiplexed wheel rotation detectors to be decoded and reconstructed as time signals.
4. Control channel logic to be decoded for mode control.

A basic functional block diagram for the analog computer is shown in Figure V-5. All data signals are initially processed through data calibration circuits, which provide necessary zero and gain corrections and filtering.

The primary vehicle response data is processed with the following equations:

$$V_x = \int (A_x + V_y r)\,dt$$

$$V_y = \int (A_y - V_x r)\,dt$$

$$\psi = \int r\,dt$$

$$\phi = \int \dot{\phi}\,dt$$

$$x = \int (V_x \cos\psi - V_y \sin\psi)\,dt$$

$$y = \int (V_y \cos\psi + V_x \sin\psi)\,dt$$

$$\tan\beta = V_y / V_x$$

$$1/R = \frac{\dot{\beta} + r}{(V_x^2 + V_y^2)^{1/2}}$$

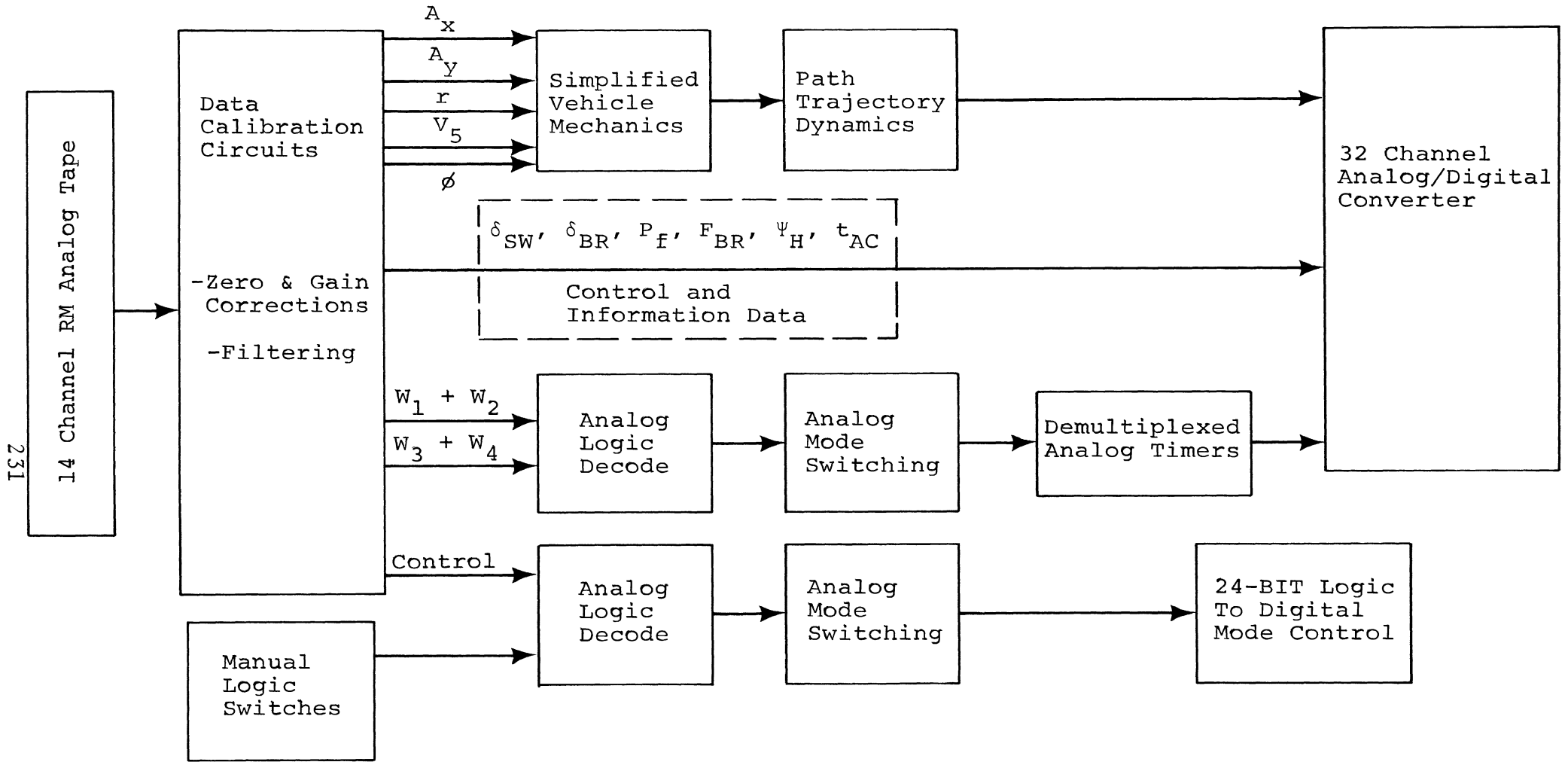

FIGURE V-5

Basic Analog Block Diagram

Definition of these terms can be found in Table V-2. All of these computations are initiated at the beginning of test mode by logical switching; all integral computations are initialized at zero except for V_x, which is initialized by the instantaneous fifth wheel velocity, V_5.

The wheel rotation detectors are triggered by light-sensitive photo-cells to create discrete voltage levels. Each wheel generates a square wave with a period equal to the wheel's rotational period; the square waves from an axle of wheels are assigned different magnitudes and then added together (analog multiplexed) to form one signal and conserve tape channels. This combined signal is de-multiplexed by the analog logic; the multiplexed signal drives analog comparators set to detect thresholds between the four possible voltage values. The logic states of the comparators are combined and used to trigger time duration amplifiers synchronously with wheel rotation rates.

The control channel information is decoded in a manner similar to the wheel rotation signals. The control signal is a DC voltage with a unique value for each mode. This signal drives a set of analog logic elements to switch states in the vehicle mechanics circuits, control the peripheral equipment and signal the digital computer.

TYPICAL SEQUENCE

It will be illustrious to consider the computer activities for a typical sequence. As shown in Figure V-4, the digital computer has primary control in the initial phases. Parameter data is read from punched cards to identify the analog elements in use and to specify various data values for filtering effects, calibration magnitudes, etc. The digital computer then sets the analog coefficient devices to the proper magnitudes and performs a static check of all

analog voltage elements to test the analog circuit. When these steps are completed satisfactorily, the analog and digital tape machines, the Brush recorders and X-Y plotter are readied. Main control is then passed to the analog computer and decoded logic signals, based on the control channel, control the sequence.

The first expected mode is Initialize Sequence (IS). During IS, the digital computer stores certain control indicators on the magnetic tape and sets internal logic switches for later reference.

During Zero Calibration (ZC) mode, the digital computer reads the initial analog stage ten times and computes the necessary voltage offset to correct for tape machine and signal processing errors. The offset values are set into the analog and the voltages are read again as a check. All of this information is also stored on the digital output tape.

During Full Scale Calibration (FSC) mode, the digital computer again reads the initial analog stages ten times and computes the gains through these amplifiers. The desired gain is known from the input deck; the actual gain will be slightly wrong due to variations in the complete system hardware. Gain control potentiometers are reset to correct for these errors and the voltages are read again as a check. All of this information is also stored on the digital output tape.

During Zero Data (ZD) mode, the digital computer repeats the procedure and equations of the ZC mode. Voltage offset errors generated by the transducers are nulled at this time.

The hybrid system is now ready for vehicle test samples. The next mode is data and the digital computer switches to read the 32 ADC channels. At the start of test mode, these channels are digitized and stored on the magnetic tape at a

rate of 50 samples per second per channel until the end of the test mode. Table V-2 identifies the samples stored. This digitizing process creates an output tape file for each test sample.

Upon encountering End of Sequence (EOS) mode, the digital computer closes the magnetic tape output, clears certain indicators and prompts the operator to initiate the next test sequence or branch elsewhere. Validity checks may be performed by dumping the digital tape file data to the main printer or creating digital plots.

DIGITAL ANALYSIS AND NUMERIC DEFINITION

The output of the analog-to-digital conversion process consists of digital magnetic tapes containing the 32 digitized variables stored in sequential files. Each data file represents one test sample and contains a discretized time history of each of the 32 variables. At the beginning of each file is a header record containing information on that file's contents. The information contained in this header gives the type of maneuver being performed, the vehicle identification, the condition code, the sample number, the test and processing dates, the file number, the number of records or data points in the file, and the file type. Calibration data associated with each data sequence is stored in calibration files before and after every sequence of data files.

The structure of the digital processing programs is shown in Figure V-6. The overall operation is controlled by a main-option control program which reads the header record of a file and determines what branching or tape control is required. At the next lowest level are six subprograms which are accessed from the main-option control program. Each subprogram performs the required numeric calculations

TABLE V-2. IDENTIFICATION OF VARIABLES

Identification Number	Symbol	Description
1	A_x	Longitudinal acceleration
2	A_y	Lateral acceleration
3	r	Yaw rate
4	V_5	Fifth wheel velocity
5	δ_{sw}	Steer wheel angle
6	W_1+W_2	Multiplexed wheel rotations, front axle
7	W_3+W_4	Multiplexed wheel rotations, rear axle
8	P_b	Brake line pressure
9	F_{BR}	Brake pedal force
10	δ_{BR}	Brake pedal position
11	tac	Time base of automatic controller
12	$\dot{\phi}$	Roll rate
13	ψ_H	Vehicle heading angle, as measured
14	CONT	Control channel (MC)
15	t_{AD}	Time base on AD-4
16	REF	AD-4 voltage reference
17	V_x	Longitudinal vehicle velocity, body axis
18	V_y	Lateral vehicle velocity, body axis
19	x	x-Displacement, fixed axis
20	y	y-Displacement, fixed axis
21	ψ	Vehicle heading angle, as computed
22	Tanβ	Tangent of vehicle sideslip angle
23	β	Vehicle sideslip angle
24	$\dot{\beta}$	Derivative of vehicle sideslip angle
25	W_1IND	Wheel rotation indicator, left front

TABLE V-2 (Cont)

Identification Number	Symbol	Description
26	W_2IND	Wheel rotation indicator, right front
27	W_3IND	Wheel rotation indicator, left rear
28	W_4IND	Wheel rotation indicator, right rear
29	$\dot{x}$	x-Direction velocity, fixed axis
30	$\dot{y}$	y-Direction velocity, fixed axis
31	1/R	Path curvature
32	ϕ	Roll angle

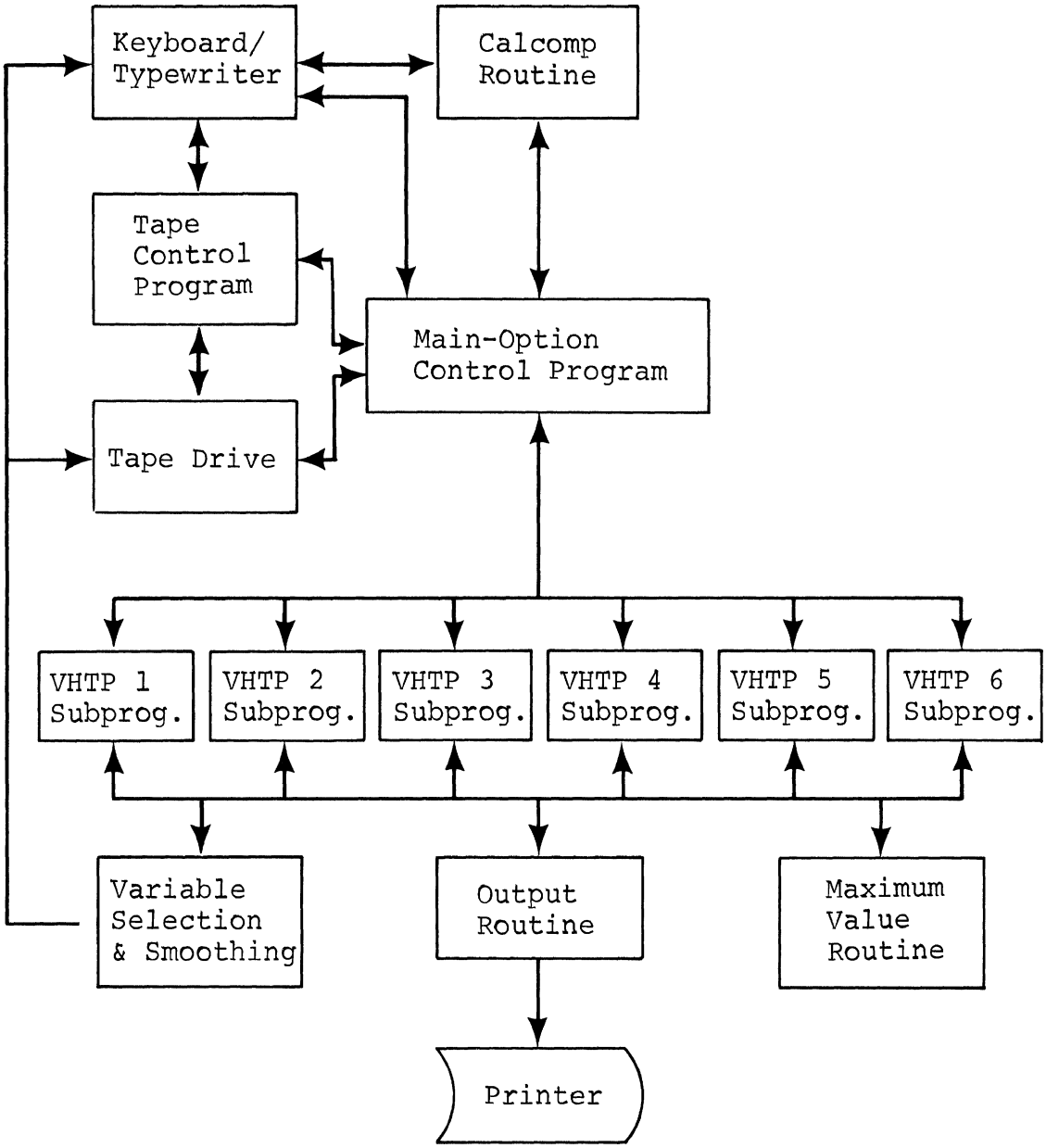

Figure V-6

BLOCK DIAGRAM OF DIGITAL PROGRAM STRUCTURE

associated with a particular VHTP maneuver. These subprograms, in turn, interact with various subroutines which are used for smoothing, finding maximum values, and printing out the results.

The processing operation is completely automatic with no need for any operator interaction. The numerics computed for each VHTP test sample are printed out in tabular form on the line printer during this mode. However, the processing may be interrupted at any time and controlled completely from the keyboard/typewriter, with additional options available such as Calcomp plotting of any two variables, complete control of the tape unit, and arbitrary subprogram branching.

The following sequence is typical of the operations that the digital processing program performs. The main-option control program first reads the header record of the present file and determines whether or not it is a data file. If it is not (hence, a calibration, initialize sequence, or end of sequence file), it skips over the present file to the next file. Once a data file is encountered, the program determines what type of maneuver is being performed and then branches to the subprogram associated with that particular VHTP maneuver. The VHTP subprogram identifies the variables needed for its particular numeric calculations and passes this information to the variable selection and smoothing subroutine, which reads these required variables from the tape to core storage, smooths, and returns them to the VHTP subprogram. The VHTP subprogram then performs the necessary numeric calculations, using these smoothed variables, and outputs the results to the line printer. Program control is then returned to the main-option control program which reads the next file header record, and the above cycle is repeated.

If the processing is interrupted for keyboard/typewriter control, the variables used in numeric calculations for the last data file remain in core storage and are not lost until the next file is processed. This eliminates any requirement to re-position the tape and read data that normally would have been lost upon completion of the calculations of the last file. Hence, many operations may be performed on this same data from the keyboard/typewriter such as Calcomp plotting, printing, searching for maximum values, or even further smoothing.

The following defines and explains the individual numerics that were calculated for each VHTP maneuver:

VHTP 1: a) $(A_x)_{ave} = \frac{1}{t_1 - t_o} \int_{t_o}^{t_1} A_x \cong \frac{1}{i} \sum_{i=1}^{n} A_{x_i}$

= average longitudinal deceleration.

where

A_x is the longitudinal deceleration

A_{x_i} is the discretized representation of longitudinal deceleration

t_o is the initial time at V = 35 mph

t_1 is the final time at V = 10 mph

i is the integer count of data points over the summation interval

V is the velocity

t is time

VHTP 2: a) $(A_x)_{ave} = \frac{1}{t_1 - t_o} \int_{t_o}^{t_1} A_x \, dt \cong \frac{1}{t_1 - t_o} \sum_{i=1}^{n} A_{x_i}$

= average longitudinal deceleration

where

A_x, A_{x_i}, t_1, t_o, i, V, t are defined the same as under VHTP 1 a).

VHTP 2: b) $R_o(\frac{1}{R})_{av} = \frac{(\frac{1}{R})_{av}}{(\frac{1}{R})_o}$ = average path curvature ratio

where

$$(\frac{1}{R})_{av} = \frac{1}{1} \int_{t_2}^{t_2+1} (\frac{1}{R}) dt \cong \frac{1}{s_f} \sum_{i=1}^{s_f} (\frac{1}{R})_i$$

$$(\frac{1}{R})_o = \frac{1}{R}\Big|_{t_2} \cong (\frac{1}{R})_i \quad , \quad i=0$$

and,

$(\frac{1}{R})_i$ is the discretized representation of path curvature

$(\frac{1}{R})$ is path curvature

$(\frac{1}{R})_o$ is the path curvature at the time the brakes are applied

$(\frac{1}{R})_{av}$ is the average path curvature for 1 second after the brakes are applied

t_2 is the time the brakes are applied

t_2+1 is the one second following brake application

s_f is the digitizing rate in samples/second.

VHTP 2: c) $\beta_p(t)$ = Maximum absolute value of sideslip angle.

where

t is defined over the interval $[t_2, t_2+1]$

t_2, t_2+1 are defined as under b).

VHTP 2: d) $\dot{\beta}_p(t)$ = Maximum absolute value of rate of change of sideslip angle.

where

t is defined over the interval $[t_2, t_2+1]$

t_2, t_2+1 are defined under b).

VHTP 3: a) $R_o(\frac{1}{R})_{av} = \frac{(\frac{1}{R})_{av}}{(\frac{1}{R})_o}$ = average path curvature ratio.

where

$$(\frac{1}{R})_{av} = \frac{1}{1} \int_{t_3}^{t_3+1} (\frac{1}{R}) dt \cong \frac{1}{s_f} \sum_{i=1}^{s_f} (\frac{1}{R})_i$$

$$(\frac{1}{R})_o = \frac{1}{R}\Big|_{t_3} \cong (\frac{1}{R})_i \quad , \quad i=0$$

and,

$(\frac{1}{R})$, $(\frac{1}{R})_i$ are defined the same as under VHTP 2 b).

t_3 is the time the vehicle enters the grid.

t_3+1 is the time 1 second after the vehicle enters the grid.

$(\frac{1}{R})_{av}$ is the average of $\frac{1}{R}$ over the above defined interval $[t_o, t_o+1]$.

$(\frac{1}{R})_o$ is the value of $\frac{1}{R}$ at the time the vehicle enters the grid.

VHTP 3: b) $\beta_p(t)$ = Maximum absolute value of sideslip angle.

where

t is defined over the interval $[t_3, t_3+1]$.

t_3, t_3+1 are defined as in a).

VHTP 3: c) $\dot{\beta}_p(t)$ = Maximum absolute value of rate of change of sideslip angle.

where

t is defined over the interval $[t_3, t_3+1]$.

t_3, t_3+1 are defined as in a).

VHTP 4: a) A_{yp} = Maximum lateral acceleration over the entire maneuver time interval.

VHTP 4: b) r_p = Maximum yaw rate over the entire maneuver time interval.

VHTP 4: c) $R_o(\frac{1}{R})_{av} = \frac{(\frac{1}{R})_{av}}{(\frac{1}{R})_o}$ = Average path curvature ratio.

where

$$(\frac{1}{R})_{av} = \frac{1}{2}\int_{t_4}^{t_4+2} (\frac{1}{R})dt \cong \frac{1}{2s_f}\sum_{i=1}^{2s_f} (\frac{1}{R})_i$$

$$(\frac{1}{R})_o = \frac{1}{R}\Big|_{t_4} \cong (\frac{1}{R})_i \ , \quad i=0$$

and

t_4 is the time of the steering input

t_4+1 is the time 2 seconds after the steering input

$(\frac{1}{R})_{av}$ is the average path curvature over the above defined interval $[t_4, t_4+1]$

$(\frac{1}{R})_o$ is the path curvature at t_o.

VHTP 4: d) $\beta_p(t)$ = Maximum absolute value of sideslip angle over t.

where

t is defined over the interval $[t_4, t_4+2]$

t_4, t_4+2 defined as in c).

VHTP 4: e) $\dot{\beta}_p(t)$ = Maximum absolute value of rate of change of sideslip angle over t.

where

t is defined over the interval $[t_4, t_4+2]$

t_4, t_4+2 defined as in c).

VHTP 4: f) $\Delta\beta = \beta_p(t) - \beta(t_4)$

where

t is defined over the interval $[t_4, t_4+2]$

$t_4 m t_4+2$ defined as in c)

$\beta(t_4)$ = the value of sideslip at t_4.

VHTP 5: a) $$\Delta = \frac{1}{T}\int_{t_5}^{t_5+T} |y-12|dt \cong \frac{1}{T\cdot s_f}\sum_{i=1}^{T\cdot s_f} |y_i-12|,$$

for right-left steer.

$$= \frac{1}{T}\int_{t_5}^{t_5+T} |y+12|dt \cong \frac{1}{T\cdot s_f}\sum_{i=1}^{T\cdot s_f} |y_i+12|,$$

for left-right steer.

where

t_5 is the time of the steering input

T is the length of time of the maneuver, usually 3.4 seconds

y is the time history of the lateral displacement of the vehicle after t_5

y_i is the discretized representation of y

s_f is the digitizing rate.

VHTP 5: b) $\beta_p(t)$ = Maximum absolute value of sideslip angle.

where

t is defined over the interval $[t_5, t_5+T]$

t_5, t_5+T defined as in a).

VHTP 5: c) $\Delta\psi(t_5+T)$ = Heading angle at the time (t_5+T)

where

t_5, T are defined as in a).

VHTP 6: a) ϕ_{max} = Maximum absolute value of roll angle over the entire maneuver time interval.

APPENDIX VI

RECOMMENDATION OF THE MINIMUM PHYSICAL REQUIREMENTS FOR THE CONDUCT OF OPEN-LOOP LIMIT HANDLING TESTS

In Figure VI-1 is shown a general requirement for the minimum size test area required for open-loop limit handling tests. This layout is configured with the intention of imposing the minimum spatial requirement on high quality paved surface. Thus a lesser quality graded "runout" surface is defined along with an "obstacle-free" margin. The dimensions of the test surface derive from the trajectories which accompany open-loop turning tests. The dimensions of the recovery areas are determined by the needs of automatic controller operation from 60 mph. In the case of the 60 mph sinusoidal steer test , for example, the vehicle can finish the maneuver with a terminal heading rotated as much as 60° from its initial heading. Under such circumstances, a margin is needed for operator judgment, plus a smooth braking transition and finally a turn-around.

Although no clear basis exists for establishing a maximum test surface inclination, a grade of 1 1/2% provides adequate drainage for most climates and contributes a relatively small distortion to the "horizontal plane" idealization of the test condition.

Since many of the vehicle response categories discussed in the text are not currently normalizeable to account for surface friction properties, there appears to be no clear statement which can specify minimum or maximum friction of the test area. Nevertheless, it would seem that a "high coefficient" property as characterized by ASTM dry "skid numbers" of 70 and above would provide for the large acceleration conditions under which the vehicle design can play a significant role in determining tire/vehicle system response.

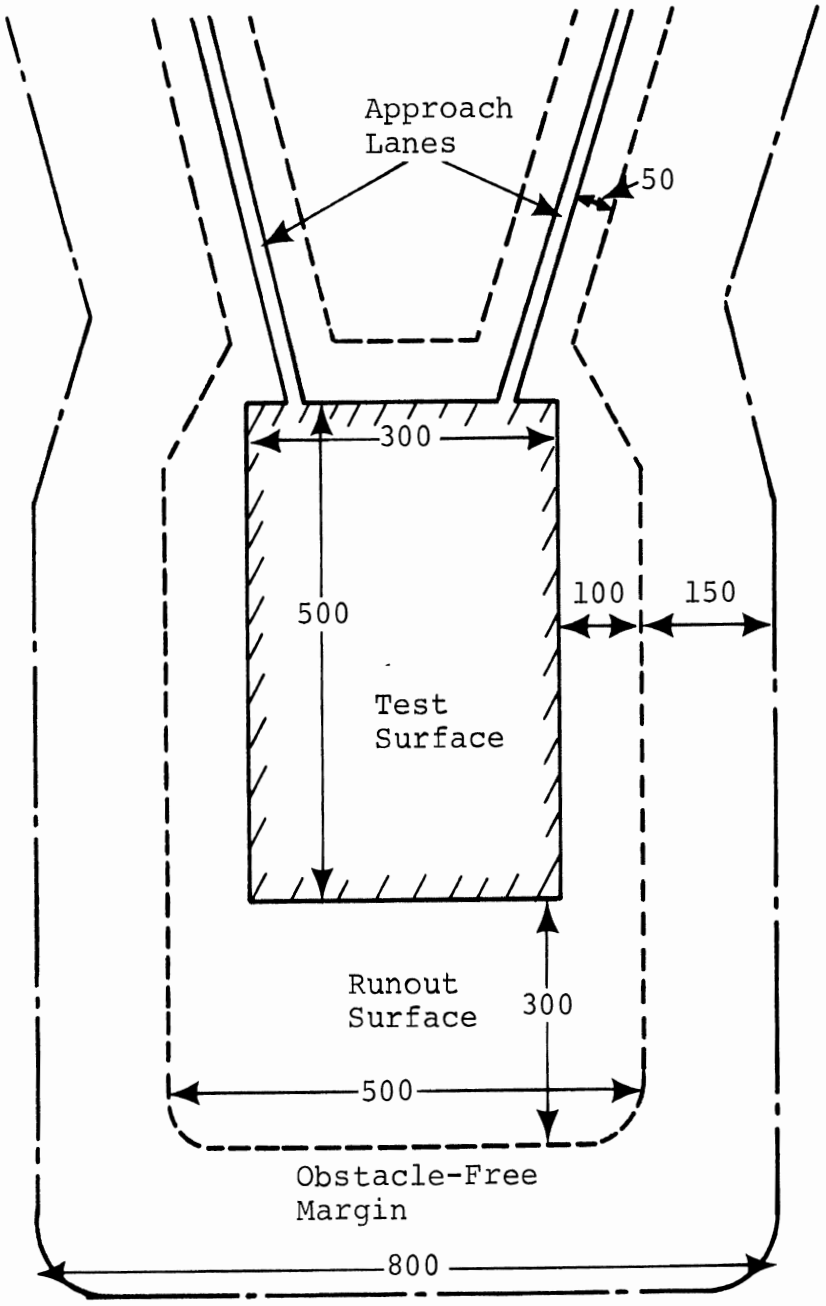

FIGURE VI-1

Minimum Recommended Test Area Dimensions

Further facilities requirements include the following, for maintenance of a full-time test effort:

- -Machine shop
- -Welding shop
- -Garage and hoist facilities with
  - -front end alignment apparatus
  - -tire changer
- -Electronics shop with full complement of modern diagnostics equipment for maintenance of analog circuits
- -Instrumentation calibration facility
  - -rate gyro pendulum or rate table
  - -precision inclinometer and table for accelerometer calibration
  - -gauge calibrator
  - -fifth wheel calibrator
  - -thermocouple calibration

The test apparatus required for the conduct of the six open-loop procedures would necessarily include the following:

1. Steering Limiter mechanism, capable of providing a mechanical stop at any steer wheel position from 500° clockwise to 500° counterclockwise. This device should have an adjustment for correcting the "zero" displacement position as testing progresses to account for tire wear and front end misalignment.
2. Brake Level Limiter - capable of constraining braking inputs to adjustable levels of either pedal force or line pressure, over the range of levels achievable within 250 lbs. of pedal force.

3. Anti-rollover outriggers.

4. Wheel rotation detectors.

5. Brake lining temperature readout device (100° to 400°F).

6. Fifth wheel-type velocity transducer capable of repeated operation over a road roughness course and under spinout conditions.

7. Automatic controller, of a design configuration capable of providing

   a. Steering trapezoids of 0.4 sec. ramp time, and adjustable level to 500° cw and ccw.

   b. Steering sine waves of 2 second period with amplitude adjustable to 360°. Sine wave must be provided initially cw or initially ccw.

   c. Combined steering and braking inputs, by which a half sine wave of steering is followed by a trapezoidal brake input. The level of the steering and braking as well as the phase relationships must be adjustable. Brake input ramp time is .050 seconds and the steer half sine wave is of 1 second half period.

8. Data acquisition and processing apparatus is needed to permit the ultimate gathering of body sideslip, path curvature, and c.g. trajectory time histories. Sufficient information can be obtained with transducers measuring A_x, A_y, r, and V_5 as per this study, or with frame-fixed

accelerometers and A) rate gyros (r, $\dot{\phi}$, $\dot{\theta}$) or B) vertical gyros - (ϕ and θ) plus a yaw rate gyro (r). Other multiple accelerometer solutions are also possible to permit the computation of body sideslip, path curvature, and trajectory. Analog to digital conversion equipment is needed at some point in the processing, such that digital computation of response numerics can be effected.